Quaternary activity of the Hluboká Fault

Abridged translation of updated final report for project

"Paleoseismology of the fault structures near NPP Temelín"

funded by the State Office for Nuclear Safety
(VaV project No. 1/2009; Jan 2009 to Dec 2010)

PETR ŠPAČEK[1], IVAN PRACHAŘ[2], JAN VALENTA[3],

P. ŠTĚPANČÍKOVÁ[3], J. ŠVANCARA[1], J. PISKAČ[2], J. PAZDÍRKOVÁ[1], R. HANŽLOVÁ[1], J. HAVÍŘ[1], J. MÁLEK[2]

[1)] Institute of Earth Physics MU Brno

[2)] Energoprůzkum Praha

[3)] Institute of Rock Structure and Mechanics ASCR

Quaternary activity of the Hluboká Fault

The research team and technical support

P. Špaček[1]	*responsible investigator, field research in fault segments 1C, 2B, 3, 4A and 5; chief editor; author/co-author of Chapters 1-6*
I. Prachař[2]	*field research in fault segments 1A-C, 2A-B; author/co-author of Chapters 2.1, 3.1, 4.2, 4.3, 4.4, 4.5, 4.6, 5, 6*
J. Valenta[3]	*management of geophysical survey and data processing*
J. Švancara[1]	*author/co-author of Chapters 2.2 and 3.2*
P. Štěpančíková[3]	*fieldwork in trenches; author/co-author of Chapters 4.7 and 5*
J. Piskač[2]	*management of technical fieldwork*
J. Pazdírková[1]	*author/co-author of Chapters 3.1 and 3.2*
R. Hanžlová[1]	*author/co-author of Chapter 3.2*

Scientific, technical and administrative support:
J. Havíř[1], J. Málek[3], R. Gaždová[3], P. Kolínský[3], Z. Sýkorová[1], T. Kratochvíl[1], P. Zacherle[1]

1) Institute of Earth Physics MU Brno, Tvrdého 12, 602 00 Brno; spacek@ipe.muni.cz
2) Energoprůzkum Praha, s.r.o., Pod svahem 757/11, 147 00 Praha
3) Institute of Rock Structure and Mechanics ASCR, v.v.i., V Holešovičkách 41, 182 09 Praha

Abridged and translated by P. Špaček, Brno, August 2011

CONTENTS

Abstract

We performed a detailed study of the Hluboká Fault, a conspicious marginal fault of Cretaceous sedimentary basin with distinct morphology, located in the area of Temelín Nuclear Power Plant. The main objective was to assess the present-day tectonic potential of the fault and to get new data which would serve as a basis for the revision of regional seismic hazard in South Bohemia. Extensive amount of data relevant for the assessment of Quaternary slip in the fault zone was gathered at several localities on different fault segments, using observations on surface, in trenches, geophysical sections and boreholes, and dating of sediments overlying the fault zone.

Numerous observations of continuous stratigraphy of Miocene, Pleistocene and Holocene sediments across the fault zone suggest a long-term tectonic quiescence at the Hluboká Fault. In some trenches it was proved that the morphological escarpment associated with margin of the Budějovice basin is not linked with any active fault which continues into Miocene and Quaternary sediments. The present-day morphology of the escarpment is explained mainly as due to the differential erosion of unconsolidated sediments of the basin fill and long-term, probably multiphase, degradation of the fault scarp since Tertiary.

In central segment of the fault some young OSL dates of higher sedimentary relics of apparently alluvial origin are in conflict with the constant thickness of the lower terrace of the Vltava river across the fault. We propose an additional research which will bring more data and help resolve these ambiguities.

Revision of catalogues of historical and instrumental records of regional seismicity performed in this project indicate only minor activity with magnitudes not exceeding $M_l=3.2$ in period 1591-1991 and $M_L=2.6$ in period 1991-2009. The Hluboká Fault has not produced any recorded seismic events within the period of observation and is regarded as seismically inactive.

1

INTRODUCTION

1. INTRODUCTION

This is an abridged translation of the updated final report for the two-year research project *„Paleoseismology of the fault structures near Temelín Nuclear Power Plant“*, funded by the State Office for Nuclear Safety (project No. 1/2009; Jan 2009 to Dec 2010). The project followed from the agreements of the Czech-Austrian parliamentary commission, implementing the „Conclusions of the Melk Process and Follow-up“ (Brussel Protocol). The expert team nominated by this commission agreed during the official meeting in Vienna (November 2007), that it is desirable to perform a paleoseismological research which would enable the assessment of seismogenic potential of the faults near Temelín Nuclear Power Plant. One of the key issues in the long-term negotiation process, repeatedly accented by the Austrian party, is the possibility of seismogenic re-activation of the Hluboká Fault. This fault, although not in direct proximity of the power plant, is conspicious by its pronounced morphology, which suggests that it could be potentially active in Quaternary. For this reason the Hluboká Fault has always been in focus of interest on expert IAEA missions to NPP Temelín, during informal discussions and in other sources (e.g. in „ETE RoadMap 2005“ report by Austrian experts for Austrian Federal Ministery for Agriculture, Forestry, Environment and Water Resources).

The current research project was therefore aimed at the investigation of the activity of the Hluboká Fault mainly in terms of its age and production of strong seismic events in Late Quaternary. The main objective was to assess the present-day neotectonic potential of the fault and to gather new data which would serve as a basis for the revision of seismic hazard in NPP Temelín. The research was based on detailed field survey, which included extensive drilling, exposing the upper parts of the fault in trenches, and dating of the sediments relevant for the fault slip history. In addition to the geological field research, revision of catalogues of historical and instrumental records of seismicity in the region was carried out.

As agreed on 2007 Vienna meeting the research was carried out in the form of two parallel interfacing research projects, funded respectively by Czech (CIP, Czech Interfacing Project) and Austrian (AIP, Austrian Interfacing Project) parties. The purpose of this strategy was to allow the effective transfer of know-how and to support the open discussion. Both members of CIP and AIP teams cooperated in field research and in laboratory dating of the rock samples. More than 10 joint field excursions and working meetings were organised during the two-year project, where both parties have informed each other about the work progress, and the results of the discussions were then taken into account in the following steps of the research. Regarding the political context of the problem investigated, the independent (external, both Czech and foreign) experts were invited for the inspection of the trenches to ensure the complexity of the interpretations and broader acceptability of the conclusions.

2

GEOLOGICAL SETTING

2. GEOLOGICAL SETTING

2.1 GEOLOGY OF THE SOUTH BOHEMIAN BASINS

In southern part of the Bohemian Massif two basins with Cretaceous and Tertiary fill are developed within the Moldanubian unit of Variscan orogeny: the Budějovice and the Třeboň Basins, together also called the South Bohemian basins (Figs. 2.1-1, 2.1-2 and 2.1-5). These basins occupy an area of approx. 2300 km^2 and are associated with prominent NW-SE to WNW-ESE oriented terrain depressions with relatively flat relief, divided by N-S striking elevation of crystalline rocks (the Lišov horst). The basin fill is assymetric, having largest thickness (300-370 m) near the steep marginal faults of NW-SE and NNE-SSW strike, in the E and NE parts of the Budějovice Basin and SW part of the Třeboň Basin (Fig. 2.1-4). The area under study is situated at the NE margin of the Budějovice Basin.

The crystalline fundament is represented by biotite, biotite-sillimanite or biotite-cordierite paragneisses to migmatites, granulites, local intercalations of amphibolites, orthogneisses and quartzites of the Moldanubian unit, and intrusions of Late Variscan granitoids. Continental clastic sediments of Upper Carboniferous and Lower Permian age occur at the E margin of the basin, representing the relicts of NNE-SSW oriented, fault bounded, Blanice Graben formed during the post-collisional extension. In Permian and during Mesozoic these units were subject to deep denudation and formation of low-elevation peneplain which was covered by thick kaoline-rich eluvium.

In Upper Cretaceous a long period of extensive faulting and reactivation of pre-existing crustal discontinuities began in the Bohemian Massif, as a result of convergence between Africa and Europe, gradual closure of the Alpine Tethys and collision of Adriatic microplate with epi-Alpine Europe (e.g. Ziegler et al. 2006). In this period the South Bohemian basins were formed most probably due to the heterogeneous slip on NW-SE and NNE-SSW striking, mostly pre-existing faults and simultaneous fill-up of the resulting depressions in Cretaceous, Tertiary and Quaternary (see Table 2.1.1).

The most important part of the basin-fill are the Upper Cretaceous fluvial and lacustrine clastic sediments of the **Klikov Formation** which were derived mainly from kaolinite-rich eluvium of crystalline rocks (Domácí, 1979). Coarse-grained kaolinic sands/sandstones, fine-grained gravels or conglomerates, dark grey organic-rich sands to clays and brown to red-brown or greenish clays are the most abundant lithologies. At the southern margin of the Třeboň Basin (between Třebeč and Nové Hrady), coarse-grained (5-7 cm pebbles) conglomerates are developed. The maximum thickness of the Klikov Fm. is 320 - 340 m. The age of Klikov Fm. is dated by macroflora (e.g., Pacltová 1961) as Upper Coniacian to Santonian and according to Malecha and Pícha (1963) it is analogical to the Gossau beds in the Alpine region. According to Slánská (1961, 1974) the similar sedimentary record indicates that in both basins deposition was controlled by the same tectonic evolution. This, together with the sedimentary relics on the Lišov horst, suggests that the two basins belonged to single depositional system and the Lišov horst was formed after deposition. In spite of the fact that the present-day shape of the basins is mostly post-depositional, we suggest that at least some faults of the NW-SE strike were active during sedimentation (compare with the situation in the Bohemian Cretaceous Basin, Uličný et al., 2008). This is supported by the coarse-grained conglomerates developed at the S margin of the Třeboň

Basin, near the Stropnice fault system, interpreted as marginal sedimentary facies deposited near actively slipping syn-sedimentary fault.

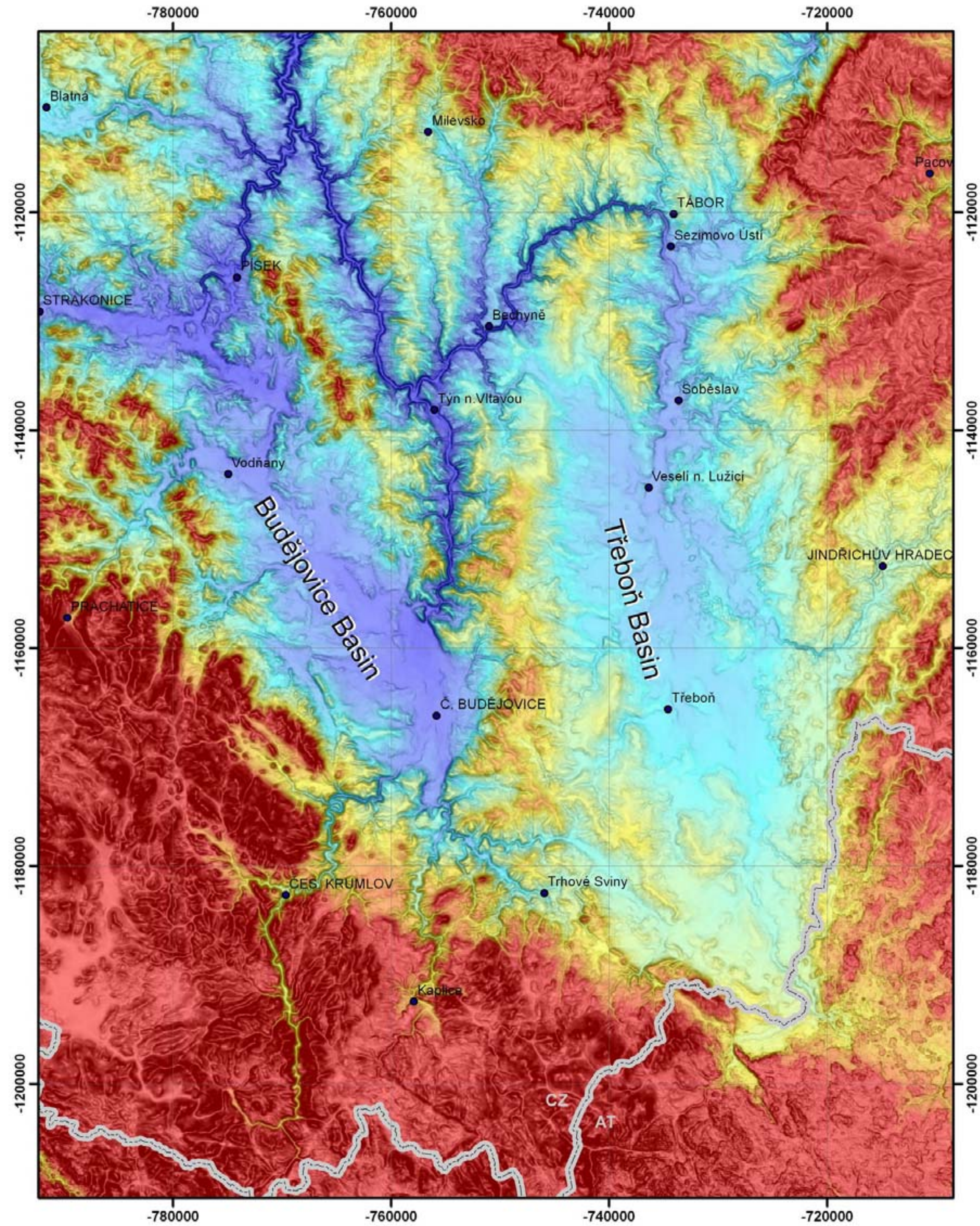

Fig. 2.1-1.: Relief map of the South Bohemain basins and adjacent areas. Note the difference in mean elevation of the two basins which is about 50 m (red - higher elevation, blue - lower elevation). S-JTSK system with 20 km grid.

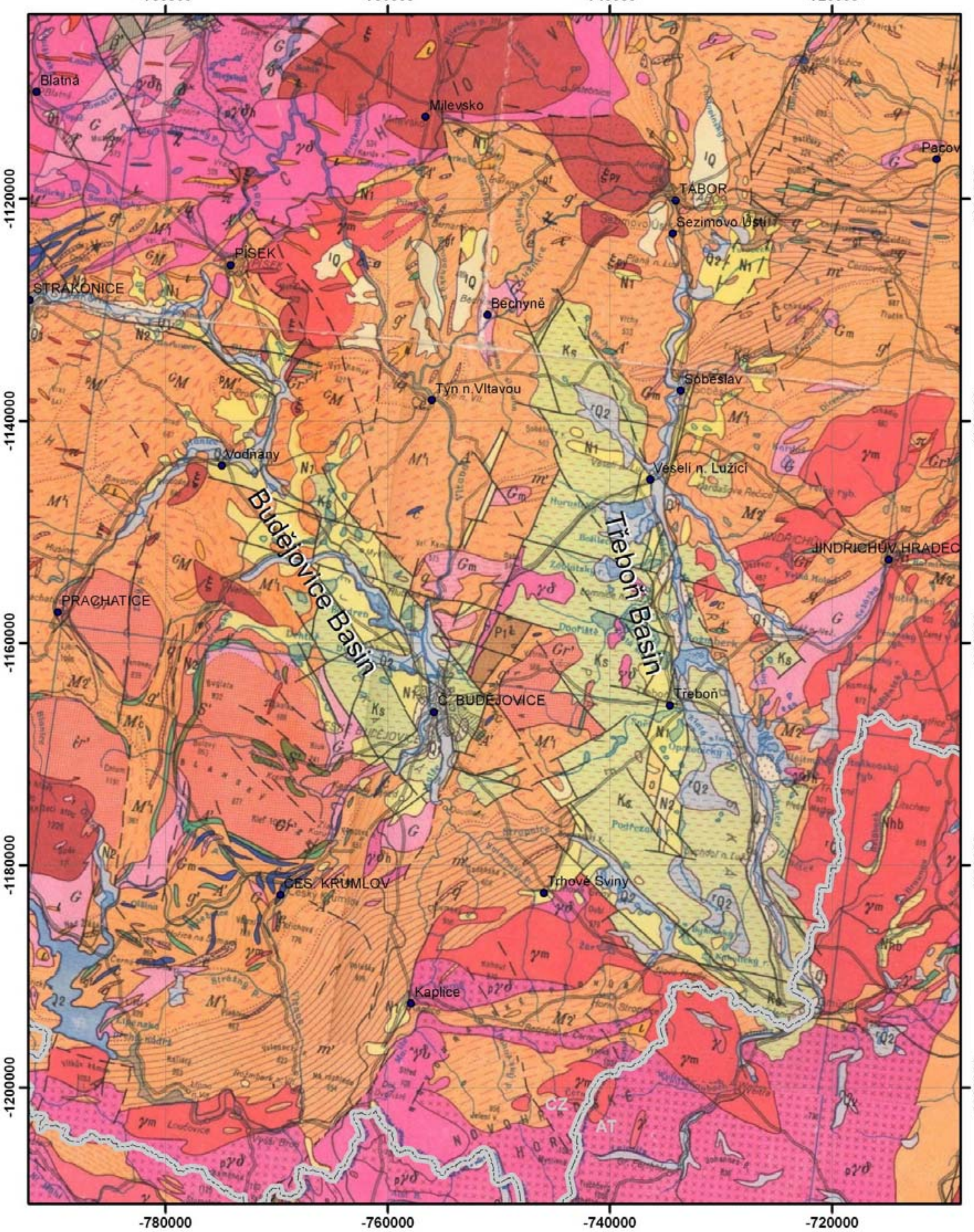

Fig. 2.1-2.: Simplified geological map of the South Bohemian basins area (Czech Geol. Survey, 1967) S-JTSK system with 20 km grid.

In the NE margin of the Budějovice basin the syn-sedimentary faulting is indicated e.g. by small-scale blind faults which were exposed in an old quarry N of Zliv (Fig. 2.1-3). Generally, the deformation of Cretaceous sediments exposed on the surface is very weak, mostly limited to small-scale slickensides with striation (Zahájí quarry) displaying only small slips of several centimetres. It is therefore difficult to assess the syn-sedimentary activity of the faults.

The major post-sedimentary deformation related to faults are mainly documented by large deformations of the Klikov Fm. strata observed in the SE part of the Budějovice Basin (at the crossing of NW-SE and NNE-SSW striking faults, in trenches near Úsilné, Chapter 4.7) and by the fold-like structure of the assumed Klikov Fm. strata in the reflection seismic profile Munice (Chapter 4.3).

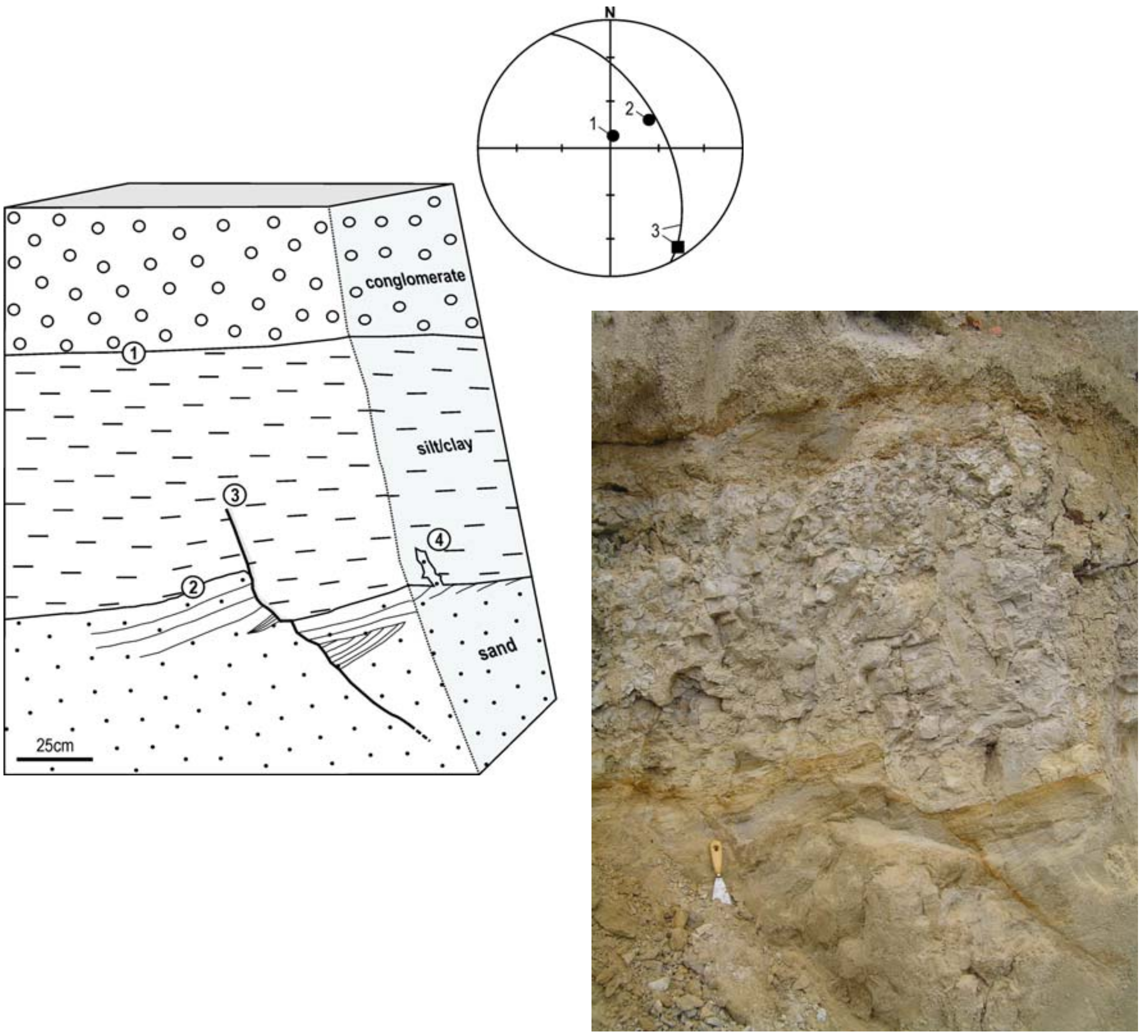

Fig. 2.1-3. Photograph and schematic drawing showing the blind fault in the Klikov Fm. exposed in the old quarry near Zliv. Viewed from SE. Stereodiagram shows the orientations of main structural features, including the weakly developed, sub-horizontal striation on the fault. Note the offset and rotation of the lower bed and the undeformed upper bed. Syn-sedimentary subhorizontal slip on the NW-SE oriented fault is inferred.

After the deposition of the Klikov Fm. the Bohemian Massif was probably mostly dry again until Eocene and the development of kaolinite-rich eluvia continued. In the Třeboň Basin 25-35 m thick sequence of clastic sediments of unknown age (Lipnice Fm.) is locally preserved in a small occurence, suggesting the continuing deposition, probably in fluvial environment. Oligocene age has been suggested by lithological similarity to other relics in the Bohemian Massif (Malecha et al. 1964). The silicification of the upper part of these strata indicates the ongoing kaolinite weathering. Numerous belevelled surfaces observed in the present-day relief possibly correspond to this period.

The **Zliv Formation** is represented by <20 m thick sequence of sandy clays and poorly sorted sands or fine-grained gravels. Similarly as in the Lipnice Fm., the upper part of these sediments is strongly silicified, and its relics are locally well preserved. Locally, fragmented diatomic fauna was found in these sediments, indicating Miocene, probably Ottnangian (Burdigalian) age and marine or brackish environment (Řeháková 1963, Gabrielová et al. 1964). Since paleontological findings are rather diverse, we approach this unit as a lithostratigraphic marker of paleosurface rather than sedimentary formation with uniform deposition age. Its lithology, however, is characteristic and we used its relics near Zliv and Hluboká as a local marker for the assessment of the slip on the Hluboká Fault.

The most extensive period of Tertiary sedimentation started in Karpathian (Upper Burdigalian (e.g. Čtyroký and Fejfar 1962, Řeháková 1963). Fluvial and fluvio-lacustrine sediments of the **Mydlovary Formation** were deposited over an area which largely extended that of the Klikov Fm. and which defines the present-day extent of the basins. The main centres of early deposition were linear, striking in NW-SE and NNW-SSE directions (Pištín depression in the Budějovice Basin, Soběslav and Šalmanovice depressions in Třeboň Basin). The lithology of the sediments seems to have been controlled by the relative elevation of the region to Paratethys and varied from clayey sands and clays to lignites and diatomites. Mainly during the deposition of the upper part of the Mydlovary Formation (Lower Badenian, Langhian) periodic ingressions of Paratethys are inferred from variations of diatomic assemblages (e.g. Řeháková 1963) and sediment lithology was dominated by diatomic clays with montmorillonite. The maximum thickness of the Mydlovary Fm. is 80-90 m, in extreme cases 120 m.

After regional uplift the following sedimentation was of local shallow, continental character, depositing lacustrine montmorillonitic clays or diatomic clays of Domanín Fm. (Middle to Upper Badenian, the Třeboň Basin), or gravels (Vrábeč sands to clays and Koroseky sandy gravels, Upper Badenian, southern parts of the Budějovice Basin) and later the fluvio-lacustrine clay-dominated sequence of the Ledenice Formation (Lower Pliocene, SW part of the Třeboň Basin and other local occurences). The main elevation of the Lišov horst was probably taking place after this period, likely causing significant changes in regional hydrography and possibly leading to significant denudation of the basin sediments (mainly in the Budějovice Basin). Since the Middle Pliocene the sediment accumulation was taking place only in fluvial terraces. (in the Vltava valley 2 Pliocene and 6-7 Pleistocene terraces are distinguished, see Chapter 4.2). The extent of Quaternary loesses is limited.

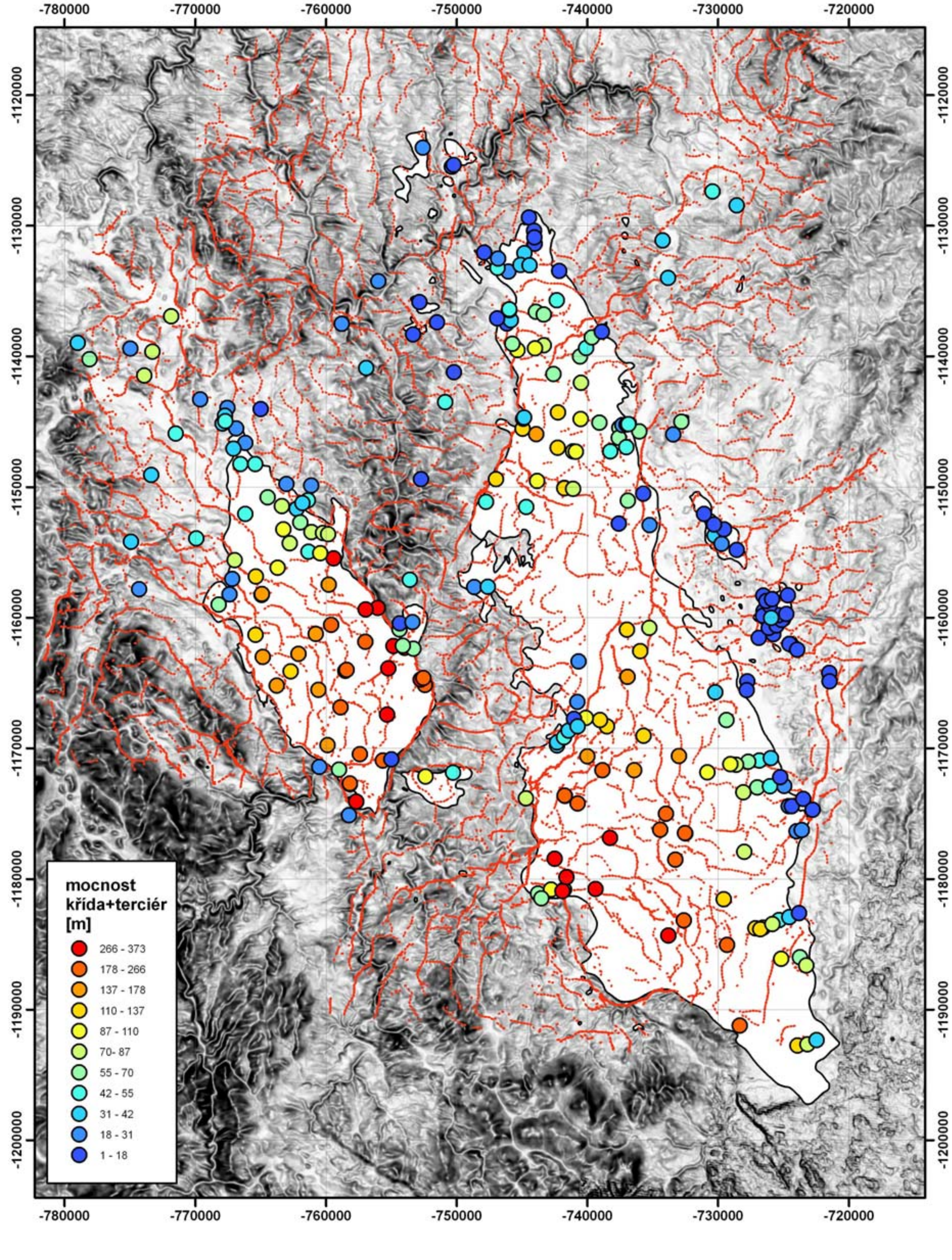

Fig. 2.1-4. Overall cumulative thickness of Cretaceous-Quaternary sediments observed in deeper boreholes over the area of the Budějovice and Třeboň basins (extent of Cretaceous shown in white). Data were compiled from original reports and digital databases of Geofond Prague. Also shown are Linsser indications of density contacts (red lines) derived from gravity field (see Chapters 2.2 and 4.2).

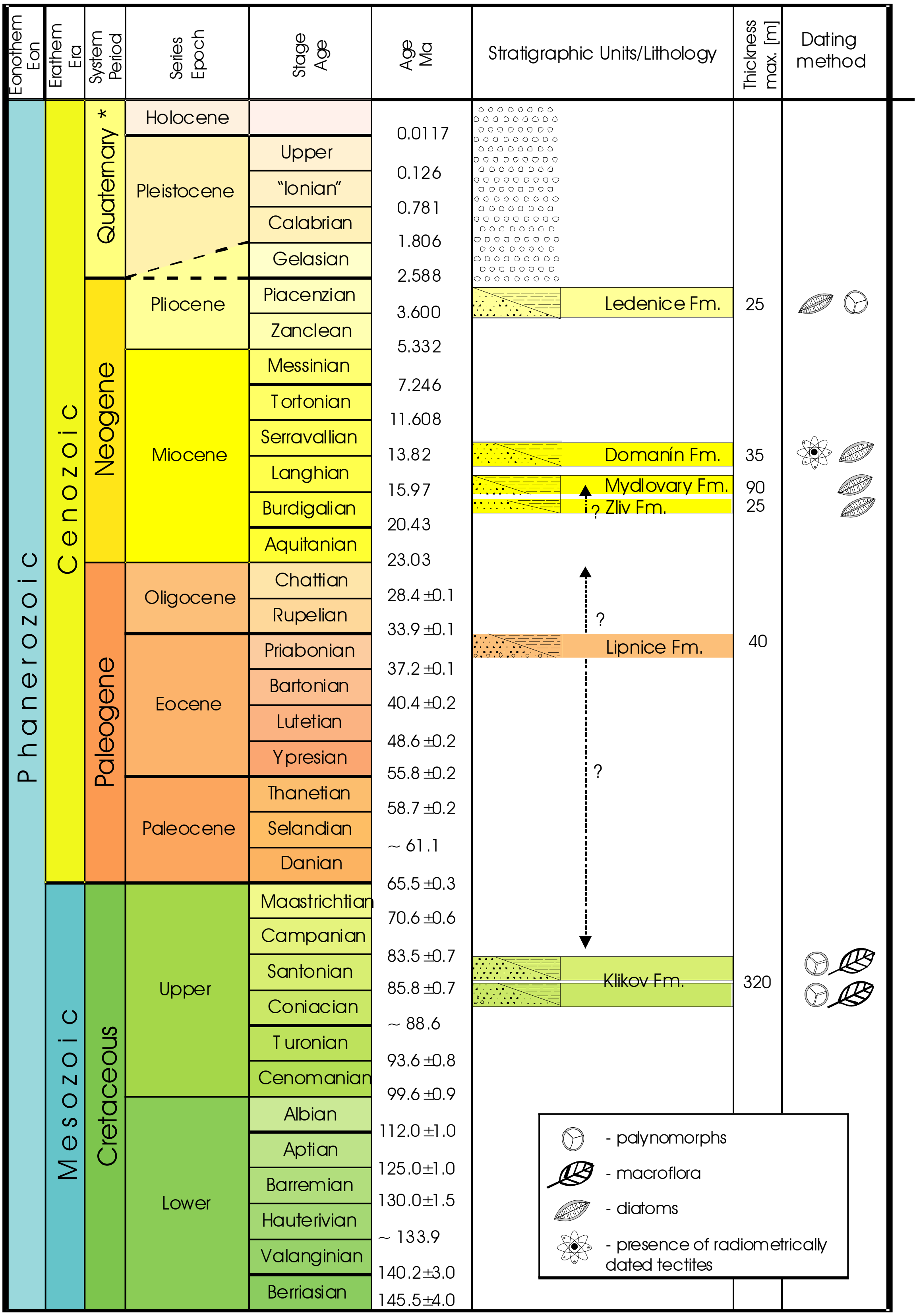

Table 2.1-1. Stratigraphic chart of the sedimentary formations in the South Bohemian basins. Compiled from numerous original sources.

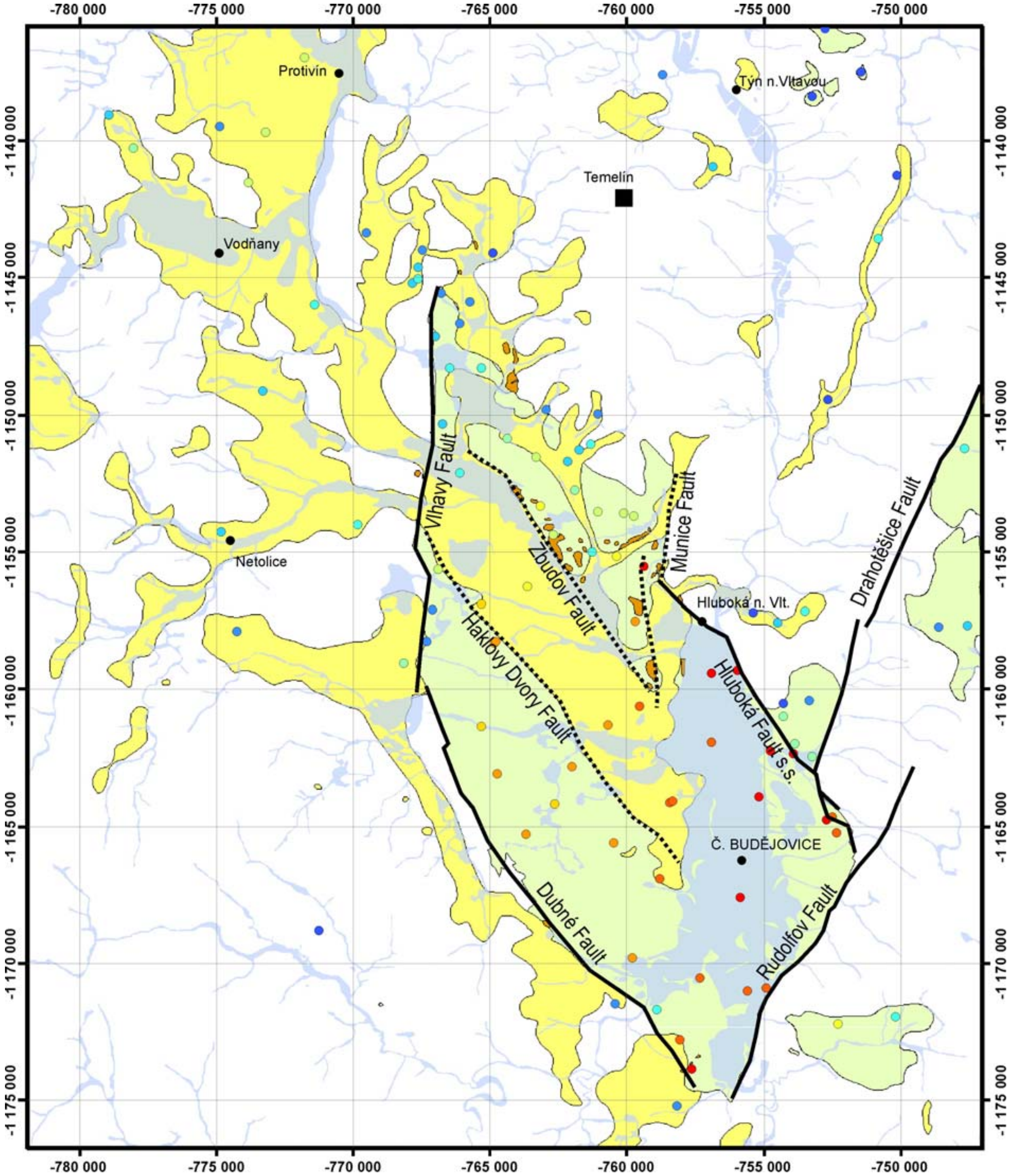

Fig. 2.1-5. Schematic map showing the extent of the main stratigraphic units in the Budějovice Basin and major faults. Green - Klikov Fm., Cretaceous, orange - Zliv Fm., Miocene, yellow - Mydlovary Fm., Miocene, Blue - Quaternary fluvial sediments. Cumulative thickness of sediments observed in boreholes is shown by coloured circles (red - deep, blue - shallow). S-JTSK system with 5 km grid.

2.2 GRAVITY FIELD OF THE BUDĚJOVICE BASIN AREA

Gravity field was used to give additional information on the structure of the basin and the older units beneath and adjacent to it. This information was used to complement the geological observations and data from boreholes, which are given in more detail in Chapter 4 for each area studied.

The maps of Bouguer gravity anomalies were derived using point measurements from detailed gravity mapping with average density of 4-6 points per square kilometre (Geofyzika Brno, Kadlec et al., 1975). In the area of Hluboká Fault, between Hrdějovice and Dubičné the gravity field was refined using detailed mapping with 28 measurement points per square kilometre (Sedlák et al., 2009). Bouguer gravity anomalies were calculated using the S-Gr95 system and a reduction density of 2.67 g/cm^3 (Švancara, 2004). These data were interpolated into regular 250×250 m grid and regional and residual gravity maps were derived using wavelength filtering. The regional gravity map (Fig. 2.2-1) was derived as an analytical continuation of gravity field into the height of 1000 m of the upper half-space. The residual gravity map (Fig. 2.2-2) was calculated as a difference between Bouguer anomaly and regional gravity. Zero isolines in the residual gravity map can be viewed as the boundaries between the density anomalies. Linsser filtering was used to constrain the location of contacts between lithological bodies at shallow depths of 250 m (Linsser, 1967; Šefara, 1973). Linsser indications are shown in Fig. 2.2-2 as rectangular symbols oriented parallel to isolines of gravity field, with stroke pointing towards higher density domain. The area of each symbol is proportional to the product of the density difference and height of vertical step in the modelled contact (see Chapter 4.2.2.1 for details on this method).

Regional gravity field

In the regional gravity map (Fig. 2.2-1) the most dominant positive anomaly correlates with mafic and ultramafic rocks associated with the granulite body of Blanský les. The NE part of this anomaly is located in the Budějovice Basin (area of Čejkovice, Dasný, Zavadily and Kaliště u Lipí) and fully supresses the gravity effect of the basin. Another, less pronounced positive anomaly to the east of the basin correlates with the Lišov granulite body, which is again associated with mafic (amphibolites) and supposed ultramafic rocks (pyroxenites).

From the NW a large negative anomaly extends to the basin between Vodňany and Hluboká. The regional component of this anomaly is explained as due to the hypothetical Putim batholith (Tomek 1974), which is supposed to exist in shallow depths between Vodňany, Písek and Strakonice. The effect of shallow sediment deposits of the Mydlovary Fm., which are abundant in the NW part of the basin, is assumed to be of minor importance. The SE part of this anomaly near Munice as well as the negative anomaly near České Budějovice and Kamenný Újezd correlate with the deep part of the basin. These features are well defined in the residual gravity field and are described below.

Other negative anomalies in the regional field are associated with low-density granites and granodiorites. The NNE-SSW oriented anomaly near Ševětín correlating with the position of Ševětín granodiorite is parallel to the Drahotěšice Fault. The strong anomaly in the SE is supposed to be due to the granitoids of the Central Bohemian Pluton.

Residual gravity field

The residual gravity map (Fig. 2.2-2) is most suitable for correlation with lithological bondaries on geological maps. In the first approximation it can be expected that rocks with natural densities below 2.67 g/cm³ (sedimentary rocks, granites and some granodiorites, felsic granulites) are associated with negative residual anomalies, while the rocks with higher densities (amphibolites, ultramafic rocks, mafic granulites) will produce positive anomalies.

Assuming a homogeneous crust beneath the sedimentary basin, its low density fill (2.2-2.3 g/cm³ for sediments of the Klikov Fm.) would be expected to result in clear, well defined negative gravity anomaly with the amplitude proportional to the sediment thickness. In reality, however, the situation in the Budějovice Basin is complicated by the heterogeneity of the crystalline units beneath the basin. This is well seen in the SW part of the basin, between Dasný, Homole and Břehov where the negative effect of 130-270 m thick sedimentary sequence is suppressed by positive anomaly of the Blanský les granulite body. A satisfying correlation is observed in the deepest parts of the basin adjacent to the Hluboká and Rudolfov Faults, where boreholes indicate thickness exceeding 300 m. The N-S striking negative anomaly between Vráto and Kamenný Újezd and the NW-SE striking negative anomaly between Vráto and Munice are in accordance with similar sediment thickness in the two elongated structures indicated by boreholes (300-340 m). Small-scale (tens of meters) variation in basin floor topography is suggested by several local minima along the Rudolfov Fault and larger minimum between České Budějovice and Nemanice. Some effect of low-density lithologies posibly associated with NNE-SSW striking Rudolfov-Drahotěšice Fault system can not be ruled out. The pronounced local gravity minimum near Kamenný Újezd (-2.75 mGal) can be explained as due to the combined effect of large sediment thickness and low-density granulites (Krasejovka body). The origin of similar local negative anomaly near Munice (-2.5 mGal) is not clear, but it is assumed to be due to local increase of sediment thickness, possibly associated with subsided block at the crossing of the Hluboká and Munice Faults.

The small sedimetary relic near Nová Ves (thickness 100 m) situated at the Lišov horst correlates well with local negative anomaly (1.0 mGal)

The Permo-Carbonidferous basin relic (the Lhotice basin) is not pronounced in the gravity field. The negative anomaly near Lhotice is more probably due to the effect of low-density granitoids beneath the basin. The density of these sediments (2.5 g/cm³ for arcoses with 10-15 vol% porosity and possibly higher for siltstones) is apparently too close to that of crystaline rocks in the area.

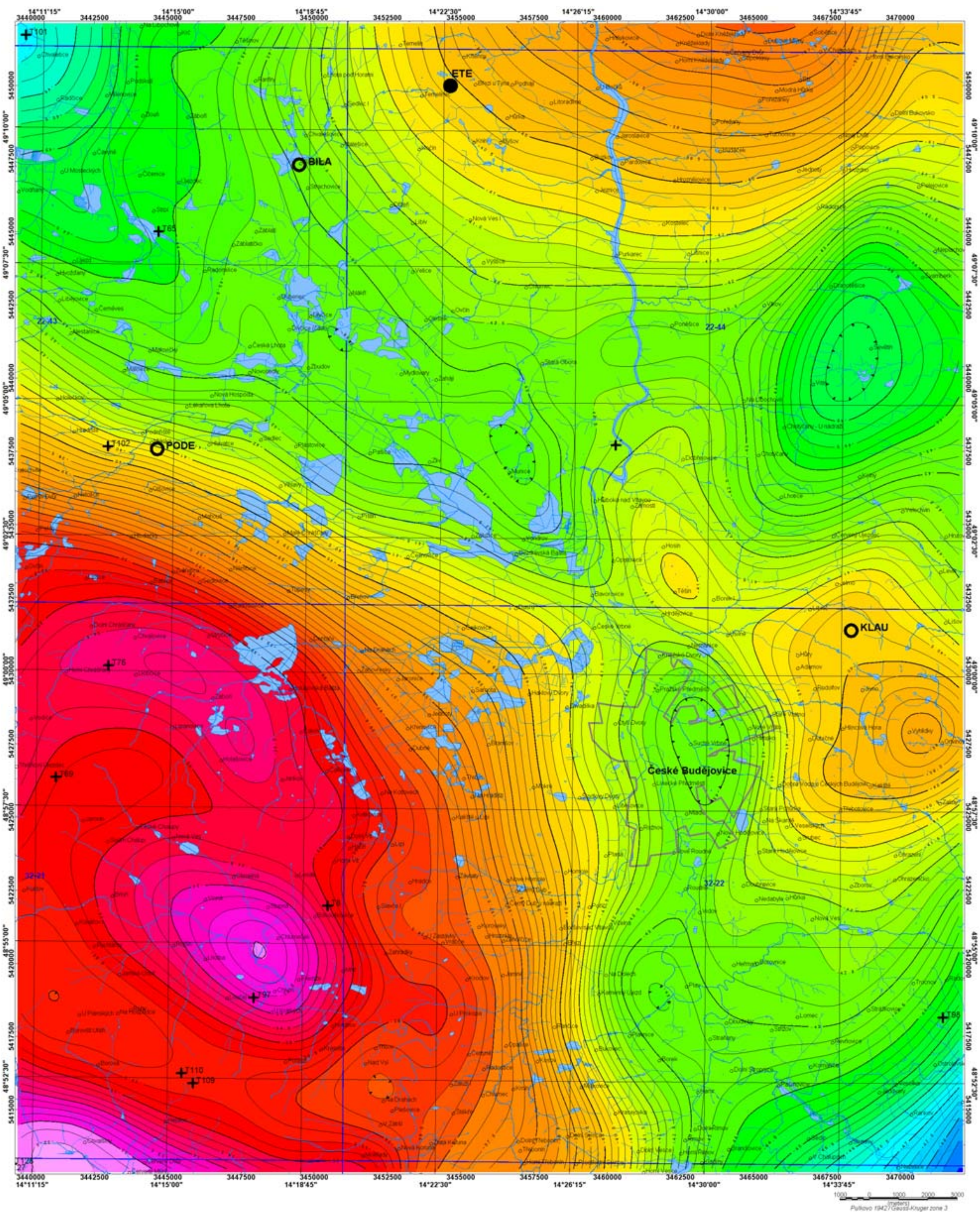

Fig. 2.2-1: Regional gravity field map of the Budějovice Basin and adjacent areas. Contour interval 0.25 mGal.

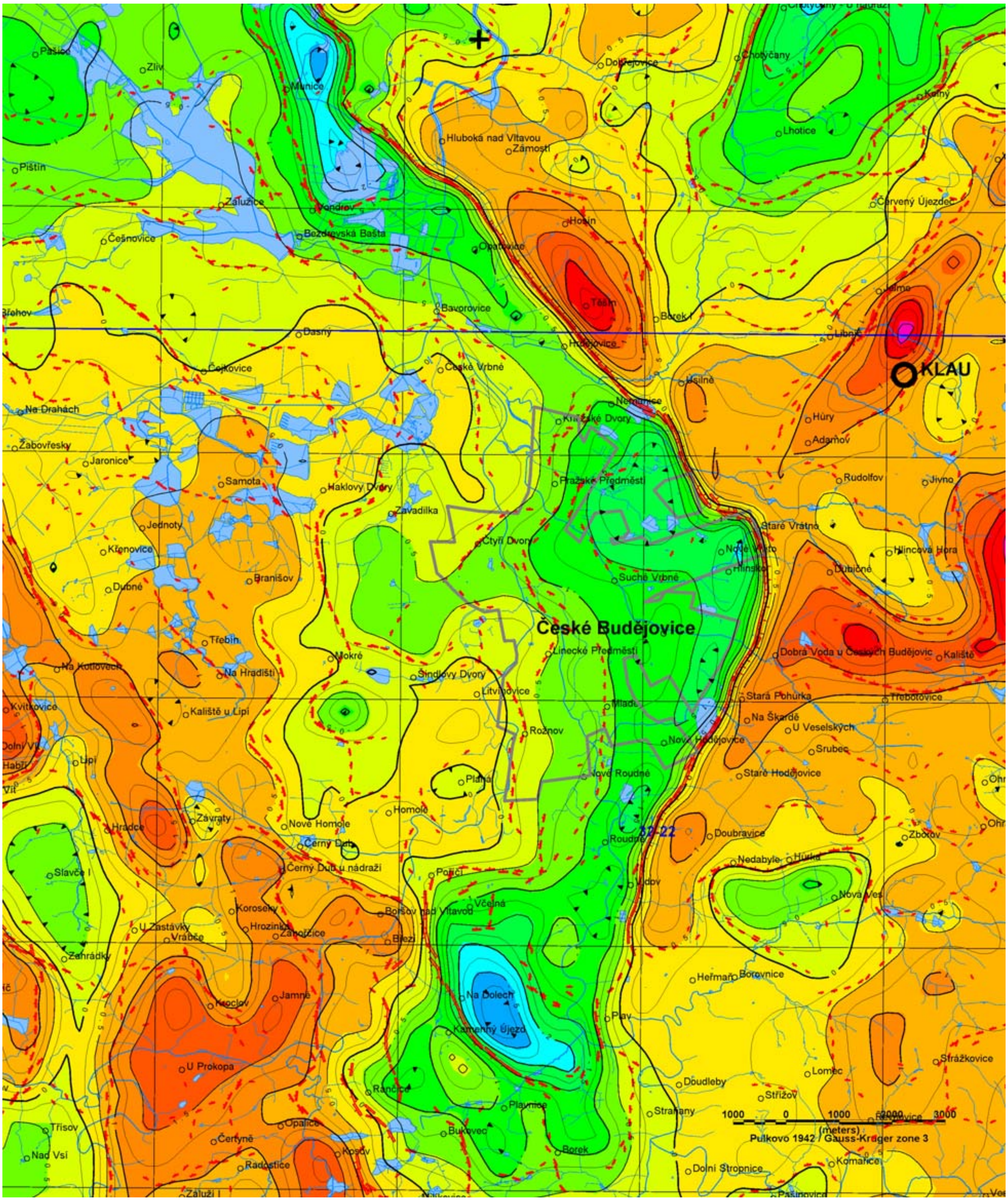

Fig. 2.2-2: Residual gravity field map of the eastern Budějovice Basin and adjacent areas. Contour interval 0.25 mGal. Also plotted are Linsser density contact indications (red symbols) calculated for 250 m depth.

3

REGIONAL AND LOCAL SEISMIC ACTIVITY

3. REGIONAL AND LOCAL SEISMIC ACTIVITY

3.1 MACROSEISMIC OBSERVATIONS

Local macroseismic effects are often observed for earthquakes with magnitudes 2-3 and higher, in some exceptional cases even lower than 2. The detection limits depend on many factors, e.g. hypocentre depth, time of origin (day vs. night), local geological conditions, density of population etc. The first instrumental data have been recorded since the early 20th century and their small number and low sensitivity in most cases did not allow to record weak seismic events until the period of approximately last four decades. For Temelín area the first instrumental records of seismic events date back to 1970s. For older periods historical macroseismic observations are the main source of data on seismic activity at higher magnitude range, since paleoseismological data from geological record are difficult to acquire and are generally limited to magnitudes larger than 6.

By far the most important factor limiting our knowledge on historical seismicity is the incompleteness of written historical record. In Central Europe the oldest written texts preserved come from the 9th and 10th centuries. The old text records - chronicles, diaries, mail correspondence, articles in newspapers and scientific journals usually report only such earthquakes which had strong effects and caused some material damage or which were exceptional in some other way. The first written records of earthquakes available for our region date back to the first half of second millenium when the population density was still very low, and these are limited to the strongest events only. Towards the younger periods the number of records and their completeness increase continually. However, many of the written historical texts were destroyed deliberately or by accident and, conversely, it can be expected that some information yet undiscovered is still in the archives.

The first catalogues of historical earthquakes in the Czech Republic were compiled in 1920s (Koláček 1921, Michal 1928). Later, Macroseismic Archive was founded by Emanuel Michal (Geophysical Inst. ASCR, Prague), data compilation became more systematic and two key catalogues aiming to give complete lists of all available reports were published: „Erdbebenkatalog der Tschechoslowakei bis zum Jahre 1956“ (Kárník et al., 1957) and „Catalogue of earthquakes for the territory of Czechoslovakia for the period 1957-1980“ (Kárník et al., 1981).

These two works served as a basis for our revised catalogue of historical earthquakes in the South Bohemian region which can be used in future for seismic hazard reassessment. We performed a revision of all original sources, older catalogues and hand-written notes from the Macroseismic Archive available for the events with epicentres within 0-70 km distance from Temelín. Numerous mistakes, incorrect locations and misinterpretations were discovered and eliminated. These included several misinterpretations of local effects of distant earthquakes and sound effects of storms and bolides as to be due the local earthquakes. The list of data sources is given in Appendix 3.

The revised catalogue comprises only 33 items, but some of these earthquakes were described as groups of up to 70 individual events (Tab. 3.1-1, Fig. 3.1-1). The oldest events from 16th and 17th centuries are of unclear origin and remain without closer location. The list should not be taken as final, since it is likely that some reports on earthquakes were lost or not found. It is also necessary to stress that the location of events can have large errors.

Y	M	D	Time	Lat.	Long.	Z	M_I (n)	M_I (1km)	M_L	I_0	Locality	State	Source	Q	S	E
1591	4	29								5,0	České Budějovice	CZ	KMM	0		25
1592	6	10								5,0	České Budějovice	CZ	KMM	0		25
1592	12	15								5,0	České Budějovice	CZ	KMM	0		25
1593	4	29								5,0	České Budějovice	CZ	KMM	0		25
1662	3	20								4,0	Žimutice?	CZ	revised	0		35
1796	2	6		48,79	14,78		2,6	1,8		3,0	Nové Hrady	CZ	KMM	0		53
1818	5	28	23	48,64	14,34	-	3,4	2,6		4,5	Vyšší Brod	CZ	revised	1		60
1856	1	26	19:45	48,94	15,02	-	3,7	2,9		5,0	Litschau, Josephstal	A	ZAMG	1	31, 5 y.	54
1860	9	28	20:45	49,01	14,92	-	3,4	2,6		4,5	Stráž n. Nežárkou	CZ	revised	1	4, 3 d.	44
1877	12	8	3:00	49,00	14,77	-	3,1	2,3		4,0	Třeboň	CZ	KMM	1		35
1880	2	1	20:15	48,88	14,18	-	3,1	2,3		4,0	Chvalšiny	CZ	revised	1		36
1893	3	17	8:45	48,70	13,80	-	2,6	1,8		3,0	Breitenberg	D	revised	1		68
1893	3	17	9:25	48,70	13,80	-	2,6	1,8		3,0	Breitenberg	D	revised	1		68
1897	1	5	6:45	48,85	13,60	-	4,0	3,2		5,5	Grafenau	D	revised	1	4, 4 d.	68
1897	11	26	8:39	48,75	14,00	-	2,9	2,1		3,5	Zvonková	CZ	revised	1		55
1897	11	26	8:50	48,75	14,00	-	2,9	2,1		3,5	Zvonková	CZ	revised	1		55
1897	11	29	3:45	48,67	13,91	3	1,9	2,3		4,0	Ulrichsberg	A	ZAMG	1		66
1900	2	11	23:20	48,86	14,20	-	3,5	2,6		4,5	Chvalšiny	CZ	KMM	1		38
1905	9	9	2:25	48,68	13,91	3	1,2	1,8		3,0	Ulrichsberg	A	ZAMG	1		65
1909	9	9	3	49,02	13,73	-	3,1	2,3		4,0	Lipka u Vimperka	CZ	revised	1	4, 3 d.	50
1909	10	20	10	49,11	14,08	-	3,1	2,3		4,0	Bavorov	CZ	KMM	0		23
1910	5	20	6	48,98	14,50	-	3,1	2,3		4,0	České Budějovice	CZ	KMM	0		24
1914	3	14	10:20	48,66	13,87	3	1,6	2,1		3,5	Julbach	A	ZAMG	1		69
1925	1	20	18:40	49,05	15,08	-	3,2	2,3		4,0	Kunějov	CZ	KMM	1	70, 11 m.	53
1932	12	23	11:07	48,93	15,24	4	2,3	2,6		4,5	Kautzen	A	ZAMG	1	5, 2 w.	69
1973	8	6	11:00	48,90	13,80	-	3,2	2,3		4,0	Lenora	CZ	KPB	1		52
1980	5	13	20:30	48,87	15,12	3	3,4	2,6	1,7	4,5	Heidenreichstein	A	ZAMG	1		64
1988	6	30	11:12	48,62	14,03	2	1,4	2,3		4,0	St.Oswald	A	ZAMG	1		67
2000	2	10	18:37	49,57	14,19	4	2,6	1,8	1,4	3,0	Orlík	CZ	revised	1		45
2002	12	2	9:36	48,73	15,01	0	3,7	2,9	1,7	5,0	Waldenstein	A	revised	1		68
2007	1	13	8:30	49,56	14,19	9	3,2	2,3	2,3	4,0	Orlík	CZ	revised	1		44
2009	5	5	16:54	48,78	14,03	3	2,6	1,8	1,8	3,0	Horní Planá	CZ	revised	1		51
2009	5	6	22:45	48,78	14,03	1	2,6	1,8	1,8	3,0	Horní Planá	CZ	revised	1		51

Table 3.1-2. Catalogue of macroseismically observed earthquakes with epicentral distance of 0-70 km from Temelín. See Fig. 3.1-1 for a map.

Items and abbreviations used in catalogue:

Y, M, D – year, month and day of origin
Time – time of observation, UTC
Lat. – latitude in °N
Long. – longitude in °E
Z – hypocentral depth in km
M_I (n) – macroseismic magnitude calculated from epicentral intensity I_0 for unknown hypocentral depth (catalogues KMM, KPB and revised data) or adopted from Austrian catalogue
M_I (1 km) – macroseismic magnitude calculated from epicentral intensity I_0 for hypocentral depth 1 km
M_L – local magnitude
I_0 – epicentral intensity in MSK scale
State: CZ - Czech Republic, A – Austria, D - Germany
Source - KMM – Kárník et al. (1957); KPB – Kárník et al. (1981); ZAMG – Austrian catalogue, Lenhardt et al. (2007) and Lenhardt and Hammerl (2010); revised – events revised in current work
Q – relative credibility: 0 – low credibility, 1 – credible location and intensity
S – number of events and duration of earthquake series
E – epicentral distance fro ETE in km

The macroseismic intensity of earthquakes (I_0) is given in MSK scale. For comparison with instrumentally recorded events the intensity is converted to magnitude using empirical equations given by Kárník et al. (1981):

$M_I = 0.55 \times I_0 + 0.95$ [1]

$M_I = 0.55 \times I_0 + 0.93 \log Z + 0.14$ [2],

where M_I is calculated magnitude and Z is hypocentral depth. The equation [1]1 was used because it does not require hypocentral depth, which is missing for most of historical earthquakes. The conversion introduces large uncertainties, regardles of which equation is used. We performed a simple comparison of magnitudes of 5 events from the last decade (localities Orlík, Waldenstein and Horní Planá) which had macroseismic effects and were also recorded and located by local seismological network (Tab. 3.1-2). The magnitudes calculated from instrumental data and from macroseismic observations using equation [1] and equation [2] for different hypocentral depths, are largely inconsistent. The equation [2] with hypocentral depth of 1 km gives the best fit for all events, independent of depths calculated from instrumental data. We therefore prefer these values as the best approximation, although small number of empirical relations observed does not allow to make this assumption general. For those events which were adopted from Austrian catalogues original values of M_I or M_L are given.

Date	Locality	I_0	M_L	M_I (n)	M_I (1 km)	M_I (2 km)	M_I (5 km)	M_I (10 km)
2.10.2000	Orlík	3	1,4	2,5	1,8	2,1	2,4	2,7
2.12.2002	Waldenstein	5	1,7	3,7	2,9	3,2	3,5	3,8
13.1.2007	Orlík	4	2,3	3,1	2,3	2,6	3,0	3,3
5.5.2009	Horní Planá	3	1,8	2,5	1,8	2,1	2,4	2,7
6.5.2009	Horní Planá	3	1,8	2,5	1,8	2,1	2,4	2,7

Table 3.1-1. Comparison of local and macroseismic magnitudes calculated for events observed both instrumentally and macroseismically. I_0 – epicentral intensity, M_L – local magnitude (based on instrumental record), M_I – macroseismic magnitude calculated from epicentral intensity for different hypocentral depths (n - unknkown depth, see text for details).

It can be concluded from the revised catalogue that credible earthquakes with macroseismic effects were observed only since the 19th century. Their epicentres are mainly located in Šumava Mts. and its foothills, roughly in the area Jindřichův Hradec – Nová Bystřice – České Velenice – Třeboň. The epicentral intensities typically range between 3 and 4° MSK. The strongest event with I_0 = 5.5° MSK near Grafenau (1897, Germany) is located in a distance of 68 km from Temelín NPP. Some events seem to be isolated while other repeat at similar positions with various periodicity (3 days to 5 years) and number of events (4-70). Some events were accompanied by acoustic effects (blow, hum, rumble).

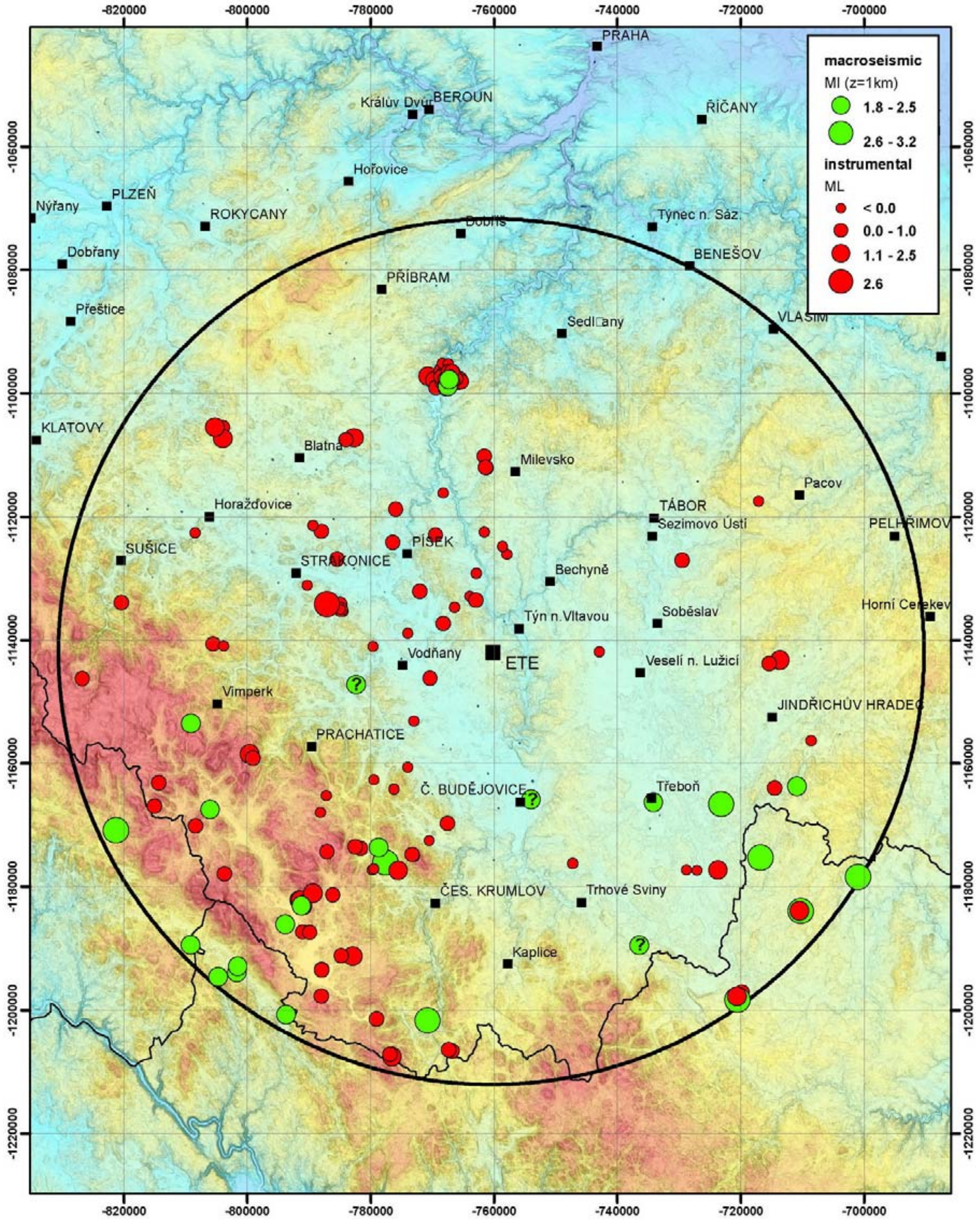

Fig. 3.1-1. Epicentre map of seismic events in the region of Southern Bohemia. Events with epicentral distance of 0-70 km from Temelín („ETE“) are plotted. Green circles - events from macroseismic catalogue, symbol size proportional to M_I (1 km); red circles - instrumentally located events from period 1993-2009, symbol size proportional to M_L.

3.2 INSTRUMENTAL OBSERVATIONS

3.2.1 Seismological networks

In broader region the first stations with digital seismometers were installed in 1970s, e.g. KHC (Kašpersské Hory) in 1973 or MOA (Molln, Austria) in 1976. Due to their small number as well as inconvenient position, these stations did not contribute significantly to the monitoring of weak seismic activity in region of our interest. To date, only 4 events with epicentres possibly lying within 70 km from Temelín were identified on these records (Tab. 3.2-1). Their locations were adopted from bulletins of Geophysical Institute ASCR (www.ig.cas.cz/cz/seismicka-sluzba/seismicke-bulletiny) and catalogue of Austrian Zentralanstalt für Meteorologie und Geodynamik (ZAMG; Lenhardt and Hammerl, 2010). The coordinates and magnitudes given in Tab. 3.2-1 are only approximate.

Date	Time UTC [hh:mm:ss]	Coordinates S-JTSK X [m]	Y [m]	Depth [km]	M_L	Dist. from ETE [km]	Locality	Source
20.08.1978	06:44:22	1181075	789338	0,0	2,5	48,6	Horní Planá	GFU
13.05.1980	20:30:00	1183896	710450	3,0	1,7	64,4	A, Heidenreichstein	ZAMG
29.04.1983	16:59:00	1134215	787071	0,0	2,6	28,4	Strakonice	GFU
27.05.1985	11:28:52	1177420	775472	0,0	2,5	38,3	Chvalšiny	GFU

Table 3.2-1. Earthquakes from within 70 km to Temelín observed instrumentally before 1991.

Since 1991 systematic seismological monitoring of Temelín Nuclear Power Plant has been provided by Institute of Earth Physics, based on safety recommendations of IAEA 2002. The monitoring was launched on 1.9.1991 using a local network of seven digital short-period stations. At the end of the year 1994 (after 3-year monitoring period required by IAEA) the number of stations was reduced to 5. In the period 1995-2005 number of stations and network geometry were changed several times. Based on recommendations of 2003 IAEA mission held in Temelín a profound re-configuration and update of the network was carried out within the research project No. 9/2003 financed by the State Office of Nuclear Safety. Since 2006 till present a new network of five highly sensitive short-period stations is in operation (Nehybka et al. 2006, Hanžlová et al. 2007a). Location and time of operation of individual stations used are given in Table 3.2-2 and Fig. 3.2-1. Details on the results of monitoring are periodically summarized in annual reports to ČEZ a.s. (e.g. Hanžlová et al. 2010). A simplified technical overview of the network configurations is given below:

Local seismological networks 1991 - 2005
- 4 to 7 stations
- three-component Mark L-22 sensors (eigenfrequency 2 Hz; sensitivity 120 V/m/s)
- seismometer Lennartz 5800, sampling rate 125 Hz
- off-line recording in trigger regime, manual data transfer, delayed proccessing (2 weeks)
- manual picking and location processing

Local seismological network 2006 - present *(in testing regime since October 2005)*
- 5 stations
- continuous recording
- VE-53 Geosig sensors (eigenfrequency 1 Hz; sensitivity 1000 V/m/s)
- Reftek DAS 130–01 seismometer, sampling rate 250 Hz
- near real-time radio and internet transmission to sub-centre, fast processing (1 day)
- manual picking and location, complementary automatic picking/location

Station	**Code**	**Coordinates S-JTSK X [m]**	**Y [m]**	**Elevation [m a.s.l.]**	**Dist. from Temelín [km]**	**Period of operation**
Struha	STRU	1145490	758360	443	3,4	01.09.91-31.12.05
Hláska	HLAS	1153470	771380	435	15,9	01.09.91-31.12.05
Bílá Hůrka	BIHU	1144550	765315	429	5,8	01.09.91-14.08.95
Kouba	KOUB	1145885	778745	558	19,1	01.09.91-23.07.01
Helfenburg	HELF	1143520	786302	568	26,5	24.07.01-31.12.05
Paseky	PASE	1132660	764840	479	11,0	01.09.91-31.12.05
Nuzice	NUZI	1133615	751890	409	12,0	01.09.91-30.11.94
U Janečků	JANE	1155465	756515	450	13,4	01.09.91-09.12.92
Jelmo	JELM	1161035	748845	514	21,5	10.12.92-30.11.94 10.06.98-31.12.05
Vrchy	VRCH	1131448	739142	525	23,4	**since 07.10.05**
Doubravka	DOUB	1131487	759409	496	11,0	**since 07.10.05**
Bílá	BILA	1144485	765258	435	5,8	**since 07.10.05**
Podeřiště	PODE	1153522	771311	441	16,0	**since 07.10.05**
Klauda	KLAU	1162714	748592	563	23,1	**since 07.10.05**

Table 3.2-2. Stations used for seismological monitoring near NPP Temelín.

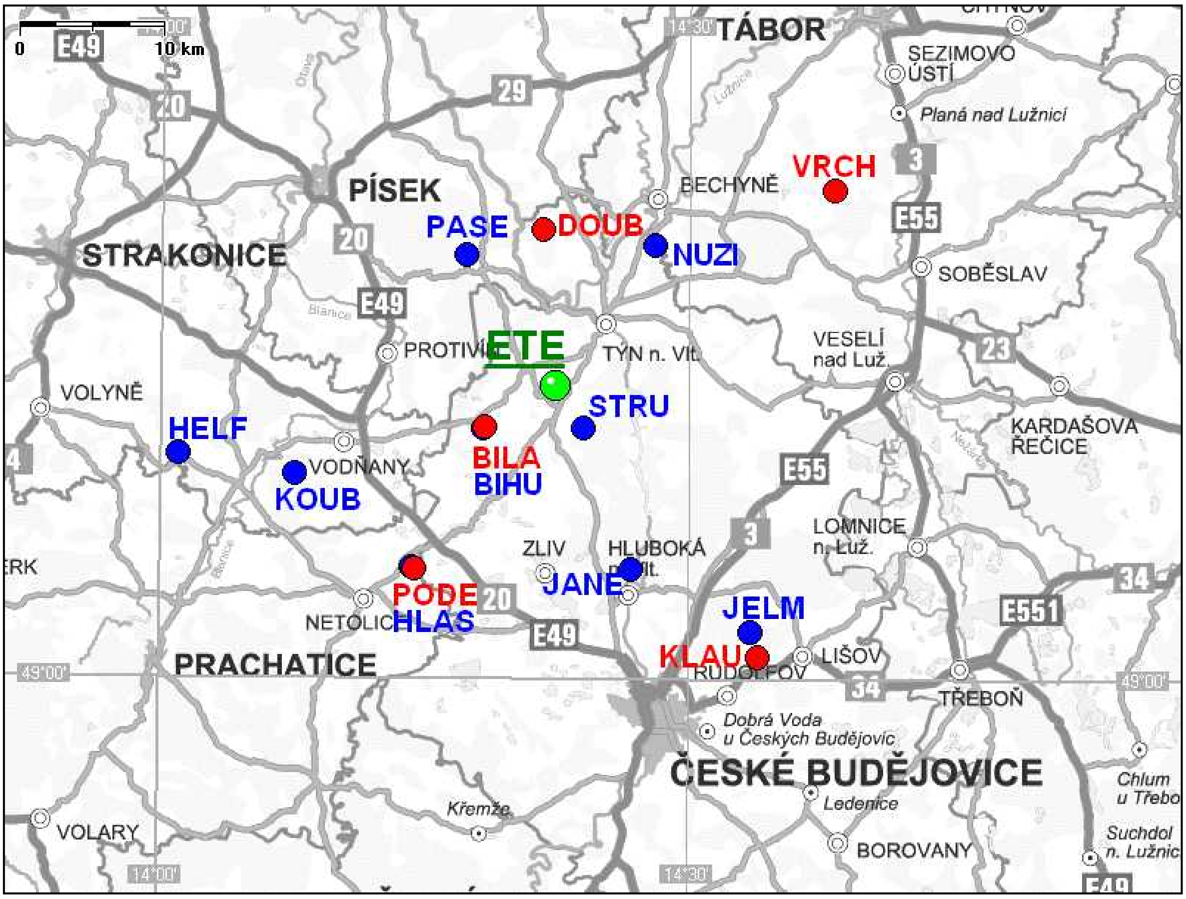

Fig. 3.2-1. Schematic map of stations used for seismological monitoring of NPP Temelín. Blue - stations operationg in the period 1991-2005; red - currently operating stations.

3.2.2 Revised catalogue of local microearthquakes

A thorough revision of all previously recorded events was caried out within current project, with emphasis on events with epicentres within 70 km from Temelín. All events were re-located in a unified way, using some newly acquired data from other stations in the region, which were formerly inaccessible. Elimination of industrial or military blasts was not necessary since this has been already carried out for original catalogues, using databases of quarries and other blasting areas (and personal verifications for some unclear events). Waveform correlations allowed to perform simple master event locations for some multiple events with close epicentres. Based on this post-processing, 15 previously recorded events were newly located and added to the revised catalogue, while those earthquakes with epicentral distances >70 km were discarded. The effects of re-location are relatively small - in 86% located events the epicentre shift was lower than 1km. In total, 133 microearthquakes of tectonic origin was located in the period 1. 9. 1991 - 31. 12. 2009. Table 3.2-3 lists all events with $M_L \geq 0$. All earthquake epicentres are shown in Fig. 3.1-1 together with events from macroseismic catalogue. Table 3.2-4 gives a simple statistical summary of the events in terms of epicentral distance and magnitude.

Table 3.2-3

ID	Date	Time UTC [hh:mm:ss]	Coordinates S-JTSK X [km]	Y [km]	Depth [km]	M_L	Dist. from Temelin [km]	Locality
T1	15.02.93	17:57:10	1135	770	9,3	0,1	9,9	Protivín
T2	**18.02.93**	**11:30:50**	**1105**	**785**	**9,2**	**1,1**	**42,0**	**Myštice**
T3	04.06.93	12:45:33	1100	770	7,8	0,9	45,5	Orlík
T6	29.01.94	23:47:47	1110	785	5,4	0,5	42,5	Myštice
T7	**14.02.94**	**18:21:13**	**1190**	**785**	**0,0**	**1,7**	**54,0**	**Lipno**
T8	06.03.94	03:35:00	1170	770	0,0	0,5	28,4	Křemže
T9	20.04.94	02:21:46	1125	775	4,0	0,0	24,7	Písek
T11	**10.05.95**	**22:24:28**	**1205**	**765**	**2,7**	**1,0**	**64,5**	**Vyšší Brod**
T12	13.05.95	01:02:49	1205	765	0,9	0,6	64,4	Vyšší Brod
T15	11.11.95	05:49:21	1095	770	7,4	0,4	46,4	Orlík
T16	**02.01.96**	**05:05:18**	**1145**	**715**	**4,7**	**2,0**	**46,2**	**Jind. Hradec**
T17	**28.10.96**	**11:15:51**	**1175**	**725**	**15,0**	**1,5**	**50,2**	**Suchdol n. Luž.**
T18	30.10.96	11:52:45	1180	785	8,1	0,7	46,9	Hor. Planá -Otice
T19	30.10.96	21:36:34	1145	715	9,6	0,7	44,5	Jind. Hradec
T20	17.11.96	07:41:29	1180	805	0,0	0,5	56,4	Šumava Plechý
T21	25.01.97	20:40:04	1175	780	0,0	0,8	38,1	Třebovice (VVP)
T22	25.01.97	20:47:23	1175	785	0,0	0,2	38,5	Třebovice (VVP)
T23	20.02.97	12:24:39	1100	765	0,0	0,9	46,3	Orlík
T24	21.03.97	02:20:45	1100	770	0,0	0,2	46,3	Orlík
T25	18.05.97	01:14:54	1120	775	8,3	0,3	28,6	Vráž
T26	**31.07.97**	**17:03:14**	**1210**	**775**	**2,8**	**1,3**	**67,2**	**Vyšší Brod**
T27	04.08.97	00:39:46	1210	775	3,6	0,8	66,9	Vyšší Brod
T36	31.01.99	14:39:06	1200	780	3,3	0,7	62,0	Lipno
T38	24.03.99	20:45:39	1165	715	9,6	0,8	50,2	Nová Bystřice
T39	23.05.99	01:50:13	1140	805	12,8	0,2	45,8	Vacov
T40	19.07.99	00:38:15	1130	790	15,5	0,0	32,5	Strakonice
T42	**16.08.99**	**09:31:50**	**1100**	**770**	**8,2**	**1,2**	**46,5**	**Orlík**
T43	**18.08.99**	**22:01:21**	**1100**	**770**	**12,2**	**1,1**	**44,8**	**Orlík**
T44	**21.09.99**	**14:35:19**	**1100**	**770**	**11,2**	**1,0**	**45,6**	**Orlík**
T46	04.04.00	20:16:43	1100	770	11,3	0,2	44,4	Orlík
T50	27.09.00	21:48:02	1100	770	11,8	0,8	44,0	Orlík
T51	**29.09.00**	**05:00:52**	**1100**	**770**	**2,0**	**1,1**	**46,7**	**Orlík**
T52	**02.10.00**	**18:37:32**	**1100**	**765**	**4,1**	**1,4**	**45,0**	**Orlík**
T53	03.10.00	02:03:47	1100	765	8,9	0,4	44,7	Orlík
T54	06.10.00	03:04:55	1120	790	5,1	0,8	34,6	Radomyšl
T58	28.12.00	17:55:59	1165	815	1,1	0,9	58,4	Strážný
T59	23.01.01	22:29:53	1105	805	9,1	0,4	57,7	Kasejovice

ID	Date	Time UTC [hh:mm:ss]	Coordinates S-JTSK X [km]	Y [km]	Depth [km]	M_L	Dist. from Temelin [km]	Locality
T60	26.09.01	17:58:02	1175	785	4,7	0,7	41,9	Ondřejov (VVP)
T62	27.02.02	19:54:58	1170	810	8,9	0,5	55,9	Strážný
T63	30.05.02	01:21:25	1125	810	3,8	0,0	52,5	Hejná
T64	18.07.02	16:47:08	1135	765	1,8	0,3	9,5	Albrechtice
T64x	**02.12.02**	**09:36:53**	**1200**	**720**	**0,0**	**1,7**	**67,8**	**A, Waldenstein**
T64y	**25.12.02**	**01:43:52**	**1200**	**720**	**0,4**	**1,0**	**67,7**	**A, Waldenstein**
T65	05.05.03	03:14:00	1145	770	8,7	0,3	11,2	Číčenice
T66	24.07.03	15:37:04	1110	760	1,4	0,5	32,3	Chlumek
T70	16.05.04	22:40:25	1190	785	0,0	0,9	54,7	Lipno
T71	27.08.04	22:12:19	1130	770	9,3	0,2	16,0	Protivín
T72	10.09.04	10:40:54	1185	790	4,6	0,2	51,2	Horní Planá
T73	12.09.04	22:24:08	1185	790	4,4	0,0	51,2	Horní Planá
T74	13.09.04	20:27:45	1185	790	5,1	0,4	51,1	Horní Planá
T75	11.02.05	11:43:24	1125	785	13,0	0,4	30,0	Strakonice
T78	21.08.05	18:15:35	1125	730	14,3	0,1	34,0	Planá nad Luž.
T79	24.10.05	17:36:02	1140	745	18,3	0,0	16,9	Veselí nad Luž.
T80	18.11.05	02:36:10	1100	765	6,0	0,3	45,1	Orlík
T81	**14.07.06**	**01:17:01**	**1105**	**805**	**4,0**	**1,3**	**56,4**	**Kasejovice**
T82	**17.09.06**	**15:50:46**	**1100**	**770**	**8,7**	**1,5**	**45,1**	**Orlík**
T82a	17.09.06	15:51:54	1100	770	5,1	0,1	45,8	Orlík
T82b	17.09.06	16:07:35	1095	765	7,3	0,1	46,1	Orlík
T82c	17.09.06	16:12:26	1100	765	4,7	0,1	45,3	Orlík
T82d	17.09.06	19:48:54	1095	770	4,5	0,1	46,2	Orlík
T83	**18.09.06**	**01:18:44**	**1100**	**770**	**7,9**	**1,1**	**45,5**	**Orlík**
T84	09.10.06	00:51:04	1125	770	15,4	0,4	21,7	Písek
T85	**13.01.07**	**08:30:11**	**1100**	**770**	**8,5**	**2,3**	**44,4**	**Orlík**
T86	**24.01.07**	**11:22:00**	**1100**	**765**	**7,2**	**1,3**	**44,8**	**Orlík**
T87	06.02.07	14:36:24	1095	770	7,5	0,6	46,0	Orlík
T88	05.03.07	15:52:54	1095	765	5,4	0,1	46,6	Orlík
T89	**06.04.07**	**11:36:05**	**1105**	**805**	**6,0**	**1,0**	**58,6**	**Kasejovice**
T90	17.04.07	03:36:33	1100	770	3,3	0,2	44,4	Orlík
T92	31.05.07	17:43:32	1095	765	0,5	0,1	46,5	Orlík
T94	16.06.07	11:53:09	1175	725	3,7	0,0	47,8	Suchdol n. Luž.
T96	25.06.07	08:10:36	1160	800	4,8	**1,4**	42,9	**Boubín**
T99	28.09.07	21:28:07	1165	815	0,2	0,5	60,5	Strážný
T100	19.10.07	16:04:50	1120	715	14,9	0,0	49,5	Malešín
T103	30.12.07	16:56:49	1140	805	4,0	0,0	44,1	Vacov
T104	19.02.08	00:46:18	1135	785	6,6	0,4	26,5	Cehnice

ID	Date	Time UTC [hh:mm:ss]	Coordinates S-JTSK X [km]	Y [km]	Depth [km]	M_L	Dist. from Temelin [km]	Locality
T106	27.03.08	17:19:20	1200	790	5,5	0,2	62,1	Lipno
T107	24.04.08	02:32:35	1135	785	5,4	0,1	26,2	Cehnice
T110	**19.07.08**	**19:20:45**	**1175**	**775**	**5,7**	**1,0**	**35,0**	**Chvalšiny**
T111	26.07.08	22:28:28	1110	760	4,8	0,2	30,4	Chlumek
T111x	02.08.08	04:49:30	1185	790	14,9	0,0	54,6	Lipno
T112	02.08.08	12:30:34	1195	790	0,0	0,1	58,2	Lipno
T113	02.08.08	17:07:29	1110	760	4,6	0,3	30,5	Chlumek
T114	02.08.08	21:46:07	1195	790	1,5	0,2	58,3	Lipno
T115	16.08.08	07:36:19	1160	800	5,3	0,3	42,6	Boubín
T116	11.11.08	14:24:53	1185	790	4,0	0,3	51,1	Horní Planá
T117	11.11.08	18:37:55	1180	790	4,5	0,8	50,7	Horní Planá
T118	11.11.08	18:46:52	1185	790	3,6	0,9	50,7	Horní Planá
T119	**11.11.08**	**20:23:40**	**1180**	**790**	**1,9**	**1,1**	**50,7**	**Horní Planá**
T120	12.11.08	13:25:24	1185	790	1,9	0,7	51,0	Horní Planá
T123	**25.01.09**	**01:58:23**	**1180**	**790**	**2,2**	**1,0**	**50,8**	**Horní Planá**
T124	25.01.09	03:10:19	1180	790	2,4	0,4	50,6	Horní Planá
T125	25.01.09	04:04:32	1180	790	2,4	0,2	50,6	Horní Planá
T129	**05.05.09**	**16:54:36**	**1185**	**790**	**2,7**	**1,8**	**51,1**	**Horní Planá**
T130	**06.05.09**	**22:45:19**	**1180**	**790**	**1,1**	**1,8**	**50,7**	**Horní Planá**
T131	07.08.09	03:10:20	1100	765	6,0	0,4	44,8	Orlík
T131x	25.08.09	16:54:19	1145	825	5,8	0,4	67,1	Antýgl
T132x	25.09.09	19:46:18	1135	820	1,8	0,1	61,2	Kašperské Hory
T134	05.10.09	10:51:07	1185	790	24,0	0,4	54,0	Lipno
T136	10.11.09	04:32:28	1100	770	3,8	0,4	45,5	Orlík
T137	17.12.09	21:26:28	1095	765	2,3	0,0	46,0	Orlík

*Table 3.2-3. Revised catalogue of tectonic microearthquakes within 70 km from NPP Temelín for period 1. 9. 1991-31. 12. 2009. Only events with $M_L \geq 0$ are listed. Coordinates are rounded to 5 km (precise locations are property of NPP Temelín). Events with epicentral distance <50 km are highlighted by red colour in selected columns. Events with $M_L \geq 1$ are plotted in **bold**.*

magnitude range	*D>50 km*	*D=50-70 km*	total
M_L ≥ 1.0	13	12	**25**
1.0 > M_L ≥ 0.0	48	27	**75**
M_L < 0.0	28	5	**33**
all events	**89**	**44**	**133**

Table 3.2-4. Statistical summary of the events in terms of epicentral distance from Temelín (D) and magnitude (M_L).

3.2.3 Sensitivity of network and completness of catalogue

The sensitivity of the current seismological network was estimated theoretically by (Nehybka et al. 2006) based on the measurements of mean noise level on individual stations. Using a conservative signal/noise ratio of 4 and condition of at least 4 stations registering these authors concluded that within 50 km distance from Temelín the network should be able to locate all shallow (depth ≤10km) earthquakes with magnitude M_L ≥ 1.2. For closer epicentral distances the sensitivity increases rapidly and in its centre the theoretical location threshold is M_L = -0.3. In practice we were able to locate even weaker events and the M_L = 0 events with epicentral distances of >50 km from Temelín are not exceptional in earthquake catalogue.

After 2005 when a new network was launched a significant increase of located events with M_L ≤ 1 can be observed (Fig. 3.2-2). We assume that this is mainly due to higher sensitivity of the current network setting (mainly continuous regime of registration). However, it is also suggested that the unusual earthquake series (localities Orlík and Horní Planá) objectively increased the total number of events in the region.

The magnitude-frequency distributions of the located events (Fig. 3.2-3) suggest that the for for the period 2006 - present the catalogue should be nearly complete down to M_L = 0, at least for epicentral distances <50 km from Temelín. It is suggested that for the period before 2006 the catalogue is nearly complete down to approximately M_L = 0.8.

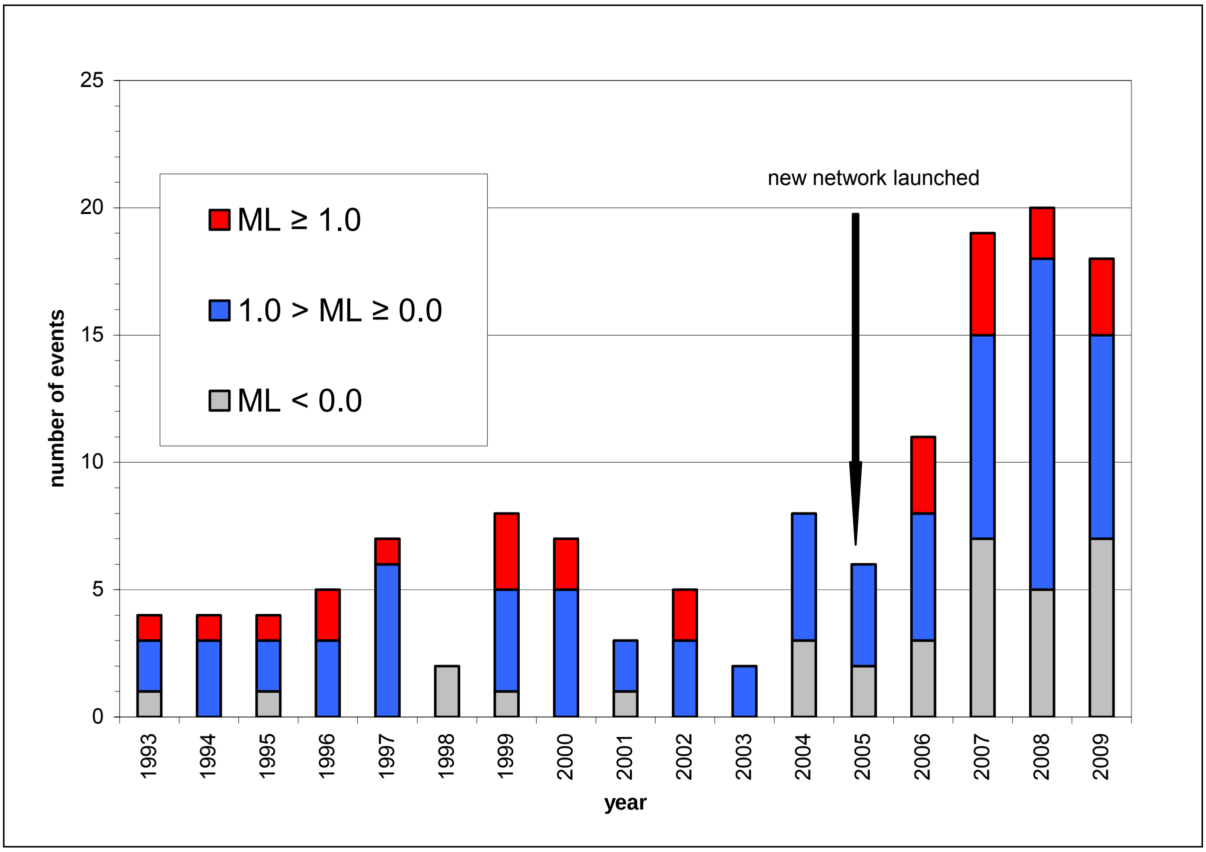

Fig. 3.2-2. Histogram showing the number of events located in individual years in a distance <70 km from Temelín.

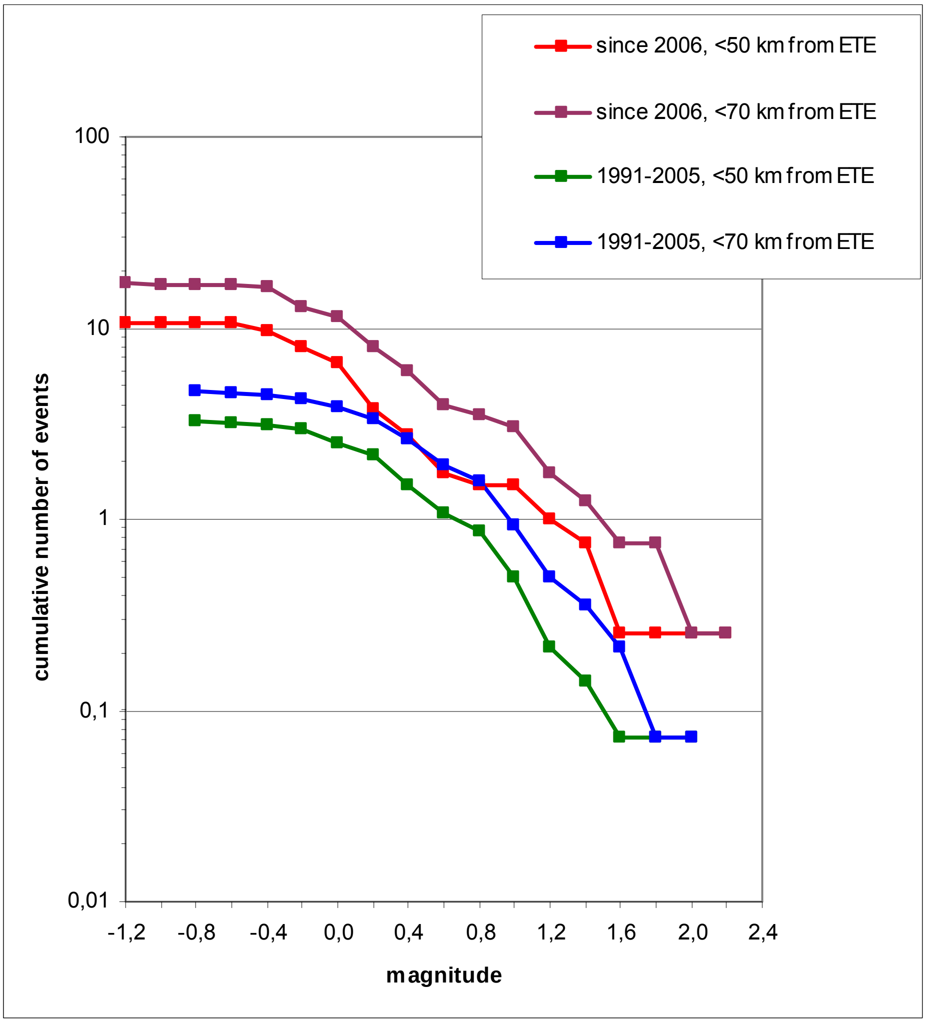

Fig. 3.2-3. Cumulative magnitude-frequency distributions of events calculated for the two periods of instrumental monitoring and two classes of epicentral distances.

3.2.4 Basic features of epicentre distribution

The seismic activity of the region studied is very weak and the possibility to correlate the observed events with geological structures mapped at the surface is largely limited. The spatial distribution of the seismicity is relatively diffuse and to understand the preferrential alignment or clustering of epicentres into well defined geometries requires long times of observations. Even after 20 years of instrumental monitoring large part of microseismic events can be regarded, in the first approximation, as due to more or less accidental relaxation of homogeneously stressed upper crust. Low magnitudes of the events and limited number of seismic stations in the region disallow the calculation of reliable focal mechanisms, which could possibly help to attribute some events to the surface structures. In case of several events with good quality records on 5 or more stations, focal mechanisms were numerically estimated based on polarities and amplitude ratios of direct waves. However, these estimates can have large errors and have to be treated with caution.
On the other hand at least some distribution heterogeneities which could be pre-conditioned by geological structure, are clearly present. Also, some spatial correlation of microseismic and historical macroseismic events can be observed (Fig. 3.1-1), which suggests that this preferrential occurence might have longer-term character. Some features of the most active areas are briefly described below (see Fig. 3.2-4 for geographical reference).

The most distinct group of epicentres is situated near the Orlík dam, approximately 45 km N of NPP Temelín. Here, 32 events have been observed since the early period of instrumental monitoring (1993) and it continues till present-day. Multiple events are characteristic for this locality. Magnitude range is M_L = -0.6 to 2.3 and the stongest event (T85, 2007) had macroseismic effects in several villages near Orlík, having maximum intensity I_0 = 4° MSK (5° EMS-98; Hanžlová et al., 2007b; Zedník and Pazdírková, 2009). Estimated focal mechanism suggests that the event was due to the slip on NNE-SSW or WNW-ESE oriented fault, which are easy-slip orientations for the present-day regional stress field. No historical earthquakes have been reported for this locality. The close spatial focusing of the epicentres to the dam area, suggests that these events could have been possibly partly triggered by an increased hydrostatic pressure in the pre-existing fault near the dam.
Another distinct group of epicentres (17 events) is located near Horní Planá, close to Maňava village, approx. 51 km SW of NPP Temelín. Here multiple events were also observed and the strongest events had macroseismic effects (2009, I_0 = 3° MSK).
Number of other microearthquakes are located in Šumava Mts. (Vyšší Brod, Lipno, Stážný, Boubín) and also several historical earthquakes were reported from this area (see Chapter 3.1). Farther to the N and NE of this area the higher concentration of epicentres is observed in broader environs of Český Krumlov and Prachatice. The event near Chvalšiny (T110, 2008) currently represents the closest instrumentally observed event to NPP Temelín (35 km) in M_L ≥ 1 range. Two historical earthquakes were reported from this area, with maximum intensity I_0 = 4.5° MSC.
Farther to the north a number of weak events sem to be aligned in NNE-SSW direction between Lhenice, Protivín and Albrechtice, partly correlating with the Lhenice and Blanice fault zones. Some of the northern epicentres of this group (T1 with M_L = 0.1 and T64 with M_L = 0.3) are located less than 10 km from NPP Temelín. The focal mechanism estimated for T1 event suggests that it could be associated with a slip on N-S to NNE-SSW striking Blanice

fault zone (Švancara et al. 2010), which has an easy-slip orientation in the present-day regional stress field.
The larger group of epicentres farther to the NW of Temelín is spatially associated with the large negative gravity anomaly which was attributed by Tomek (1974) to the hypothetical Putim granite batholith. No historical earthquakes were reported for this area.
The Budějovice basin is largely aseismic. Only one of the 133 located events (T65, near Čičenice, ESE of Vodňany) has the epicentre in the area of possible continuation of the Hluboká Fault. The estimated focal mechanism is compatible with dextral slip on a steep, NW-SE oriented fault or sinistral slip on steep NE-SW oriented fault.

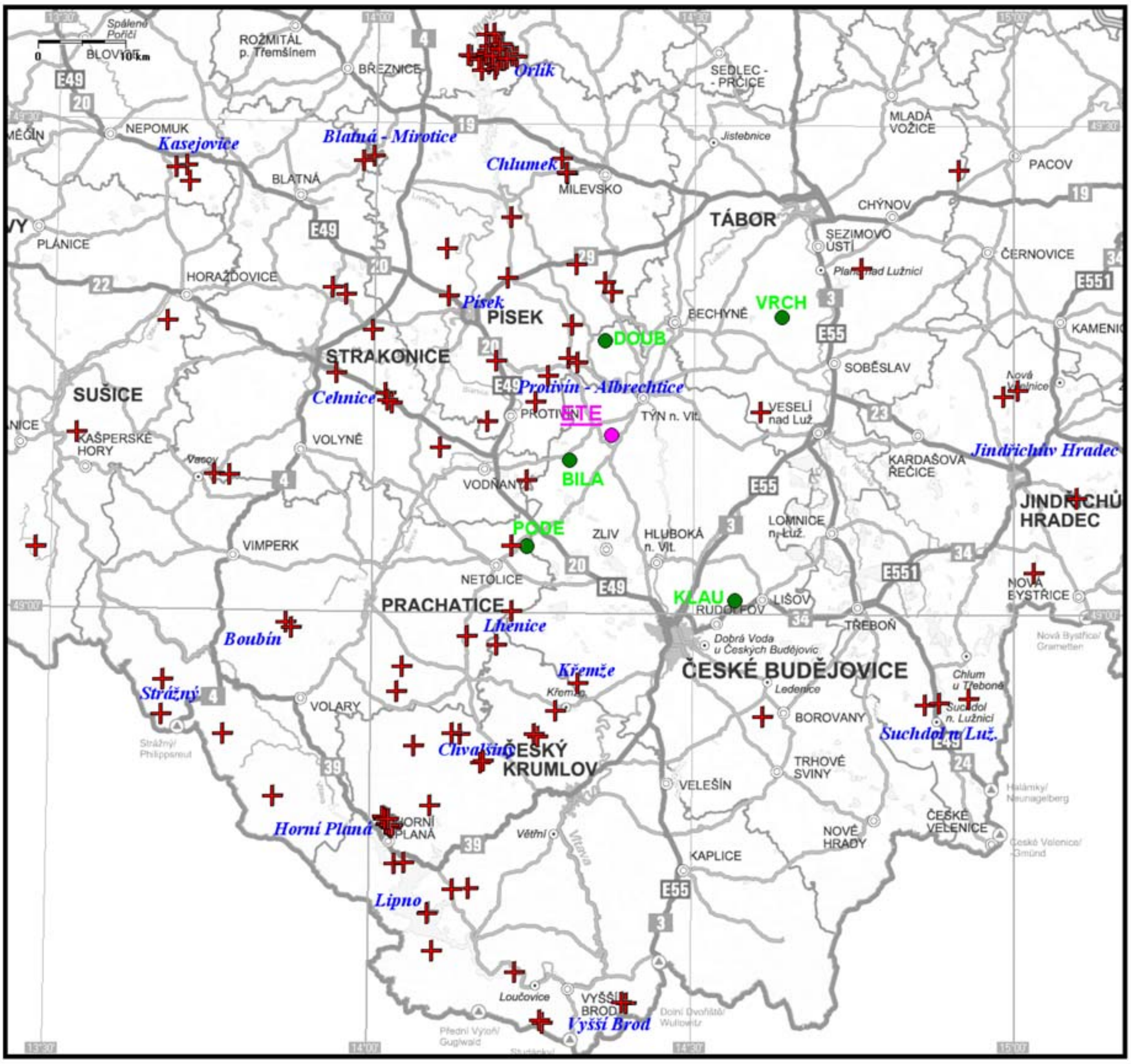

Fig. 3.2-4. Epicentre map of tectonic microearthquakes located instrumentally in a period 1991-2009 (red crosses). Stations of cuurent seismic network are shown by green dots.

4

ASSESSMENT OF QUATERNARY ACTIVITY OF THE HLUBOKÁ FAULT:

METHODS AND OBSERVATIONS

4. ASSESSMENT OF QUATERNARY ACTIVITY OF THE HLUBOKÁ FAULT: METHODS AND OBSERVATIONS

4.1. HLUBOKÁ FAULT

The Hluboká Fault is the NE marginal fault of the Budějovice basin with a pronounced morphology, which makes it the most conspicious fault structure in the area of NPP Temelín. For this reason it has been considered by some geologists an important structure in terms of young tectonic activity with possible continuation to Quaternary. The possible active tectonic slip on the Hluboká Fault and its potential impact on the seismic hazard has been repeatedly discussed on IAAE missions to the NPP Temelín.

The Hluboká fault has been defined by Malecha et al. 1966 as a fault system with generally NW-SE strike at the NE margin of the Budějovice basin. Since then the Hluboká Fault is understood in some works as a relatively long regional structure controlling the whole NE margin of the Budějovice basin, eventually continuing to the Třeboň basin farther to the SE. Such structure can be then termed as „the Hluboká Fault *sensu lato*“. In the light of the present detailed study such a broad definition is not suitable because the NW part of the structure is largely hypothetical and it is not constrained by any distinct expressions. Likewise, the geological mapping fails to clearly trace the fault in the crystalline units of the Lišov horst and its continuation towards the SE is thus purely hypothetical. For this detailed work we need to define the fault basing on the objective morphological, geophysical and geological indicators. Although we accept that the contact between the Cretaceous basin sediments and adjacent crystalline units can be of tectonic origin in most parts of the present-day basin margin, the relatively small sediment thickness in the NW part of the basin suggests the possibility of the locally transgressive margins and the existence of marginal faults can not be proved without other supporting field data.

Taking this into account, we define the **Hluboká Fault *sensu stricto*** (the simple term „Hluboká Fault“ will be used farther in this text) as a quasilinear system of faults closely associated with the main steep margin of the deep part of the Budějovice basin between the villages of Munice and Dubičné. The length of the fault with such definition is approximately 13km (Figs. 4.1-1 and 4.1-2). The term *Hluboká Fault Zone* will be used to describe those faults or hypothetical faults which are adjacent to, but not coincident at the local scale with, the main lithological boundary between Cretaceous sediments and crystalline or Permo-Carboniferous rocks.

In this part of the basin margin the course of the fault is indicated by distinct linear features in the maps of horizontal gravity gradient and in the surface morphology, and its steep dip has been proved by several boreholes. The pronounced linear maximum in the horizontal gravity gradient map can be traced nearly along the whole fault, between the NW part of the Hluboká n. Vltavou town and the Dubičné village. We explain this maximum of gravity gradient as due to the steep fault-related contact between the thick sequence of porous and less dense Cretaceous clastic sediments at the SE wing of the fault, and the denser rocks of crystalline units and consolidated Permian-Carboniferous sediments at the NE wing of the fault.*

The 300-350 m thickness of the Cretaceous sediments has been proved by a number of structural and hydrogeological boreholes, some of which constrain the minimum local dip of the marginal fault to 65-80° (Figs. 4.1-1 and 4.1-2).

In the section Hrdějovice-Úsilné the surface extent of Cretaceous sediments continues above the fault, about 3km farther to the NE. In this promontory the thickness of the sediments is strongly reduced - the maximum thickness verified in the borehole is 75m. The base of the Cretaceous rises up to 490 m a.s.l. at the northern margin of this promontory, which is about 440 m higher than the base of Cretaceous in the deepest part of the basin adjacent to the fault in its SW wing. Similar small extent promontory of shallower Cretaceous sediments behind the main gravity indication of the fault can be observed near the village of Vráto. In this area reduced sediment thickness is also proved in underground mines.

Contrastingly, in the NW part near Munice the continuous gravity indication steps aside from the basin margin into the crystalline units. We believe that here the gravity expression of the Hluboká fault can be weakened and shifted due to the cumulative gravity effects of the structures in the subcropping crystalline units and the overlying low-density Tertiary sediments which cut the original contact between Cretaceous sediments and the crystalline (see the seismic profile Munice, chapters 2.8 and 5.1).

The morphological scarp parallel with the fault is most conspicious in the section Hluboká nad Vltavou - Hrdějovice, and south of the Hosín village it reaches the height of 65m and the slope dip of 15-30° (locally 45°). Within this section the floodplain of the Vltava river adjoins the scarp in the place where the river escapes the basin, overcomes the fault and continues northwards into the upland (Fig. 4.1-1).

In the NW and SE the Hluboká Fault is terminated by steep transverse faults with vertical displacement which results in abrupt reduction of the basin fill thickness. In the SE the system od NNE-SSW faults, called the *Rudolfov Fault* terminates the basin and reduces the thickness from >300 m to 0 m (see the note above on the questionable occurence of Permian beneath the Cretaceous sediments). This fault is a part of a larger system with regional importance associated with the relics of the Blanice Graben with Permian-Carboniferous sedimentary fill. Another fault of this system, the *Drahotěšice Fault*, crosses the Hluboká Fault near Úsilné, forming the eastern termination of the above mentioned promontory of the Cretaceous sediments. In the NW the Hluboká Fault interferes with another fault system, called the *Munice Fault*. The exact trace of this fault is not well constrained but the N-S oriented promontory of the basin with large sediment thickness is associated with this structure and at the surface it seems to be terminated by quasilinear morphological scarp. The thickness of Cretaceous sediments is reduced abruptly from approx. 300 m to <120 m to the west of this fault.

*) The continuation of the Permian-Carboniferous sediments farther to south, beneath the Cretaceous sediments in the NE part of the Budějovice basin is debatable. In some boreholes sediments were found with lithologies different from the typical Cretaceous facies, classified as the Permian-Carboniferous facies aby some geologists (e.g. Woldřich 1893, Malecha at al. 1964). However, the palynological analyses of these sediments in borehole TsV-7 near Vráto (Holub and Kalibová-Kaiserová 1965) indicate the Upper Cretaceous age, which resulted in the distinguishing of separate unit called the Budějovice Formation (Slánská 1967, 1974). Taking into account that the gravity effect of the basin in this area does not indicate any shallowing of the basin relatively to its deep parts with typical lithological developement (in surface occurence the consolidated Permian-Carboniferous rocks do not display any gravity anomaly relative to crystalline rocks), we suppose that these sediments belong to the Cretaceous sedimentary sequence (see also Reininger 1909).

Farther to the NW only very inexpressive and local morphological indications of possible linear fault structures with NW-SE strike are present (the exception is the Olešnice hill) and their co-incidence with pronounced abrupt changes of sediment thickness was not observed. We see no indication for the existence of the faults traceable over longer distances, although their existence can not be ruled out. Similarly, in the SE we can not rule out that some fault segments continue behind the basin margin into the Lišov horst. We do not observe clear expression of the fault, perhaps with the exception of coincidence of a linear creek valley (Dubičný potok) with the geometrical continuation of the local strike of the Hluboká Fault.

The preliminary field survey has shown that the Hluboká Fault does not have a simple planar geometry with perfectly linear surface trace. The structure of the fault zone is complicated and it is composed of several segments with azimuth ranging between 110-160°. Since the re-activation potential of the fault depends primarily on the relative orientation of the fault plane to the stress tensor, we can not rule out the heterochronous activation of various fault segments in the fault zone. Therefore, we subdivide the Hluboká Fault to several segments with different strikes which are studied separately. These segments are further sub-divided to shorter sections based on other geological criteria and this classification is used in the chapters desribing the results of the research:

Segment 1 - Munice Fault - Vltava floodplain, length of 3.8 km, azimuth 120-130°

Section 1A - between the eastern environs of Munice and the western periphery of Hluboká nad Vltavou. Here, the contact of Creatceous sediments with crystalline units is completely buried below the sediments of Tertiary Mydlovary Fm. and its accurate trace is not known. Terrain scarp is less pronounced, having slope of 3-11°. In the area where Tertiary channel running in NE-SW direction from Zámostí crosses the fault, the dip of the slope is less than 1° (Chapter 4.3). Distinct gravity expression of the fault are only observed in the southernmost part of this section, which is probably a result of large thickness of Tertiary sediments covering the basin margin (see above). Seismic profile Munice gives an important indication of the fault position (see Chapters 2.5 and 5.1).

Section 1B - Hluboká nad Vltavou, between its western periphery and the swimming pool in Hluboká-Podskalí. The contact Cretaceous/crystalline is located close to the foot of the morphological scarp (height of ca 50 m, slope up to 25°) and it is covered by colluvia, Quaternary fluvial terraces and anthropogenic sediments (Chapter 4.3).

Section 1C - between the swimming pool in Hluboká-Podskalí and the southern environs of Zámostí. The lithological contact Cretaceous/crystalline is buried beneath the floodplain and older terraces of the Vltava river and its clear gravity indication is offset from the terrain scarp up to 300m to the SW (Chapter 4.4).

Segment 2 - Vltava floodplain - Drahotěšice Fault, length of 5 km, azimuth 140-145°

Section 2A - between the bend of the gravity indication south of Zámostí and the western periphery of Těšín. The contact Cretaceous/crystalline stays offset up to 150 m from the foot of the terrain scarp (height up to 65 m, slope 15-30°, locally up to 45°), and it is covered by fluvial sediments (Vltava floodplain and terraces) and thick colluvia (Chapter 4.5)

Section 2B - between the western periphery of Těšín and the eastern periphery of Nemanice, the area of northward promontory of Cretaceous sediments behind the Hluboká Fault. The fault, here indicated by gravity gradient and boreholes, has no geomorphological expression at the surface and takes its course in the flat area with a relatively continuous mild slope of <2° toward SW or WSW (Chapter 4.6).

Segment 3 - the western zone of intersection with the Drahotěšice Fault, approx. length of 700m, azimuth 110-120°

Between the eastern periphery of Nemanice (the dam area of „Čertík“ pond, also called „Voselný“ pond) and the scarp associated with contact of Cretaceous/Permian south of Úsilné. The gravity indication of the fault is rather diffuse and the geomorphological expression is missing (Chapter 4.7).

Segment 4 - Drahotěšice Fault - Vráto, approx. length of 1.9 km, azimuth 150-160°

Section 4A - between the onset of the scarp on the contact of Cretaceous/Permian (south of Úsilné) and area south of „Červený vrch“ hill (near Světlík farm). The slope of the terrain scarp associated with this segment is 5-8° (Chapter 4.7).

Section 4B - between the eastern environs of the Světlík farm and the western periphery of Vráto. This segment is indicated only by pronounced expression in gravity field. The terrain scarp is missing as Cretaceous sediments extend beyond the fault segment to the NE.

Segment 5 - area of the „Červený vrch“ hill, minimum length of 500m, azimuth 125°

West of Červený vrch hill the verified NW-SE striking fault segment branches off, with unclear continuation to the SE. An exotic block of crystalline rocks was emplaced into Permian-Carboniferous sediments along this fault (Chapter 4.8). This segment has been called the „Reininger Fault“ in the old literature (Reininger 1909). The slope of the associated terrain scarp is up to 9° and to the south of it Cretaceous sediments occur, reaching beyond the gravity indication of the main fault (segments 4b and 6).

Segment 6 - Vráto - Rudolfov Fault, length of 800 m, azimuth 100-110°

In this segment the fault is only indicated in the gravity field which, together with the deep boreholes, proves very steep contact of the pre-Mesozoic consolidated rocks with the Createaceous sediments of the basin.

Segment 7 - zone of interference with the Rudolfov Fault, approx. length of 900 m, azimuth 160°

Both geomorphological and gravity indications prove the position of fault, which is again associated with the surface lithological contact between Cretaceous sediments and crystalline units. The transition of fault structures with prevailing NW-SE strike into the NNE-SSW strike is continuous and distinguishing between the Hluboká and Rudolfov Faults is purely formal in this area.

In addition to the above given segments with unequivocal fault-slip origin, we define an additional hypothetical segment H as a structure whose surface trace corresponds to the foot of the main terrain scarp (azimuth 140-145°) in the proximity of segments 1C and 2A. The purpose of distinguishing this segment is the dissociation of the linear scarp from the margin of the Cretaceous sediments and its geometrical continuation in the strike close to that of the segment 2 (see Chapter 4.4). Theoretically, this structure can continue towards the NW where it could coincide with some less expressive linear scarps in terrain.

In the present work we studied segments 1-4A, 5 and the hypothetical segment H. The segments 4B, 6 and 7 were not studied mainly because no suitable effective methods of research into its structure and Quaternary activity have been available. The results of the research are given in the following chapters in accordance with the above used classification.

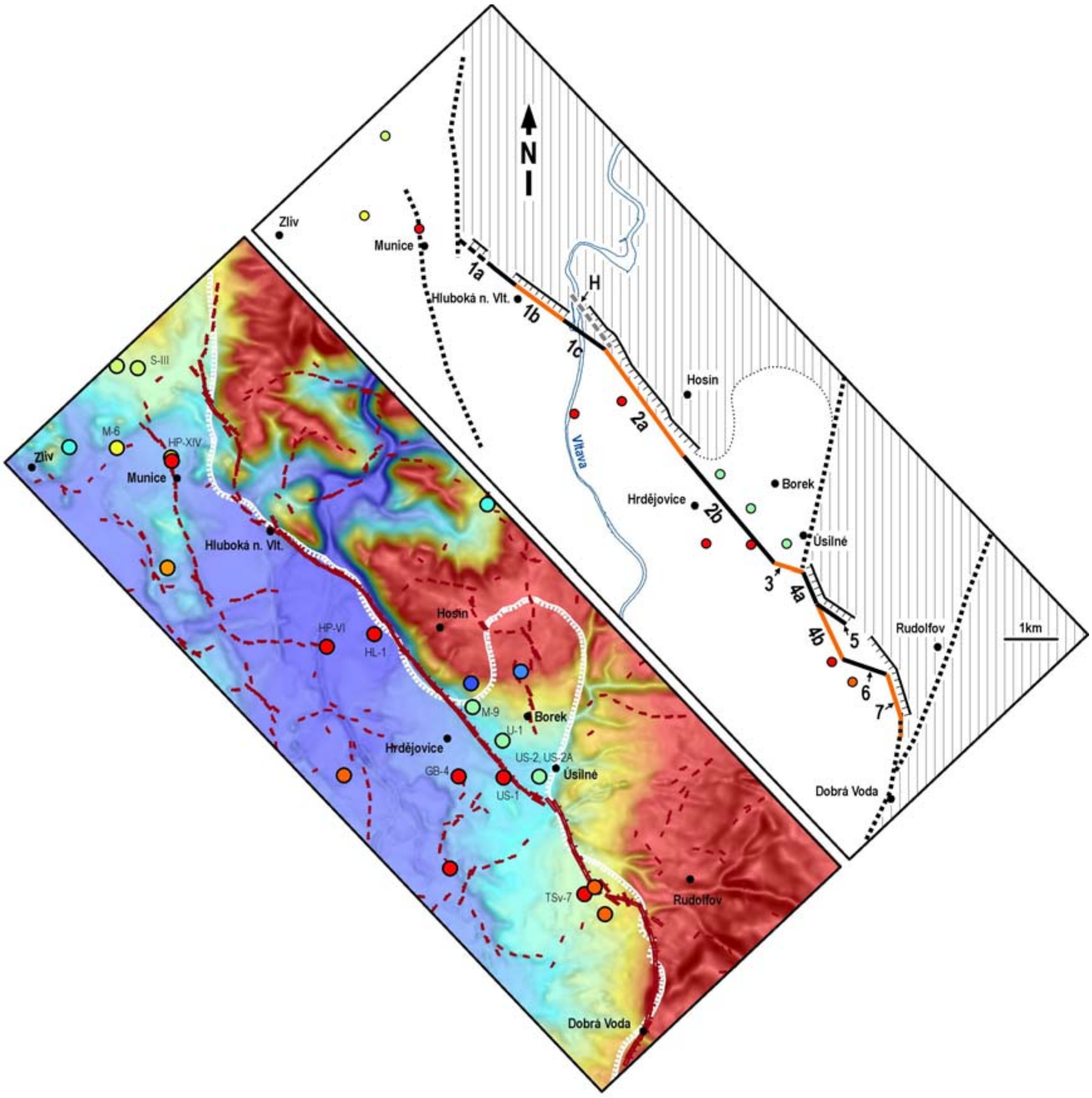

Fig. 4.1-1: Definition of the Hluboká Fault sensu stricto*. Lower-left: map showing the colour-shaded DEM with gravity indications of the faults (Linsser indications, brown symbols), the extent of Cretaceous sediments (composite white line; the dotted side indicating the basinward side), and the position of deep boreholes (circles, colour-coded according to thickness of the post-Permian sediments; red - large, blue - low). Upper-right: schematic map showing the inferred trace of the Hluboká Fault, classification into the segments/sections defined in the text (bold black and orange lines). White and vertically hatched areas show the extent of Cretaceous sediments and the crystalline units not covered by Cretaceous (Tertiary not shown). Distinct terrain scarps shown schematically by barbed lines. Other important faults shown schematically by bold dotted lines.*

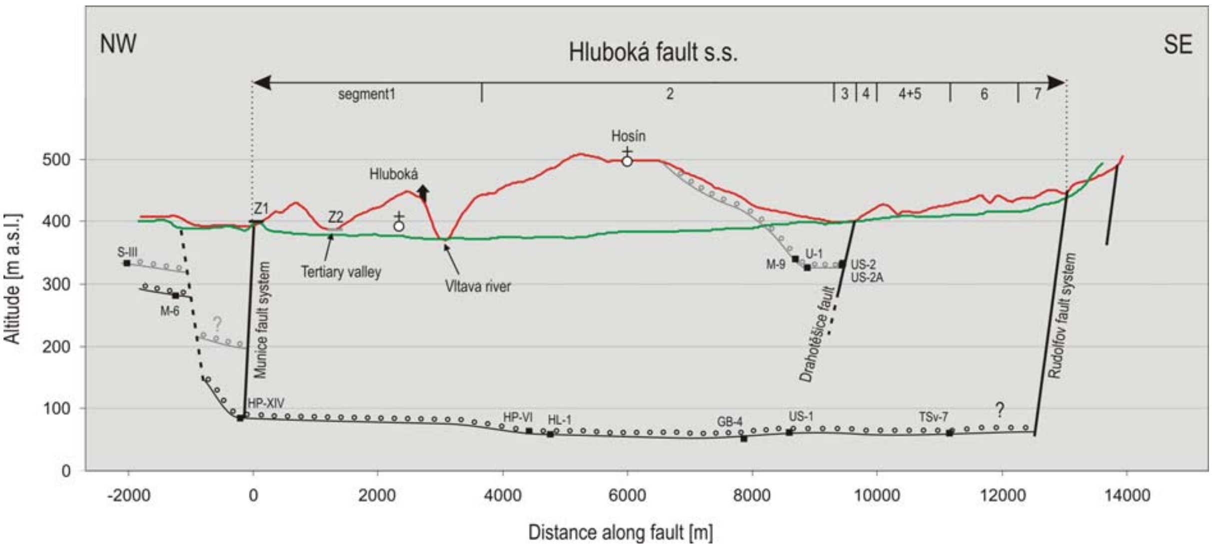

Fig. 4.1-2: Schematic longitudinal fault-parallel vertical profile through the blocks adjacent to the fault viewed from the basin to NE. Green and red lines - terrain elevation profiles in the basin and in the crystalline. Full lines with open circles indicate the approximate position of the base of Cretaceous sediments interpreted from boreholes and geophysics (black - basin block, grey - crystalline block). Crucial boreholes shown as black squares with names (see Fig. 4.1-1 and the note in the text above on the debatable Permo-Carbiniferous in the borehole TSv-7). Approximate traces of the transverse faults shown as solid and hatched bold black lines.

4.2. METHODS AND OVERVIEW OF KEY ACTIVITIES AT THE STUDIED LOCALITIES

4.2.1. Compilation of geological and geophysical data and digital elevation model

A detailed compilation of available data relevant for our understanding of geological structure, stratigraphy and evolution of the Budějovice and Třeboň basins was carried out. Database of horizontal and vertical extent of Cretaceous and Tertiary stratigraphic horizons was compiled based on available geological maps, boreholes and geophysical data (see Fig. 2.1-4 for illustration).

Official maps of Czech Geological Survey were used, in the Budějovice basin mainly the sheets 22-443 „Hluboká nad Vltavou“, 22-444 „Ševětín“, 32-221 „České Budějovice“ and 32-222 „Lišov“ in the scale 1:25000 and sheet 22-44 „Hluboká nad Vltavou“ in the scale 1:50 000 (including the unified digital version GEOČR50). We also used unpublished mapping reports which include descriptions of documentation field points.

Important data on geological structure of the basin and on the extent of the stratigraphic units in the basin fill were acquired from extensive archive of manuscripts and electronic databases of boreholes in Geofond archive. The relevant information was extracted and stored in our own databases.

Vectorised elevation contour lines from digital topographic maps ZM10 (ZABAGED databases; Czech Office for Surveying, Mapping and Cadastre, 2008-2009 release) were used to interpolate digital elevation models (DEM) of the Budějovice basin and adjacent areas with 10-20 m horizontal resolution (Fig. 4.2.1-2). The interpolation was carried out using „Topo to Raster“ technique (iterative finite difference method) in ArcGIS environment. Taking into account the vertical interval of contour lines (1 m in flat areas, 2 m in higher slopes) the expected vertical error of the DEM is close to 1 m for most of the area.

The gravity field maps were derived using point measurements from a detailed gravity mapping with average density of 4-6 points per square kilometre (Geofyzika Brno, Kadlec et al., 1975). In the area of Hluboká Fault, between Hrdějovice and Dubičné the gravity field was refined using detailed mapping with 28 measurement points per square kilometre (Sedlák et al., 2009). Analysis of residual gravity field and horizontal gravity gradient and mainly the Linsser filtering of the gravity field proved useful for defining the Hluboká fault and its precise location (see Chapters 2.2, 4.2.2.1 and Figs. 2.1-4, 2.2-1, 2.2-2, 4.1-1).

The results of previous geophysical survey using vertical electrical sounding (Bárta and Benda, 1966) was also used to reconstruct the basin morphology.

All relevant data were assembled in ArcGIS environment giving a basis for model of present-day structure of the Budějovice and Třeboň basins and their evolution in Creatceous and Cenozoic. Such models allow to assess the relative structural importance of the faults which shaped the basin and help identify those faults which can be potentially active. Based on these data we selected localities at the Hluboká Fault which were then surveyed in detail by field geological reconnaissance, geophysical profiling, shallow boreholes and trenches.

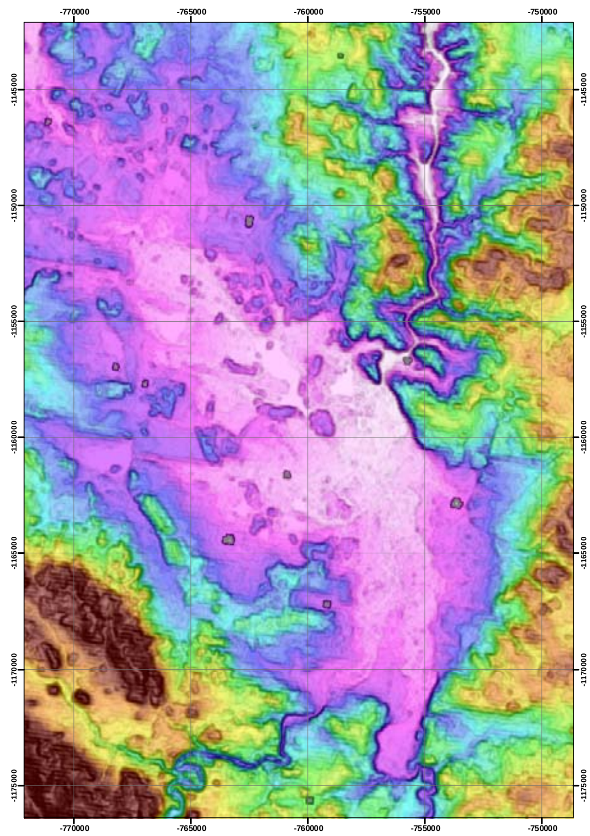

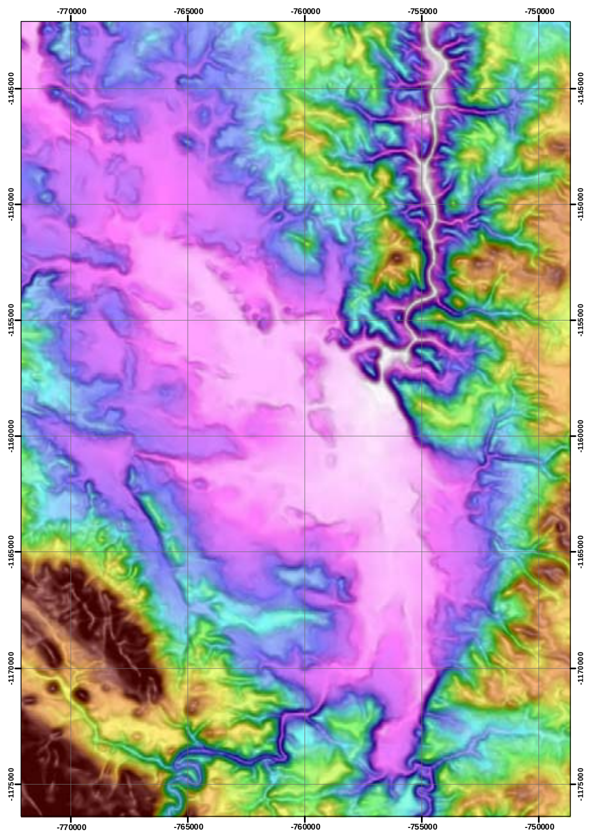

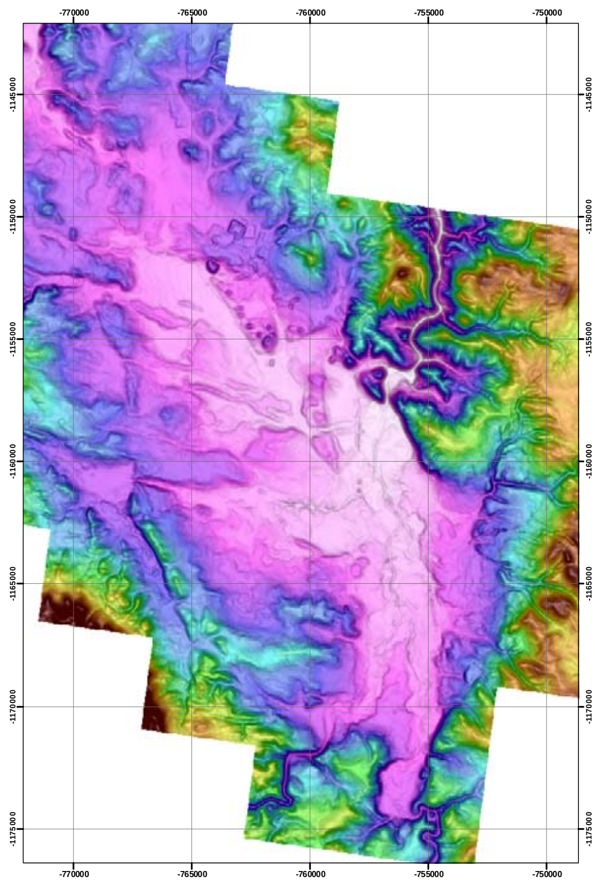

Fig. 4.2.1-2. Digital elevation models compiled from three different data sources, to compare their quality. Top left: SRTM2 model based on satelite radar altimetry. Note the artifacts and regular rastering due to systematic errors in elevation. Top right: Model interpolated from DMÚ-25 (VTOPOÚ Dobruška) contourlines. Note the smoothing of details in relief due to low density and imperfect topology of contourlines. Bottom left: DEM interpolated from ZABAGED (ČÚZK Prague) contourlines. The precise topology and high density (1-2 m in elevation) of contourlines, terrain edges and river bank lines result in high fidelity of the model showing reasonably detailed morphology even in relatively flat areas. Artifacts are reduced to few flat areas with low density of contourlines.

4.2.2. Geophysical and borehole survey

The basic step for analysis of geometry of the fault zone was the location of the main lithological boundary between Cretaceous or Tertiary sediments in the SW wing and crystalline or Permo-Carboniferous rocks in the NE wing of the Hluboká Fault. The precise location was required to minimise the costs of the detailed survey in trenches to reasonable level. Since the position of the lithological boundary often differed from the morphological escarpments (if present) in topography, and because of thick Quaternary beds developed above it, it was necessary to perform geophysical and borehole survey of the sub-surface levels at each locality to be studied.

The procedure of survey was as follows:

Geological reconnaissance was performed to improve geological maps in places with unclear or complicated situation. When necessary, samples of rocks for laboratory analyses were taken during the field survey in shallow diggings or shallow manual boreholes to depths of <1 m. Geodetic positioning was performed using regular or differential GPS.

Geophysical survey was then performed on profiles (or areas) crossing the assumed position of the fault zone with lithological boundaries. The geophysical method was selected based on the expected lithology, desired resolution and specific site conditions. Electric resistivity tomography was used in most cases, however, since the results were often inconclusive, it was necessary to combine several geophysical methods (geoelectric, seismic, gravimetric) and verify the interpretations by direct observations in boreholes, shallow diggings etc. The overview of the geophysical methods used is given below, the position of the surveyed sites is given in Fig. 4.2.2-1 and the results are given in Appendix 4.2-1 and in the following chapters describing individual sites.

Borehole survey was used to verify the interpreted geophysical profiles, specify the lithogies, and sample relevant stratigraphies for further laboratory analyses. Deeper core drilling was performed by *Stavební geologie - Geoprůzkum České Budějovice* company using UGB 50 driling set (20 cm diameter). For shallower boreholes to depths of 1-3 m we used manually lead percussion driller with cores (5 cm diameter) stored in special plastic bags. Overall, 31 deeper boreholes and 21 shallow manual boreholes were made at 10 localities (Tab. 4.2.2-1 and Fig. 4.2.4-1). The cores were described in the field, photographed and sampled (see Appendix 4.2-2 for lithological profiles and photographs).

Borehole sampling, together with OSL dating, was used as the main research method in the floodplain of Vltava river (fault segments 1C, 2A and H) where it was not possible to expose the fault in a trench. Here, the continuity of fluvial sediments across the fault was studied instead and the drilling cores were the only way to sample the lower parts of the terraces (see Chapter 4.4).

name	x (JTSK, m)	y (JTSK, m)	z (BPV, m)	depth	date
MUN-1	-758729.68	-1155589.56	404.55	23.5	31-VIII-2009
MUN-2	-758904.74	-1155628.80	403.15	10.0	31-VIII-2009
MUN-3	-758934.00	-1155723.61	400.20	14.0	24-XI-2009
MUN-4	-758947.67	-1155756.41	398.81	8.4	24-XI-2009
MUN-5	-758976.66	-1155774.31	398.83	8.2	24-XI-2009
MUN-6	-758931.60	-1155686.21	401.50	7.5	1-VII-2010
MUN-7	-758917.18	-1155656.29	403.05	13.0	15-VII-2010
M-3	-758077.95	-1156501.05	387.53	10.0	31-VIII-2009
HL-4	-756523.77	-1157955.09	373.15	4.9	26-XI-2009
HL-5	-756556.03	-1157984.79	373.44	7.0	26-XI-2009
HL-6	-756574.70	-1158001.90	373.21	7.2	26-XI-2009
HL-7	-756219.00	-1158204.00	373.00	5.7	1-VII-2010
HL-8	-756647.56	-1158528.57	373.58	7.5	27-IV-2010
HL-9	-756583.58	-1158431.92	372.97	7.0	27-IV-2010
HL-10	-756690.72	-1156808.21	372.49	4.0	27-IV-2010
HL-11	-756752.21	-1156801.47	372.11	5.0	27-IV-2010
HL-12	-756360.75	-1158224.80	373.43	8.1	26-IV-2010
HL-13	-756337.19	-1158202.23	373.44	10.0	26-IV-2010
HL-14	-756303.43	-1158169.58	373.13	14.0	26-IV-2010
HL-15	-756253.44	-1158214.86	372.68	8.0	2-VII-2010
HLB-9	-756509.00	-1157966.66	373.5	1.2	X-2009
HLB-10	-756547.53	-1158000.63	373.5	2.2	X-2009
HLB-11	-756567.42	-1158018.44	373.5	1.2	X-2009
HLB-3	-756584.40	-1158033.36	373.5	1.2	X-2009
HLB-5	-756592.69	-1158040.40	373.5	1.2	X-2009
HLB-6	-756603.04	-1158049.52	373.5	1.2	X-2009
HLB-7	-756621.69	-1158066.09	373.5	1.9	X-2009
HLB-12	-756626.23	-1158069.60	373.5	2.1	X-2009
HLB-8	-756659.80	-1158099.65	373.5	2.1	X-2009
HLB-18	-756418.69	-1158264.12	373.5	1.2	X-2009
HLB-17	-756436.91	-1158281.93	373.5	1.2	X-2009
HLB-16	-756456.80	-1158301.41	373.5	2.1	X-2009
HLB-15	-756494.09	-1158336.62	373.5	1.2	X-2009
HLB-14	-756567.83	-1158408.29	373.5	1.2	X-2009
OP-1	-755937.27	-1159244.00	374.44	6.0	1-IX-2009
OP-2	-755893.78	-1159235.23	374.24	10.0	1-IX-2009
OP-3	-755816.00	-1159217.90	374.30	3.5	25-XI-2009
OP-4	-755803.70	-1159214.40	375.10	3.8	25-XI-2009
OP-5	-755736.26	-1159207.88	388.50	12.7	26-XI-2009
OP-6	-755720.51	-1159203.54	391.20	5.0	25-XI-2009
HR-1	-754931.46	-1160825.75	387.32	6.0	2-IX-2009
HR-2	-754952.97	-1160847.11	386.59	9.5	2-IX-2009
NE-1	-753883.60	-1162457.20	392.36	6.2	15-XI-2010
NE-2	-753816.23	-1162422.99	392.82	7.0	15-XI-2010
NE-3	-753718.75	-1162383.26	394.25	6.0	15-XI-2010
USI-1	-753176.69	-1163203.77	402.42	1.2	2-VII-2009
USI-3	-753164.88	-1163135.92	402.82	2.1	3-VII-2009
USI-4	-753151.81	-1163132.23	403.88	2.8	3-VII-2009
USI-5	-753198.42	-1163054.37	403.01	1.9	3-VII-2009
USI-6	-753188.53	-1163052.29	403.97	2.3	3-VII-2009
CVR-1	-752889.70	-1163773.40	409.70	1.1	2-VII-2009
CVR-2	-752921.40	1163791.80	408.80	1.1	2-VII-2009

Table 4.2.2-1. List of boreholes (> 1 m deep) performed within the curent project.

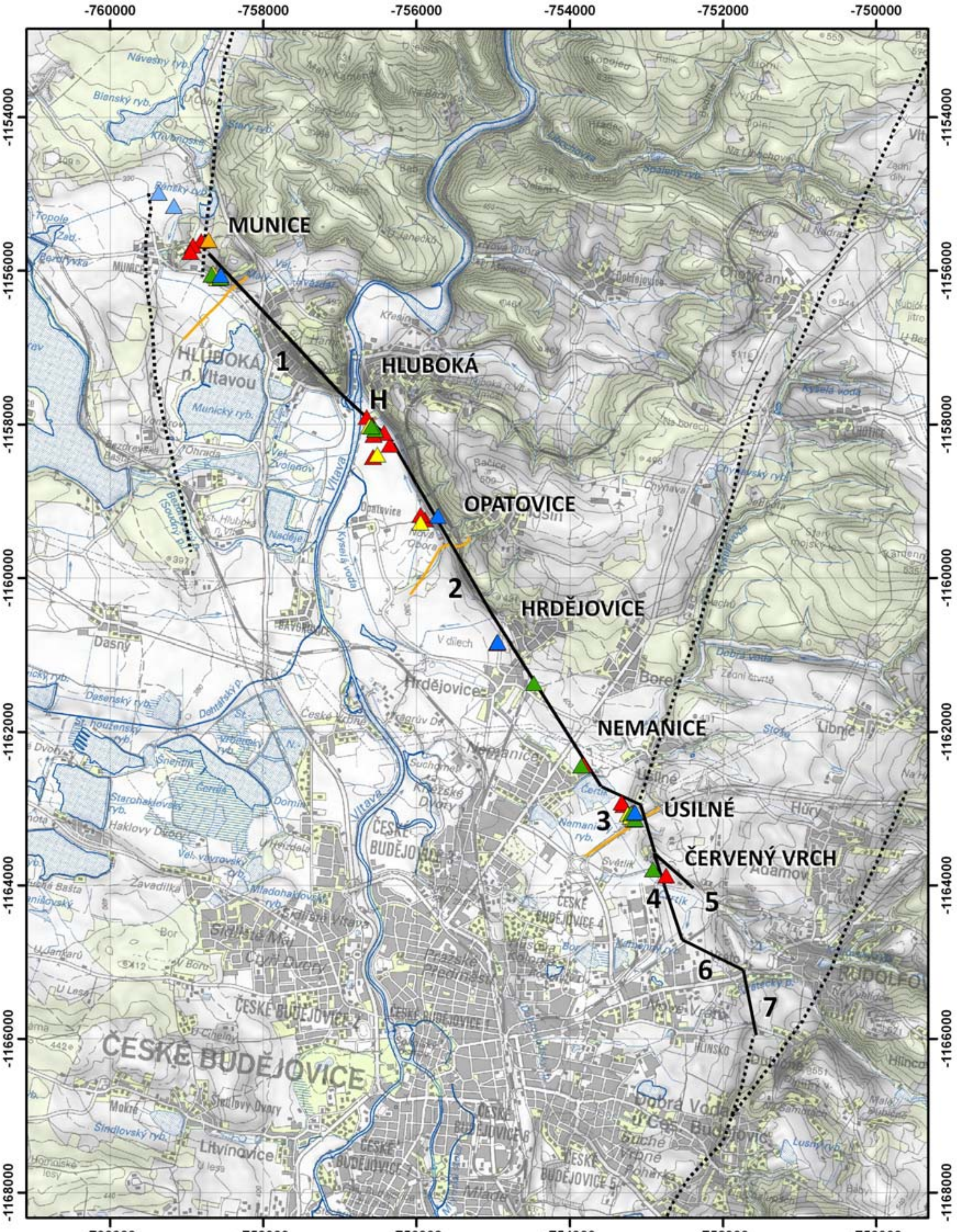

Fig. 4.2.2-1. Schematic map showing geophysical measurements carried out at individual localities studied within the current project. Approximate positions of geophysical profiles shown as coloured triangles: red - multielectrode resistivity tomography, yellow - pole-dipole and/or DEMP profiling, orange - VES, green - GPR, dark blue - shallow seismic refraction, light blue - gravimetric profiles. Orange lines show the three reflection seismic profiles made by AIP team. Individual segments of the Hluboká Fault shown by black line with numbers. Black dotted line shows approximate positions of major oblique faults. S-JTSK grid woith 2 km step.

4.2.2.1 Geophysical methods used

Resistivity methods

Surface electrical resistivity surveying is based on the principle that the distribution of electrical potential in the ground around a current-carrying electrode depends on the electrical resistivities and distribution of the surrounding soils and rocks. The resistivity of soils and rocks is governed primarily by the amount of pore water, its resistivity and the arrangement of pores. Commonly, zones of distinctive resistivity can be associated with specific lithological domains on the basis of local field or borehole evidence, and the resistivity surveys may be used to detect anomalies that can be further investigated by complementary geophysical methods and/or boreholes. The usual practice in the field is to apply an electrical direct current (DC) between two electrodes implanted in the ground and to measure the difference of potential between two additional electrodes that do not carry current. The distribution of potential can be related theoretically to ground resistivities and their distribution for some simple cases, notably, the case of a horizontally stratified ground and the case of homogeneous masses separated by vertical planes (e.g., a vertical fault with a significant throw).

Following resistivity methods were used in the current survey:

Pole-Dipole Profiling

This is a simple technique for locating areas of particular interest. The four-electrode aray in fixed geometry is moved along a line and measurements are repeated at intervals. For example, traversing techniques might be employed to locate steep inhomogenities as low resistivity fracture zones in a high resistivity rock, where there is soil or alluvium concealing the solid geology. The depth of geological structures can not be inverted, but can be roughly estimated as ¼ of separation of current electrodes. Interpretation is generally qualitative, the results were further tested by other methods.

Vertical Electrical Sounding (VES)

This method was used to investigate the vertical variation of resistivity. The centre point of the four electrodes is fixed and the electrode spacing is increased between measurements. In this way current is forced to flow to increasingly greater depth with the result that the resistivity measurement also responds to changes with depth. In case of horizontally stratified lithology the depth of geological structures can be estimated as ¼ of separation of current electrodes. Using number of VES measurements along a profile, 2D section was obtained.

Multielectrode Resistivity Tomography

This method incorporates a combination of both traversing and sounding. As the process calls for a large number of measurements, the survey is carried out using large linear array of electrodes which are alternately used as current and potential, and the collection of data is automatically controlled by computer. The high density of data allows for computer inversion procedures to produce an image of the 2D (or 3D in case of planar geometry of electrodes, not used in the current project) variation of rock resistivity along the line of the survey. Electrical tomography is particularly useful in areas of complex geological structure where conventional techniques are unsuitable. By using a knowledge of the relative resistivities of common rocks, resistivity images can be interpreted in geological terms. In the current project we used the *Res2dInv* (M.H. Loke) which implements a forward modelling subroutine to calculate the apparent resistivity values, and a non-linear least-squares optimisation technique for the inversion routine (Loke & Barker 1996, Loke & Dahlin 2002). This method proved as the most suitable in the area studied.

Dipole Electromagnetic Profiling (DEMP)
This method is suitable for fast measurement of the apparent conductivity of shallow ground using two dipoles, one of which emits the electromagnetic waves which are transformed into secondary electromagnetic field in the sub-surface and recieved by second dipole. The in-phase component of the induced magnetic field is characteristic for buried metal objects and permits their identification. The main advantage of this method is the contactless transmission of the signal which allows fast gathering of data at long profiles or areas. Similarly as other methods based on electrical resistivity, DEMP was used to distinguish qualitatively lithologies with contrasting grain size. Theoretical depth range of the measurements in the current project is 6-9 m.

Ground Penetrating Radar (GPR)
This method uses polarized electromagnetic pulses in a microwave band and detects signals reflected from subsurface boundaries with different dielectric constants.
The transsmission of the signal is contactless which allows fast recording of variations in the reflected return at the profile. The method gives high resolution images, but the depth range is limited, controlled mainly by the electrical conductivity of the ground and the transmitted center frequency. In highly conductive, moist, clay-rich sediments which are so abundant in the area investigated, the penetration depth was only several meters even for 50 MHz frequency measurements.

Shallow refraction seismics
This method is based on the measurement of the travel time of seismic P-waves refracted at the interfaces between subsurface layers of different velocity. Seismic energy was provided by 5 kg hammer, which produces seismic signal that can be detected as far as 100 m away. Travel times of refracted waves were read using linear array of geophones. The inversion of travel times to velocities was performed using t_0 method (Hagedoorn 1959) and seismic tomography (Lehmann 2007). The results were interpreted in terms of lithology and depth of main refraction horizon to assess structural contrasts at both wings of the fault.

Gravimetry
This method was applied to detect faults based on gravity effect of the density contrasts associated with marginal basin faults that have large throw and large sediment thickness.
Use of the regional Bouguer gravity data and derived maps was of key importance for locating the main lithological boundary associated with the Hluboká Fault on regional to local scales. Some details on the source data and processing methods were outlined in Chapter 2. Here we give additional information on Linsser filtering which was used as a surveying method.

Linsser Indications of Density Contacts

Spatial changes in the density of rocks are responsible for gravity anomalies. Linsser filtering is a unique technique for fault mapping based on the assumption that faults are associated with steep contacts of rocks with contrasting densities. The original technique was proposed by Linsser (1967) and later modified by Šefara (1973). Linsser method is based on the assumption, that the gravity profile over a fault or a density contact can be described as a linear combination of gravity master curve and regional gravity field:

$$\Delta g(x) = E \times M(x) + R \times B(x)$$

where $\Delta g(x)$ is the measured gravity profile,
$M(x)$ is the gravity master curve for specified depth level,
E is the amplitude of the fitted gravity master curve,
$B(x)$ is the spatial variation of regional field,
and R is a multiplicative coefficient describing regional gravity field.

For the gravity data processing presented in this report we have used approach of Šefara (1973), where the gravity master curve is calculated for the thin sheet model approximating the fault (Fig. 4.2.2-2) and the regional field is considered to be constant, i.e. $B(x) = 1$. The comparison of gravity data, locally re-interpolated to the direction perpendicular to the horizontal gravity gradient, with master curves enables the estimation of fault amplitude and the regional gravity. The density contact indication is plotted on the map in a position where the Linsser coincidence criterion C defined in Fig. 4.2.2-2 has a pronounced maximum. An additional requirement for the construction of a density contact indication is the existence of a maximum of the coincidence criterion C also on two adjacent parallel profiles. This reduces significantly the fragmentation of the density contact patterns. Linsser filtering is performed by analyzing a set of depth levels using master curves the length of which is at least 6 times greater than the gravity grid cell size (seven-point convolution operator with the length 1500 m). Linsser indications are plotted in maps as rectangular symbols oriented parallel to isolines of gravity field, with stroke pointing towards higher density domain. The area of each symbol is proportional to the product of the density difference and height of vertical step (E×C) in the modelled contact.

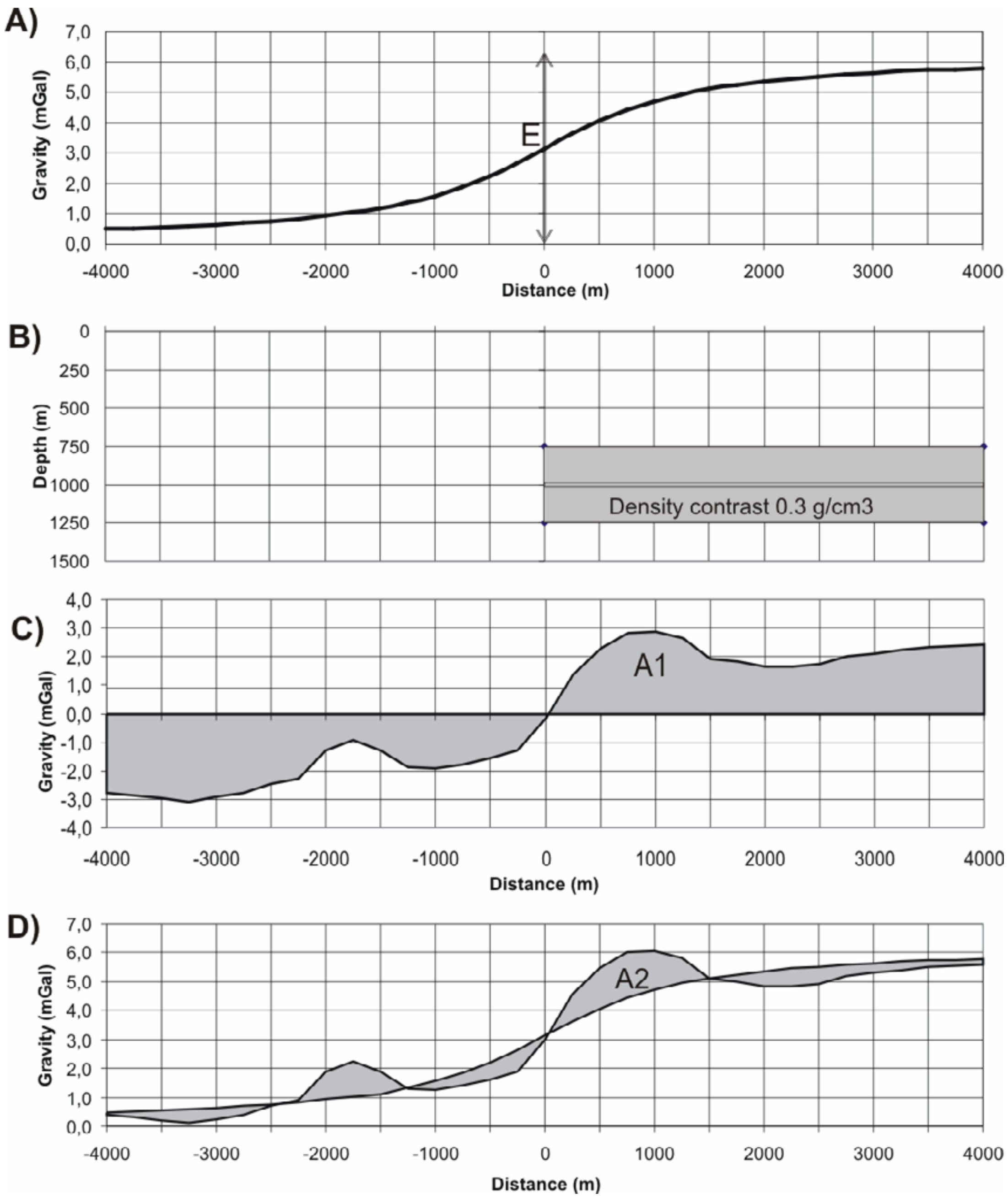

Fig. 4.2.2-2: Principle of the Linsser filtering technique for determination of fault parameters. A) Gravity master curve corresponding to the geological model. E is the amplitude of the gravity effect of the master curve. B) Cross section of the density contact model approximated by a 2D horizontal thin sheet. C) Measured gravity profile running across the density contact. A1 is the area between the regional field and the measured gravity. D) Comparison of the measured gravity profile with the gravity master curve. A2 is the area between the master curve and the measured gravity. The coincidence C between the measured gravity and the master curve is defined by the expression C(%) = 100 × (A1-A2)/A1.

4.2.3. Trenching

According to the intention of the project the Hluboká Fault should have been reached in its shallow parts by trenching to allow direct detailed study and eventual paleoseismological analysis in the exposed profiles. Selection of the sites suitable for trenching was, in addition to geological situation, mainly controlled by technical/economical ascpects, including the possibility to reach the fault in reasonable depths, hydrological aspects, situation of roads, mains and developed areas, or land use and ownership. From this point of view the situation on the Hluboká Fault appeared to be rather unfavorable. High scarp associated with the fault between Hluboká and Hrdějovice derives thick colluvia and alluvial fans which disallow the precise location of the fault and reaching its sub-Quaternary levels by a simple trench. The railway and busy major road Hluboká-Hrdějovice, both located close to the foot of the scarp, further complicate the situation. In the SW part trenching is made impossible by high level of housing development (Hluboká town). The high level of water table disallows the trenching in Vltava floodplain.

For these reasons the survey for trenching sites focused preferrentialy on the external parts of the fault, where only low scarps are developed and built-up area is not so extensive. Based on geological, geophysical and geomorphological aspects the survey was confined to two localities - Munice in the NW part of segment 1A, and area to the S-SE of Úsilné in segments 3, 4A and 5. In central parts of the fault indirect alternative methods of research had to be used.

After detailed geological mapping and geophysical and shallow borehole survey four trenches were excavated at two localities (Munice and Úsilné). These had simple geometries and dimensions optimised to the local requirements ensuing from the current observations during the digging. Taking into account safety regulations, mechanical properties of the material and the demands on easy documentation, the combined single- or double-benched trench cross-sections with laid-back walls were used (see Chapter 4.7).

After multiple cleaning of the trench walls a 0.5×0.5 m to 1×1 m reference grid was constructed and geodetically referenced. A detailed documentation was then carried out incuding the compilation of orthorectified photomosaic, description of lithologies, logging, structural measurements and sampling. The observations were interpreted in terms of tectonic structures related to fault slip and stratigraphy of the overlying sediments.

On-site inspections and discussions with members of AIP team and other co-operating specialists in the fields of paleoseismology, structural and Quaternary geology allowed an open, complex interpretation founded on broad spectrum of views.

4.2.4. Dating

Dating of sediments studied was performed using OSL method (Optically Stimulated Luminescence) on samples taken from trench profiles and drilling cores. Dating by radiocarbon method was not carried out due to the small content of organic matter in sediments studied.

A key advantage of OSL dating is that the luminescence of quartz and feldspar grains is reduced to a low definable level after a few minutes of sunlight exposures. An important limiting factor to applicability of this method is the age of sediment dated which, in most cases, must not be higher than 150-200 thousand years.

In order to derive an optically stimulated luminescence (OSL) age both the palaeodose (De - the amount of absorbed dose since the sample was buried) and the dose rate (the estimated radiation flux for the sedimentary bodies) have to be determined. The age is calculated as the ratio of palaeodose (expressed in Grays) and the annual dose rate (Grays/yr). An inherent assumption in these age calculations is that the sediment was fully reset or 'bleached' by exposure to sunlight during the last transport event or whilst in situ prior to burial and that no post-depositional sediment disturbance has occurred. To calculate the dose, single aliquot regeneration method was applied to coarse (90-250 μm) quartz grains extracted from the samples. An IR-SAR approach was adopted to measure the concentrations of naturally occurring potassium, thorium, rubidium and uranium, which were then converted to annual dose rates taking into account the attenuation factors relating to sediment grain sizes used, density and palaeomoisture, and the contribution to dose rates from cosmic sources.

At the beginning of the project it was agreed with AIP team that the samples taken for OSL dating by CIP team wil be shared and, according to the needs and ability, dated at the expense of AIP or CIP. The results were available to both teams and the interpretation was independent. In this way we took the advantage of funding from two interfacing projects and the total number of the dated samples was increased.

In the current project the samples were dated in laboratory of Sheffield Centre for International Drylands Research (Dr. M. Bateman). Within the AIP project the samples were dated in laboratory of University of Vienna (Institute of Applied Geology a Department of Geodynamics and Sedimentology, Dr. J. Lomax). From total of 67 samples, 32 were dated and the remaining 35 samples were archived. The list and location of dated samples is given in Tab. 4.2.4-1 and Fig. 4.2.4-1 and described in more detail in following chapters.

sample	locality	x (JTSK) [m]	y (JTSK) [m]	z (sample) [m, BPV]	age [ky±1sigma]	min-eral	dating lab
HL-4D	Hluboká	-756524	-1157955	369.60	**22.2±1.6**	qtz	Sheffield
HL-5A	Hluboká	-756556	-1157985	372.40	**13.2±0.8**	qtz	Sheffield
HL-5B	Hluboká	-756556	-1157985	371.90	**13.8±0.7**	qtz	Sheffield
HL-6A	Hluboká	-756571	-1158007	372.60	**8.9±0.5**	qtz	Sheffield
HL-6C	Hluboká	-756571	-1158007	371.85	**14.7±0.8**	qtz	Sheffield
HL8-1	Hluboká	-756648	-1158529	372.18	**7.08±0.68(fel), 163(qtz)**	fel+ qtz	Vienna
HL8-3	Hluboká	-756648	-1158529	369.33	**48.62±4.80**	fel	Vienna
HL8-4	Hluboká	-756648	-1158529	368.33	**78.80±8.35**	fel	Vienna
HL-11B	Hluboká	-756752	-1156801	370.26	**33.80±2.0**	qtz	Sheffield
HL-11C	Hluboká	-756752	-1156801	369.61	**3.42±0.17**	qtz	Sheffield
HL-11C	Hluboká	-756752	-1156801	369.61	**4.45±0.44(fel), 75.27(qtz)**	fel+ qtz	Vienna
HL-11D	Hluboká	-756752	-1156801	367.61	**5.53±0.41**	qtz	Sheffield
HL-12E	Hluboka	-756361	-1158225	368.59	**53.50±4.0**	qtz	Sheffield
HL-14C	Hluboka	-756303	-1158170	368.93	**41.40±3.5**	qtz	Sheffield
DH-007	Zámostí	-756223	-1156231	388,1	**>150**	fel	Vienna
HL-16	Zámostí			381.80	**to be specified**	fel	Vienna
DH5-1	Zámostí	-756934	-1156668	376.00	**23.42±2.54**	fel	Vienna
HLR1_2	Zámostí	-756690	-1156091	375.00	**23.33±2.29**	fel	Vienna
OP-1	Opatovice	-755937	-1159244	372.94	**15.97±0.9**	qtz	Sheffield
OP2-1	Opatovice	-755894	-1159235	370.09	**>230**	fel	Vienna
OP2A	Opatovice	-755894	-1159235	369.79	**>153**	qtz	Sheffield
OP-7	Opatovice	-755736	-1159244	376.00	**42.40±2.70**	qtz	Sheffield
NO-1	Skelná Huť	-755635	-1159594	383.00	**16.27±0.84**	qtz	Sheffield
HR-1	Hrdějovice	-754931	-1160826	385.95	**53.58±6.12**	fel	Vienna
USI-2A	Úsilné-R1	-753192	-1163053	402.00	**48.70±2.60**	qtz	Sheffield
USI-4B	Úsilné -R2	-753153	-1163134	401.50	**21.8±1.2**	qtz	Sheffield
US3-1A	Úsilné -R3				**8.38±0.46**	qtz	Sheffield
US3-3A	Úsilné -R3				**8.22±0.44**	qtz	Sheffield
DH-20-1	Úsilné	-753083	-1162468	399.00	**24.05±2.73**	fel	Vienna
DH-20-2	Úsilné	-753083	-1162468	400.00	**19.13±2.08**	fel	Vienna
NE-1B	Nemanice	-753884	-1162457	390.26	**13.63±0.86**	qtz	Sheffield
NE-1D	Nemanice	-753884	-1162457	387.06	**39.70±2.40**	qtz	Sheffield
NE-3A	Nemanice	-753719	-1162383	391.60	**9.27±0.51**	qtz	Sheffield

Table 4.2.4-1. List of samples dated by OSL method and their ages. Included are results of AIP team which are referred to in this report (blue - CIP data, yellow - AIP data).

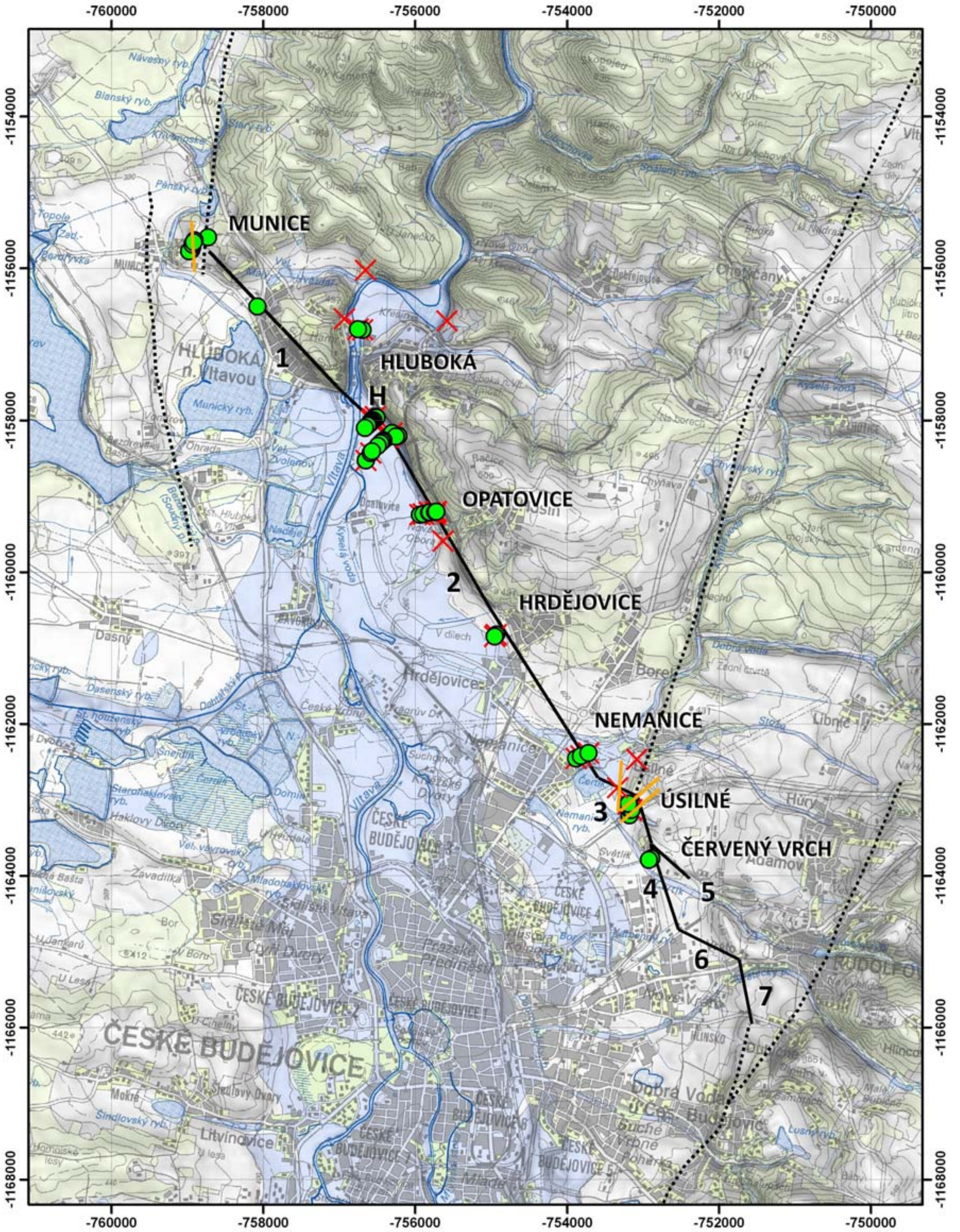

Fig. 4.2.4-1. Schematic map showing the positions of shallow boreholes made within current project (green circles), trenches (orange lines) and sampling sites for OSL dating (red crosses). Blue-shaded area shows the extent of fluvial sediments, mostly associated with Vltava river. Individual segments of the Hluboká Fault shown by black line with numbers. Black dotted line shows approximate positions of major oblique faults. S-JTSK grid woith 2 km step.

4.3 SEGMENTS 1A AND 1B: MUNICE - HLUBOKÁ NAD VLTAVOU

The NE segment of the Hluboká Fault with azimuth of 120-130° is defined between its crossing with Munice Fault to the NE and the Vltava floodplain, SE of Hluboká nad Vltavou. Our investigation focused on three areas (Fig. 4.3-1): Munice, Northern River channel, and Hluboká-town, which are described separately in following chapters.

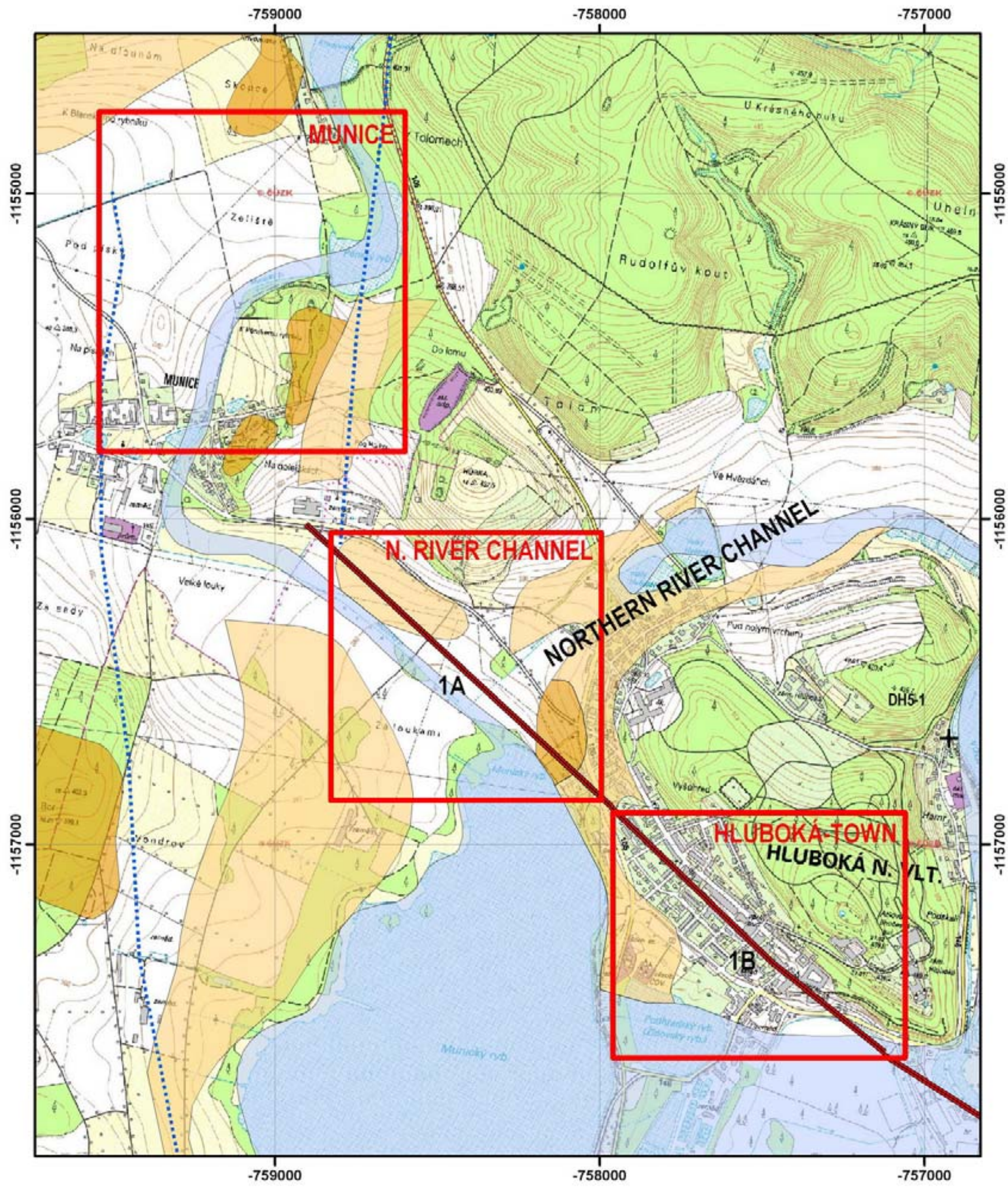

Fig. 4.3-1: Situation map of the segments 1A and 1B of the Hluboká Fault showing the three areas of interest described in following chapters. Beige, ocre brown and light blue areas show the extent of Mydlovary Fm., Zliv Fm. and Quaternary fluvial sediments according to geological map. Red bold line is the approximate trace of the Hluboká Fault. Dotted blue lines indicate the approximate position of the Munice Fault. S-JTSK projection with 1 km grid step.

4.3.1 The Northern River channel area (segment 1A)

This area is of key importance for understanding of long-term activity of the Hluboká Fault in its NW part, because it is covered by sediments of the Neogene Mydlovary Fm., which continue farther to NE as a fill of narrow valley sometimes called the Northern River channel (Figs. 4.3-1). On the other hand, the large thickness of these sediments and relatively dense development of the area in a proximity of Hluboká town, make the detailed survey difficult.

Fig. 4.3.1-1: Overview of the „Northern River channel" and adjacent parts of Hluboká town viewed from NW. Red arrows indicate the position of the Hluboká Fault (left arrow – fault trace behind the scarp). Blue arrow indicates the local axis of the "Northern Channel" in the present-day Vltava valley. The channel continues in the local valley towards the Hluboká Fault (towards red arrows).

The area was studied during the earlier period of survey (1993-1995; Šimůnek et al., 1995), using vertical electrical sounding on several profiles parallel and oblique to the Northern River channel, and two boreholes, M-1 and M-2 (Fig. 4.3.1-1 and Appendix 4.2-2). The M-1 borehole reached the base of the Mydlovary Fm. in depth of 46.7 m below surface which is comparable to the level at which the flat, horizontal base of this unit is interpreted in the seismic section located < 300 m to the west (see below). Borehole M-2 reached the crystalline at the depth 28 m. It seems likely that the M-1 borehole was located close to the paleo-thalweg of the Northern River channel and that this level represents the erosional base in the area prior to deposition of the sediments of the Tertiary Mydlovary Fm. This, however, would have serious implications as regards to the activity of the Hluboká Fault, because the M-1 borehole and the horizontal base of the Mydlovary Fm. in the seismic section lie on the opposite wings of the fault. Therefore we made an effort to gather additional data to support or exclude the assumption of the absence of vertical slip on this fault segment since Miocene.

In the current survey we carried out new electrical resistivity measurements across the NW-SE striking terrain scarp near Hůrka hill (elevation 432 m). A complementary borehole M-3 was made in the eastern part of the Northern River channel. We documented the profile exposed by a shallow drainage trench built for construction purposes between the Munice and Malý Hvězdář ponds, which crossed the surface trace of the fault. An important source of information is the reflection seismic section measured in 2009 by AIP team on a profile crossing the fault which is summarised below.

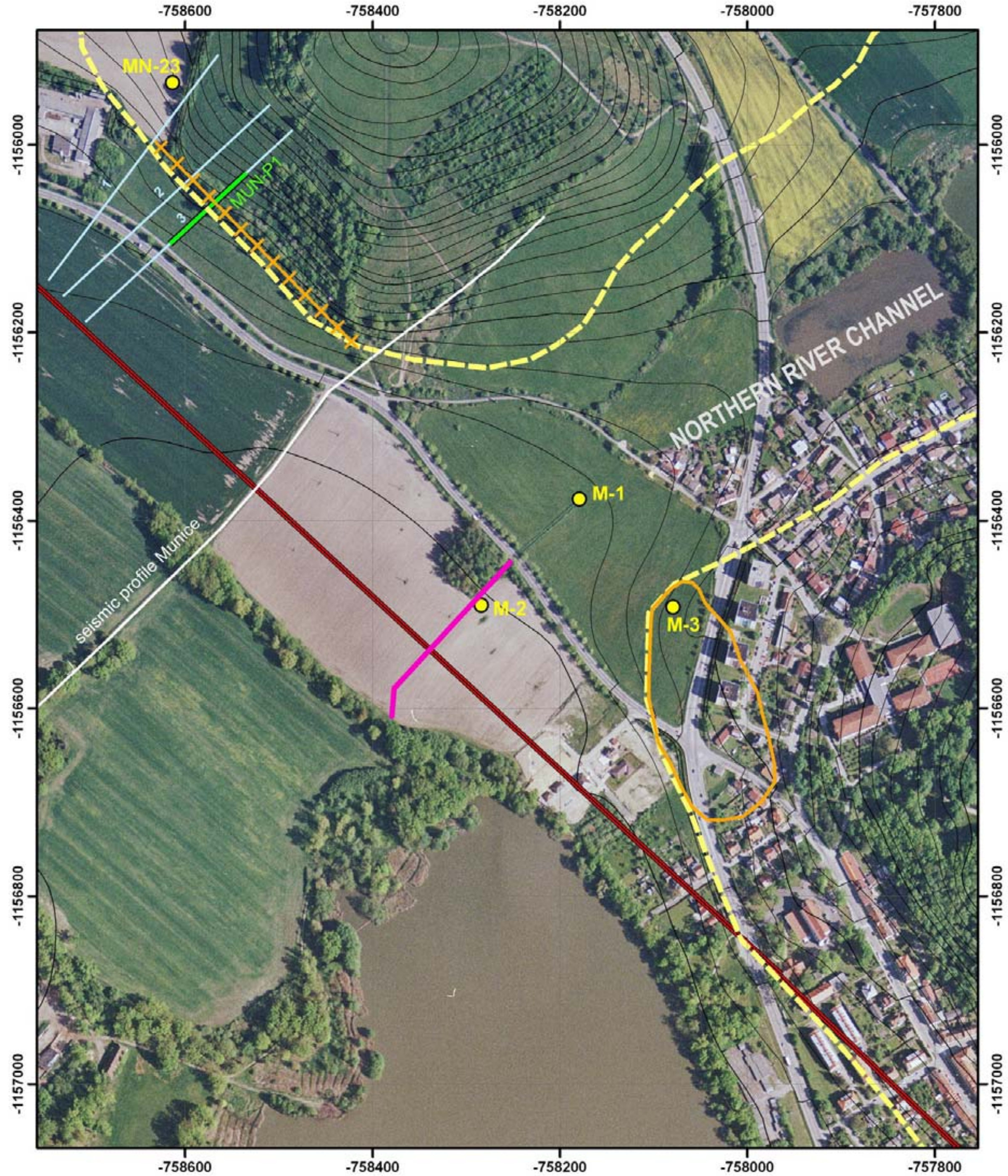

Fig. 4.3.1-1: Situation map of the Northern River channel area between Hluboká and Munice showing the positions of transects 1-3 (light blue lines) with electrical resistivity profile Mun-P1, seismic reflection profile Munice (white line), shallow drainage channel (purple bold line), boreholes M-1, M-2 and M-3 and documentation point MN-23 referred to in text (yellow dots). Approximate position of the Hluboká Fault shown by red dash-and-dot line. Approximate extent of sediments of the Mydlovary Fm. and Zliv Fm. is shown by yellow dashed line and orange line, respectively. Also shown is the scarp at the SW slope of the Hůrka hill (orange cross-line). S-JTSK projection with 200 m grid step.

Reflection seismic section Munice

Seismic profile Munice (map in Fig. 4.3.1-1, results and interpretation in Fig. 4.3.1-2) made in the year 2009 by AIP team (Decker, 2010a), was designed to cross the expected fault trace and the associated escarpment between Hluboká and Munice. Neogene sediments of the Mydlovary Fm. are exposed beneath the Holocene topsoil in the area (Fig. 4.3-1). Its base is situated in the central part of the section at the distinct sub-horizontal boundary at 100ms TWT, i.e. approx. 50-70 m below surface. The lower domain, interpreted as the Klikov Fm., displays bended reflections reoriented in the NE into direction sub-parallel to the 60° inclined base reflection, which most likely corresponds to the surface of crystalline at the Hluboká Fault. Clear angular unconformity is developed between the two sedimentary units. The continuous, horizontal reflections within the upper domain suggests that sedimentary sequence of Mydlovary Fm. was not disturbed by significant offsets on faults. In the SW part of the section the uneven, step-like character of the boundary between the two domains could be interpreted (but not necessarily) as due to faulting in the early periods of sedimentation of the Mydlovary Fm.

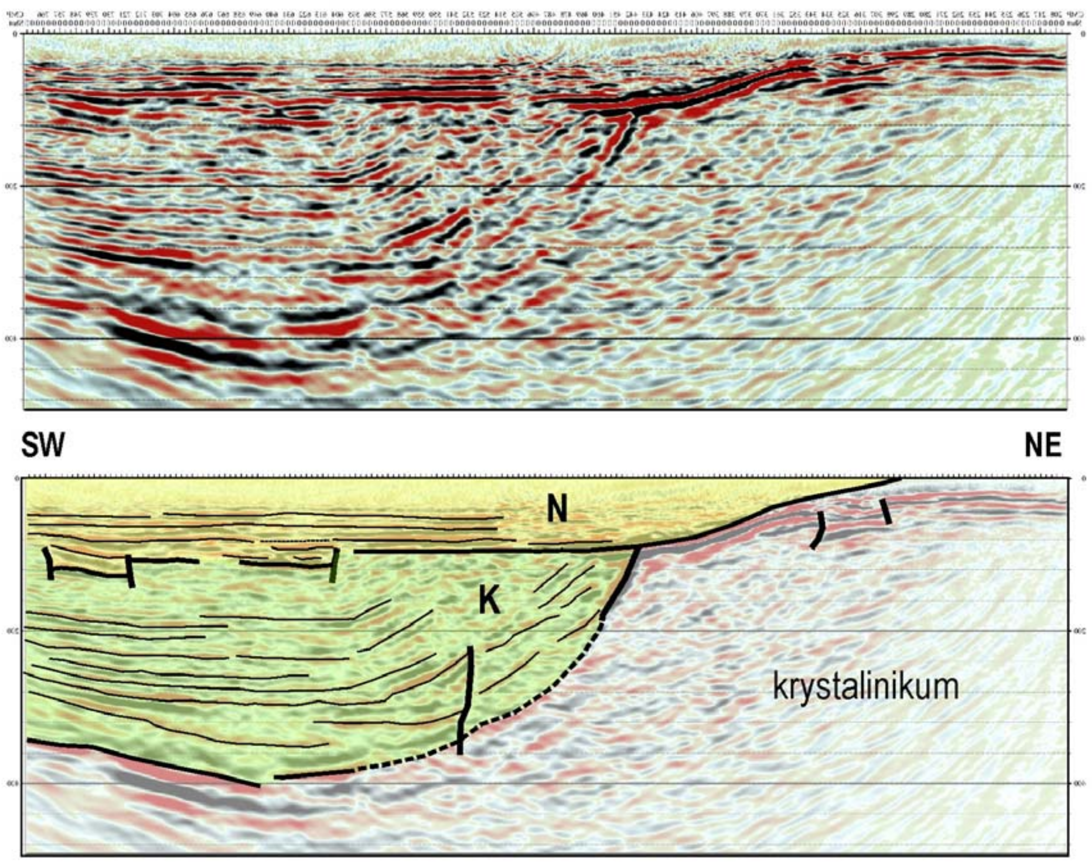

Fig. 4.3.1-2.: Reflection seismic section Munice (above; AIP team, Decker et al. 2010a; courtesy K. Decker) and its re-interpretation (below, CIP team). Length of profile - 1100 m. Green and yellow domains represent the suggested extent of Cretaceous Klikov Fm. (K) and Neogene Mydlovary Fm. (N), respectively. Bold, sub-vertical lines indicate possible faults. No fault-related offsets are observed in sediments of the Mydlovary Fm.

In the NE part of the section the base of the Mydlovary Fm. is found at the distinct reflection inclined to the SW, which most likely coincides with the top of crystalline on the NE wing of the Hluboká Fault. The smooth, continuous trace of the reflection attributed to the base of the upper domain at a long portion of the section suggests the transgressive character of the Mydlovary Fm. above the buried Hluboká Fault, which has not been active after the deposition.
Farther in the NE part the seismic line is oriented in a high angle to the slopes of the Northern River channel. Although here only the lower part of the main reflection multiplet is observed (the upper part is cut off), it is well seen in both migrated and non-migrated sections as a smooth line without offsets (only lateral discontinuity is observed near the road Hluboká-Munice). Thus it seems that significant vertical offsets can be excluded for whole section between CDP 290 and CDP 600 - this is in accordance with the resistivity profile MUN-P3 located at the base of the scarp farther to west (see below).

Borehole M-3

In borehole M-3 the extent of the small occurence of the Zliv sandstones (Zliv Fm.) near Hluboká was verified. This denudation relic is situated at the NE wing of the fault, lying on the crystalline rocks (see Appendix 4.2-2 for lithological description). The elevation of the base is 383,03 m a.s.l., which is close to (and lower than) the base elevations of similar relics of the Zliv Fm. in the area, which lie on top of the Cretaceous Klikov Fm., i.e. at the SW wing of the fault and to the west of the Munice Fault (390-400 m a.s.l. west of Hluboká and 380-394 m a.s.l. south of Hluboká; see geological maps and several documented localities, including borehole MUN-2 in the following chapter). This is an important observation suggesting the absence of significant uplift of the NE block of the Hluboká Fault at this segment.

Geophysical survey at the escarpment near Hůrka hill (432 m a.s.l.)

Geophysical measurements were carried out at three transects located at the lower part of the SW facing slope of the Hůrka hill (Fig. 4.3.1-1) to assess its sub-surface structure and possible tectonic origin. Based on the results of the dipole electromagnetic profiling (DEMP) and the pole-dipole profiling the multielectrode electrical resistivity and shallow refraction seismic measurements were carried out on shorter selected segments. Geological interpretation is based on the 110 m long electrical resistivity tomography profile MUN-P1 on the transect 3 (Fig. 4.3.1-3) which is most informative. The profile was located in the central/NE part of the transect (from the bicycle path to the NE). Two domains of distinctively contrasting resistivities, divided by a relatively broad zone of high gradient are readily recognised in the tomographic profile. The wedge-shaped domain of low resistivities is interpreted as clay-rich sediments of the Mydlovary Fm. The mild, 20-30° dip of its base, further steepening with increasing depth, and the coincidence of its termination with the base of the terrain escarpment suggest that its structural position is transgressive rather than tectonic. The high gradient boundary zone is interpreted as the weathered surface of crystalline rocks. The high resistivity domain in the scarp could represent the rocky colluvia derived (naturally or artificially) from the outcrops and quarries in the paragneisses higher in the hillslope. In these parts the crystalline rocks are fresh or only slightly weathered, while the typical elluvium with the apperance of sandy mica-rich clays was only observed in a shallow probe farther to the east (MN23 in Fig. 4.3.1-1).

It is inferred from the observations in the broader area that the studied escarpment is coincident with the margin of river channel now filled with clays, sandy clays and clayey sands of the Mydlovary Fm. This channel can be tracked farther to the NW (see the results from the Munice area desribed in the following chapter) and it is suggested that it was formed in Tertiary by a right-hand tributary of the Northern River.

Regarding the geological situation and the observations in the seismic profile which indicates the position of the steep contact of crystalline vs. Cretaceous beneath the 50-70 m thick beds of the Mydlovary Fm., some 200 m farther to the SW from the scarp, we suggest that the scarp is not linked directly to the fault slip but it is rather of exogenic origin, representing a degraded fault scarp partly modeled by the river erosion.

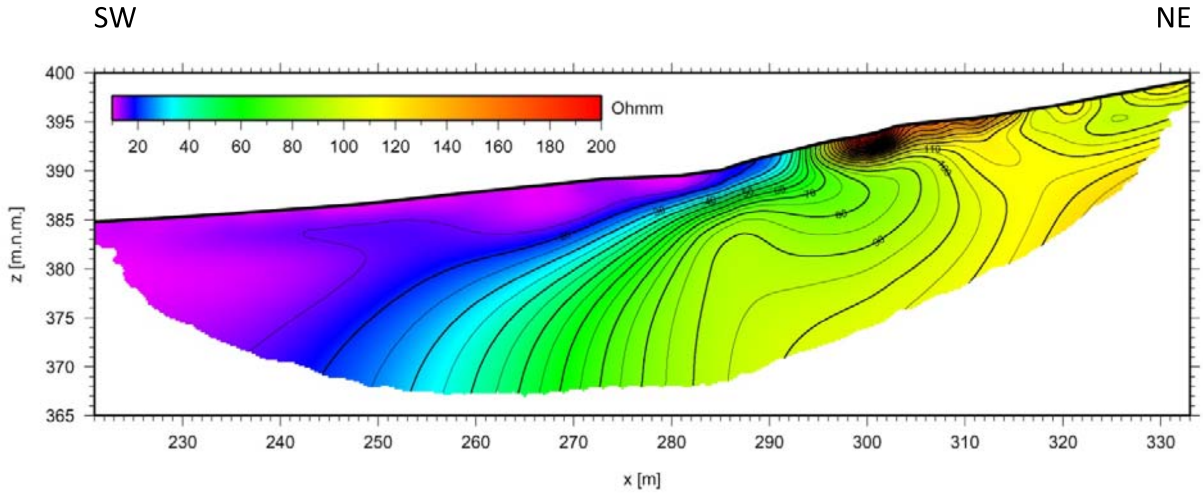

Fig. 4.3.1-3: Electrical resistivity tomographic profile Mun-P1.

The shallow drainage trench

In 2009 a shallow drainage trench was built for construction purposes between the Munice and Malý Hvězdář ponds. The trench exposed the clays of uppermost part of the Mydlovary Fm. in a >200 m long profile which crossed the expected surface trace of the buried Hluboká Fault in the axial area of the Northern River channel (Fig. 4.3.1-1). The gray brown clays, covered by 40-50 cm thick topsoil bed (Fig. 4.3.1-4), displayed a monotonous horizontal bedding in the whole profile and no traces of tectonic offset were observed despite a thorough survey. This observation, contraindicative to the existence of an active fault in the area of the profile (i.e. between the Munice pond and the road Hluboká-Munice) is in accordance with the above desribed observations in the geophysical transects farther to the NW.

Fig. 4.3.1-4: Monotonous, horizontally bedded clays of the Mydlovary Fm. exposed in the NW wall of drainage channel between Hluboká and Munice.

4.3.2 The Munice area (segment 1A)

In the area to the N and NE of Munice village the Hluboká Fault is terminated at the crossing with the NNE-SSW striking Munice fault (Fig. 4.3.2-1).

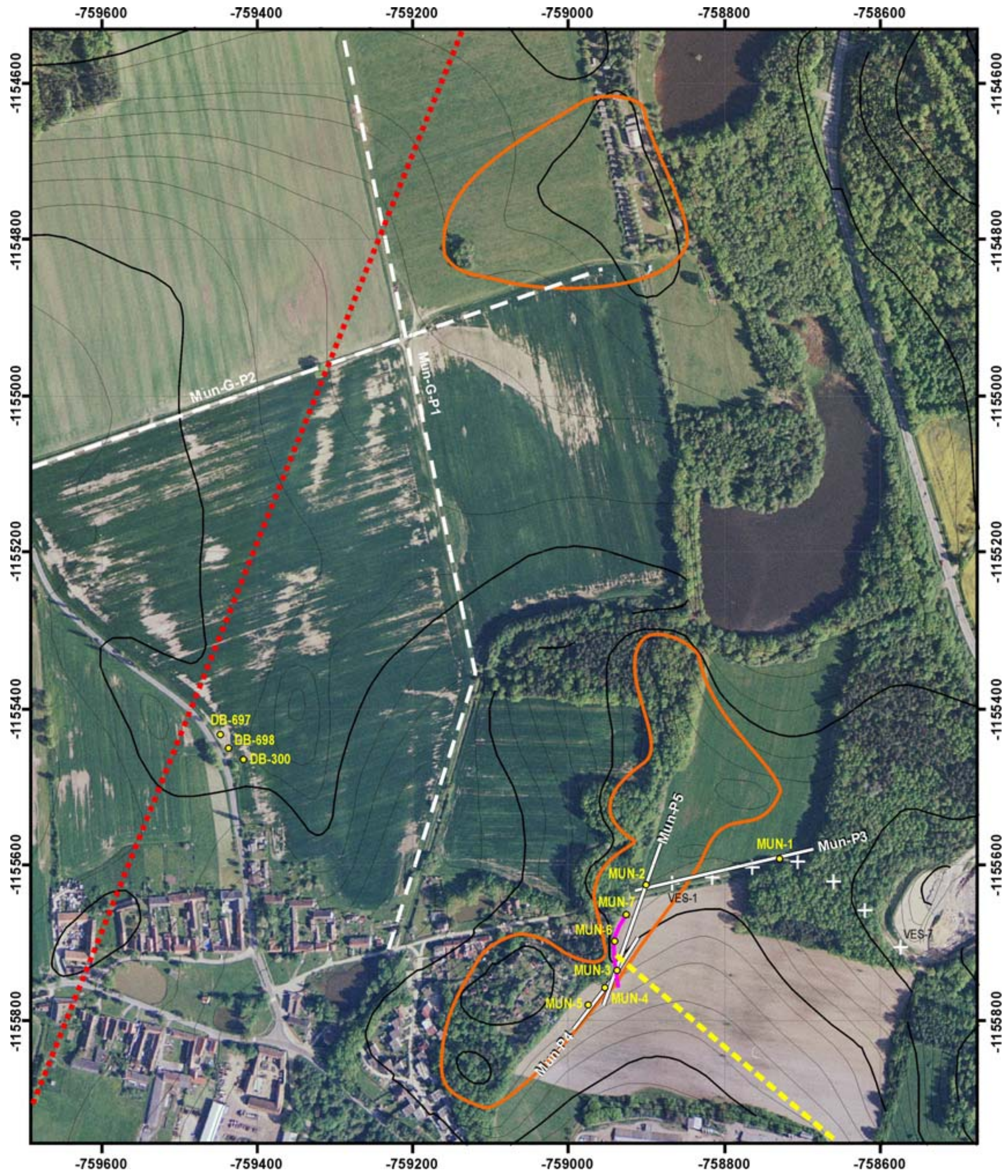

Fig. 4.3.2-1: Situation map of the Munice area. Yellow dashed line indicates the geometrical continuation of the escarpment (see Chapter 4.3.1). Red dotted line shows the approximate position of the eastern margin of the Munice Fault zone. Orange line shows the extent of the Zliv Fm. White dashed lines - gravimetric profiles;, white solid lines - multielectrode resistivity profiles; white crosses - VES profile; white circles - boreholes; purple line - trench Munice. S-JTSK projection with 200 m grid step.

Although the exact position and the detailed geometry of the fault structures in this area are not completely understood, our working model based on the borehole data, gravity field and surface geology, assumes that a small, N-S oriented subsided block with high (around 300 m) thickness of Cretaceous sediments is developed at the fault crossing. In the adjacent blocks to the west of the crossing the thickness of Cretaceous sediments is reduced to 100-170 m. To the N and NW of Munice the relics of 6-8 m thick, silicified Zliv sands cover the eastern part of the fault crossing zone and the terrain morphology does not correspond to the lithological contact crystalline/Cretaceous.

The mapping of the fault structure N of Munice was complicated by the absence of contrasting lithologies and the geophysical survey was based on gravity measurements. These should be theoretically sensitive to the abrupt changes of sediment thickness associated with faults and indicated by borehole data (change of thickness of Cretaceous sediments from 300 m to 40-100 m between boreholes DB-300, DB-698 and DB-697 in Fig. 4.3.2-1). However, the results of the gravity measurements on two profiles (Mun-G-P1, Mun-G-P2) were not conclusive and the survey of this locality was closed.

The survey was then focused on the area NE of Munice, where theoretically the fault associated with the Hluboká Fault could be expected in continuation of the escarpment described in previous chapter. A detailed mapping (including shallow probes) and geophysical survey (electrical resistivity profiles) were carried out, seven boreholes (MUN-1 to MUN-7) were drilled and a trench was excavated to understand the geological situation at this locality (Fig. 4.3.2-1).

Geological mapping and shallow probes confirmed that the channel filled with sediments of the Mydlovary Fm., described in previous chapter, continues to this area from SE. The geophysical and boreholes survey were mainly designed so that we could learn about the structure and lithology of this channel. Vertical electrical sounding (VES) and multielectrode electrical resistivity measurements were performed on a set of transects arranged to cross the Tertiary channel, the relic of the Zliv sandstones and the contact crystalline vs. Cretaceous buried beneath them (Figs. 4.3.2-3, 4.3.2-4, and 4.3.2-5). The VES profile shows the extent of the channel as a domain of higher resistivity with maximum depth of approx. 30 m. The more detailed tomographic profile suggests that the lithology of the channel fill is rather heterogeneous possibly with sands localy developed in the upper levels. The borehole MUN-1 revealed the predominance of fine-grained, clay-rich sediments and confirmed their large thickness (borehole collapsed at 23.5 m due to water break out).

The boreholes MUN-2 to MUN-7 (see Appendix 4.2.2) and transects M-3, M-4 and M-5 (Figs. 4.3.2-4 and 4.3.2-5) prove the existence of more or less continuous bed of Zliv sandstones (Zliv Fm.) whose extent has been mapped on the surface, with uneven base at < 7 m (e.g., 6.2 m below surface in MUN-2 borehole). The underlying Cretaceous Klikov Fm. is represented mainly by clay-rich sediments. The specific lithology of the sediments reached by MUN-3 borehole, coincident with the steeply dipping contact of high and low resistivity domains in profile M-4, was originally interpreted as a potential fault zone. Its structure was verified in the N-S oriented trench excavated in June 2010. The profiles exposed in nearly 100 m long and locally 4.5 m deep trench (Figs. 4.3.2-6 to 4.3.2-8), however, have not confirmed the existence of the fault.

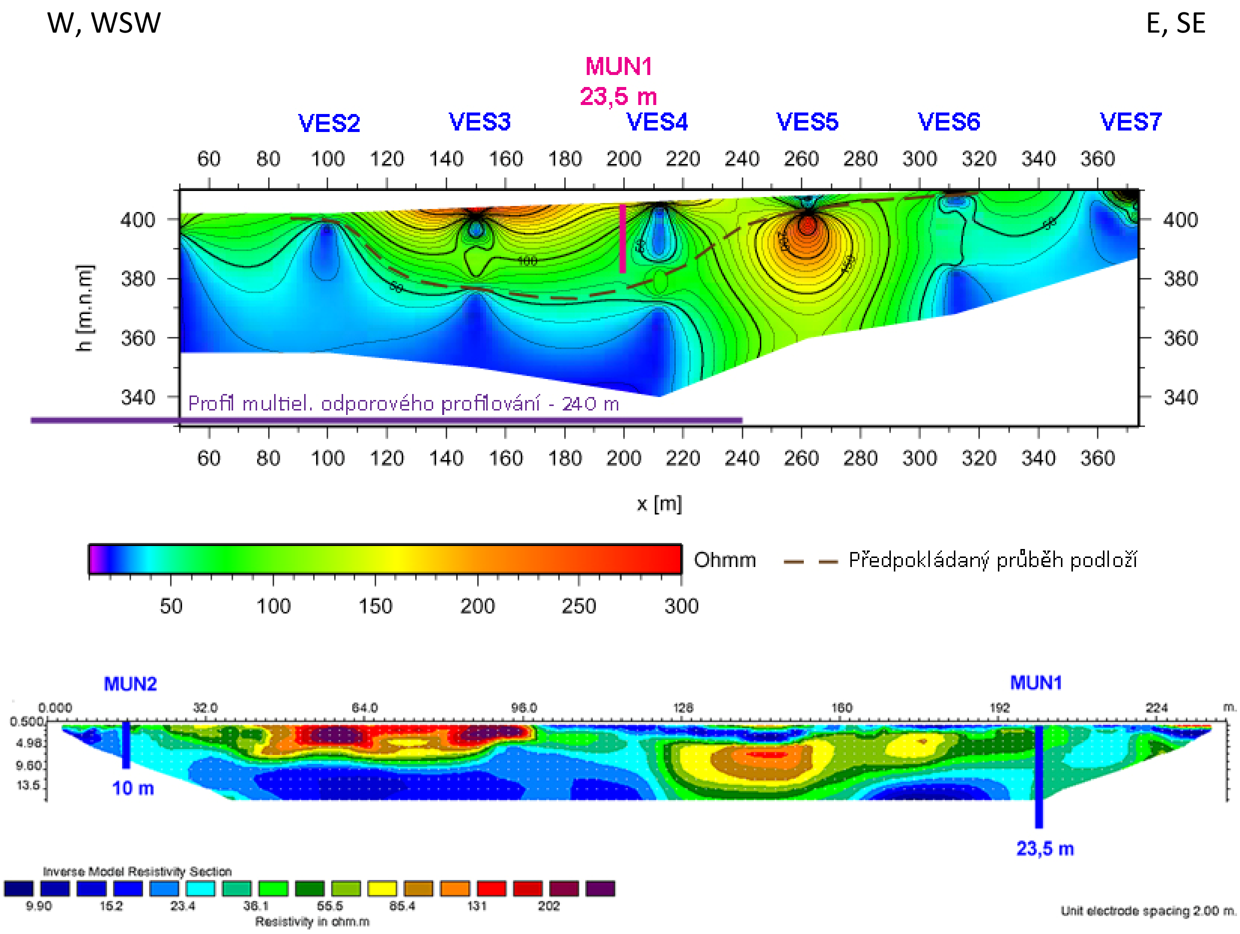

Fig. 4.3.2-3: Electrical resistivity profiles on M-3 transect and position ofboreholes MUN-1 and MUN-2. Top – profile interpolated from vertical electrical sounding. Dashed brown line shows schematically the expected position of Tertiary channel bottom. Violet line shows the extent of the multielectrode profile; Bottom – western part of the transect, tomography from multielectrode measurements. The Tertiary channel is not well defined here - it begins around distance point 100 m and continues to the E. The high resistivity domain in the W part of the profile corresponds to the silicified Zliv sands.

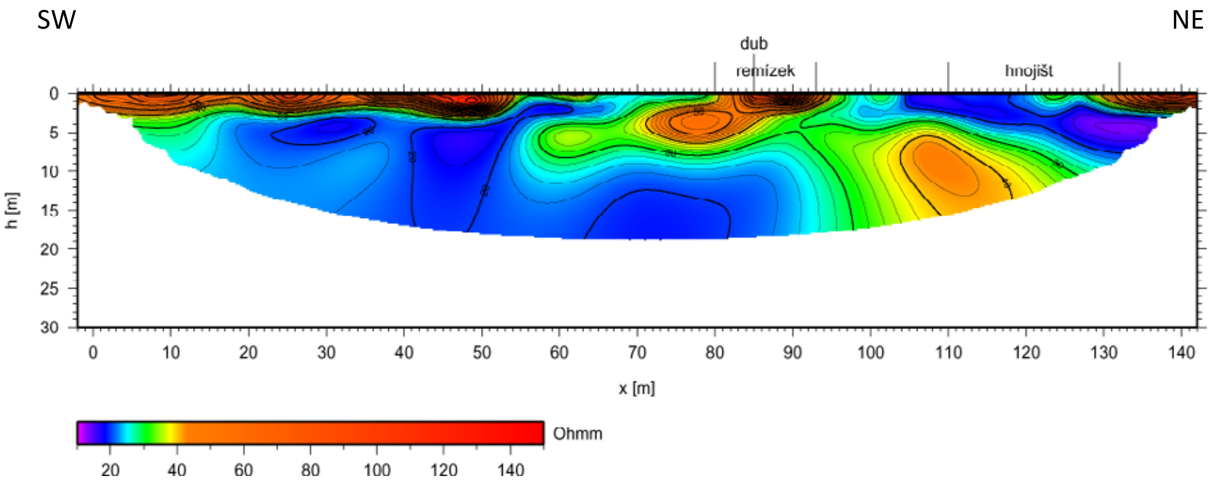

Fig. 4.3.2-4: Electrical resistivity profile M-4.

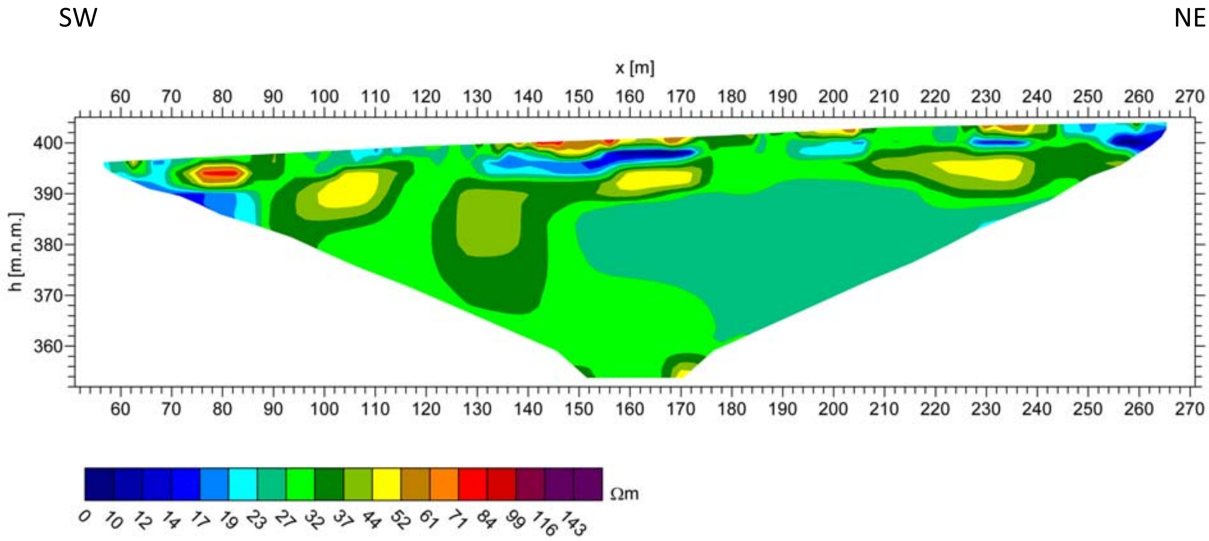

Fig. 4.3.2-5: Electrical resistivity profile M-5.

Fig. 4.3.2-6: The deeper northern part of the Munice trench viewed from south.

Fig. 4.3.2-7: The shallow southern part of the Munice trench (viewed from south).

Fig. 4.3.2-8: Silicified sandstones of the Zliv Fm. exposed in trench.

4.3.3 Hluboká-town (segment 1B)

The trace of the fault segment 1B is located in the central part of the Hluboká town (Figs. 4.3.3-1 and 4.3.3-2). Its position is confined by numerous, mostly shallow engineering boreholes whose descriptions were taken from databases of Geofond archive.

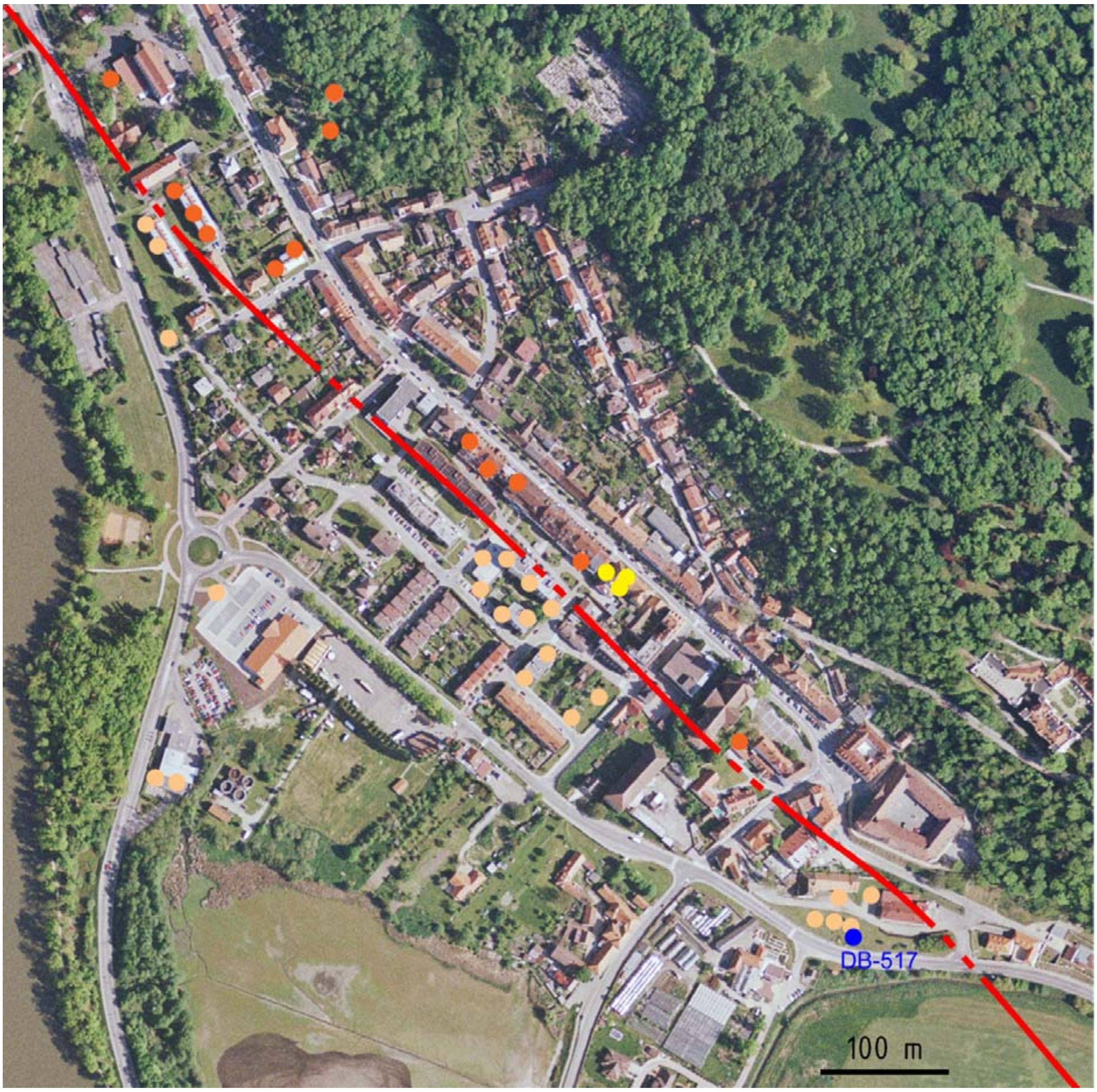

Fig. 4.3.3-1: Situation in the Hluboká-town section showing the boreholes used for mapping of the fault, colour-coded according to the stratigraphy of the Quaternary subcrop: cream yellow – sediments of the Klikov or Mydlovary Fm. (non-differentiated), brick red – crystalline, yellow – probably sandstones of the Zliv Fm. Borehole HRC-1 (DB-517) referred to in text shown as blue dot. Approximate inferred position of the Hluboká Fault shown by red line.

Fig. 4.3.3-2: Overview of the Hluboká town and the fault scarp viewed from SW (Munice pond at the front).

The borehole data suggest that the contact between crystalline rocks and basin sediments follows approximately the local contour line 386 m a.s.l. The description of the HRC-1 borehole (DB-517 in Fig. 4.3.3-1) suggests that this borehole reached the fault plane (Šimůnek et al., 2005) in a depth of approx. 40 m. Detailed information on the fault-related lithologies is not available since the borehole was drilled without core. Nevertheless, taking into account the well-confined surface trace of the fault, it is suggested that the fault has only moderate dip (30-50°) in its upper part.

Three boreholes near the church of Hluboká (V1, V2 a V3; Karlín, 1987, yellow dots in Fig. 4.3.3-1) reached the lithologies strongly reminding of typical development of the silicified Zliv sands at the elevation approx. 388 m a.s.l. The base of these strata was not reached in the shallow boreholes, but it is likely that they lie on top of crystalline rocks.

4.4 SEGMENT 1C AND HYPOTHETICAL SEGMENT H: THE VLTAVA FLOODPLAIN

In its SE part the segment 1 continues with an unchanged azimuth of 120-130° to the Vltava floodplain. The sub-segment 1C is defined between the swimming pool in Hluboká-Podskalí and the southern environs of Zámostí. Here the lithological contact Cretaceous/crystalline is buried beneath the floodplain and older terraces of the Vltava river and its clear gravity indication is offset from the terrain scarp up to 300m to the SW. The detailed survey in this area is described in detail in Chapter 4.4.1.
As stated in Chapter 4.1 we define an additional hypothetical segment H as a structure whose surface trace corresponds to the foot of the the main terrain scarp in the proximity of segments 1C and 2A. The purpose of distinguishing this segment is the dissociation of the linear scarp from the margin of the Cretaceous sediments and its geometrical continuation in the strike close to that of the segment 2 (azimuth 140-145°, see Chapter 4.5).

The situation in the area of fault segments 1C and H is unfavorable with respect to trenching. The fault can not be reached in reasonably shallow level because the sediment thickness is too large. The high level of water table in the Vltava floodplain, high density of mains, major road and ownership situation of private land would further complicate the trenching. As an alternative way of research into the fault slip in Quaternary, we performed the analysis of continuity of Vltava fluvial sediments in broader area adjacent to the above defined fault segments (Fig. 4.4-1).
The fluvial sediments of the Vltava river between České Budějovice and Týn nad Vltavou have been studied by several authors (Ambrož, 1935; Engelman, 1938; Mazáčová, 1961; Bučková, 1962; Chrobok and Mazáčová, 1963; Chábera 1965; Chábera and Novák, 1975). Dating of the terraces was approximate, based solely on the relative elevations above the present-day Vltava river using the analogy with other regions in the Bohemian Massif and the Alps (see Tab. 4.4-1). By this approach, however, the absence of tectonic slip on faults which cross the terrace systems, is assumed *a priori*. Therefore, it was necessary to employ an independent stratigraphical tool to verify the age at a local scale. The OSL dating on quartz (or feldspar) grains was used since organic-rich sediments were absent in the sedimentary sequences studied.

The complex survey in this area included:
1) mapping of the fault trace and of the continuity of Quaternary sediments using geophysical and borehole survey,
2) analysis of the pre-Quaternary sediments and crystalline rocks buried below the Quaternary and cropping out within the fault scarp and,
3) research into the terrace sediments of the Vltava river, including their dating.

Archival data from borehole databases of Geofond were largely used (see Tab. 4.4-2).

The same methodical approach was used for the research in segment 2A, where the situation is similar.

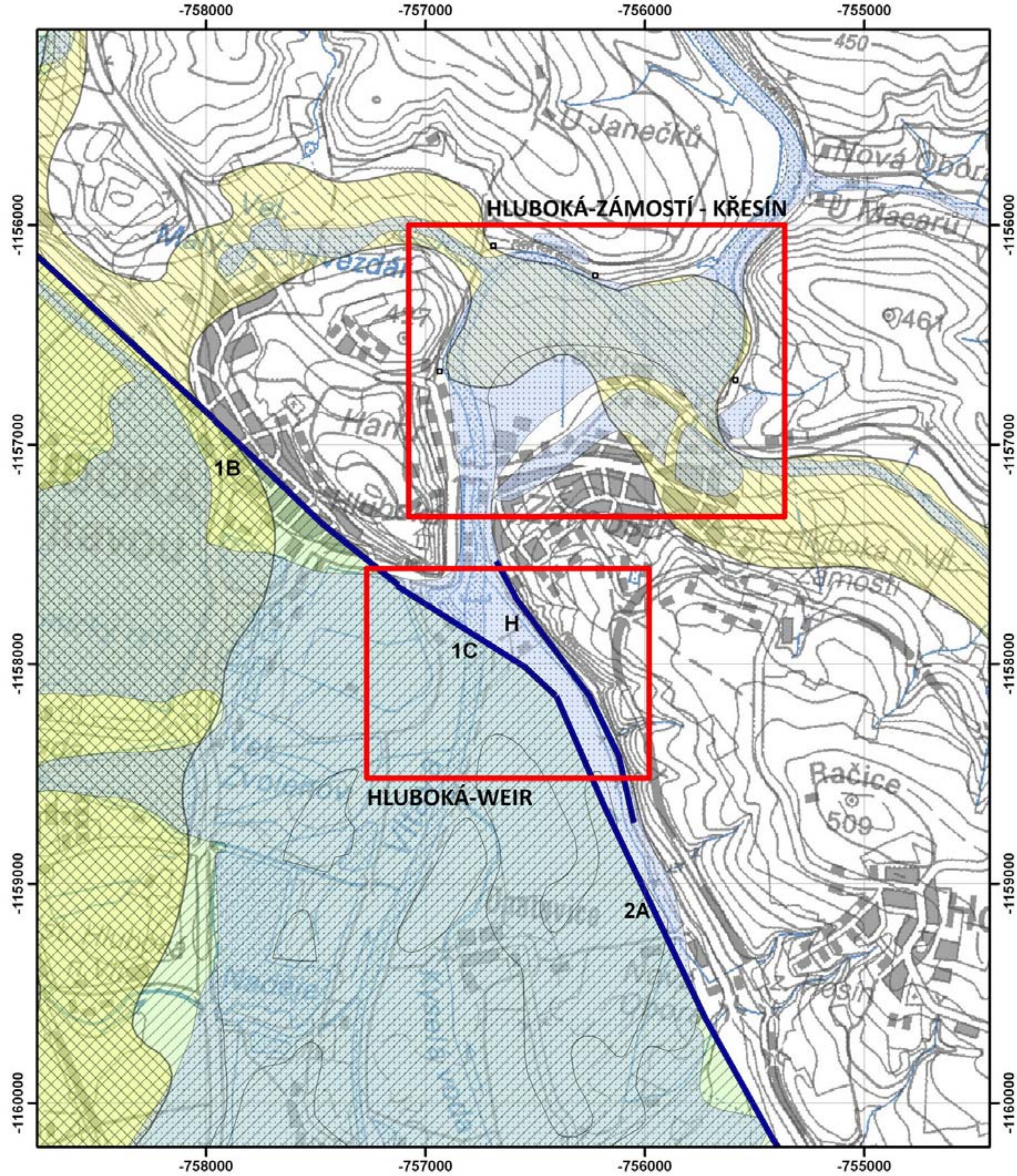

Fig. 4.4-1. Situation map of the investigated area adjacent to the fault segments 1C and H. Yellow hatched area - sediments of Tertiary Mydlovary Fm.; green hatched area - sediments of Createceous Klikov. Fm.; cross hatched area - Mydlovary Fm. on top of Cretaceous Fm.; blue dotted area - fluvial sediments. Blue line - approximate position of the Hluboká Fault. The approximate extent of two areas of interest given in separate sub-chapters is shown by red rectangles.

Section	Hluboká nad Vlt. – Purkarec		Hluboká nad Vlt.- Týn nad Vltavou		Pašice-Purkarec		environs of Purkarec		Purkarec-Jehnědo		Hluboká nad Vlt.- Týn nad Vltavou	
(Reference)	(Ambrož, 1935)		(Engelman, 1938)		(Mazáčová, 1961)		(Bučková, 1962)		(Chrobok a Mazáčová, 1963)		(Chábera and Novák, 1975)	
Tertiary	105											
					I.	66-88			61-70		T1	72-74
					II.	51-65			51-62		T2	56-58
Donau	middle terrace	50-55			III.	43-52			I.	43-56	I.	47-53
										38-42		
Günz												
					IV.	32-38			II.	32-38	II.	33-39
Mindel	lower terrace	20-25			V.	18-28	I.	20-25	III.	17-28	III.	17-29
			O-Terasse	15-20	VI.	10-20	IIa.	15-22/25	IV.	10-20	IV.	10-21
Riss							II.	10-15				
					VII.	6 -13	III.	5/6-7/10	Va.	6-13	Va.	8-14
			U-Terasse	5-10	VIII.	3-10	IV.	3-5/6	Vb.	3-10	Vb.	3-10
									VI.	?-3	VI	-1-4
Würm					floodplain sediments				VII.	?-1,5	VII.	-1-2

In Mindel, Riss and Würm the first and second numbers correspond respectively to the lowest and highest relative elevations of the terrace base and top above Vltava. In older terraces (Günz, Donau, Tertiary) the numbers corrspond to the range of the extent of gravels on relic terraces.

Table 4.4-1. Overview of the classification of Vltava terraces between Hluboká nad Vltavou and Týn nad Vltavou (modified from Chábera and Novák 1975).

Table 4.4-2

Borehole	JTSK coordinates		Z [m a.s.l.]	base Q [m a.s.l.]	Subcrop	Reference
	X	Y				
1/9	-757139	-1158280	372,7	366,3	K	Malecha & Mrázek 1960
B-17	-757752	-1160054	376,8	371,3	K	Volšan 1961
BP-4	-756721	-1158682	373,14	366,64	K	Homolka 2004
HL-1	-756043	-1159262	374,04	358,54	K	Dornič et al. 1966
HL-1	-756741	-1156708	371,73	366,23	N	Šimůnek et al. 1994
HL-10	-756691	-1156808	372,49	368,89	XX	this study
HL-11	-756752	-1156801	372,11	367,56	XX	this study
HL-12	-756361	-1158225	373,39	368,39	K-N	this study
HL-13	-756337	-1158202	373,41	368,51	K-N	this study
HL-14	-756308	-1158178	373,13	367,48	K	this study
HL15	-756253	-1158215	373,68	368,43	XX	this study
HL-2	-755809	-1156395	371,47	363,27	N,XX	Šimůnek et al. 1994
HL-3	-756613	-1158036	374	369,6	K	Šimůnek et al. 1994
HL-4	-756524	-1157955	373,15	369,45	XX	this study
HL-5	-756556	-1157985	373,44	368,04	XX	this study
HL-6	-756571	-1158007	373,21	369,01	K	this study
HL-7	-756219	-1158204	374	368,65	XX	this study
HL-8	-756648	-1158529	373,58	366,48	K-N	this study
HL-9	-756579	-1158435	372,97	368,72	K-N	this study
HP-VI	-756967	-1159375	373,94	367,94	K	Petr 1977
HP-VII	-756935	-1159385	373,94	364,44	K	Petr 1977
HP-VIII	-756939	-1159357	374,05	364,55	K	Petr 1977
HV102	-756720	-1157806	374,39	368,29	XX	Rout 2008
HV103	-756724	-1157762	374,45	367,55	XX	Rout 2008
HV104	-756722	-1157713	374,37	369,17	XX	Rout 2008
HV105	-756720	-1157664	374,47	367,87	XX	Rout 2008
HV106	-756717	-1157613	373,91	368,11	XX	Rout 2008
HV107	-756716	-1157543	373,72	370,32	XX	Rout 2008
J-1	-756703	-1157022	372,75	367,75	XX	Karlín 2007
J-2	-756778	-1157127	370,41	366,51	XX	Pupík 2007
J-2	-756813	-1157009	372,75	367,25	XX	Karlín 2007
JV101	-756721	-1157884	374,35	367,05	XX	Rout 2008
OP-1	-755937	-1159244	374,44	370,64	K	this study
OP-2	-755894	-1159235	374,24	367,74	XX	this study
OP-3	-755816	-1159218	374,3	371,8	XX	this study
OP-4	-755804	-1159214	375,1	372,5	XX	this study
OP-5	-755736	-1159208	388,5	376,9	XX	this study
OP-6	-755721	-1159204	391,2	389,7	XX	this study
PV-503	-756849	-1157447	373,4	368,2	XX	Šetina 1981
PV-504	-756834	-1157446	373,73	367,93	XX	Šetina 1981
PV-505	-756818	-1157445	373,8	368	XX	Šetina 1981
PW555	-756806	-1156216	374,67	369,97	N	Šetina 1981
V1	-756837	-1157865	373,35	367,35	K	Plachký 1999
V1	-756829	-1157549	374,87	368,37	XX	Plachký 1996
V101	-756825	-1157765	374,22	367,22	?	Šimek 2002
V2	-756854	-1157886	373,35	367,05	K	Plachký 1999
V2	-756830	-1157573	375	367,4	XX	Plachký 1996
V3	-756867	-1157867	373,35	367,45	K	Plachký 1999

Borehole	JTSK coordinates		Z [m a.s.l.]	base Q [m a.s.l.]	Subcrop	Reference
	X	Y				
V3	-756830	-1157588	375	369,7	XX	Plachký 1996
V-34	-756754	-1158278	373,4	368,9	K	Chocholáč 1985
V-35	-756858	-1158258	374,8	369,9	K	Chocholáč 1985
V-36	-757002	-1158231	372,4	369,7	K	Chocholáč 1985
V501	-756849	-1157489	373,68	367,98	XX	Šetina 1981
V502	-756829	-1157477	373,64	368,14	XX	Šetina 1981
V-506	-756845	-1157403	373,28	367,48	XX	Šetina 1981
V-507	-756820	-1157401	373,59	367,59	XX	Šetina 1981
V-508	-756831	-1157402	373,73	367,93	XX	Šetina 1981
V-509	-756687	-1157703	374,31	368,31	XX	Šetina 1981
V-510	-756658	-1157685	374,25	368,45	XX	Šetina 1981
V-561	-756877	-1157501	373,94	368,54	XX	Šetina 1981
V-562	-756829	-1157522	374,06	367,46	XX	Šetina 1981
V-563	-756815	-1157529	374,17	367,77	XX	Šetina 1981
V-904	-756580	-1159347	375,66	369,86	K	Cepák 1967
W523	-756282	-1156712	375	367,8	XX	Šetina 1981
W528	-755820	-1156647	370,05	365,25	N	Šetina 1981
W556	-756741	-1156031	378,54	374,94	N	Šetina 1981

Table 4.4-2: List of boreholes used for the research into Quaternary terraces in the areas adjacent to the fault segments 1C and H near Hluboká nad Vltavou. Coding of subcrop stratigraphy: XX - crystalline, K - Cretaceous, N - Neogene.

4.4.1. THE FAULT ZONE AND THE SW WING: HLUBOKÁ WEIR

To the south of the terrain scarp the research was focused on the floodplain of the Vltava river near the Hluboká weir (Fig. 4.4.1-1).

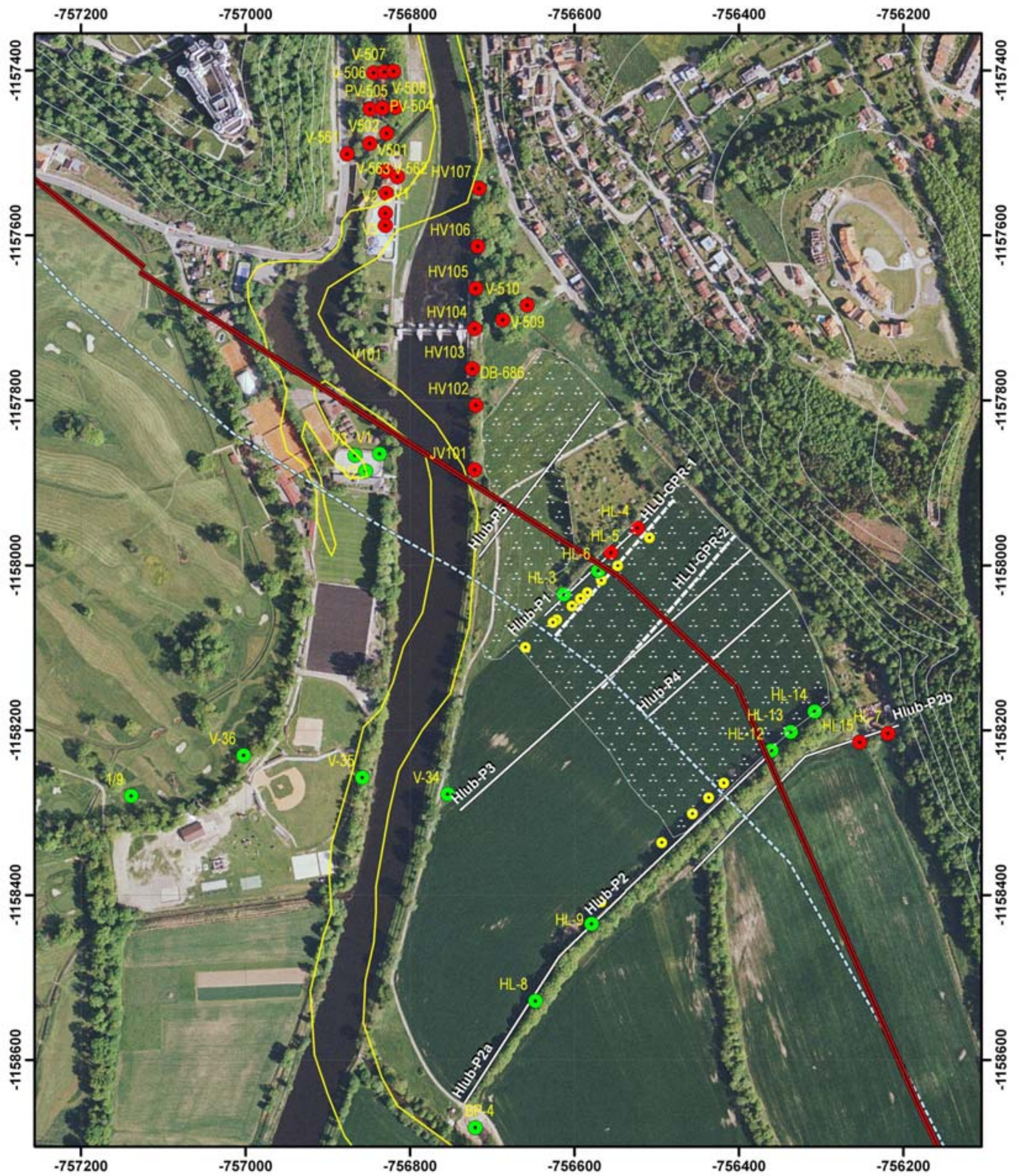

Fig. 4.4.1-1: Situation map of the Hluboká-weir area showing the resisitivity profiles P1-P5 (white solid lines), GPR profiles 1 and 2 (white dashed lines), extent of DEMP measurements (white-dotted area), and boreholes sampling the deep and shallow parts of terraces (large and small circle symbols; colour denoting the reached stratigraphy - red - crystalline, green - pre-Quaternary, yellow - Quaternary). The gravity indication of the main basin margin shown as dashed blue line. The approximate trace of the Hluboká Fault is shown by red line. Yellow lines show the approximate position of Vltava river channel around 1850. S-JTSK grid with 200 m step.

The position of the strong linear maximum of horizontal gravity gradient indicates that the segment 1C of the Hluboká Fault corresponding to the margin of the Cretaceous basin, is buried below the fluvial sediments within the floodplain.

The fault trace does not correspond with the foot of the distinct terrain scarps SE of Hluboká n. Vlt. and in the area of the Hluboká weir it is shifted as far as 300 m basinward. This fault segment, similarily as the major part of the segment 2A, does not display morphological expression at all. However, this does not rule out the continuing vertical slip because the sedimentary environment in the floodplain is highly dynamic and is capable of destroying the growing scarp very quickly. The geometry of the gravity indication suggests that the fault changes its direction from 120° to about 140°. Although higher structural complexity can be expected in this part of the fault zone, we work with a starting simplistic geometrical model in which the segments 1C, 2A and H represent the boundaries of the fault zone. To learn about the possible slip with vertical component in Quaternary we therefore studied the continuity of the terrace sediments across the whole fault zone.

It should be noted that the survey in some parts of this area is complicated by shifting and reshaping of the Vltava channel during the building of the weir near the basin margin in 1930s. The anthropogenic landfill of the old channel is not necessarily easily distinguished from natural sediments which makes the interpretations and lithological correlations difficult in relevant places. The approximate position of the river channel prior to its regulation is shown on the historical map and photographs in Figs. 4.4.1-2 to 4.4.1-4.

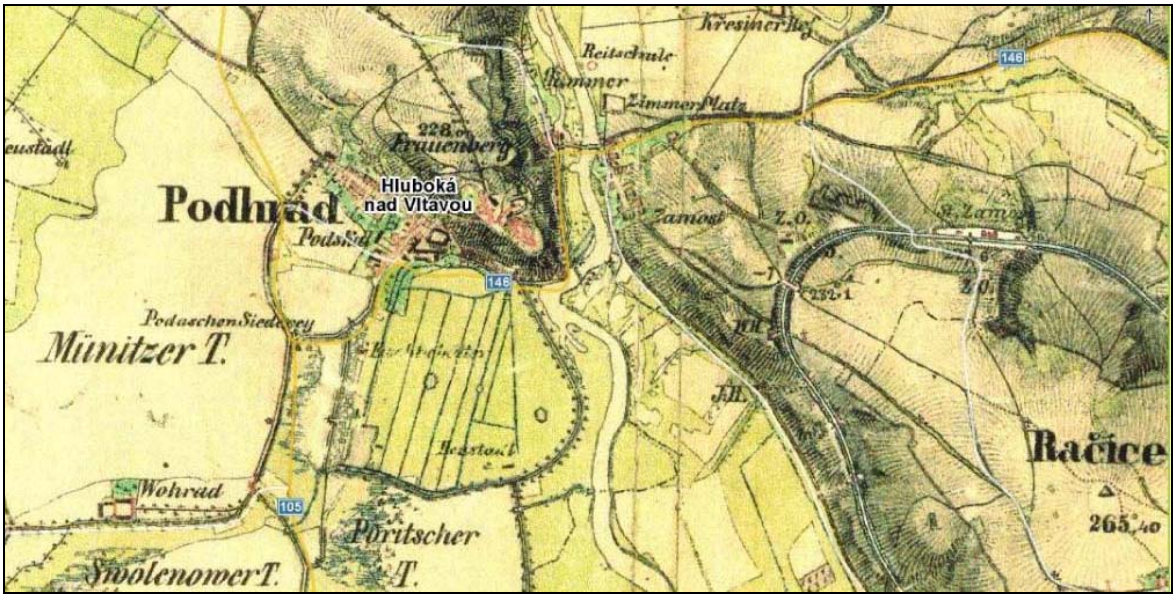

Fig. 4.4.1-2: The 2nd military survey map (Austrian State Archive) from the years 1836-1852 showing the position of the Vltava channel prior to its regulation.

Fig. 4.4.1-3: Historical photography (before the year 1930) showing the original channel of Vltava viewed from south. Courtesy Archive of South-Bohemian Museum in České Budějovice.

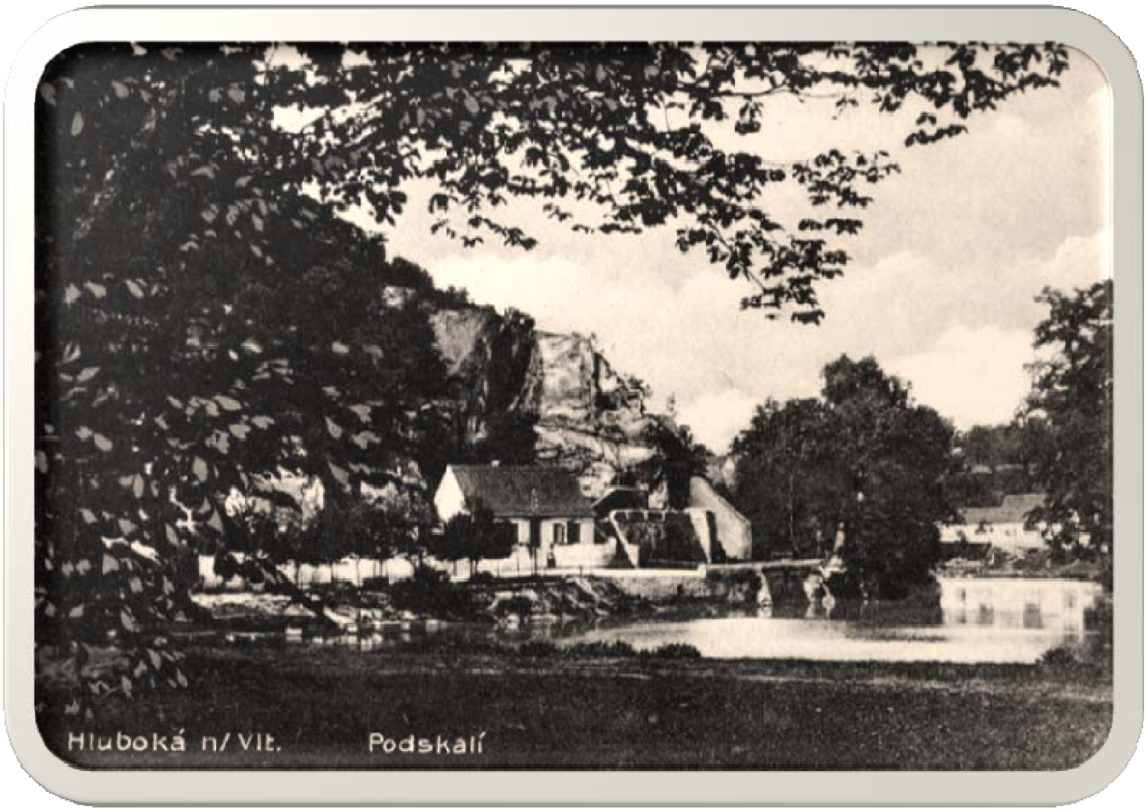

Fig. 4.4.1-4: Historical photography showing the original position of the Vltava channel near the swiming pool in Hluboká-Podskalí, viewed from southwest. Courtesy Archive of South-Bohemian Museum in České Budějovice.

The area of interest was covered by 6 electrical resistivity profiles, Hlub-P1, P2 (+P2a, P2b), P3, P4 and P5. In addition, two 50 MHz GPR profiles were measured, HLU-GPR-1 and 2 and DEMP mapping was performed to roughly approximate the 3D image of the area between the line profiles.
Several boreholes were made along two profiles to study the lithology of Quaternary fluvial sediments and subcropping rocks in detail and to take samples for dating: boreholes HL-3 to HL-6 on Hlub-P1 profile, and HL-7 to HL-9 and HL-12 to HL-15 on the Hlub-P2 profiles (HL-3 borehole was made within older survey in 1983-1985). In addition, several shallow boreholes (HLB-series, manual percussion) were made into the fine-grained upper parts of the terraces within the testing pilot study.

The positions of boreholes and geophysical profiles are shown in Fig. 4.4.1-1. The results of geophysical measurements are given in Appendix 4.2-1 and later in this text. The lithological profiles from boreholes (except the shallow HLB-series) are given in Appendix 4.2-2. The list of boreholes used for mapping of the buried basin margin and for study of the Quaternary sediments is given in Table 4.4-2.

On the profile Hlub-P1 and farther to the west the continuation of crystalline rocks away from the terrain scarp into the basin are confirmed by a number of borholes which reach the base of Quaternary terraces.

In the eastern part, on the profile Hlub-P2, however, the crystalline rocks or their residua were not reached in analogous positions behind the gravity indication of the basin margin. The boreholes indicate that the subcrop of the river terraces is formed by variegated clay-rich sediments with unclear stratigraphical position, which have a minimum thickness of 8 m in HL-14 borehole. The crystalline in shallow depths was only confirmed much closer to the foot of the terrain scarp than indicated in the gravity field. The structural interpretation is problematic mainly because of the uncertain stratigraphy of the sediments with untypical lithology which can be of both Cretaceous or Tertiary age.

Unfortunately, the geophysical profiles do not bring much light into the problem. The variability of the resistivity on the interpreted sections indicates a rather complicated lithology, varying both in horizontal and vertical directions. In deeper parts of the sections many apparent steep to vertical boundaries can be observed, which are, however, difficult to clearly associate with the faults.

Pre-Quaternary sediments of the Budějovice Basin

The extent of pre-Quaternary sediments beneath the Quaternary fluvial terraces of the Vltava is shown in Fig. 4.4.1-1 (borehole symbols) together with its spatial relation to the gravity indicaton of the basin margin.

In spite of clear lithological differences betwen the Cretaceous Klikov Fm. and younger Tertiary sediments on a regional scale (e.g., Slánská 1963), the petrographical and mineralogical similarity of some lithologies makes their distinction problematic when studied in short profiles on a local scale. This is also the case of the SE part of area studied, where clay- and silt-rich sediments of variable colours underlie the Quaternary fluvial sediments. Unlike the light-grey to white sands and sandstones with kaoline-rich matrix reached in the boreholes HL-3 and HL-6, which are characteristic for the Klikov Formation, the lithology of these sediments does not correspond with characteristic development of the Klikov Formation and they can represent younger strata. On the other hand, beds of kaoline-rich sands similar to those described above, were reached also in boreholes HL-12 and HL-14. The X-ray diffractometry of the clay-rich sediments revealed the predominance of well organised 1T-type kaolinite, which is characteristic for Klikov Fm. according to Slánská (1963). However, the low elevation of the base of Mydlovary Fm. in adjacent area to the west allows that these sediments eventually represent the top of the Cretaceous rocks resedimented over short distances (without change in mineralogy) in Neogene.

In any case, the extent of the pre-Quaternary sediments beyond the gravity indication of the basin margin, closer to the terrain scarp, indicates a step-like geometry of the sub-Quaternary crystalline ledge. This geometry can be a result of (1) subsidence of a small-scale crystalline block with Cretaceous cover between multiple faults, (2) formation of erosional pediment within crystalline at the foot of the single fault scarp and subsequent deposition of >8m thick post-Klikov Fm. sediments on top of it, or (3) combination of both scenarios.

It is necessary to stress, however, that independent of lithology, all pre-Quaternary sediments in the boreholes display sub-horizontal bedding, which indicates that they were not affected by deformation related to the fault slip (see Fig. 4.4.1-5).

Fig. 4.4.1-5. Photograph of part of the core from HL-6 borehole, cut along two perpendicular planes. Kaolinic sands/sandstones, probably belonging to the Klikov Fm., display sub-horizontal bedding. The bending of the strata is a result of core deformation during drilling.

Quaternary fluvial sediments

Quaternary fluvial sediments cover the whole flat terrain in front of the narrow valley near the weir and, according to the geological maps, they extend to the Munice pond in the west.

Pleistocene sediments are mainly represented by clast-supported sandy gravels of Würmian age and silts/clays to sands of Holocene age (see Table 4.4.1-1). Quartz, migmatites, quartzites, granulites and gneisses dominate in the pebble material of gravels.

The total thickness of Quaternary sediments is 4-6 m, locally 7-9.5 m. Farther to south (near Opatovice) larger thickness reaching 15 m has been reported from HL-1 borehole, but we believe that such extreme value could be affected by technical problems usually encountered when drilling water-saturated loose gravels.

The results of DEMP mapping indicate lateral lithological variability in the upper part of the floodplain (Fig. 4.4.1-6), which agrees with the observations made in shallow boreholes and with the results of the electrical resistivity profiles. Gravels often reach the shallowest ploughed levels, as indicated by visual mapping and DEMP measurements. Together, the geophysical measurements indicate that the high resistivity gravels form more or less continuous bed, which may only locally disintegrate into fragmented structure.

Detailed geophysical and borehole survey allowed the construction of conceptual structural models of the fluvial sediments on top of the buried basin margin along two profiles, P1 and P2+P2a+P2b (Figs. 4.4.1-6 to 4.4.1-8).

The data suggest that the fluvial Quaternary terraces have uneven base with local, mostly long-period depressions with amplitudes of up to 3-4 m. We assume that these structural depressions represent abandoned channel segments and their position is linked to local river dynamics, perhaps also partly controlled by the lithology of subcropping sediments. It is often seen in boreholes that the onlap of gravels over clays is sharp, with mixing zone 20 cm or thinner, while the contact zone of gravels with subcropping sands and silts is thicker. We assume that the clay-rich domains tend to be associated with elevations in the base of Quaternary, owing to their higher resistance to erosion in river channel bottom.

No indication by any of the survey method (including GPR, see Appendix 4.2-1) of tectonic discontinuity in the Quaternary terraces was found near the contact of Cretaceous sediments and crystalline rocks located by boreholes or in the area of the gravity indication of the basin margin.

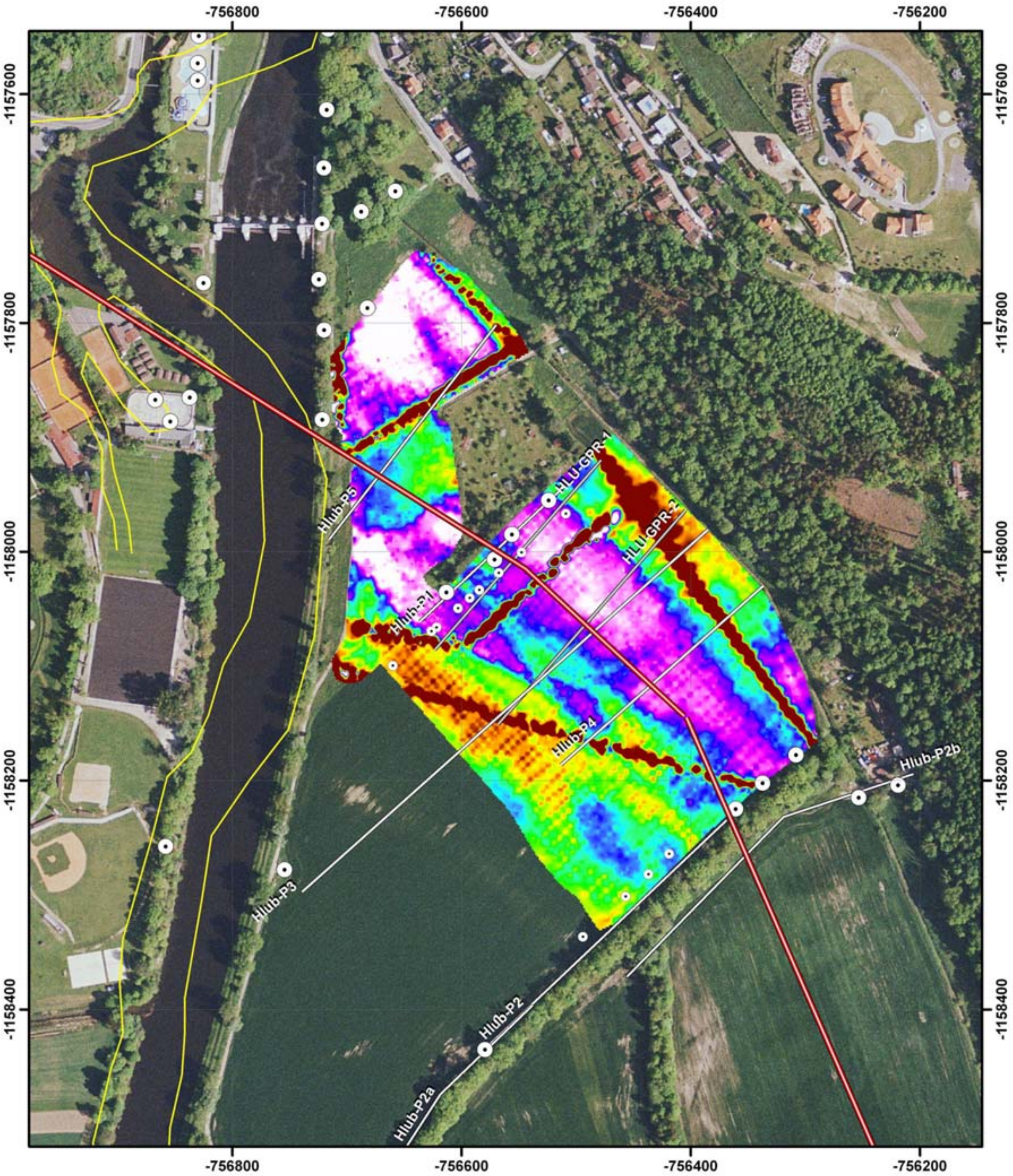

Fig 4.4.1-6: Electrical conductivity map of the floodplain on right riverbank of the Vltava river, measured by DEMP method. Effective values are integrated from approximate interval 0-8 m. The variations correspond primarily to the extent of sediments with different grain size (gravels - low values, white and violet; silts/clays - high values, green and yellow). Linear maxima are response to four subsurface artificial conductors. Authors: A. Létal and P. Špaček. Positions of boreholes, geophysical profiles are also shown (white symbols) together with approximate position of the Hluboká Fault trace.

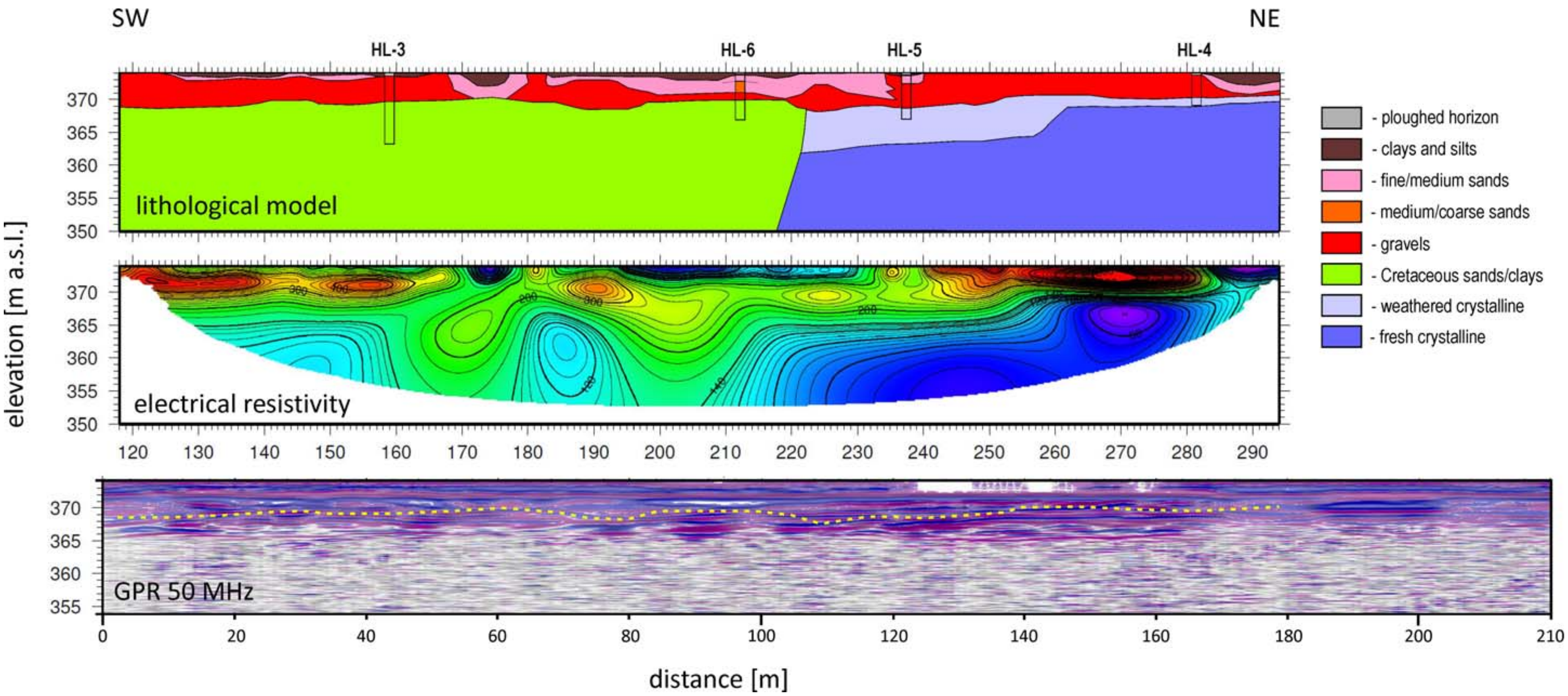

Fig. 4.4.1-7. Profile Hlub-P1. Detailed lithological model based on the boreholes HL-3 - HL-6, the electrical resistivity profile, and GPR profile (50MHz). Yellow dotted line on GPR profile shows the base of Quaternary inferred from the resisitivity profile and boreholes. Note that the GPR profile is offset up to 25 m from the resistivity profile with boreholes. Non-exaggerated.

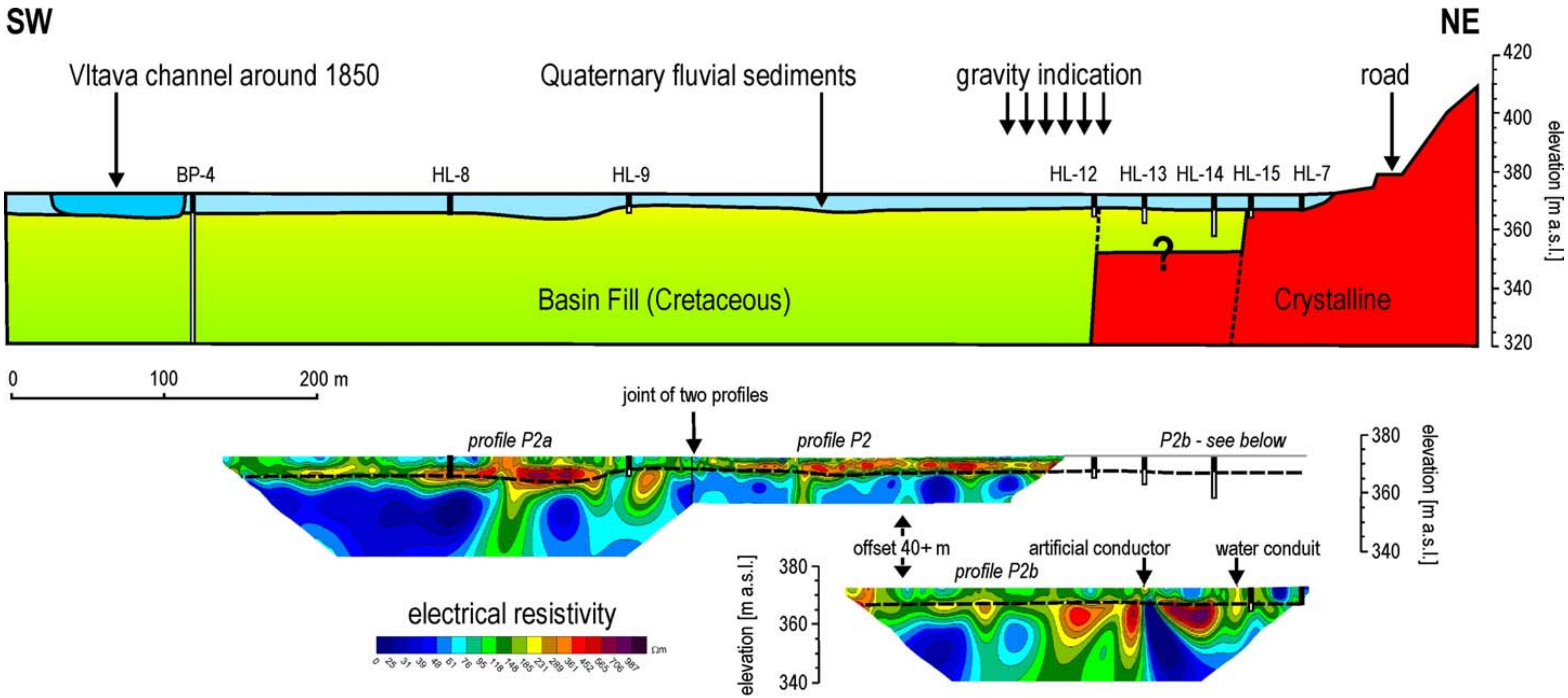

Fig. 4.4.1-8: Profile Hlub-P2+P2a+P2b. Schematical conceptual model of the basin margin showing the thickness of fluvial Quaternary sediments and the assumed step-like margin of the basin (top), based on the borehole survey and geophysical data (below). Profile P2b with boreholes HL-7 and HL-15 is offset 40 m and more from the profile P2. Subhorizontal dashed lines show the approximate base of Quaternary. Steep dashed lines show schematically possible faults. Vertical exaggeration approximately 2×.

The sediments of terraces were dated by OSL method on 10 samples from selected boreholes. In some of these boreholes, only the upper parts of the sequence could be dated, because of the absence of fine-grained fraction in well-sorted gravels (HL-5, HL-6). The results suggest the existence of continuous Late Pleistocene to Holocene sequence uninterrupted by vertical offset on faults (Table 4.4.1-1, comp. with map in Fig. 4.4.1-1).

sample	**elevation [m a.s.l.]**	**lithology, position**	**age [ka ± 1 σ]**	**method, laboratory**
HL-4D	369.6	sandy matrix of gravels, base of terrace above crystalline	22.20 ± 1.6	quartz, Sheffield
HL-5A	372.4	fine-grained sand, upper part of terrace above crystalline	13.20 ± 0.80	quartz, Sheffield
HL-5B	371.9	fine-grained sand, upper part of terrace above crystalline	13.80 ± 0.70	quartz, Sheffield
HL-6A	372.6	loamy, fine- to medium-grained sand, uppermost part of terrace above Cretaceous sands	8.90 ± 0.50	quartz, Sheffield
HL-6C	371.9	fine- to medium-grained sand, upper part of terrace above Cretaceous sands	14.70 ± 0.80	quartz, Sheffield
HL-8-1	372.2	loamy sand, upper part of terrace above Cretaceous clays	7.08 ± 0.68	feldspar, Vienna, Decker et al. 2010b
HL-8-3	369.3	sandy matrix of gravels, middle part of terrace above Cretaceous clays	48.62 ± 4.80	feldspar, Vienna, Decker et al. 2010b
HL-8-4	368.3	matrix of sand-rich layer in sandy gravels, lower part of terrace above Cretaceous clays	78.80 ± 8.35	feldspar, Vienna, Decker et al. 2010b
HL-12E	368.6	sandy matrix of gravels, base of terrace above ?Cretaceous sands	53.50 ± 4.00	quartz, Sheffield
HL-14C	368.9	sandy matrix of gravels, lower part of terrace above ?Cretaceous sands	41.40 ± 3.50	quartz, Sheffield

Table 4.4.1-1: Samples from locality Hluboká-weir dated by OSL method.

4.4.2. NE FAULT WING: HLUBOKÁ-ZÁMOSTÍ – KŘESÍN

Although not closely spatially associated with the Hluboká Fault, the area Hluboká-Zámostí – Křesín forms the immediate NE wing of the hypothetical segment H. Hosting the terraces of the Vltava river, it carries useful information for comparing the relative elevations of Quaternary sediments with same age across both wings of the fault (se Fig. 4.4.2-1).

Unfortunately, the extent and density of urbanised area complicates the situation in this area. The research in the lower river terraces is limited by the regulations at the right riverbank, in the area of top-water-level of the Hněvkovice reservoir in Hluboká-Zámostí. In case of higher terraces, the research is also strongly limited by their small extent (only relics are preserved), which often disallows ruling out the possibility of post-accumulation transport in alluvial/proluvial environment due to solifluction.

A characteristic morphological feature of this area is the natural amphitheatre formed at the crossing of two channel systems – the „Northern Channel" filled with sediments of Neogene age and the present-day Vltava river valley with lower terrace filled with Pleistocene and Holocene sediments (Figs. 4.4-1, 4.4.2-1). While the Northern Channel was probably formed by a river flowing generally to the south, the present-day Vltava flows in the opposite direction, to the north (Fig. 4.4.2-2).

The correlated occurences of Neogene sediments (Mydlovary Formation) with bases generally lowering in a southward direction seem to form a relic of a single, once continuous channel system (Šimůnek et al., 1995). In the area under study the Neogene sediments form a continuous body on the line Dobřejovice - Luční potok valley - Křesín - Zámostí - Malý a Velký Hvězdář Ponds - Munice Pond further continuing to the Pištín Graben in the central part of the Budějovice basin (see Chapter 4.3). In the area Křesín-Zámostí the Neogene sediments were verified by several boreholes, one of which reached their base on top of crystalline subcrop (HL-2, Fig. 4.4.2-1 and Table 4.4-2).

The sediments of the lower Quaternary terrace cover crystalline rocks and Neogene sediments, having the thickness of 4-8 m. Unfortunately, in this area only 5 boreholes are available in the floodplain and it is not possible to draw a complete detailed model of the terrace. Large parts of the floodplain have been regulated and modified anthropogenically into depths of at least 2 m (Fig. 4.4.2-1). Two new boreholes, HL-10 and HL-11 were made, but for technical reasons, we were not able to make more boreholes into deper parts of the lower terrace (see the proposal of continuation of the research in Chapter 6).

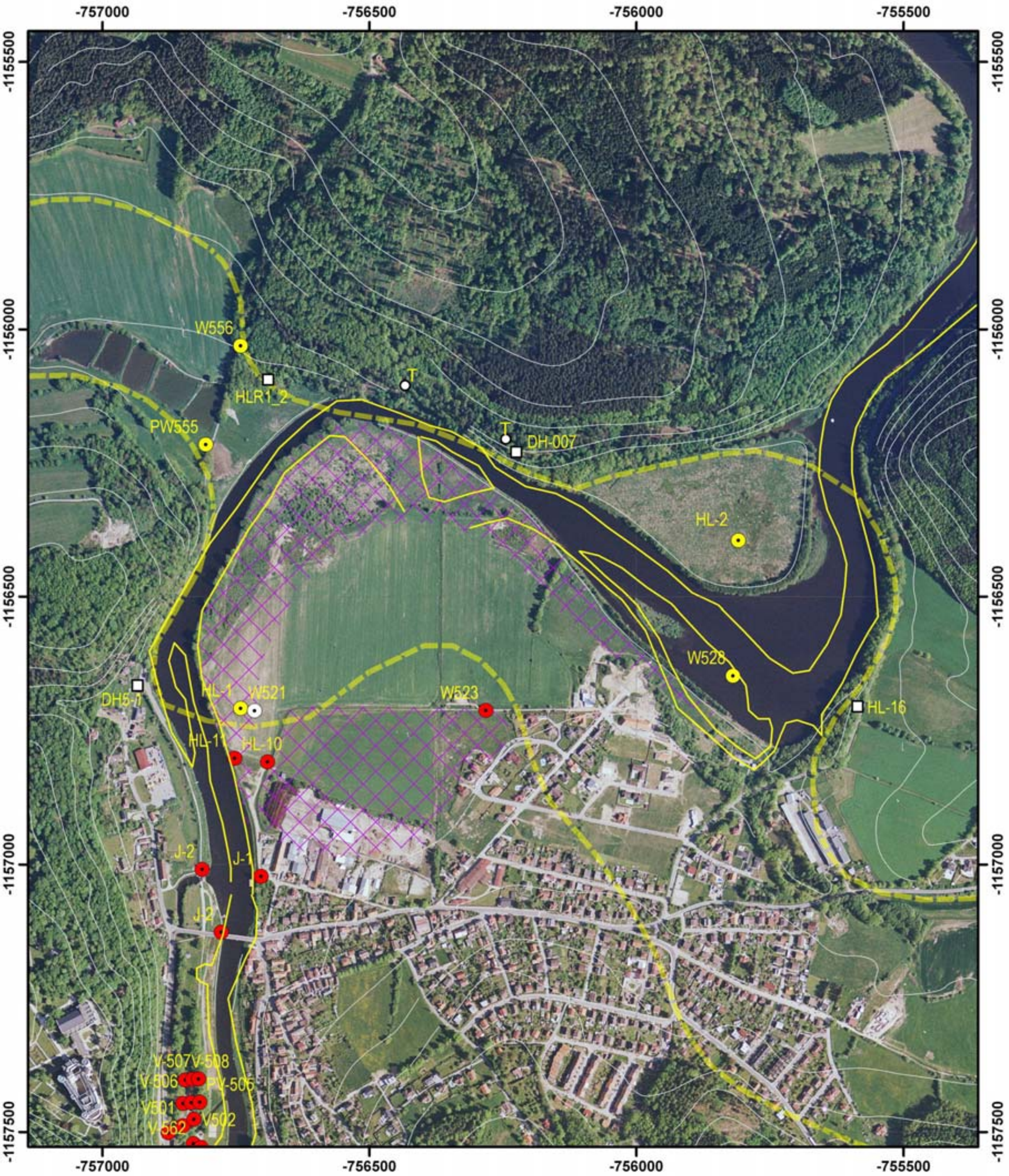

Fig. 4.4.2-1: Situation map of the area Hluboká-Zámostí – Křesín showing the boreholes used for modeling of Quaternary terraces (circles with colour denoting the subcropping stratigraphy - red - crystalline, yellow - Neogene, white - unknown). White squares show sampling sites in Quaternary of higher levels. Purple cross-hatching shows the main areas of anthropogenic modifications in the floodplain. Bold dashed yellow line shows the approximate extent of Neogene sediments. Thin yellow line shows the approximate position of Vltava river channel around 1850. White lines are relief contour lines with 10 m step. S-JTSK grid with 500 m step.

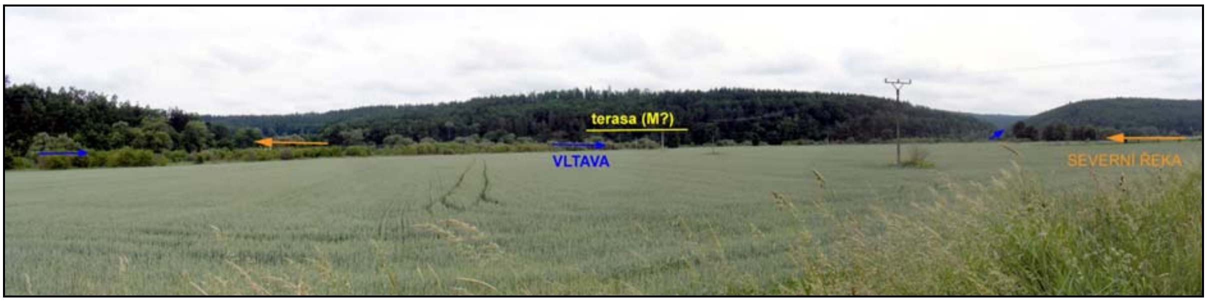

Fig. 4.4.2-2: View of the northern slope of the valley near Hluboká-Křesín. Flow directions of Vltava and „Northern Channel" river are indicated by orange and blue arrows, respectively. Yellow line shows the top of relict higher terrace. Viewed from south.

Fig. 4.4.2-3: Relic of higher terrace with sandy gravels preserved on a platform shown in Fig. 4.4.2-2.

Similarly as in the area of Hluboká weir, the lower part of the terrace is represented by clast-supported coarse-grained gravels 2-5 m thick, with the base reaching locally the elevation of 363.3 m a.s.l. (HL-2 borehole). On top of the gravels up to 3 m thick loamy sediments are developed.

Dating of the lower terrace is restricted to borehole HL-11, which is situated very close to the present-day river channel, in the place with moderate thickness of Quaternary. The lowest parts of the terrace thus remain undated. The OSL dating revealed that both sands from the middle parts and gravels from the base of the Quaternary sequence are of Holocene age (Table 4.4.2-1). This is in accordance with the occurence of hard crystalline rocks in the bottom of the present-day Vltava channel in the narrow neck of the valley in Hluboká-Zámostí, which suggests that the older (Late Pleistocene, Würm) terraces were destroyed by continuing erosion in the river channel and are not preserved in some parts of this area. We assume, however, that Würmian sediments are represented in the lower parts of the terrace downstream, which are well below the present-day bottom of the river channel. We also can not rule out that these deeper terraces are actually preserved in paleo-thalweg to the west of borehole HL-11, since somewhat larger thickness of Quaternary sediments is also documented in borehole J-2 situated >200 m upstream (Fig. 4.4.2-1 and Table 4.4-2, Karlín 2007).

The relict character of higher terraces makes their recognition and dating problematic and it should be complemented by further research in future.

A prominent relic of old terrace was found on top of the rocky slopes in the left part of the river valley, north of Zámostí (Fig. 4.4.2-1, marked by *T* letters). The terrace is represented by sub-horizontally bedded sandy gravels and the elevation of its top level is 393,90 (west) to 391,85 (east) m a.s.l., i.e. approximately 24 m above the Vltava river. The base of the terrace lies at approximately 387 m a.s.l. The OSL dating of the sandy matrix of gravels performed by AIP team revealed an age of > 140 ka (sample DH-007, Decker et al. 2010b). According to classification of Chábera and Novák, 1975 (Tab. 4.4-1) the elevation corresponds to older Mindel, when the absence of tectonic offsets is assumed.

At the NE periphery of Hluboká-Zámostí, near the road Hluboká-Poněšice a >2 m thick relic of Quaternary sediments of alluvial/fluvial character is exposed in a landslide cut-off (Fig. 4.4.2-4). The sequence is formed by sands hosting approx. 40 cm thick bed of sandy gravels. The base elevation is approx. 381 m a.s.l., i.e. 13.2 m above the reconstructed Vltava surface-level. Although the gravel material is probably fluvial in origin, re-deposition in alluvial/proluvial environment can not be ruled out. Furthermore, strong re-working by cryoturbation is indicated for the whole sequence. One of the samples taken by AIP team was dated by OSL method, giving Late Pleistocene, early Würmian age (D. Homolová, pers. comm.).

At lower elevations the sediments of possible fluvial origin were studied in two localities. The well-sorted sands were sampled in a shallow probe HLR5-1 in the left bank of the river in the „Northern Channel“, in the elevation 375 m a.s.l. The OSL dating performed by AIP team (Decker et al. 2010b) reveals Late Pleistocene age. Similar age has been determined for clay-laminated sands studied by D. Homolová in an artificial outcrop in the slope of the left part of the valley 376 m a.s.l. (sample DH5-1). Although the fluvial origin is assumed by AIP team (Decker et al. 2010b), the dated sediments do not form characteristic terrace morphology and other sedimentary environment can not be ruled out.

sample	elevation [m a.s.l.]	lithology, position	age [ka ± 1 σ]	method, laboratory
HL-11B	370.26	sandy matrix of gravels, top of terrace above crystalline; likely anthropogenic influence	33.80 ± 2.0*	quartz, Sheffield
HL-11C	369.61	fine-grained sand, upper part of terrace above crystalline	3.42 ± 0.17	quartz, Sheffield
HL-11C	369.61	same sample as above, dated in two laboratories to cross-compare the methodologies	4.45 ± 0.44	feldspar, Vienna, Decker et al. 2010b
HL-11D	367.61	sandy matrix of gravels, base of terrace above crystalline	8.90 ± 0.50	quartz, Sheffield
DH-007	388.1	sandy matrix of gravels (rusty colour), artificial outcrop (roadcut) with relic of high terrace	> 140	feldspar, Vienna, Decker et al. 2010b
DH5-1	376.0	clay-laminated sand, outcrop in the wall of the river valley	23.42 ± 2.54	feldspar, Vienna, Decker et al. 2010b
HLR1_2	375.0	silty sand with gravel, 1 m deep probe below soil in slightly sloping terrain	23.33 ± 2.29	feldspar, Vienna, Decker et al. 2010b
HL-16	381.8	sand with gravel, relic of sediments above crystalline, profile in the landslide cut-off	to be specified	feldspar, Vienna, D. Homolová, pers. comm.

*Table 4.4.2-1: Samples from area Hluboká-Zámostí - Křesín dated by OSL method. Included are samples taken and dated by AIP team in Vienna. *) The unrealistic age of the sample HL-11B indicates the anthropogenic overturning of the sequence in its upper part.*

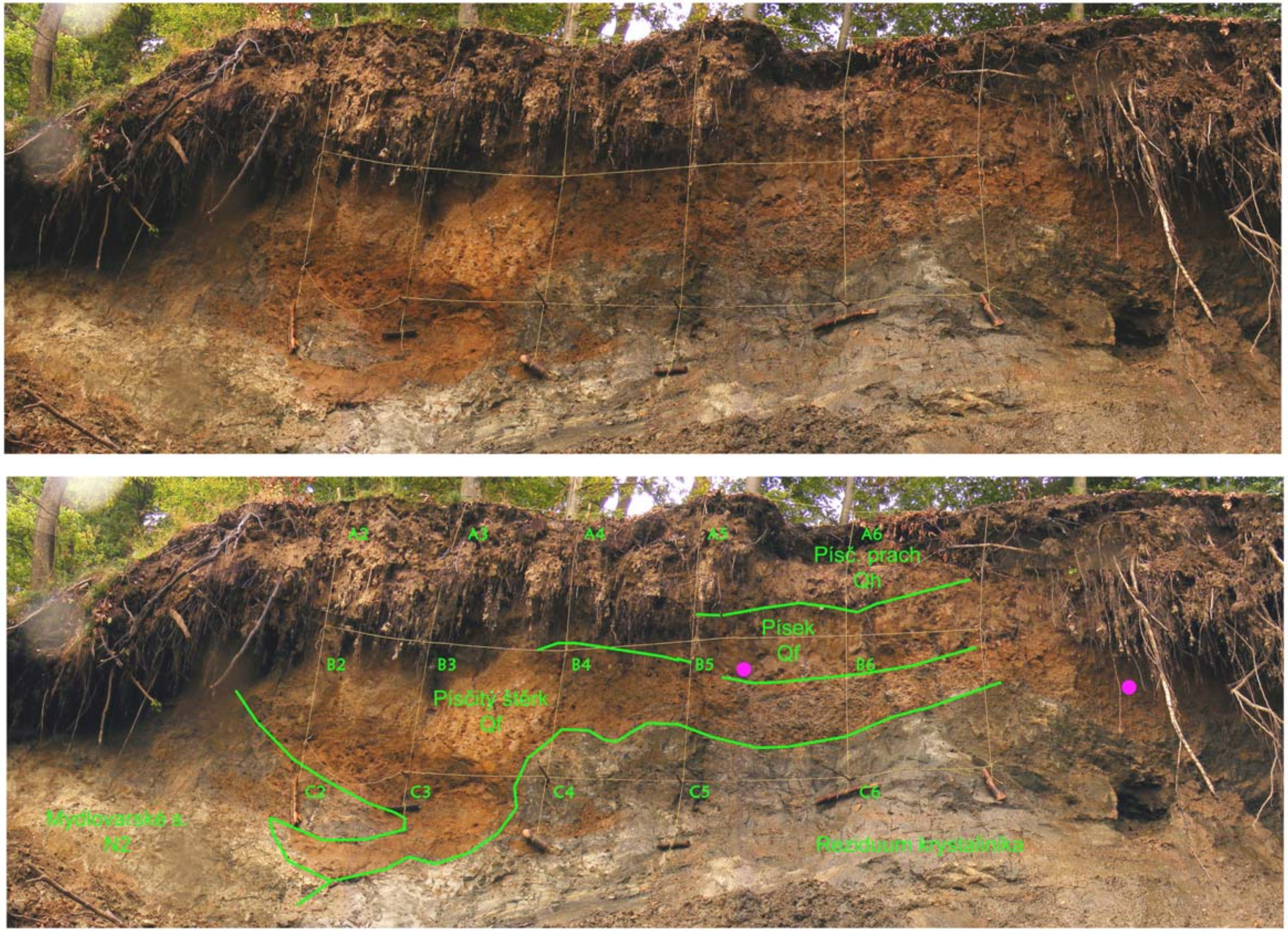

Fig 4.4.2-4: A profile through relict Quaternary sediments residing on weathered crystalline rocks, landslide cut-off near Zámostí – Křesín (photograph and simple log). Location of samples for OSL dating (HL-16) shown by purple dots. Grid step: 2 m.

4.4.3 CONTINUITY OF THE LOWER RIVER TERRACE ACROSS THE FAULT ZONE

As outlined above, in the area of Vltava floodplain in the eastern neigbourhood of Hluboká nad Vltavou the fault zone is defined by verified segments 1C and 2A which form the main margin of Cretaceous basin, and hypothetical segment H which is associated with a prominent terrain scarp. Although we can expect rather complicated geometry of the fault zone in the area where these fault segments meet, we made a simplistic working model with three blocks divided by these segments: block A, representing the main part of the basin, southwest of the segments 1C+2A, block B, representing the transition between basin and crystalline between the segments 1+2 and H, and block C, representing the crystalline to the northeast of the segment H (Fig. 4.4.3-1). Our main aim was to test the continuity of the terrace sediments across the whole fault zone to learn about the possible slip with vertical component in Quaternary. As explained above, we focused on the lower terrace in this phase of research, since the sampling of the relict higher terraces was problematic.

We compiled the database of geological profiles from all available boreholes which reached the base of fluvial Quaternary sediments in the area (Fig. 4.4.3-1). Then we analysed the variations in elevation of its base, which could be due to vertical offsets on the fault zone. The schematic longitudinal (river-parallel) profile across the basin margin showing the thickness of Quaternary fluvial terrace is given in Fig. 4.4.3-2.

In spite of considerable lateral variability of the local bases of the lower Vltava terrace, the smoothed base level is similar, at approx. 3.5 - 4 m below the reconstructed Vltava surface-level (prior to river damming) in both the basin (block A) and on top of crystalline (block C). In several boreholes a deeper base level is indicated, both in block A (>6 m below Vltava surface-level in HP-VII and HP-VIII boreholes near Opatovice) and block C (>5 m below Vltava surface-level in borehole HL-2 near Křesín). Even larger thickness was reported from HL-1 borehole near Opatovice, but we believe this to be an artifact (see Chapter 4.4.1). On the other hand, in the narrowest part of the Vltava valley, the depth of the terrace base below Vltava surface-level seems not to exceed 2.5 - 3 m which suggests the existence of local, 1-2 m high elevation of crystalline riverbed roughly between the Hluboká weir and the bridge in Hluboká-Zámostí. However, this can also be an artifact, because the valley is narrow and none of the boreholes in this area is located in the thalweg.

Regardless of these observations, the mean thickness of the lower Vltava terrace in the basin and on top of crystalline is comparable and no substantial vertical offset of block A relatively to block C is indicated after the deposition of the lower terrace.

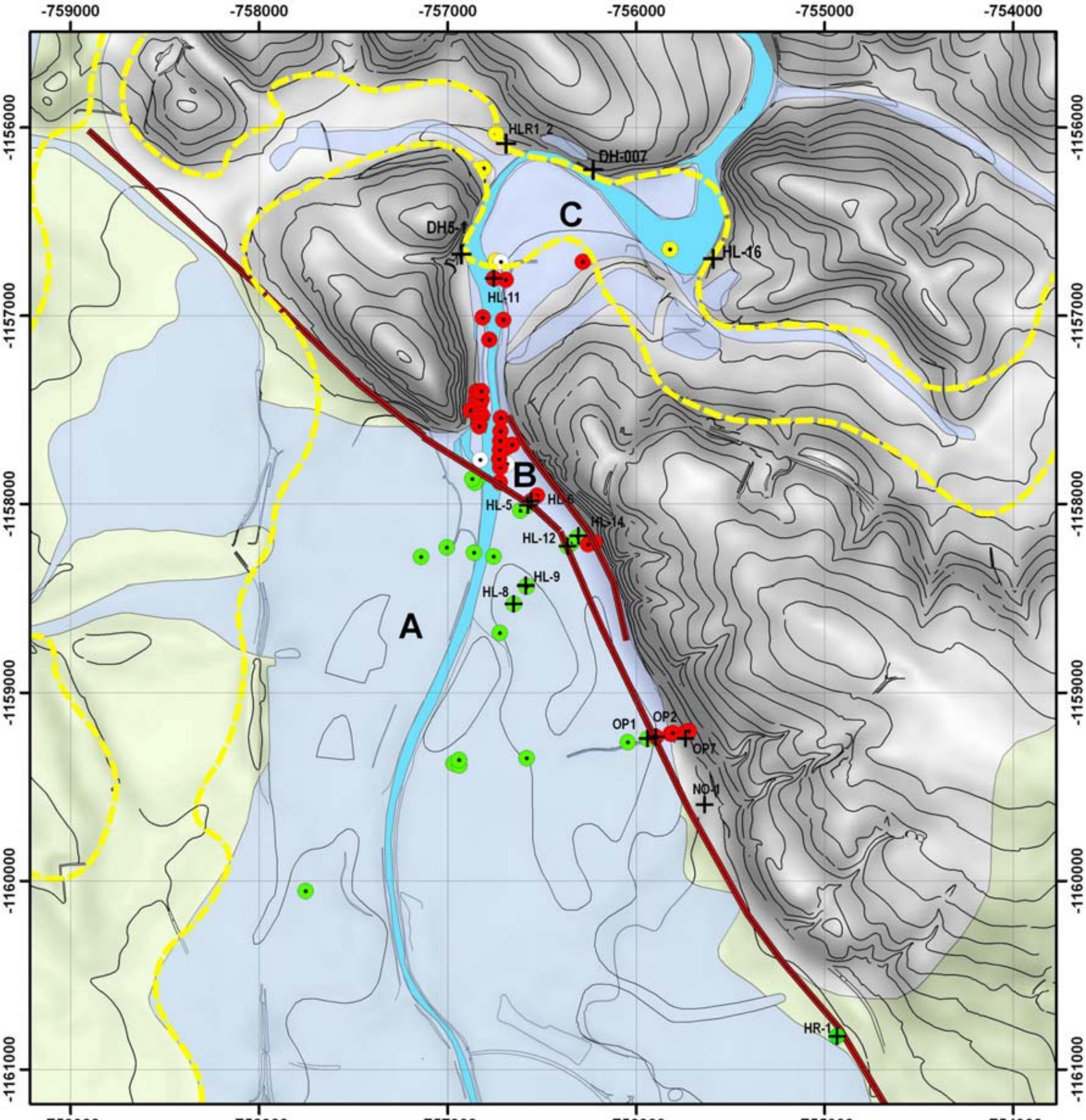

Fig. 4.4.3-1: Schematic map of the central part of the segments 1 and 2 of the Hluboká Fault and the hypothetical segment H (red lines) define the boundaries of the blocks A, B and C. The approximate extent of fluvial sediments is shown by light blue colours. The Cretaceous Klikov Fm. is shown by green colour. The approximate extent of Neogene Mydlovary Fm. is shown by bold dashed yellow line. Circles show the boreholes used for the reconstruction of the lower terace and the analysis of its lithology. The colour coding shows the stratigraphy of the sub-Quaternary bedrock: red - crystalline, green - Klikov Fm. or unknown Cretaceous/Tertiary age, yellow - Mydlovary Fm. The samples for OSL dating are shown as black crosses with labels.

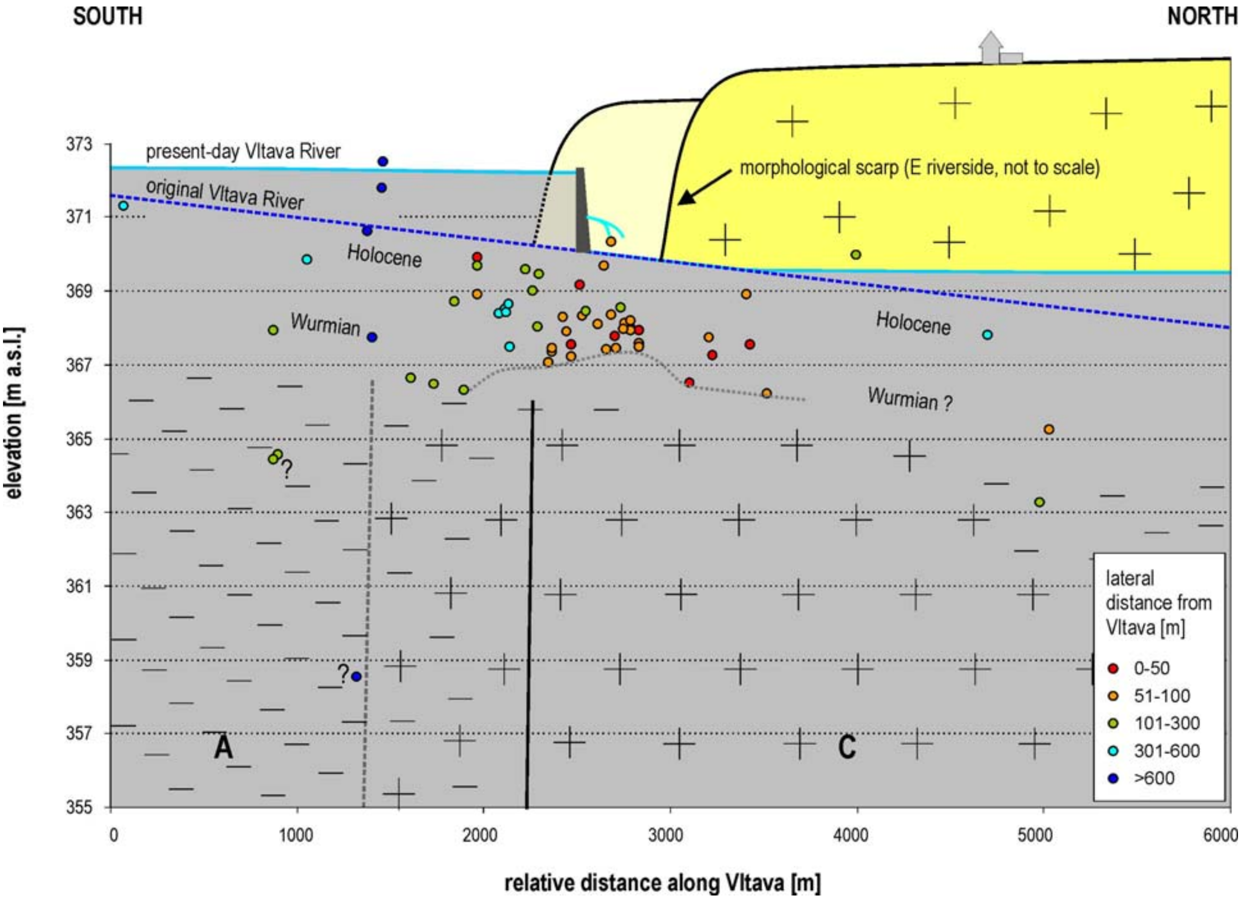

Fig. 4.4.3-2: Schematic longitudinal (river-parallel) profile across the basin margin showing the thickness of Quaternary fluvial terrace. Bases of Quaternary observed in boreholes given in Fig. 4.4.3-1 are orthogonally projected onto the profile and their lateral distance from Vltava is colour-coded. The positions of terrain scarps on both sides of the river are shown schematically. The assumed position of the Hluboká Fault is shown by two vertical lines - the solid black line corresponds with the fault trace in the plane of profile, the dashed grey line indicates the maximum extent of the laterally projected fault trace (crosses - crystalline, horizontal hatch - Cretaceous or Neogene sediments). The reconstructed level of the Vltava is shown by dashed blue line. In spite of considerable lateral variability of the local bases of Quaternary, the smoothed base level is comparable in the basin and on top of crystalline at approx. 3.5 - 4 m below the reconstructed Vltava level. The 1-2 m high elevation of crystalline is suggested in the narrowest part of the Vltava valley (roughly between the Hluboká weir and the bridge in Hluboká-Zámostí, thin dotted line). Some extremely low elevations of terrace bases are probably due to incorrect interpretation of the borehole profiles.

The results of dating of the sediments sampled in individual blocks and their elevations relative to the reconstructed level of Vltava is given in Fig. 4.4.3-3. The data are given separately for individual blocks A-C and are colour-coded according to the sediment age.

The similar age of samples taken at similar elevations in blocks A and B prove the absence of vertical slip on segments 1C/2A of the Hluboká Fault *sensu stricto* in Holocene and youngest Würm (approx. 14 ka, boreholes HL-5 and HL-6). The continuity of the lower, older Würmian part of the terrace across the Hluboká Fault is also strongly suggested by compatible results of dating for samples from boreholes HL-8, HL-12 and HL-14. However, since here the fault was not located with high enough precision (see above), we can not take this as a conclusive evidence.

Dating of sediments from block C unfortunately do not allow to assess the vertical slip on the Hluboká Fault zone (hypothetical segment H). The two boreholes made did not reach the lower levels of the terrace. The samples from borehole HL-11 give Holocene age for the whole upper part of the terrace, down to -2 m below the Vltava surface-level. It is likely that in this narrow valley older deposits were destroyed by lateral erosion of the river. More datings of the samples from boreholes situated farther in block C will be necessary in future research to assess the age of the lower part of the terrace.

As described in Chapter 4.4.2 and below in Chapters 4.5 and 4.6, several samples from higher levels above Vltava were dated. These give systematically younger ages than expected, which are in the same range as the the ages of sediments in the lower terrace. Most of these samples, however, were taken in small relics without clear morphological signature. In such position it is not possible to unequivocally assess its sedimentary environment and in-situ position. Since these data are in contradiction to other significant observations, we suggest that the ages of these sediments reflect the bleaching of their fine-grained component during re-deposition at the slopes and/or cryoturbation.

The discussion and preliminary model to explain these aparently contradictory observations are given in Chapter 5.

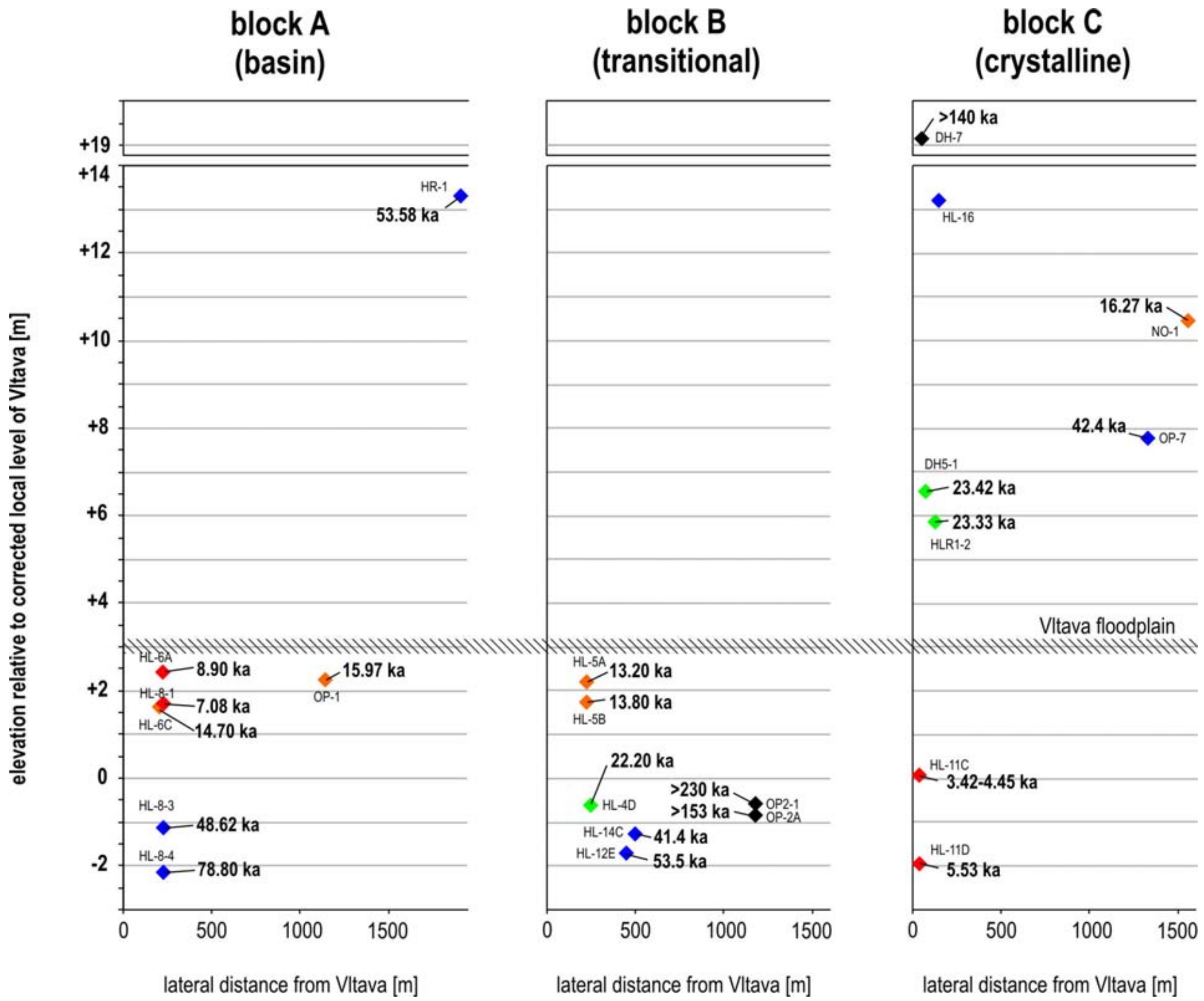

Fig. 4.4.3-3: Schematic plot showing the OSL ages and relative elevations of samples above or below the corrected surface level of Vltava. Lateral distance from Vltava is also shown. The results are shown separately for blocks A, B and C. Colour coding represents the age of the samples: black - oldest samples outside the OSL dating range, blue - older Würm (41-79 ka), green - younger Würm - 22-24 ka, orange - youngest Würm (13-16 ka), red - Holocene (3-9 ka). Note the similar patterns in the lower terrace of blocks A and B. Sediments with higher elevations, on the other hand, are younger than would be expected for the in-situ fluvial sediments. This is explained as due to the post-sedimentary bleaching rather than differential tectonic movements, see Chapter 5.

4.5. SEGMENT 2A: HLUBOKÁ-WEIR – TĚŠÍN

Segment 2A is defined by linear maximum of horizontal gravity gradient in a position near the prominent terrain scarp between the locality Hluboká-weir (south of Zámostí) and the western environs of Těšín. Both features are subparallel, having azimuth 140-145°, and roughly coincide with the contact of Cretaceous vs. crystalline buried beneath Quaternary sediments. Similarly as in other fault segments, the steep margin of the Cretaceous sediments with thickness of approximately 300 m is indicated by deep boreholes near Opatovice, by the horizontal gravity gradient, and by reflection seismic profile measured by AIP team (profile Hosín, Decker et al. 2010a).

Thanks to the prominent terrain scarp associated with this fault segment (Figs. 4.5-1 and 4.5-2) the question of its Quaternary activity was repeatedly opened in the past survey of the Temelín NPP. First research initiated by the 1992 IAEA mission focused on the testing of the assumption that the terrain scarp with its present-day position and morphology really can be associated with active tectonic fault plane. This early research carried out in the period 1992-1995 has shown, however, that the tectonic contact of Cretaceous sediments and crystalline buried beneath Quaternary sediments is offset approximately 70-140 m away to the SW from the foot of the scarp. This conclusion was drawn based on series of three boreholes in the SE part of the fault segment (Hrdějovice-1 locality, see map in Fig. 4.5-3) where >10m thick alluvial-colluvial fan is associated with the terrain scarp, extending several hundred meters away from its foot to the basin.

In this project we continued the research in the NW part of the segment (Opatovice locality, Fig. 4.5-3) where floodplain sediments approach closer to the scarp and the colluvia (or alluvial fans) are preserved only as relics just at the foot of the scarp. Since the area of segment 2A is not suitable for direct analysis of the fault in trenches, we used the same methodical approach as in case of segment 1C: 1) mapping of the fault trace and of the continuity of Quaternary sediments using geophysical and borehole survey, 2) analysis of the pre-Quaternary sediments and crystalline rocks buried below and cropping out within the fault scarp and 3) research into the terrace sediments of the Vltava river, including their dating. The results for the Opatovice locality are given in Chapter 4.5.1. The results of the past research on Hrdějovice-1 profile are given in Chapter 4.5.2 together with some additional data.

Fig. 4.5-1: Panoramic view (from SW) at the linear terrain scarp between Hluboká and Hrdějovice (Hosín church on the left). Fault segment 2A is located close to the foot of the scarp.

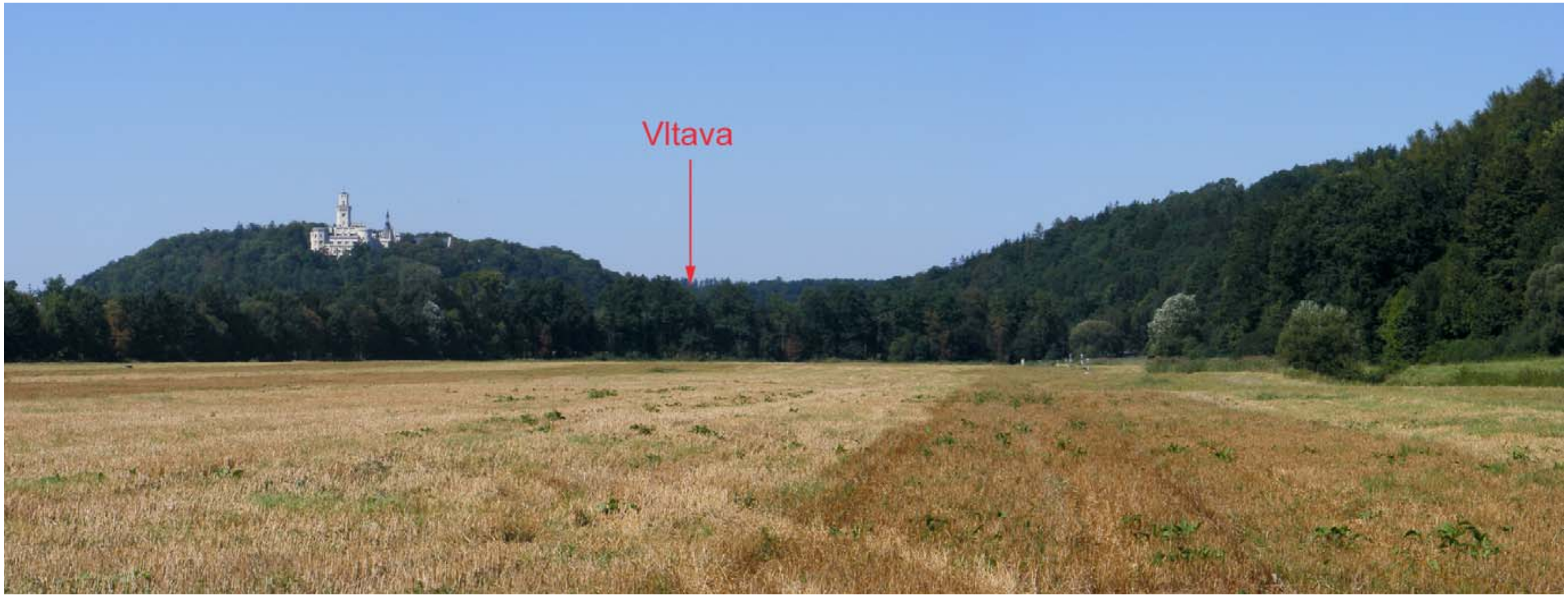

Fig. 4.5-2: View at the linear terrain scarp near Hluboká (viewed from south, chateau on the left) showing the point where Vltava river enters the hilly land through a narrow gate near Hluboká-weir.

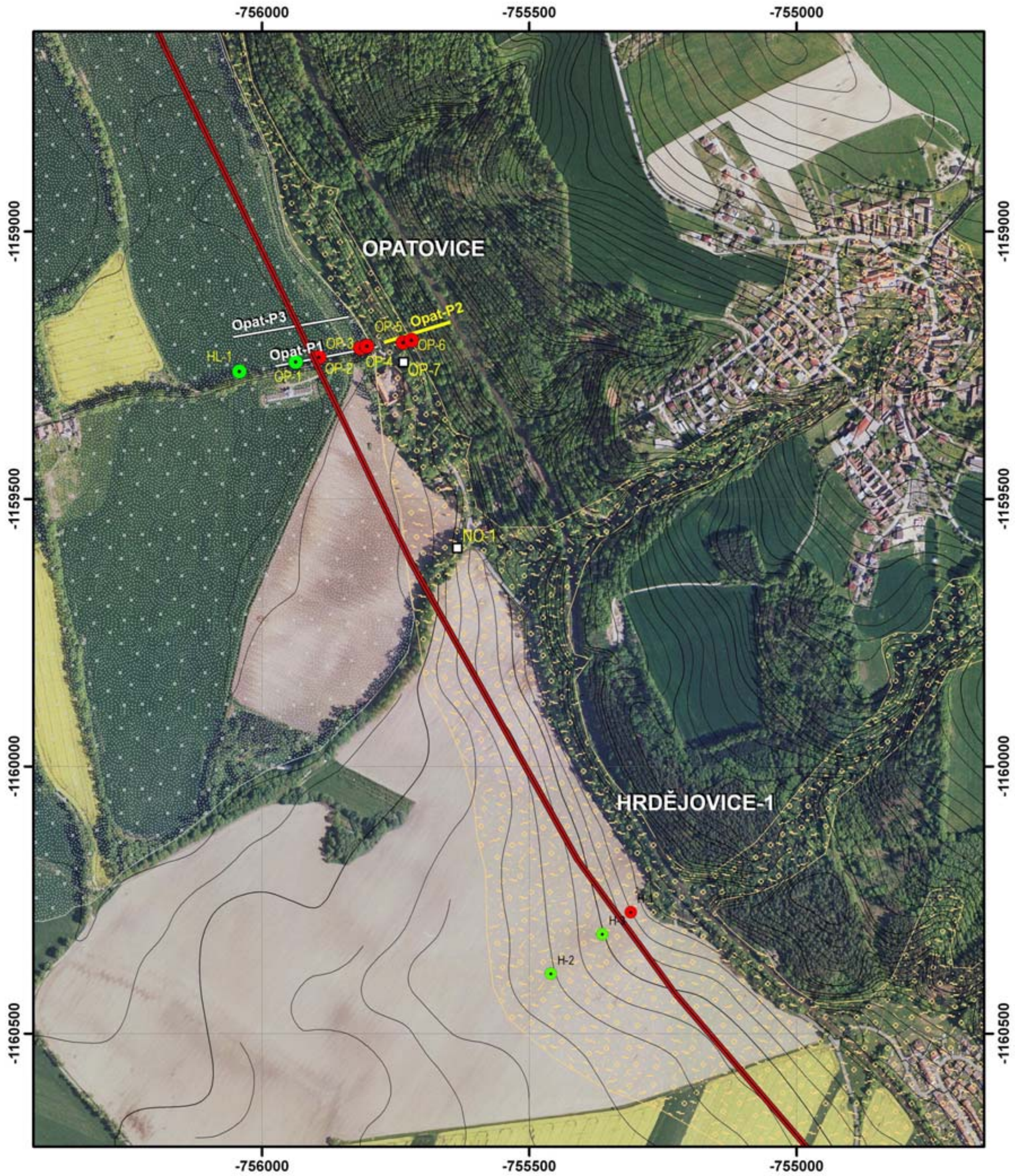

Fig. 4.5-3: Situation map of fault segment 2A showing the two localities under study - Opatovice and Hrdějovice-1 with resisitivity profiles Opatovice-P1 and P3 (white lines), seismic refraction profile Opatovice-P2 (yellow line), boreholes sampling the Quaternary sediments (circle symbols; colour denoting the reached stratigraphy - red - crystalline, green - pre-Quaternary), and locations of other shallow probes for OSL dating (white squares). Also shown is the extent of the Vltava floodplain (light-grey-dotted area, based on the 2002 flood) and the approximate extent of colluvia/alluvia (orange hatch). The approximate trace of the Hluboká Fault shown by red line. S-JTSK grid with 500 m step. Contour lines with 2 m step.

4.5.1. LOCALITY OPATOVICE

Profiles of the locality Opatovice cover the whole zone between the fault scarp and the contact of Cretaceous vs. crystalline, approximately 450 m to the east of the Opatovice village (Fig. 4.5-4). The 331 m deep HL-1 borehole described by Dornič et al. (1966), which was located in the locality of current research, proved that the Cretaceous Klikov Fm. has a local thickness of 316 m and is dominated by mudstones and sandy mudstones. The subcropping migmatitic gneiss is only slightly weathered in the first 7-9 m of depth and strongly kaolinized horizons typical for other boreholes are missing. The schematic structural/morphological section across the basin margin is given in Fig. 4.5-5.

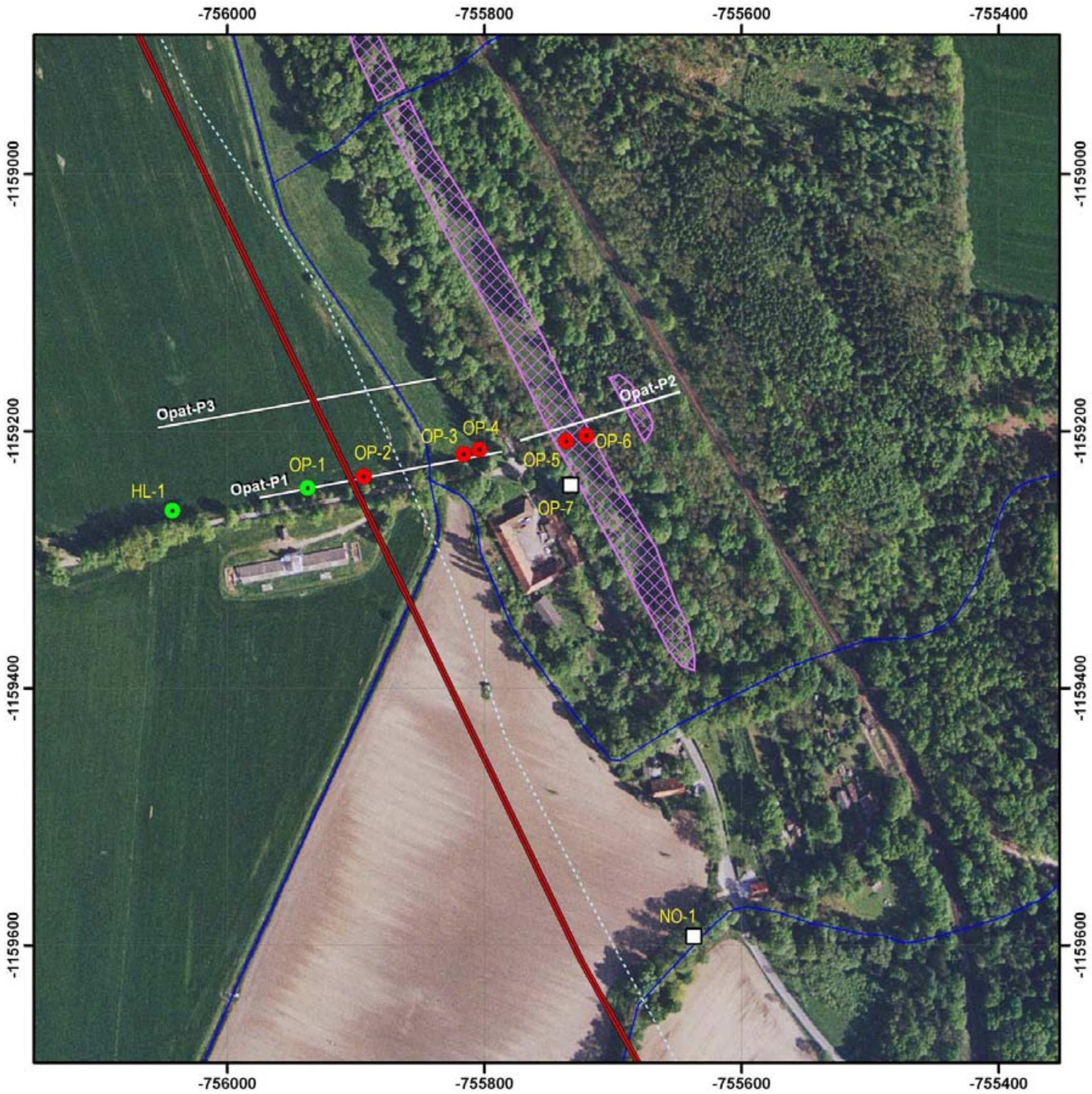

Fig. 4.5-4: Closeup map of the Opatovice locality. Light blue dashed line indicates the gravity indication of the fault. Cross-hatched violet areas correspond with the two plateaus with clastic sediments. Creeks shown by dark blue lines. See Fig. 4.5-3 for explanation of other symbols. S-JTSK grid with 200 m step.

Opatovice – overall view

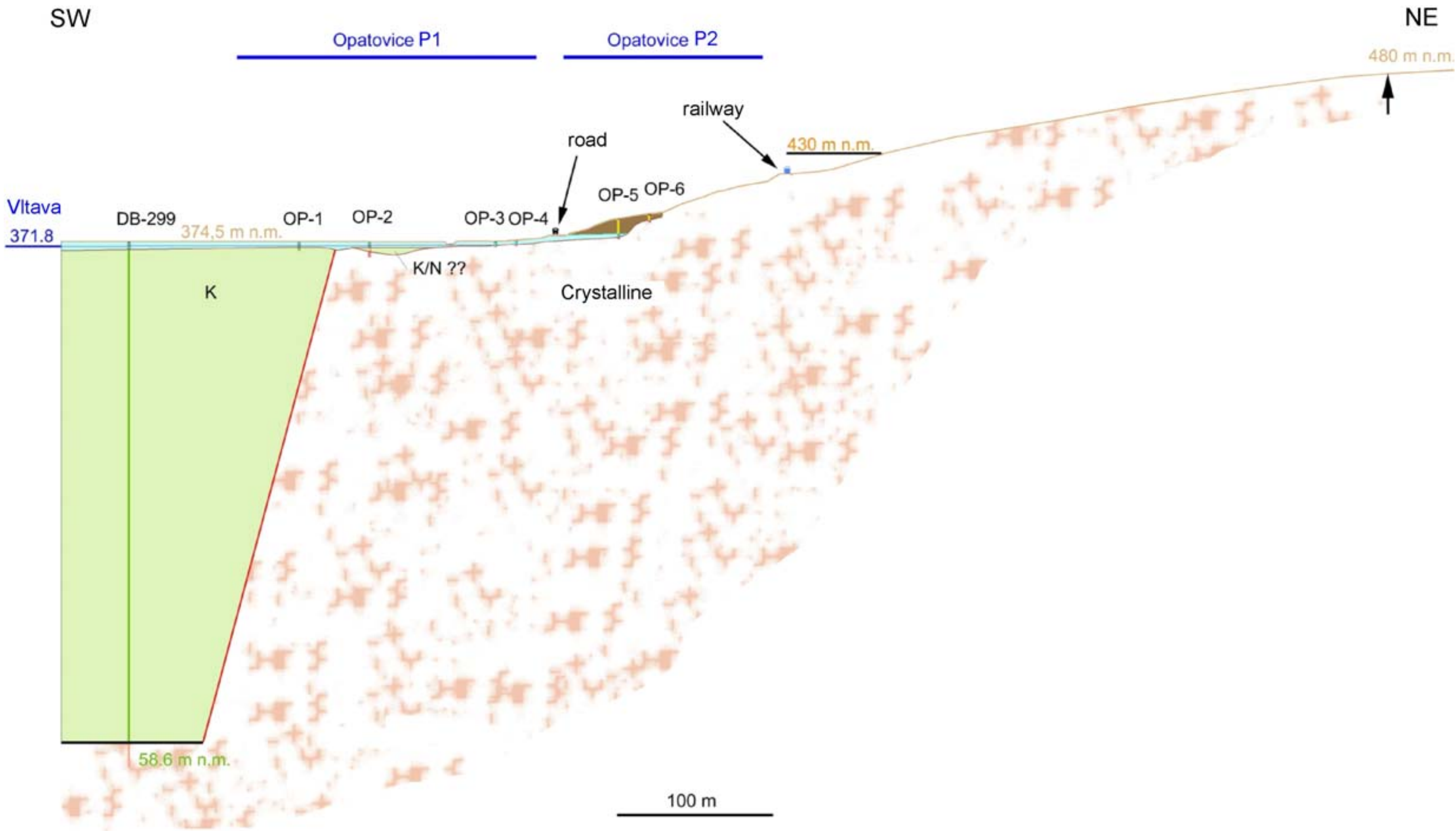

Fig. 4.5-5: The schematic section across the basin margin at the Opatovice profile showing the morphology of the fault scarp and location of the survey boreholes. Based both on archive and new data. Light blue - Quaternery terraces (including the possibly re-deposited parts in OP-5 borehole) ; brown - colluvia/aluvia; green- Cretaceous sediments of the Klikov Fm. and relict sediments of unknown age (K/N??). The marked level 430 m a.s.l. denotes the approximate assumed level of minimum vertical extent of now eroded Tertiary sediments (see the discussion chapters). The elevation profile was measured by differential GPS.

Profiles P1 and P3 - The floodplain

The electrical resistivity profile Opatovice-P1 (composite of two overlapping profiles) is located within the Vltava floodplain to cover the contact of Cretaceous vs. crystalline indicated by gravity gradient. The extent of the profile was limited by the road Hrdějovice-Hluboká. In the ENE part the data are probably affected by a causeway, gas and water pipes and regulated drainage (Opatovice creek). Four boreholes were made along the profile to study the lithology of the Quaternary terrace and of its subcrop. The inverted section (Fig. 4.5-6) shows the existence of homogeneous high-resisitivity layer at the top in a distance range -50 m to 95 m, corresponding to 3.5 - 5 m thick bed of coarse-grained, clast-supported sandy gravels having similar base level of 370.6 m and 370.2 m a.s.l. in boreholes OP-1 and OP-2. The OSL dating of sand-rich layer in the middle parts of the gravels gives an age 15.97±0.9 ka (sample OP-1). In the NE part in a distance range 100 m and 140 m the top layer is represented by approx. 2 m thick, partly gleyed, loamy sediments, locally rich in organic detritus (Fig. 4.5-9-left), while the thickness of sandy gravels beneath is reduced to 0.5 m (boreholes OP-3 and OP-4).

In OP-1 borehole the red-brown clays were found beneath Quaternary fluvial terraces, with lithological and mineralogical features characteristic for Cretaceous (well ordered kaolinite of T-type, goethite nodules; comp. Slánská 1963). In OP-2 borehole the subcrop of Quaternary is formed by colourful marbled sandy clays with preserved metamorphic structure representing the eluvia of migmatitized gneisses (Fig. 4.5-8-right), and >2 m thick sand-rich to loamy, locally organic-rich, unconsolidated sediments lying on top of it. The sand-rich sediments are relatively well sorted, composed mainly of angular to sub-angular quartz grains; locally they are cemented by Fe-oxides (Fig. 4.5-8-left). The age of these sediments exceeds the range for OSL method (>153 ka or >230 ka, samples OP-2A and OP2_1, respectively, the latter dated on feldspar by Decker et al. 2010a). The lithology does not allow for specification of the age, although the character of sediments suggests that they are post-Cretaceous. Based on the resistivity section we assume that these enigmatic sediments fill a shallow depression extending in a distance range 20 - 80 m. Regarding the lithology found in the boreholes, the buried contact between Cretaceous and crystalline is assumed to lie between boreholes OP-1 and OP-2 as indicated schematically in Fig. 4.5-6).

In contrast to OP-2 borehole, boreholes OP-3 and OP-4 reached fresh crystalline rocks (pegmatite, sillimanite-biotite gneiss) without the residual eluvia (Fig. 4.5-9-right). This observation, together with features in the resistivity section, suggest the existence of two domains in the ledge of crystalline buried beneath Quaternary terraces - one adjacent to the terrain scarp with fresh rock at the very surface (approx. 372 m a.s.l.) and another farther to the SW with thick elluvia and sediments of unknown age (top approx. at 370.5 m. a.s.l.). The occurence of thick eluvia in the latter domain indicates the exposure of the crystalline to the surface in Cretaceous or, more likely, in Tertiary.

To verify the homogeneity of the structures over a larger area we measured another electrical resisitivity section Opatovice-P3, parallel to P1, in a position 70 m to the north (Fig. 4.5-7). The high-resistivity gravel bed with base around 370 m a.s.l. seems to be well developed in Quaternary terrace, locally disrupted by finer-grained sediments (and posibly by artificial drainage which is expected around distance 110 m). The sub-vertical resistivity boundary below the Quaternary in the middle part of the section could correspond to the contact of Cretaceous and weathered crystalline. A depression-like structure similar to that in profile P1 seems to exist in a distance range 140-190 m. The fresh crystalline can be expected in the ENE part of the profile, however, the complexity of the inverted section does not allow a simple interpretation.

Opatovice-P1

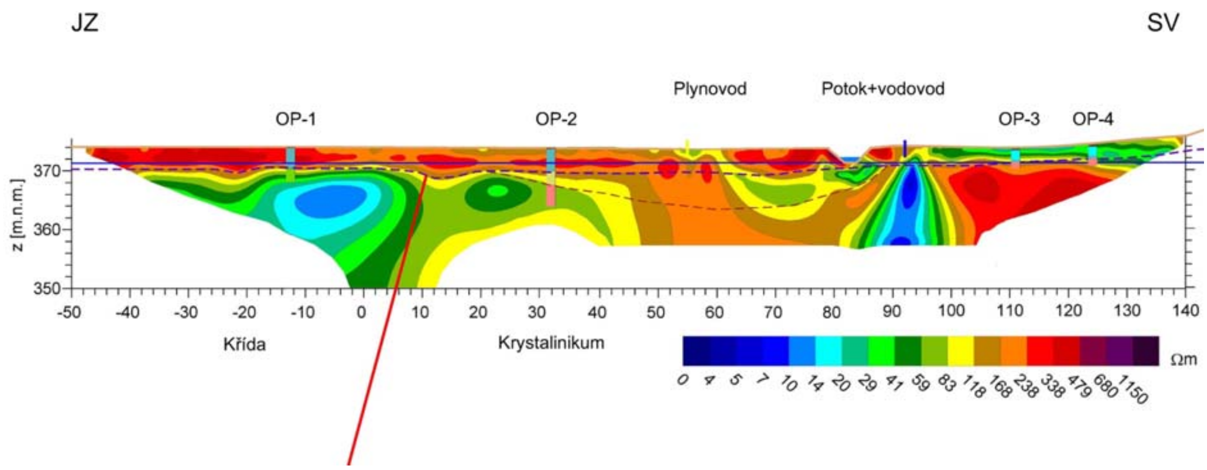

Fig. 4.5-6: Electrical resistivity profile Opatovice-P1 with positions of boreholes OP-1 to OP-4 indicated. Blue line shows the present-day level of Vltava as a reference. Dark violet dashed line corresponds to the assumed base of Quaternary terrace sediments. Light brown dashed line shows schematically the base of depression filled with sand-rich sediments of unknown age - see text for explanation. Red solid line indicates schematically the approximate position of the Hluboká Fault.

Opatovice-P3

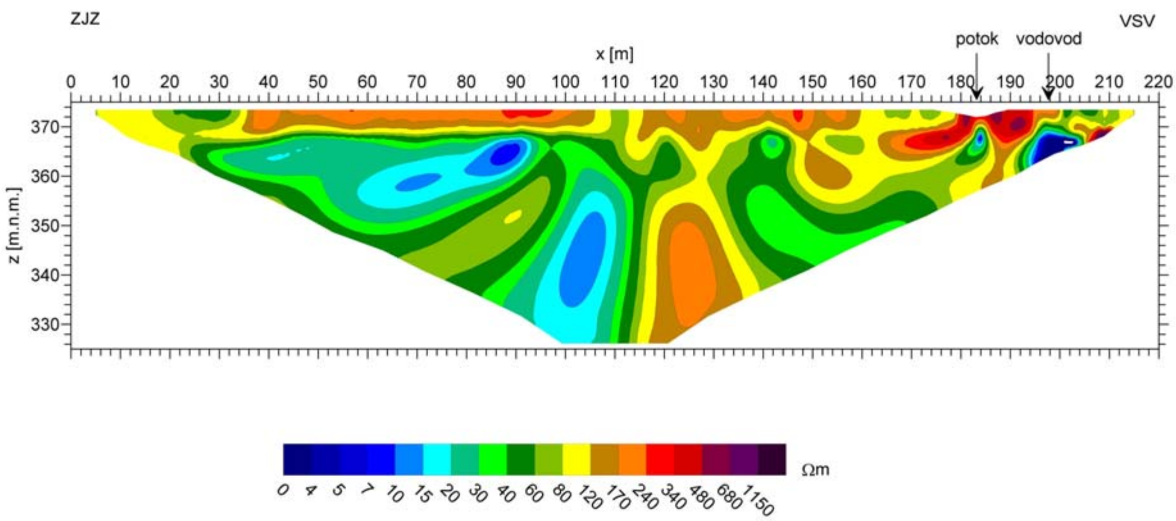

Fig. 4.5-7: Electrical resistivity profile Opatovice-P1.

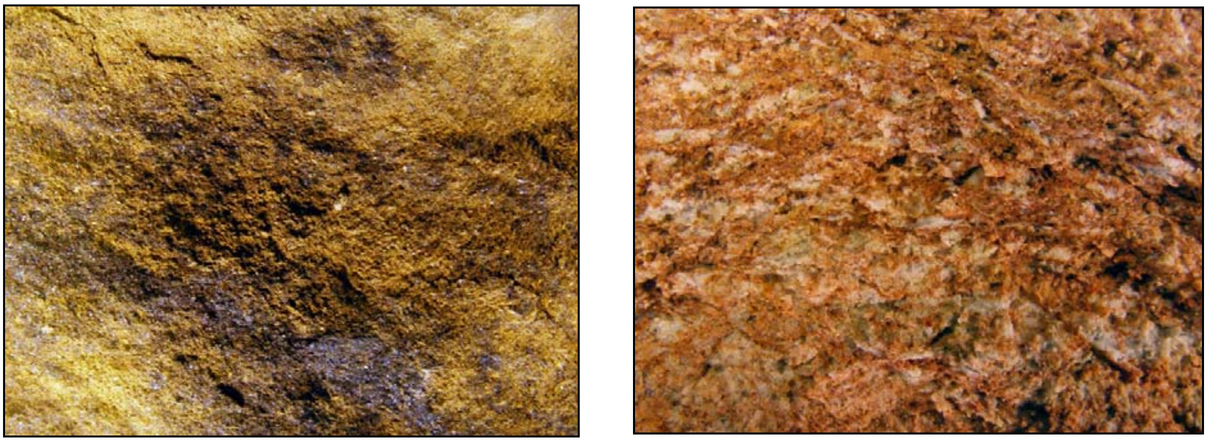

Fig. 4.5-8: Left - Sand/sandstone cemented by Fe-oxides, OP-2 borehole 6.3-6.4 m; Right – weathering rezidua (aluvium) of crystalline rock, probably migmatite, OP-2 borehole, 7.6-7.8 m. Areas shown on both photographs are 2.2 x 3 cm.

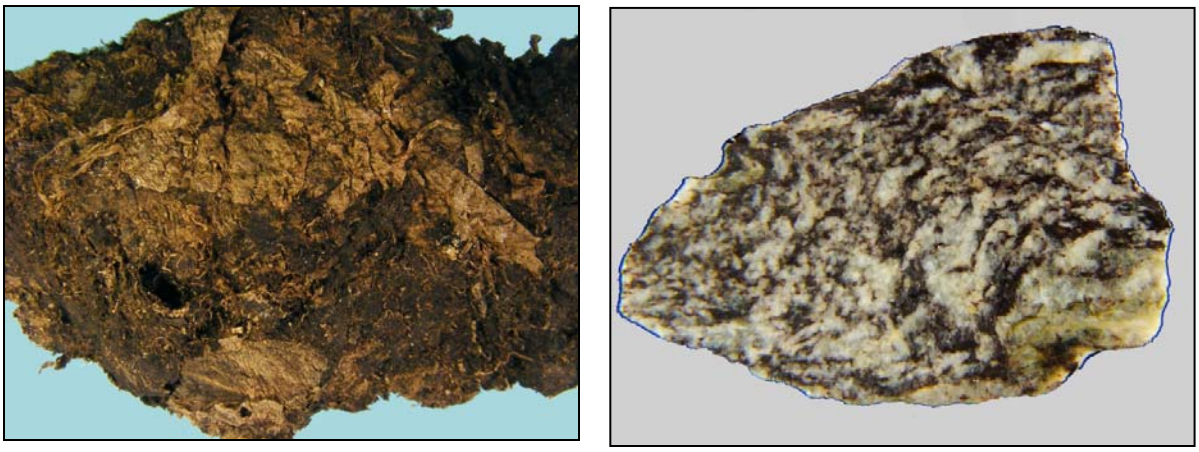

Fig. 4.5-9: Left - Organic sediment from OP-3 borehole, 1.75-2.05 m. Area 3.5 x 4 cm. Right - sillimanite-biotite gneiss from OP-4 borehole. Area 3.5 x 2.5 cm.

Profile P2 - The fault scarp

In the continuation of the profile P1 farther to the NNE the terrain scarp displays a conspicious morphology with three narrow plateaus of smaller slope at the elevations 389-393 m, 406-412 m, and 416-419 m a.s.l. (comp. Figs. 4.5-4, 4.5-5 and 4.5-14). The morphology of the upper two plateaus (Fig. 4.5-11) is very likely modified artificially during the building of the railway and since they are not easily accessed and rather small, they were not studied further in detail. In the >500 m long lower plateau (Fig. 4.5-10) the field reconnaissance revealed the occurence of sands and sandy gravels, likely representing the relict fluvial and alluvial sediments either in-situ or re-deposited on the slope. To learn about the structure and composition of these features we performed a detailed survey including two shallow boreholes and the refraction seismic profile between the road Hrdějovice – Hluboká and the railway.

Indeed, the refraction seismic profile presented in Fig. 4.5-12 shows that the two plateaus in terrain relief recognised on this section correspond to thickening of the low velocity layers covering the higher velocity fundaments with the elevations 376-378 m and 401-404 m a.s.l. These geophysical indications correlate well with the observations in boreholes OP-5 and OP-6 made within the plateau. The borehole OP-5 proves the existence of at least >9m thick beds of aluvial/colluvial sands and scree on top of 1.7 m thick bed of sandy gravels. The sands (Fig. 4.5-13) are locally mixed with silt, display variable degree of rounding and contain small angular rock fragments. In sandy gravels rounded grains prevail, but angular to sub-angular rock fragments are also represented in significant amount (Fig. 4.5-14). Beneath the gravels another thin bed of sands with angular stone fragments is developed lying upon slightly weathered migmatite without eluvia.

In the shallower OP-6 borehole sand-rich colluvia/aluvia with large angular stones were observed lying on top of 2 m thick eluvial residuum and strongly weathered migmatitic gneiss.

The base of the lower plateau can be explained as an erosional feature as supported both by its flat morphology and the lack of eluvia. The gravels deposited in the lower part of the associated sedimentary sequence likely contain significant amount of fluvial component, however, the relatively large content of poorly rounded grains is not characteristic for purely fluvial sediments of the lower Vltava terraces. Furthermore, shallow probes made into the terrain slope at the basal parts of the horizon indicate that gravels are limited in spatial extent to several meters only. The OSL dating of sample OP-7 taken from the base of the road cut (Fig. 4.5-15) gives the age 42.40±2.70 ka.

The age of the colluvial/aluvial sandy sediments was not determined on the Opatovice profile. However, these sediments can be paralleled to fine grained, ocre coloured sands, with local laminae of loamy sands or angular grains of coarse sand size sands exposed in a several meters high profile in a steep creek valley located approx. 400 m to the south. The OSL dating of the sample NO-1 taken in basal part of the exposed profile (Fig. 4.5-16) gives an age 16.27±0.84 ka.

Fig. 4.5-10: Terrain plateau in the fault scarp near Opatovice (Opatovice-P2 profile) at the elevation approx. 389-393 m a.s.l. Viewed from SE.

Fig. 4.5-11: Terrain plateau in the fault scarp near Opatovice (Opatovice-P2 profile) at the elevation approx. 406-412 m a.s.l. Viewed from NW.

Opatovice-P2

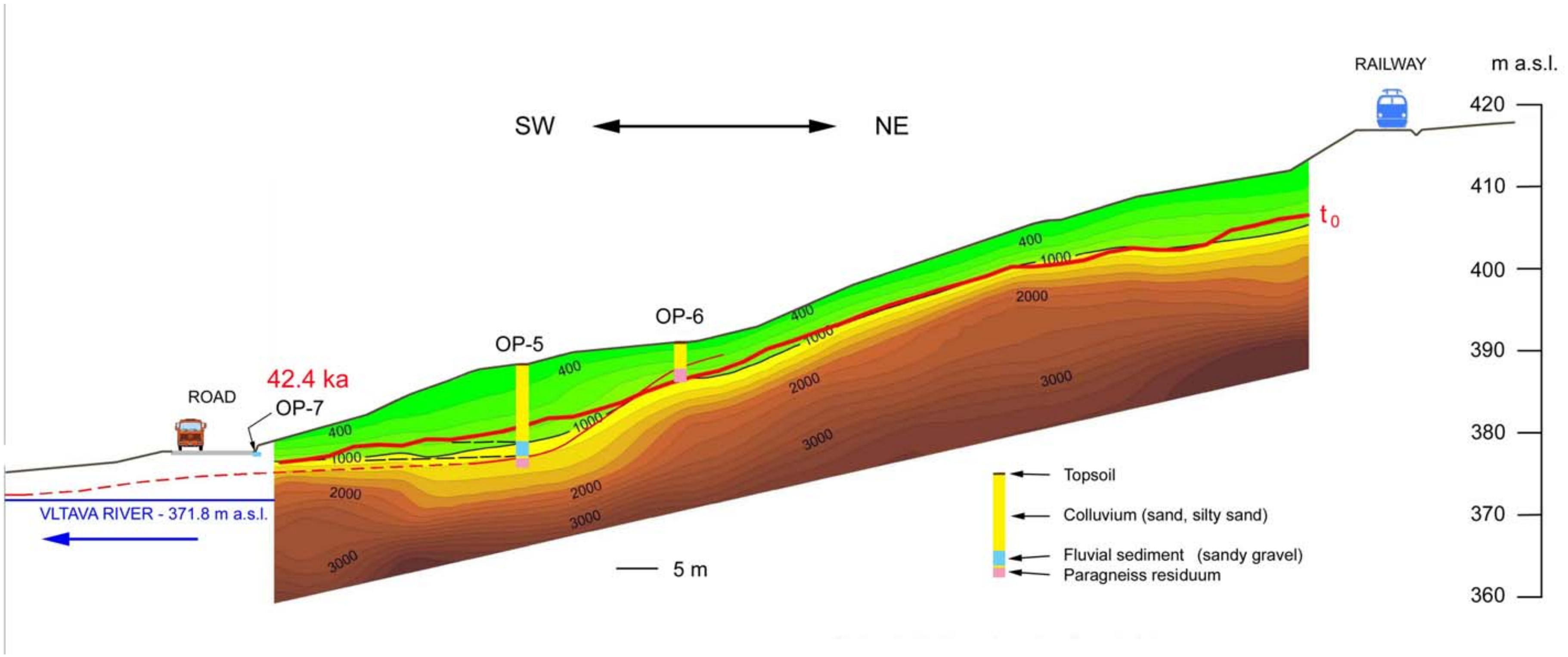

Fig. 4.5-12: Refraction seismic profile Opatovice-P2 across the lower part of the fault scarp showing the terrain morphology and position of boreholes OP-5 and OP-6 and probe OP-7. Red bold line indicates the refraction boundary determined by t_0 method. Blue line at 371.8 m a.s.l. – reference level of Vltava river; red dashed line - approximate assumed base of Quaternary; black dashed line - approximate assumed extent of sandy gravels.

Fig. 4.5-13: Characteristic colluvial/alluvial sands from borehole OP-5 (depth 3.4 m) Size 5×4 cm.

Fig. 4.5-14: Detailed view at grains from >32 mm (left) and 3-10 mm (right) fractions of gravels sampled by OP-5 borehole (depth 9.90 – 10.30 m). Note the sub-angular to sub-rounded quartz grains and angular fragments of gneisses.

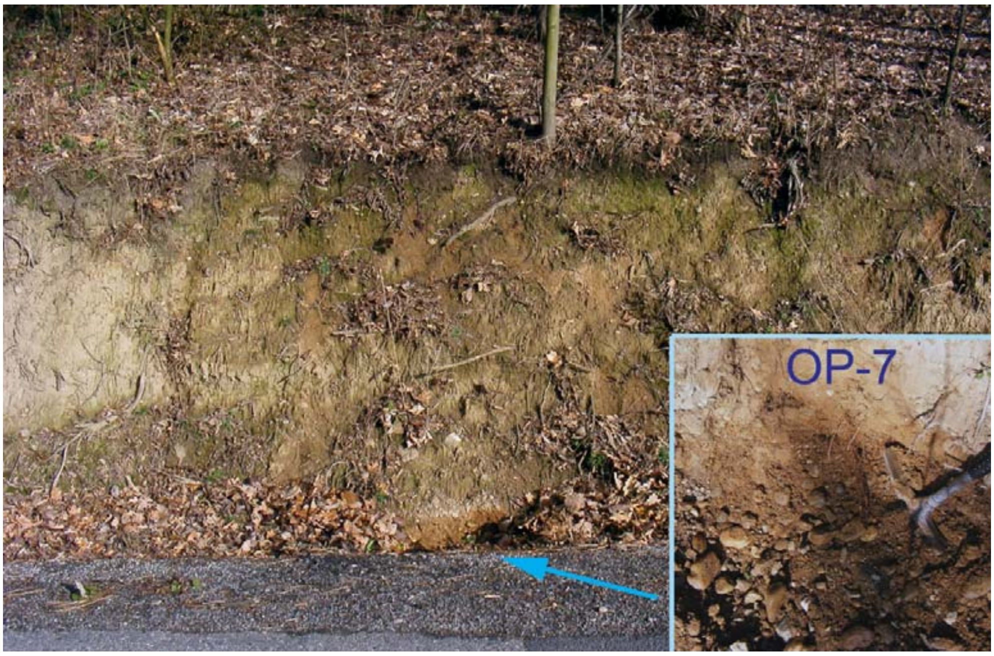

Fig. 4.5-15: Sampling site of sandy gravels exposed in a road cut below sediments of colluvial/alluvial fan (sample OP-7, road Hrdějovice-Hluboká).

Fig. 4.5-16: Sampling site of fine-grained sands exposed in a steep creek valley south of the road Hrdějovice-Hluboká (near Skelná Huť, sample NO-1).

4.5.1. LOCALITY HRDĚJOVICE-1

The locality Hrdějovice-1 is situated approx. 500 m to the NW of the Hrdějovice village, where a thick coluvial/alluvial fan is developed at the foot of a prominent terrain scarp, extending several hundred meters away from its foot to the basin (Fig. 4.5.3).

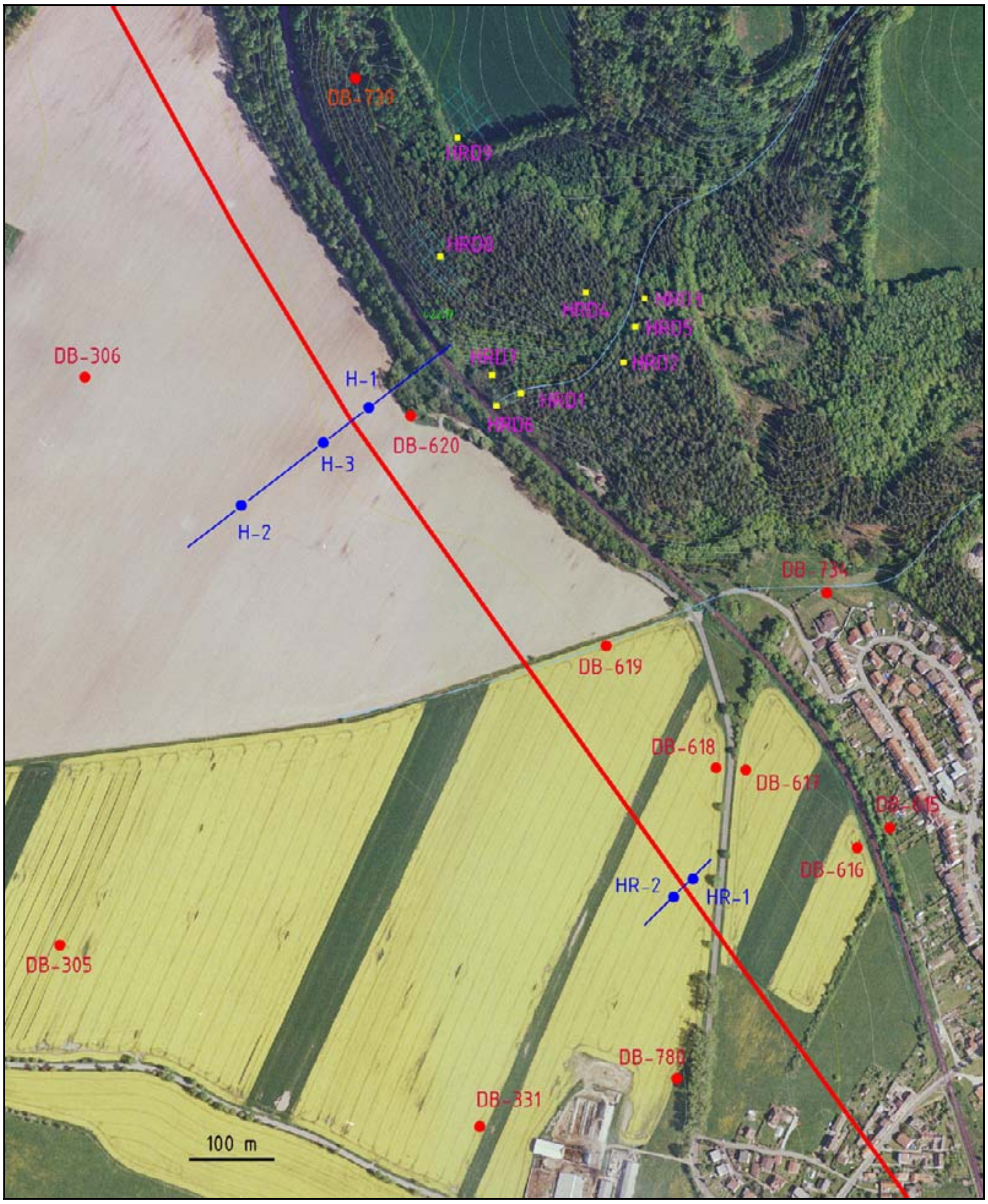

Fig. 4.5-17: Situation of the profiles Hrdějovice-1 (NW) and Hrdějovice-2 (SE, blue lines). Blue dots – new boreholes on the profiles; red dots – archived boreholes; yellow dots – field-documented outcrops; red line – approximate expected trace of Hluboká Fault. See Chapter 4.6 for details on locality Hrdějovice-2.

This locality was studied previously, in the years 1992-1995 (Šimůnek et al., 1995), using a series of three boreholes penetrating the >10m thick colluvio-alluvial fan (H-1, H-2 and H-3 in Figs. 4.5.17 and 4.5-18). The sediments are represented by poorly sorted sands or silty sands, locally well sorted sands, and in proximal parts of the fan (H-1) thick beds of angular rock debris. All three boreholes reached sandy gravels or sands below the sediments of colluvio-alluvial fan, representing the fluvial terrace sediments. The increasing amount of angular clasts in the gravels was observed with increasing proximity to the scarp. The vertical extent of fluvial sediments ranges from 376.0-380.9 m a.s.l. in H-2 borehole to 373.9-378.3 in H-1 borehole. According to the model of Chábera and Novák 1976 (see Table 4.4-1), this should represent terraces of Riss age. Unfortunately, the OSL dating has not been performed during this early period of survey.

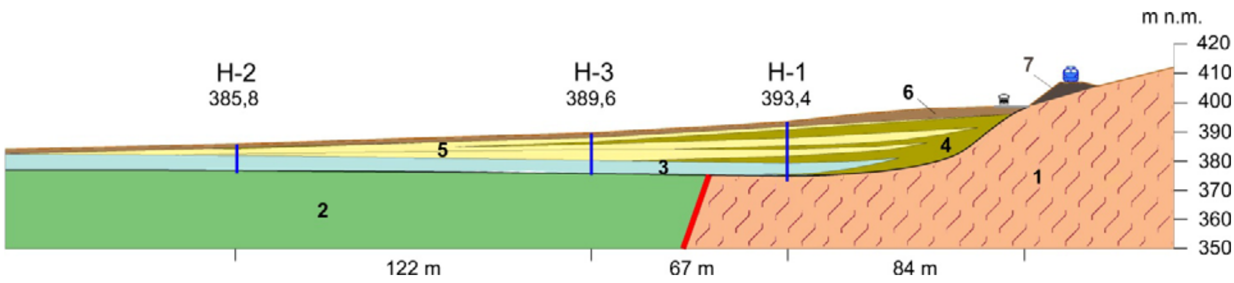

Fig. 4.5-18: Profile Hrdějovice-1. 1 – crystalline; 2 – Cretaceous (Klikov Fm.); 3 – fluvial sediments of Vltava river, 4 – rocky colluvium; 5 – sand-rich colluvium (proluvium); 6 - loamy colluvium; 7 – railway causeway; red - Hluboká Fault (schematic); H-1, H-2 and H-3 – boreholes with terrain elevations.

All boreholes reached the pre-Quaternary subcrop - Cretaceous sediments of the Klikov Fm. in boreholes H-2 and H-3, and strongly weathered (kaolinitized) migmatite in borehole H-1 situated 55 m south of the road Hluboká - Hrdějovice. This proves that, similarly as in previous localities, the tectonic contact of Cretaceous and crystalline buried beneath Quaternary sediments is offset approximately 70-140 m away to the SW from the foot of the scarp. Apparently, in the area of HL-1 borehole the basin margin was leveled by lateral erosion of the Vltava river to the corresponding erosinal base regardless of the lithology. The preservation of the strongly weathered top layer in migmatites suggests that the crystalline legde might have already existed prior to the advance of the river and could have been merely re-modeled or exhumed during Quaternary.

Although the age of coluvial/alluvial sediments overlying the buried river terrace is not known, it can be possibly estimated using OSL data from the adjacent localities with analogical structure: In HR-1 borehole situated approx. 600 m to the SE (locality Hrdějovice-2, see Chapter 4.6 and Fig. 4.5.-17) the sands lying on top of relict gravels of similar character and elevation give the age 54 ka (results of AIP team, see Chapter 4.6). The OP-7 sample described above (locality Opatovice), interpreted as the likely slope-redeposited (and re-bleached) sediment gives the age 42.5 ka. Both these samples could represent the age of the lower part of the coluvial/alluvial fan. NO-1 sample of the sands exposed approx. 800 m to the NW gives the age 16 ka, representing the approximate age of the upper part of the alluvial fan.

Fault scarp and higher plateaus

Several outcrops in the valley of the nameless creek expose the crystalline rocks of the fault scarp (HRD-1 to 4, HRD-5, HRD-7 in Fig. 4.5-17, see e.g. Fig. 4.5-19). Fresh, unweathered orthogneisses locally contain shearplanes or slickensides of NW-SE, NE-SW or N-S strike. At some places, these planes contain Riedel shears, but are generally of old age, being covered by thin layers of quartz, chlorite, or sericite. Incipient cataclasis is sometimes developed, but low temperature mylonites or clay- rich gauges have not been observed.

Two morphological plateaus, covered by Quaternary sediments, were identified in the higher part of the fault scarp (Figs. 4.5-20 and 21): 1) The plateau at the elevation approx. 422 - 424 m a.s.l. (HRD-8 in Fig. 4.5-17) is covered by loamy sands with angular fragments of orthogneiss lithologically similar to the sands of the lower colluvial/aluvial fan. No fluvial component has been observed. 2) The plateau at the elevation 430-434 m a.s.l. (HRD-9 in Fig. 4.5-17) contains relict gravels with ventifacts locally found at the small area of ploughed field. Both these plateaus are very likely of Lower Pleistocene or Pliocene age.

Fig. 4.5-19: Abandoned quarry near foot of the fault scarp, W of Hrdějovice, locality HRD-1.

Fig. 4.5-20: Terrain plateau in the fault scarp at the elevation 422 – 424 m a.s.l.

Fig. 4.5-21: Terrain plateau in the fault scarp at the elevation 430 – 434 m a.s.l. with ventifacted gravels (locality HRD-9).

4.6 SEGMENT 2B: HRDĚJOVICE-NEMANICE

Between the western environs of Těšín and the eastern margin of Nemanice, the Hluboká Fault continues in the same azimuth as in segment 2A (140-145°). This is indicated by distinct single linear maximum of horizontal gravity gradient, which reflects the abrupt change in sediment thickness. At the surface, however, Cretaceous sediments continue behind the fault with reduced thickness, making a distinct promontory to the north. The fault scarp is not developed and the fault trace is located in a flat area with slopes <2° dipping to SW and WSW (Fig. 4.6-2).

Several boreholes in the area which reached the base of the basin prove the vertical offset of >250m between the two blocks divided by the fault (Fig. 4.6-1). To the SW of the fault the sediment thickness is approximately 300-340 m. The base of Cretaceous sediments was reached by two boreholes next to the fault: GB-4 (Mrázek, 1960) and US-1 (Lána, 1973), in elevations 51.1 and 61.7 m a.s.l., respectively. Farther to the south the basin thickness 300-320 m is documented by several boreholes in the Budějovice brewery (Budvar), some of which reached the base of the Klikov Fm. (borehole no. 5, base at approx. 90 m a.s.l., e.g. Hynie 1949; HJ-1, 78.1 m a.s.l., Vašta, 1968), and others which did not reach the base at even lower elevations (HV-2, 75.5 m a.s.l., Vašta, 1969; HV-3, 71.9 m a.s.l., Kroupa, 1991; HC-2A, 82.4 m a.s.l., Homolka, 2003).

To the NE of the fault the maximum thickness verified by boreholes is 75 m. In U-1 borehole located only about 200-250 m from the fault trace, the base of Cretaceous has the elevation of 326 m a.s.l. (Kůst, 1947; incorrectly positioned in the electronic database of Geofond). At the western margin of Úsilné two boreholes reached the base of Cretaceous at 320-325 m a.s.l., with Permo-Carboniferous sediments (apparent thickness 22m) and crystalline rocks underneath (US-2, Lána, 1973 and US-2A, Koroš 2001).

Farther to the north only few boreholes reached the base of Cretaceous (e.g., HB-3, 382.5 m a.s.l., Daněk, 2001) together indicating general dip of sediment base towards the fault to the south. Likewise, assymetrical geometry of the basin promontory in the NW-SE direction is indicated, with sediment base dipping towards the Drahotěšice Fault to the SE.

We interpret segment 2B of the Hluboká Fault as a simple, single, steep to sub-vertical planar fault as shown schematically in Fig. 4.6-1.

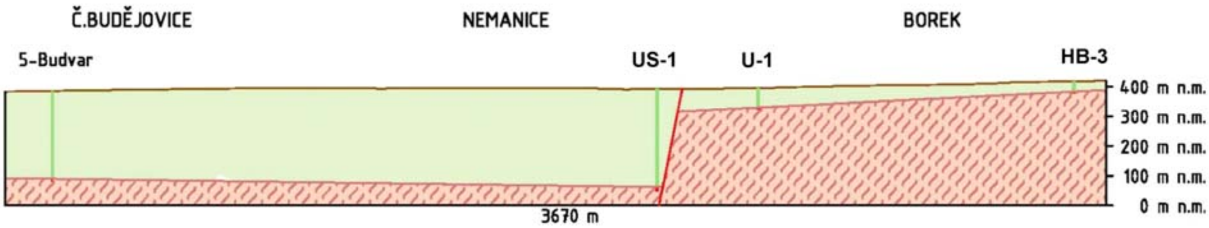

Fig. 4.6-1: Schematic interpretation of basin margin at profile Nemanice-Borek using boreholes no.5, US-1, U-1 and HB-3.

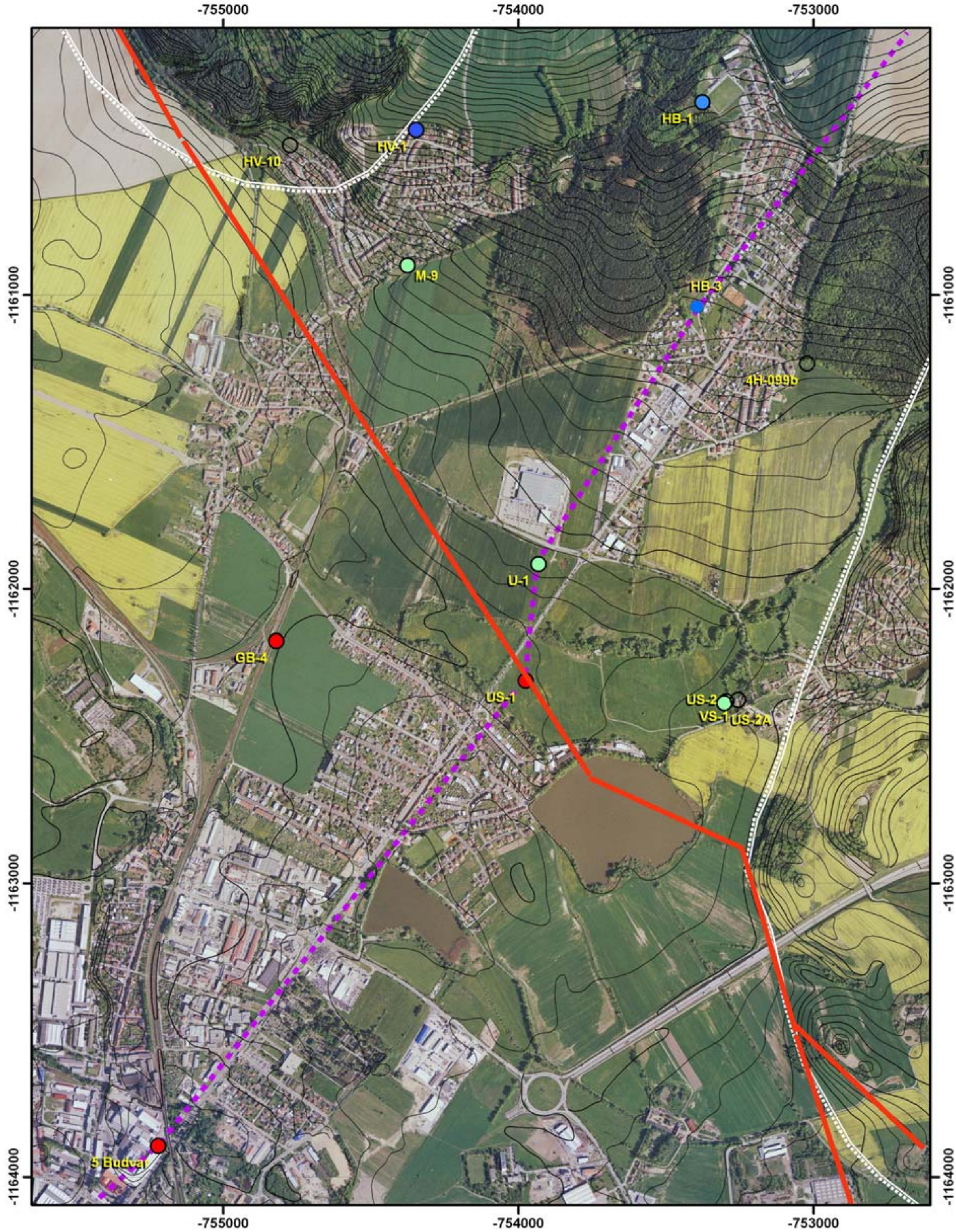

Fig. 4.6-2: Situation of segment 2A between Těšín and Nemanice. Red line - indicated trace of the Hluboká Fault; white line - approx. surfacial extent of Cretaceous sediments; purple dashed line - section intepreted in Fig. 4.6-1; coloured circles - important boreholes which reached the base of Cretaceous. S-JTSK grid with with 1 km step. Contour line step: 2 m.

4.5.1 LOCALITY HRDĚJOVICE-2

The profile Hrdějovice-2 characterizes the basin margin in the area adjacent to segment 2A, where the Hluboká Fault separates off the terrain scarp and enters the flat relief, approximately 700 m SE from the profile Hrdějovice-1 (Fig. 4.6.1-1).

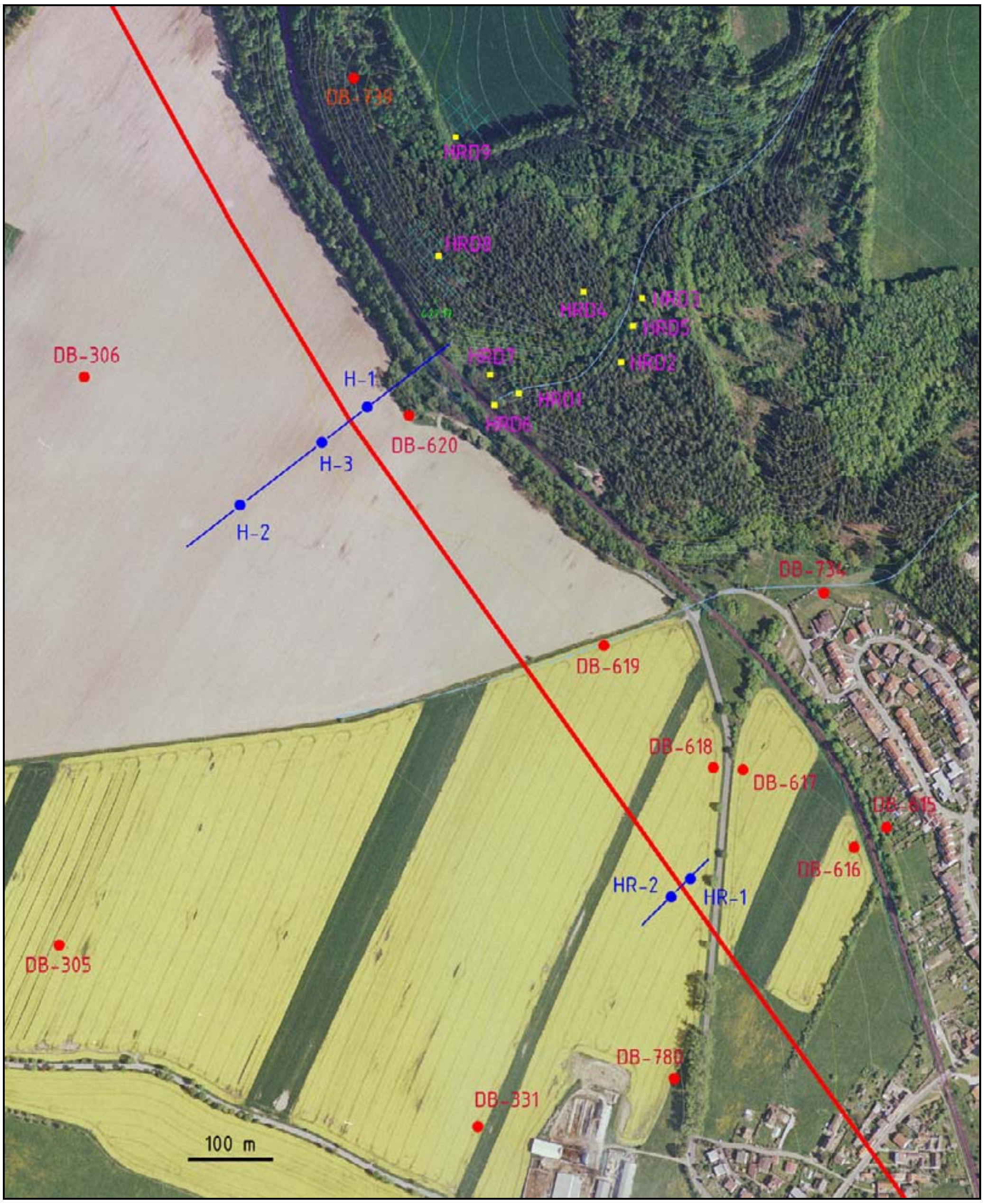

Fig. 4.6.1-1: Fig. 4.5-17: Situation of the profiles Hrdějovice-1 (NW) and Hrdějovice-2 (SE, blue lines). Blue dots - new boreholes on the profiles; red dots - archived boreholes; yellow dots - field-documented outcrops; red line - approximate expected trace of Hluboká Fault. See Chapter 4.5 for details on locality Hrdějovice-1.

According to geological maps, a contact of Cretaceous sediments and crystalline rocks was expected in relatively shalow depths below Quaternary sediments. The profiles for shallow seismic refraction and multielectrode resistivity tomography were located in the area where the fault trace was expected based on gravity indication and geometrical consideration.

The refraction seismic profile indicates the absence of steep velocity contacts down to a depth of about 20 m. The „t_o“ method indicates the base of low-velocity (< 800 m.s^{-1}) layer in depths of 3-4 m. Similar shallow low-resistivity layer of comparable thickness is indicated in electrical resistivity profile. In greater depths two sub-vertical resistivity boundaries are indicated, dividing a 20 m wide low-resistivity domain (Figs. 4.6.1-2 and 4.6.1-3).

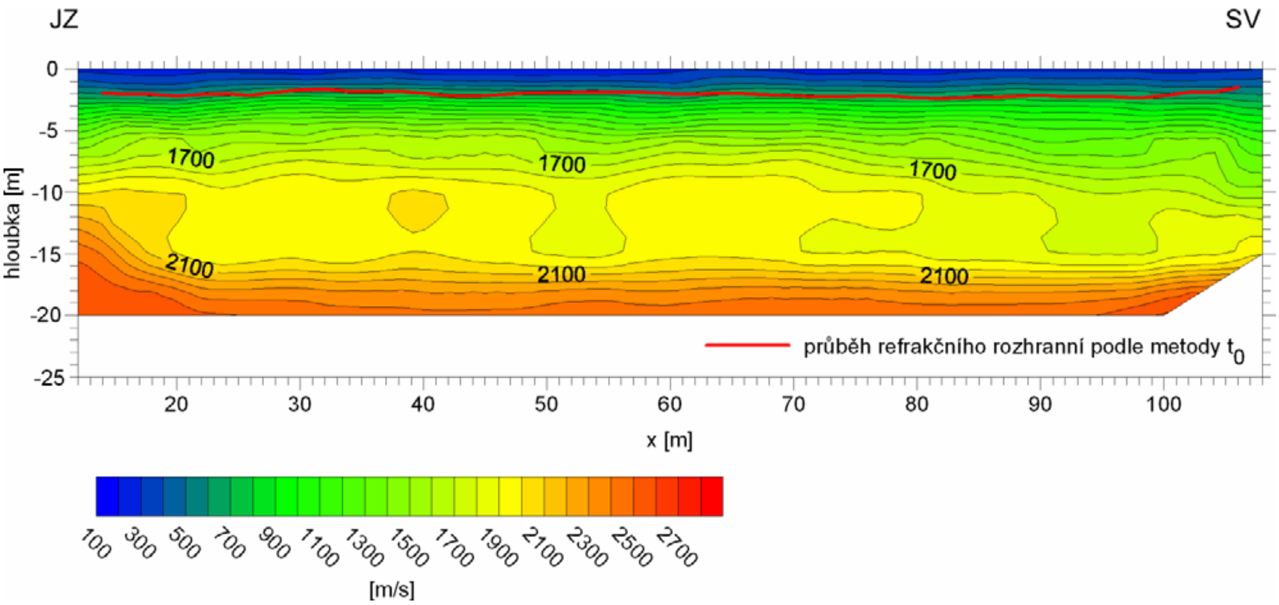

Fig. 4.6.1-2: Shallow refraction seismic profile Hrdějovice (Hrd-P1).

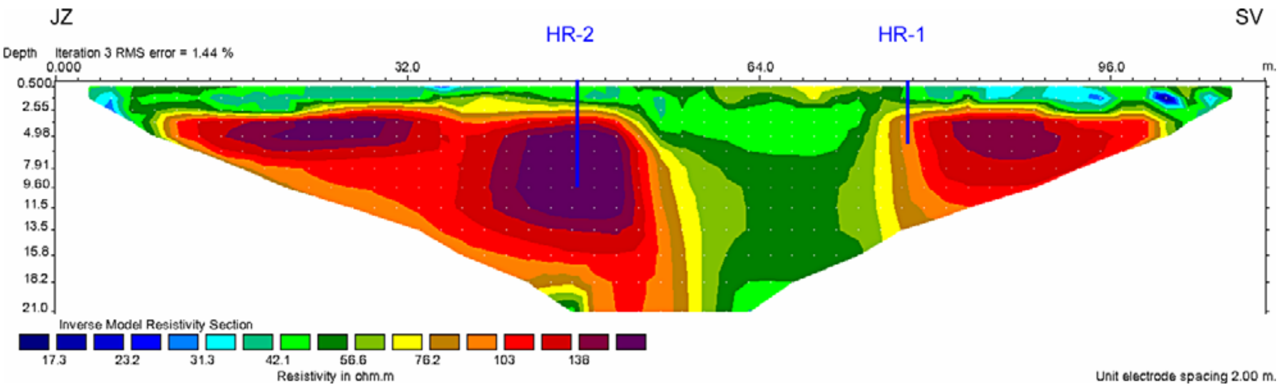

Fig. 4.6.1-3: Multielectrode resistivity profile Hrdějovice (Hrd-P1).

Two boreholes were made on both sides of the resistivity anomaly (HR-1 and HR-2) to verify the lithological differences. Both boreholes, however, reached Cretaceous clays and sands at the elevations of 382.17 (HR-1), and 382.14 (HR-2). Quaternary clastic sediments covering Cretaceous are mainly poorly sorted, fine-grained sands of yellow-brown colour or brownish gravels with argillaceous component in matrix. These lithologies are interpreted as alluvial sediments (proluvia) deposited below the terrain scarp of the Hosín hill, rather than in-situ fluvial sediments (comp. with the boreholes at profile Hrdějovice-1). Similar sediments were described from other boreholes in the area (DB-615 to DB-618; V20 to V23; Chocholáč M., 1985)

OSL dating of sands from borehole HR-1 (sample HR-1, Decker et al. 2010) gives the age of 53.58 ± 6.12 ka.

4.6.2 LOCALITY NEMANICE

In the NE environs of Nemanice near České Budějovice fluvial sediments of Pleistocene and Holocene age are deposited above the Hluboká Fault (Fig. 4.6.2-1). The analysis of present-day architecture of this sedimentary body could allow the assessment of Late Quaternary activity of the fault. If there was a slip with vertical component after the deposition of these sediments, we should be able to observe a step-like offset of their base above the fault. The boreholes archived in database of Geofond, however, do not indicate the existence of significant changes in thickness of Quaternary sediments which could be associated with the Hluboká Fault. The base of Quaternary sediments is comparable in both blocks divided by the fault and variations have only local extent. Unfortunately, the lack of boreholes in the area adjacent to the fault trace and small depth of the boreholes disallow using these data as an unambiguous proof. To find a more detailed picture of the fault and of the Quaternary sediments deposited above it, we carried out a complex analysis on NEM-1 profile, using multielectrode resistivity, GPR and three shallow boreholes (Figs. 4.6.2-1 and 4.6.2-2). This profile was located so as to transect the fault trace indicated by horizontal gravity gradient and constrained by boreholes U-1 and US-2 (see text in the introduction to Chapter 4.6).

The electrical resistivity section indicates a nearly constant depth of base of Quaternary sediments 5-6 m below surface. The sub-vertical boundary below Quaternary, in the central part of the section, may correspond with a lithological boundary developed within Cretaceous sediments due to the offset on the fault (this feature, however, can be exagerrated in the inverted section, since it is only weakly defined in the non-inverted apparent resistivity profile).

The GPR section shows several strong reflections with generally smooth variations in the upper 5 meters. As verified in the boreholes, this horizon corresponds to the fluvial sediments, and the variation can be explained by the lateral migration of the channel. The horizontal „reflections“ in the middle level (5 to 8 m) within the SW part of the section are interpreted as a result of deeper penetration due to contrasting physical properties in the near-surface level, but they can eventually correspond to clay-rich lithologies found in borehole NE-1.

The geophysical profiles indicate the absence of significant abrupt offsets in the structure of Quaternary sediments.

Two boreholes (NE-1, NE-2) were made at the profile NEM-1 and another (NE-3) near the profile, all reaching the base of Quaternary sediments (Figs. 4.6.2-1 and 4.6.2-2). The Quaternary is represented by 2.9-5.8 m thick sequence with prevailing fluvial sands and clays. The poor rounding and lithological composition of clasts in Quaternary sands and gravels indicates a short-distance transport of some clastic components with crystalline and Permo-Carboniferous provenance, probably representing deposits of the Čertík creek. In boreholes NE-1 and NE-2 the stratigraphy of the sub-Quaternary sediments is not clear because of the non-specific clay-rich lithology which can belong both to Cretaceous and Neogene, possibly re-deposited in Quaternary. In NE-2 borehole, the content of Permian-Carboniferous arcoses/siltstones in the clastic component suggests that the top of the Klikov Fm. does not correspond with the main change in lithology and colour (the Permo-Carboniferous clastic components are usually not found in Klikov Fm.). The base of Quaternary thus can not be defined clearly.

Fig. 4.6.2-1: Situation of the locality Nemanice showing approximate extent of Quaternary fluvial deposits (grey, oblique hatching; taken from geological maps) and their thickness verified in boreholes (circles with depth in meters; colour denotes the stratigraphy reached at the bottom: yellow - Quaternary, green - Cretaceous, red - crystalline, purple - Permo-Carboniferous). Red, green and blue dotted lines denote the positions of gravity indications of the fault calculated for depths of 250, 125 and 80m. Resistivity and GPR profiles shown as red and blue-dotted lines, respectively. Contour line step 1-2 m. S-JTSK system with grid step of 200 m.

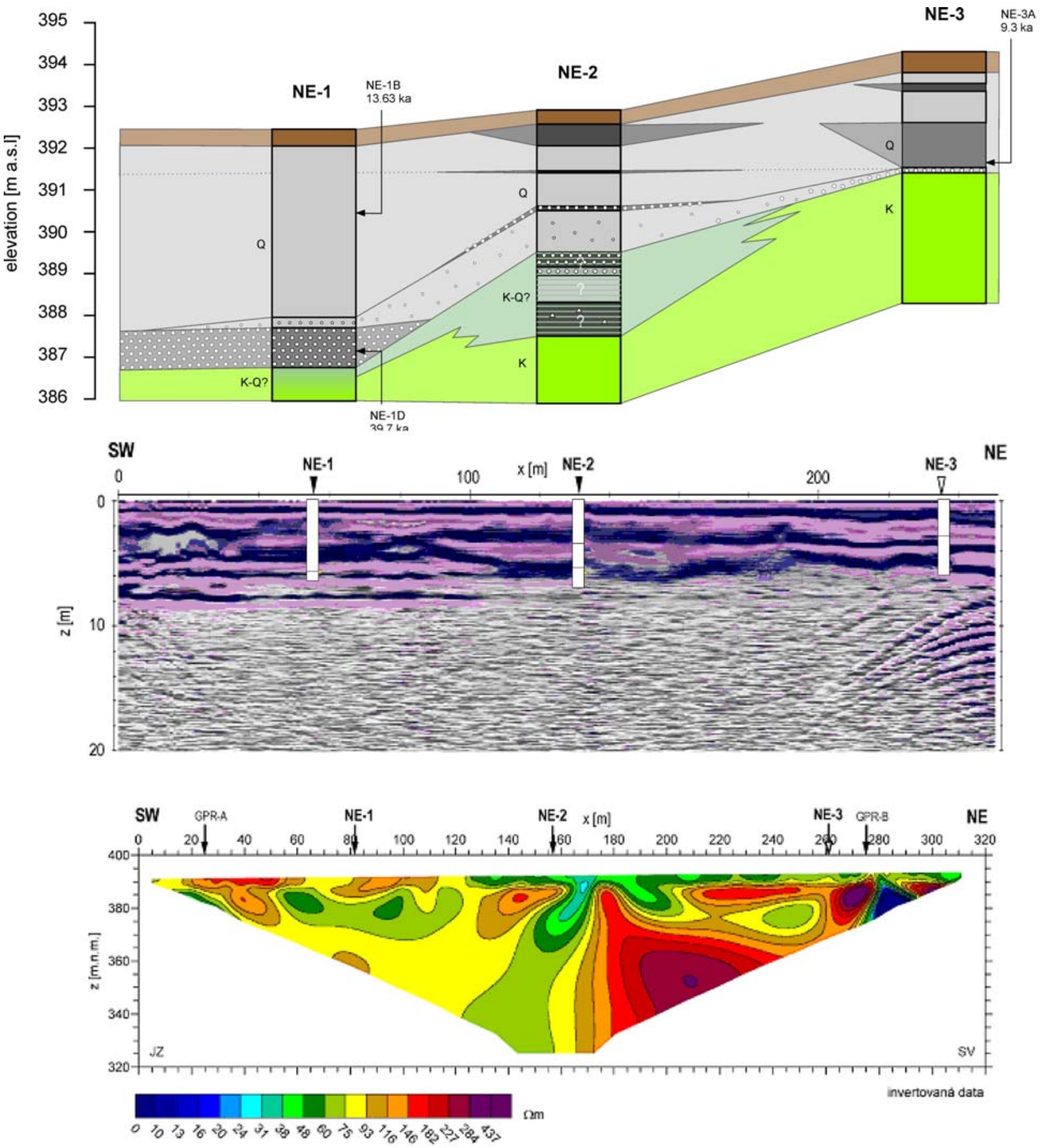

Fig. 4.6.2-2: Electrical resistivity tomographic section NEM-1 (bottom; electrode spacing 4 m), GPR section NEM-GPR-2 (centre; 50 MHz) and boreholes with suggested correlation (top; NE-1 and NE-2 on profile, NE-3 approx. 18 m to the SE of the profile). The sub-vertical boundary at base distance 175 m of the resistivity section was interpreted as the Hluboká Fault. The resistivity minimum in the NE part of the section is probably caused by local electrical facility. The position of GPR profile is marked on resistivity profile for spatial reference. Note the shallow horizon seen on both profiles corresponding to Quaternary fluvial sediments. In GPR section the base of Quaternary is indicated by horizontal strokes. No significant offset is observed.

Although the lithological variability is significant, the correlation can be made at least for the upper, sand-rich part of the sequence. The shallowing of the Quaternary sediments and the increasing content of clays towards the NE are in accordance with slightly rising elevation and can be explained as a transition to more distal parts of the fluvial sedimentary system. The often observed gravels with clay/silt-rich matrix found at the base or within fluvial deposits, could represent transitions to different alluvial sedimentary environments. With some degree of uncertainty these sediments can be correlated between the boreholes, suggesting the 40 ka age for the basal parts of Quaternary sequence across the large part of the transect NEM-1.

OSL dating of three samples from the boreholes proves Late Pleistocene to Holocene age of the fluvial sedimentary sequence covering the fault. In the borehole NE-1 the clay/silt-rich sandy matrix of gravels in the basal parts of Quaternary (sample NE-1D) has been dated at 39.70±2.40 ka. The overlying sands give the age 13.63±0.86 ka (sample NE-1B). The clay-rich pebbly sands near the base of Quaternary sequence in the borehole NE-3 (sample NE-3A) give the Holocene age 9.27±0.51. This range of ages overlaps with the ages revealed at the locality Úsilné, and suggests that the fluvial sedimentation was synchronous with alluvial sedimentation and gelifluction on the terrain scarps at least during the Marine Isotope Stages 3 and 2.

The continuity of the base of Quaternary sediments across the transect NEM-1 indicate that segment 2B of the Hluboká Fault has not experienced tectonic slip with significant vertical component at least during the large part of Holocene (10 000 years BP).

The earlier slip history can not be assessed unambiguously based on the data available, but the partial correlation of some lithological markers between the boreholes suggests an undisturbed sequence back to 40 000 years BP.

4.7. SEGMENTS 3 AND 4A: LOCALITY ÚSILNÉ

4.7.1. INTRODUCTION

Approximately 800 m south of the village of Úsilné segment 4A of the Hluboká Fault coincides with the contact of Cretaceous sediments of the Budějovice Basin and Permian-Carboniferous sediments representing the relic (so called Lhotice sub-basin) of the Blanice Graben sedimentary fill. This lithological contact is associated with mild but well defined terrain scarp (azimuth 150-160°) and nearly perfectly coinciding, pronounced maximum of the horizontal gravity gradient indicating a very steep fault. Boreholes made earlier in the broader area proved the basin-fill thickness of 330-350 m (see Chapter 4.1 for discussion on the basin fill stratigraphy). The seismic section Úsilné (Decker et al. 2010) suggests that the sediment thickness can reach >400 m near this locality.

The contact of the Cretaceous and Permian-Carboniferous sediments is easily mapped in this area since both have characteristic lithologies, the Tertiary is missing and the thickness of Quaternary fluvial and colluvial sediments is relatively small. Using geophysical and shallow borehole survey we were able to confirm the steep sub-surface lithological contact in the depth range 0-20 m and to refine its location in places with inexpressive terrain scarp (Chapter 4.7.2.1). This fault segment was exposed in two trenches (R1 and R2) located directly on geophysical profiles. The descriptions and logs of the exposed walls are given in the following chapters together with their interpretations.

In close proximity to R1 and R2 trenches the NNW-SSE striking segment 4 of the Hluboká Fault adjoins minor segment 3 with the WNW-ESE strike and approximate length of 500 m. The existence of this fault segment is inferred as a necessary geometrical link between distinct segments 2 and 4. However, the character of the gravity indication of the fault is diffuse, suggesting a complicated structure of the Hluboká Fault in this area most probably resulting from the interference with the NNE-SSW striking Drahotěšice Fault - a part of an important fault system linked to the Permian-Carboniferous Blanice Graben. In segment 3 thick sequences of Cretaceous sediments are developed on both wings of the fault and the lack of geomorphological expression at the contact of easily eroded soft sediments makes the detailed location of the fault trace difficult. Two resistivity profiles in the eastern part of the segment proved the existence of steep lithological boundaries parallel to the local fault strike. With the intent to verify the local fault trace and to study the fault-related deformation of the sediments we excavated the third trench (R3) in a flat terrain with fluvial sediments close to the contact with segment 4. The results and interpretations are given in Chapter 4.7.3.

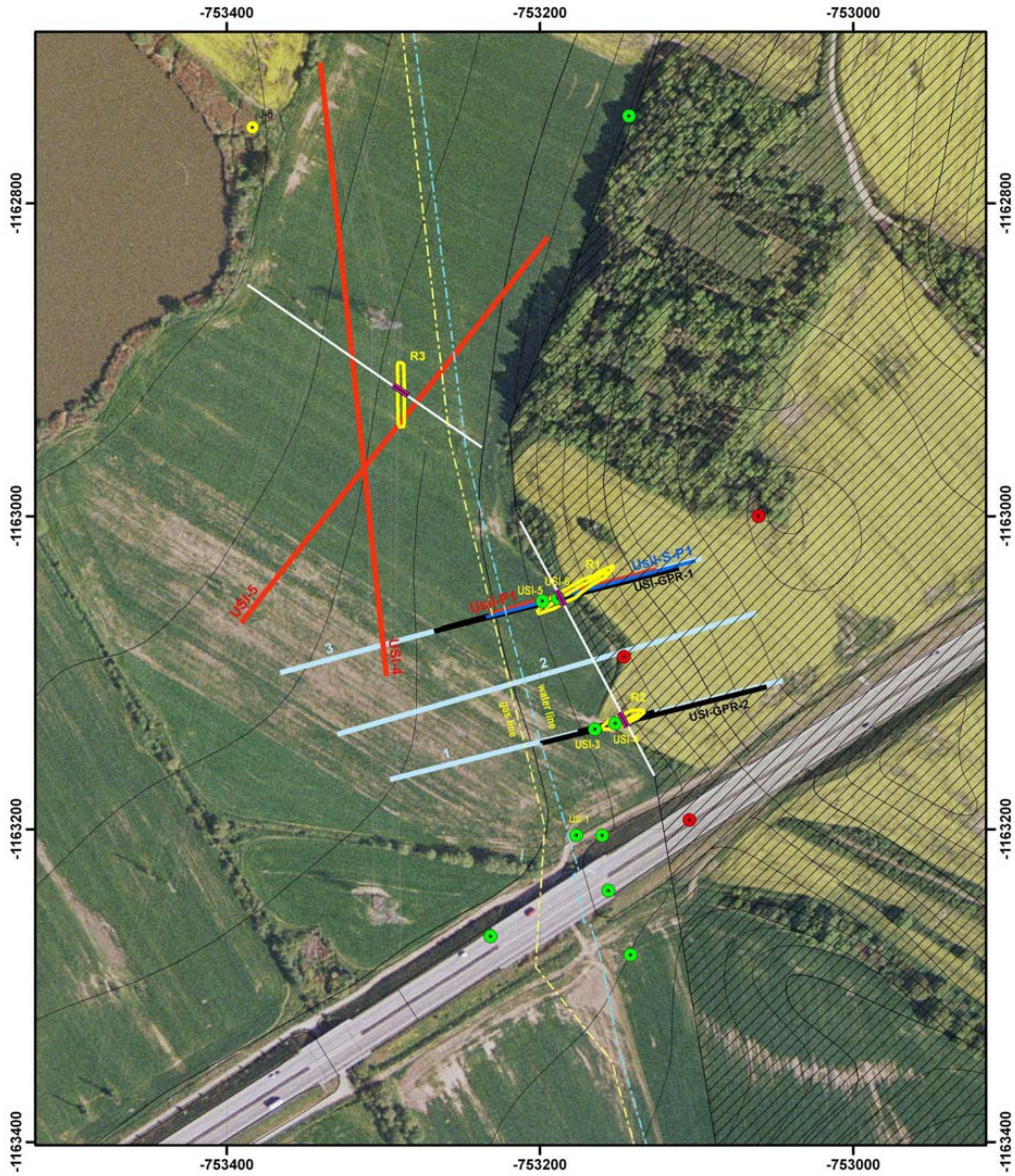

Figure 4.7-1. Situation at the locality Úsilné. Circles show the shallow boreholes, colour denoting the sub-Quaternary stratigraphy: red - Permian-Carboniferous, green - Cretaceous, yellow - not confirmed. The extent of Permian-Carboniferous shown as hatched area. Trenches R1-3 are shown as yellow lines. White lines show the expected trace of the Hluboká fault (segments 3 and 4A). Purple strokes show the position of fault/main lithological boundary verified in the trenches. Position of geophysical profiles shown with bold lines: red - multielectrode resisitivity profiles, light blue - pole-dipole profiles, blue - refraction seismic profile, black - GPR. Dot-and-dash lines show the position of gas and water pipelines. Terrain contour lines with 2 m step.

4.7.2. TRENCHES R1 AND R2

4.7.2.1. Geophysical and borehole survey

Three parallel profiles were defined on fault segment 4A oriented at about 70° to the terrain scarp (Fig. 4.7-1) and, based upon the preliminary results of the pole-dipole measurements two profiles were studied in detail, using multielectrode electrical resistivity, shallow refraction seismics (both at profile 1) and GPR meaurements (profiles 1 and 2).

Similarly as in other surveyed parts of the Hluboká Fault the resisitivity and GPR methods have shown well defined indications of lithological contacts near the expected fault trace (Figs. 4.7.2-1, 4.7.2-2) which were, however, difficult to interpret and could only be explained unambiguously after the trenching. The low-resistivity domain in the central part of the resistivity profile apparently corresponds with the fault gouges and clayey Cretaceous sediments adjacent to the fault (see the logs in Figs. 4.7.2-9 and 4.7.2-10). The promontory of this domain in shallow parts of the profile probably corresponds with the same clay-rich lithologies affected by downslope transport due to Late Quaternary gelifluction. The penetration depth of GPR was low, but relatively high contrast of the first reflection amplitudes was observed between the two parts of the profile separated by the foot of the terrain scarp (not seen in the figures). This can be explained as a combined effect of contrast in lithology and water saturation.

By contrast, the refraction seismic profile clearly shows a sharp termination of high velocity layer spatially associated with the foot of the terrain slope which later proved to correspond with the sub-vertical fault. Figure 4.7.2-3 shows the results of the three methods used at the profile 1 together with the position of trench R1.

Taking into account the low resolution of seismic profile and the ambiguous results of electrical methods we had to verify the position of the lithological boundary prior to trenching by several shallow boreholes in colluvia (see example in Fig. 4.7.2-4).

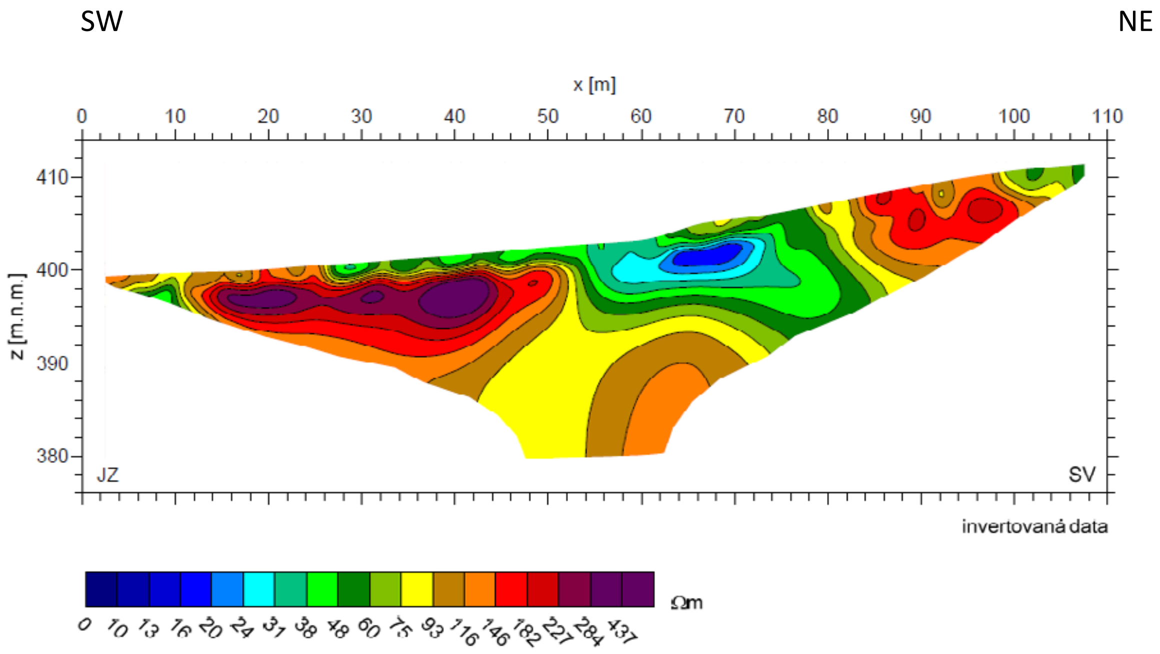

Fig. 4.7.2-1. Inverted resistivity profile USI-P1 at Úsilné locality (R1 trench site).

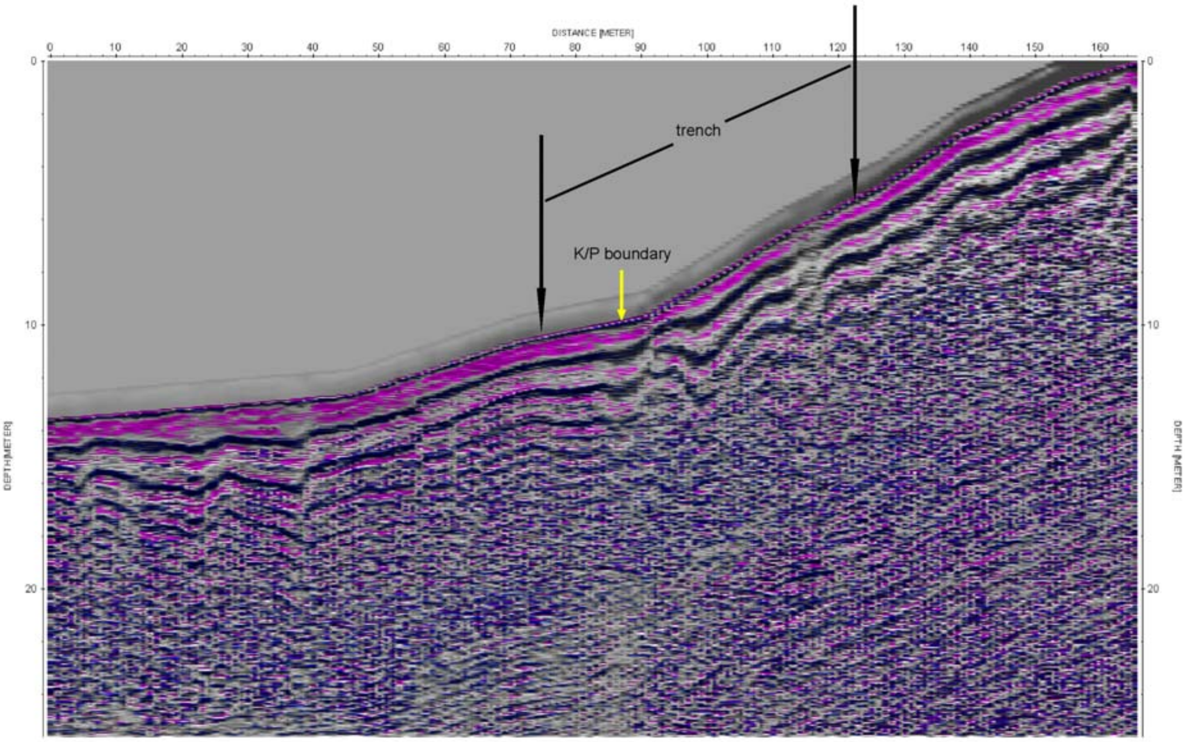

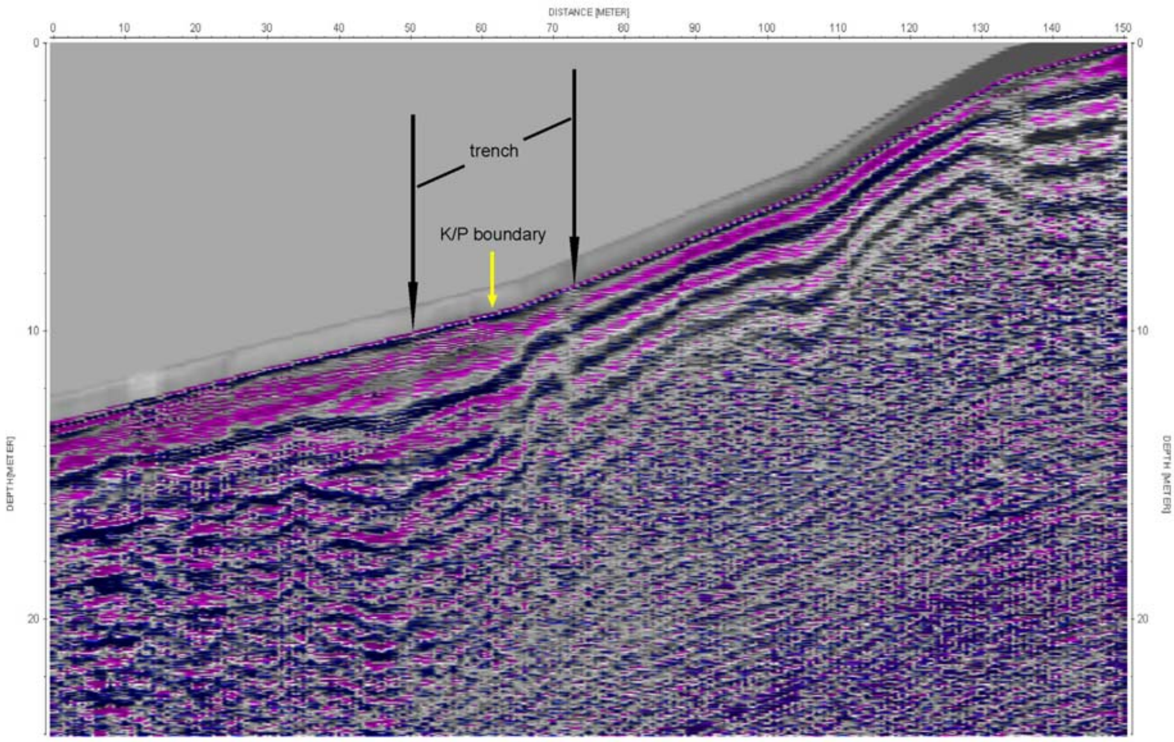

Fig. 4.7.2-2. 50 MHz GPR profiles USI-GPR-1 (top) and USI-GPR-2 (below). The position of trenches and the main lithological boundary are shown by arrows.

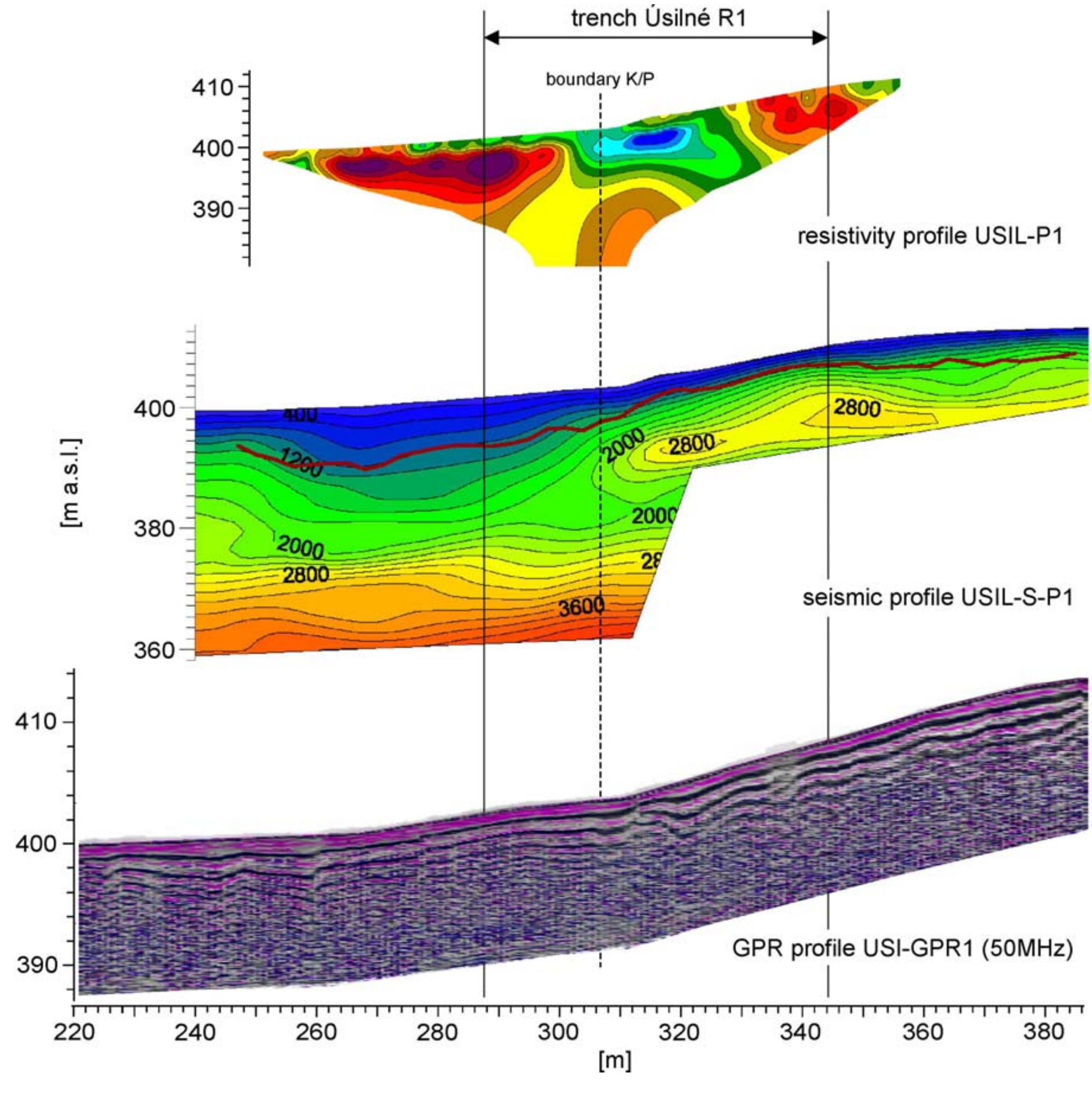

Fig. 4.7.2-3. Aligned resisitivity, refraction seismic and GPR profiles at Úsilné locality, profile 3. Also shown are the positions of trench R1 and the boundary Cretaceous/Permo-Carboniferous.

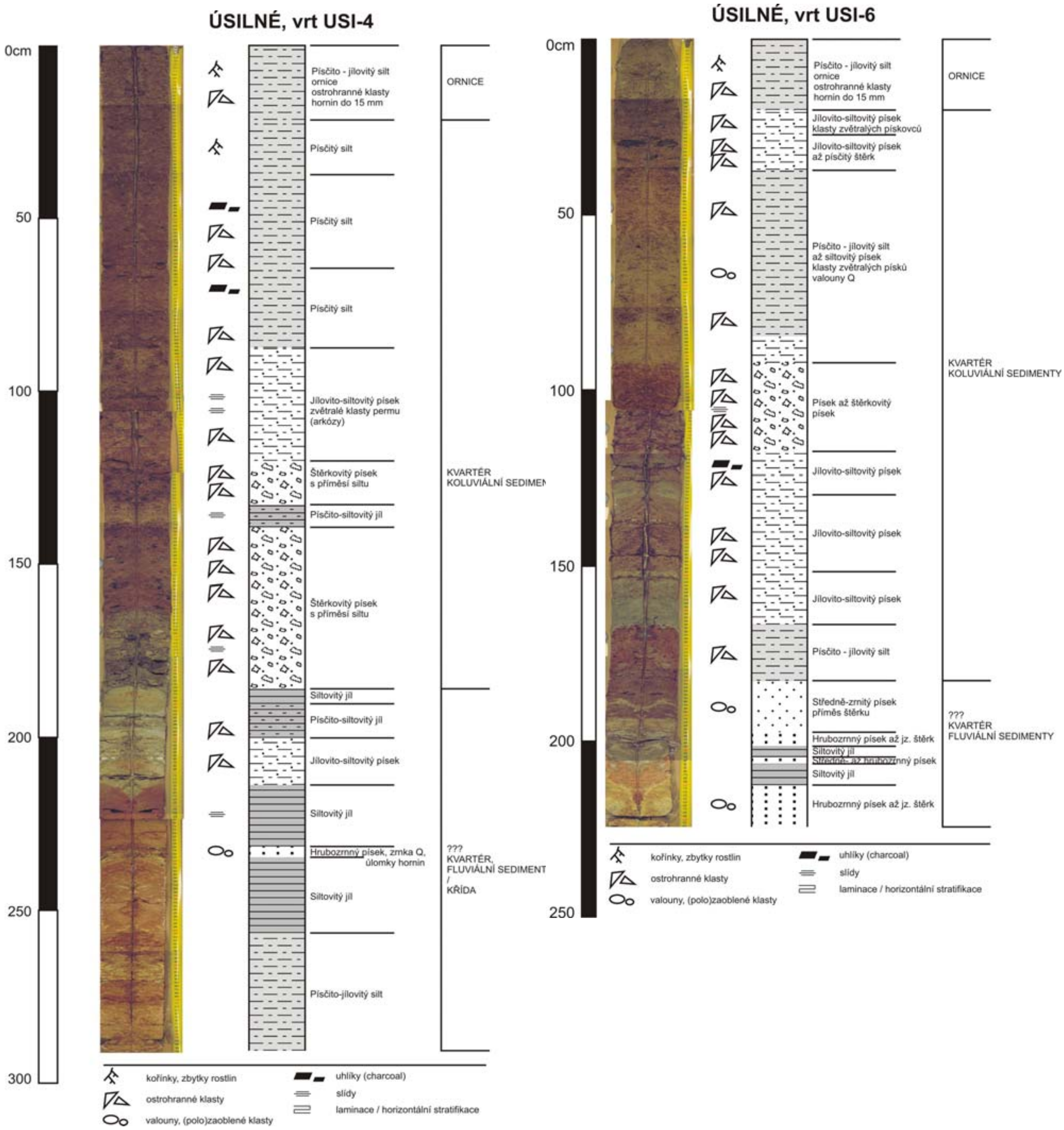

Fig. 4.7.2-4. The example profiles through the colluvia sampled by shallow boreholes below the fault scarp at the locality Úsilné (author: O. Bábek).

4.7.2.2. Trenching

After the geomorphological and geophysical mapping fault segment 4A was exposed in two trenches (R1 and R2) located right on geophysical profiles 3 and 1 (Fig. 4.7-1). Auxiliary trench R2 was excavated to enable correlation of the observed structures and assessment the structural homogeneity in the broader area. The length of the trenches was limited by the protection zones of the gas- and water pipelines which are located close below the foot of the fault scarp. Taking into account the safety regulations, mechanical properties of the material and the demands on the easy documentation, the combined single- or double-benched trench cross-sections with laid-back walls were used (Fig. 4.7.2-5).

Trench R1 was located to reach the broader area of the contact of Cretaceous and Permo-Carboniferous sediments indicated by terrain scarp and seismic profile (azimuth 47°, length 56m incl. ramps, typical depth 4m, maximum depth 5m). The location of trench R2 where morphological scarp is not developed was selected mainly basing on the borehole survey and GPR profile (azimuth 55°, length 28m incl. ramps, typical depth 3.5m).

After multiple cleaning of trench walls a 0.5×0.5 m to 1×1 m reference grid was constructed and geodetically referenced. A detailed documentation was then carried out incuding the compilation of orthorectified photomosaic, description of lithologies, logging, structural measurements and sampling.

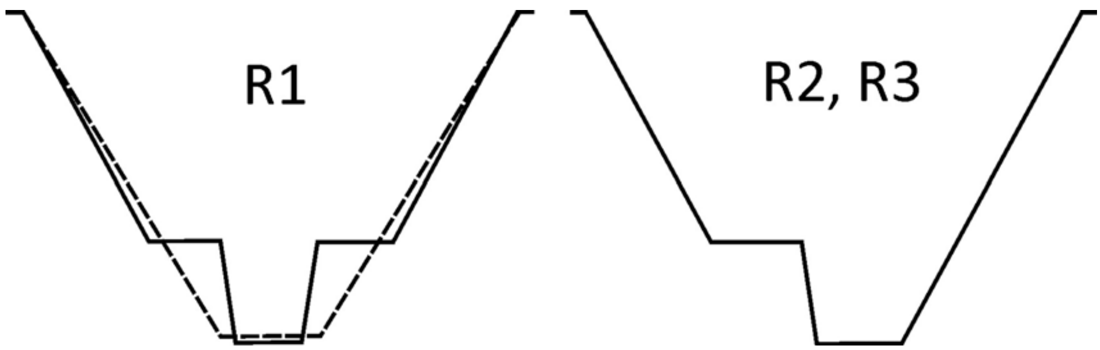

Fig. 4.7.2-5. Schematic cross-sections of the trenches. Maximum width on a terrain surface level: 4.5-8 m.

Fig. 4.7.2-6. Photographs documenting the excavation of R1 and R2 trenches and overall situation on the locality Úsilné with R1 and R2 trenches viewed from SE (Oct 2009). Yellow dashed line shows an approximate trace of the fault (segments 4A, 3 a 2B). Red line shows the position of trench R3 excavated in 2010.

4.7.2.3. The structure of the exposed fault zone and colluvia

Despite some differences the exposed fault zone displays similar lithological and structural features in both trenches (R1 and R2) with deformed Cretaceous sediments in the SW in a steep tectonic contact with Permo-Carboniferous sediments in the NE.

Photomosaics and logs of the exposed walls are shown in Figs. 4.7.2-9 to 4.7.2-11.

In Cretaceous sediments the lithological sequence is as follows (from SW to NE):

1/ Light grey coase- to fine-grained sands/sandstones,

2/ Coarse- to fine-grained sands alternating with grey, dark grey, brown, beige and red clayey beds.

In Permo-Carboniferous sediments the lithological sequence is as follows (from contact with Cretaceous to NE):

1/ Fractured and cataclastic arcoses with clay-rich fault gauges (brown to green colours),

2/ Strongly faulted arcoses with slices of mylonitized red-brown siltstones,

3/ Arcoses with intercalated siltstones less affected by tectonic deformation, with clear bedding.

Detailed photographs of some structures are given in Figs. 4.7.2-7, 8, 12, 13 and 16. Lithological boundaries within the whole exposed fault zone have generally NW-SE strike and are mostly steeply inclined to the NE. In Cretaceous sequence sub-vertical boundaries with dips both to the NE and SW prevail. The block of Permo-Carboniferous rocks is in the hanging wall position, being thrusted over Cretaceous sediments due to the post-Santonian fault slip with significant thrust component.

The most distinct structural difference between the two trenches is observed in the block of Permo-Carboniferous sediments where part of the sequence in trench R1 is disturbed by a NE-SW striking system of fault planes associated with a broad domain of mylonitized red-brown siltstones and slices of fractured arcoses with clay fault gouges.

Azimuth of the line connecting the main thrust planes in the two trenches is 155°. This orientation is identical to the strike of the local gravity indication of the fault (see Chapter 2.2).

The upper 1.5-2.8 m of the exposed profiles are represented by colluvia strongly affected by solifluction. This horizon is interpreted as a product of Quaternary weathering and gravity-driven slope movements supported by high water content due to melting of the snow-cover and the upper parts of permafrost (so called *gelifluction*). These horizons are characteristic by well developed uniform layering (locally lamination) with layers sub-parallel to the terrain surface. In both trenches domains of fine-grained, well sorted quartz-rich sands with well rounded grains, containing variable amounts of colluvia-derived component, are developed. These domains were mainly observed as parts of accumulation anomalies characterized by complex (often chaotic) structure of individual layers, mutually mingled into variable shapes. These accumulation anomalies are interpreted as the products of landslides, sandy domains being parts of alluvial bodies which were being deposited on top of the fault scarp and emplaced into gelifluted colluvia and landslides.

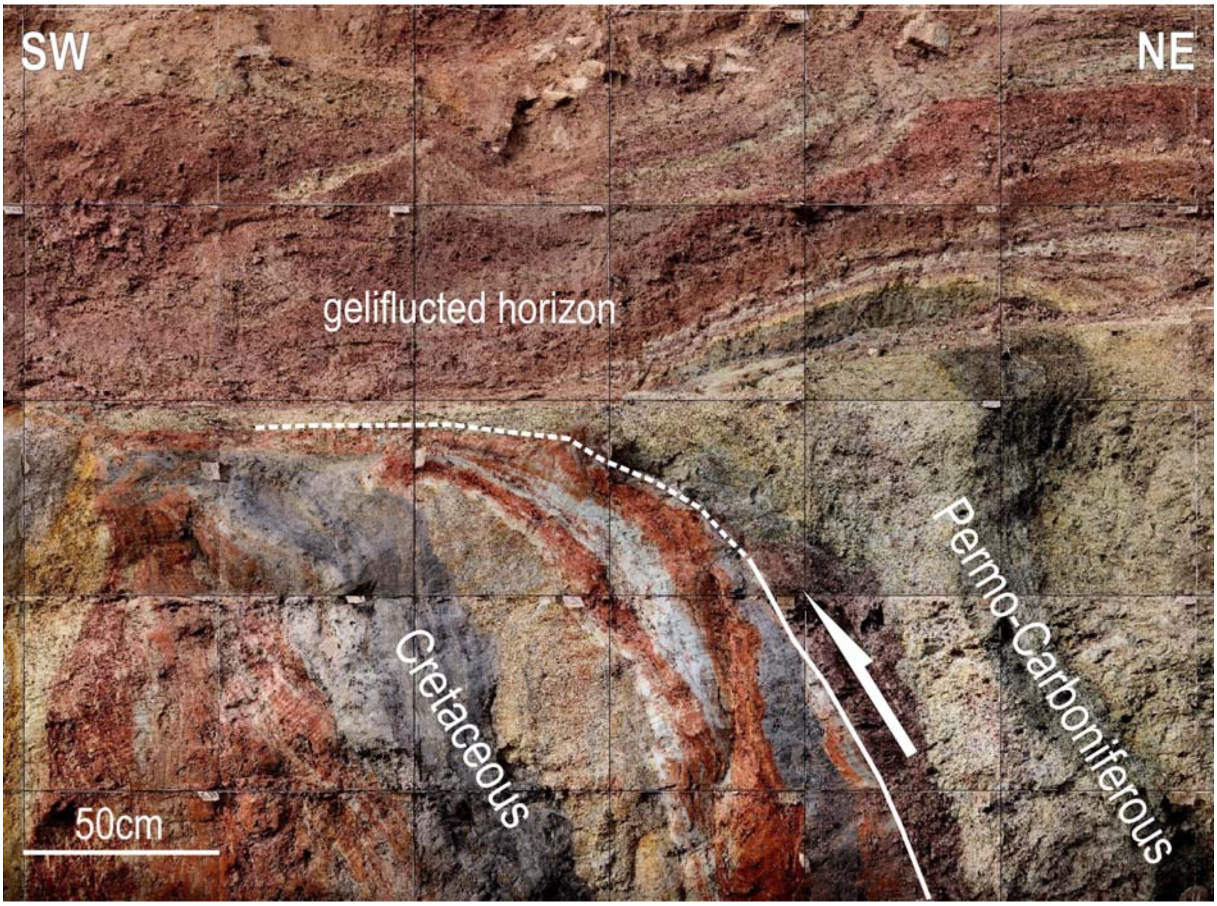

Fig. 4.7.2-7: Detail of the tectonic contact of Cretaceous and Permo-Carboniferous rocks in trench R1 (wall R1-a, view to the NW. Cataclastic arcoses with clay fault gouges (right) are thrusted over variegated Cretaceous clays and sands (left). Note that tectonic structures do not continue into the geliflucted horizon developed above the fault.

Samples taken from such sand-rich domains were dated by OSL method, assuming that these sediments were exposed to the sunlight during mixing of the their alluvial and colluvial components. Sample USI-2A from trench R1, where these sediments are part of a landslide, gives an age 48.7 ± 2.6 ka. The sample from the lower part of colluvia in the SE wall of trench R2 (profile R2-b, sample USI-4B) gives an age 21.8 ± 1.2 ka. The interpretation is given below, in Chapter 4.7.4.

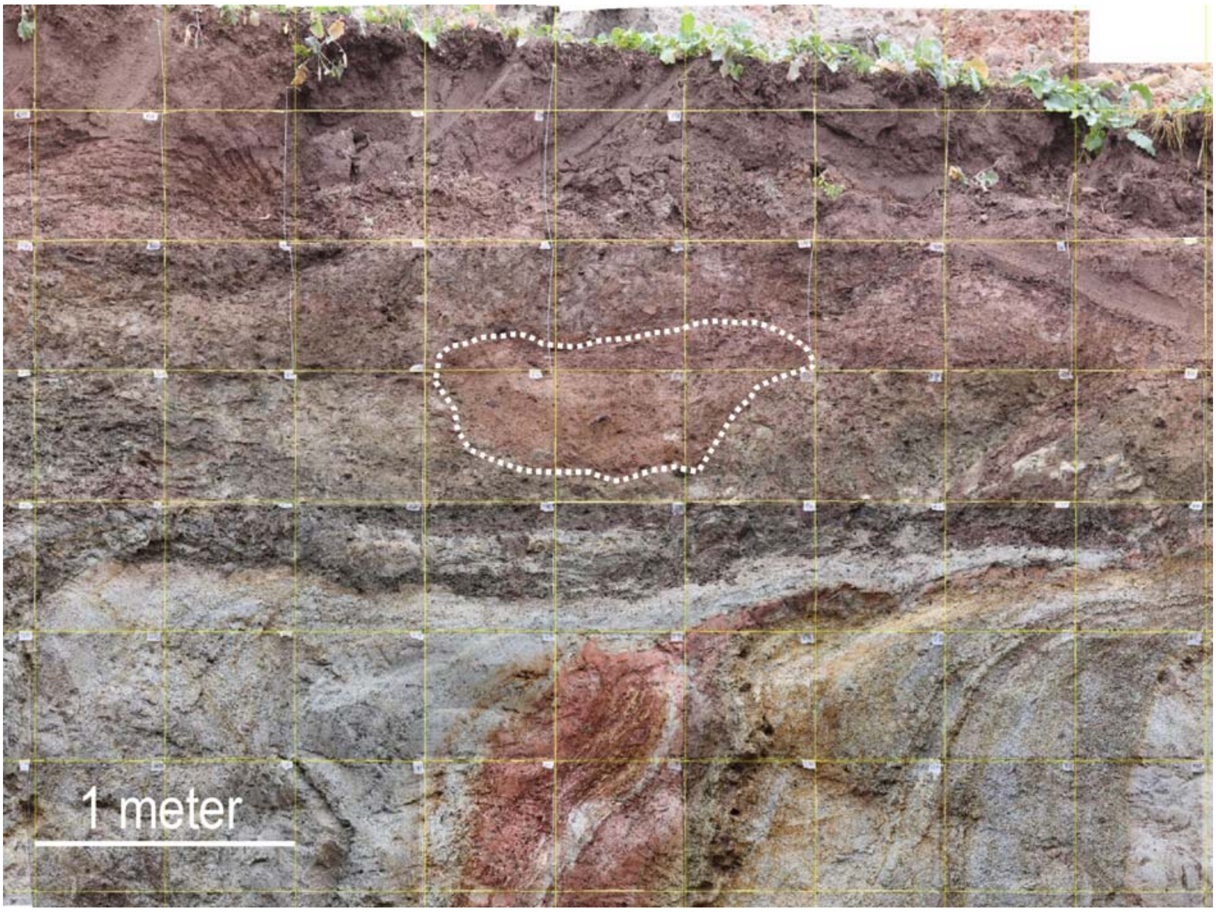

Fig. 4.7.2-8. The domain of alluvial sands mixed with colluvia-derived component emplaced into the colluvia during gelifluction. Trench Úsilné R2.

On following pages:

Fig. 4.7.2-9: Orthorectified photomosaic and schematic log of the main lithological and structural features in trench R1 (NW wall, R1-a). Thrust contact of Cretaceous and Permian-Carboniferous sediments is located at base-distance 17 m. Positions of dated sample USI-2A shown by black-and-white disc.

Fig. 4.7.2-10: Orthorectified photomosaic and schematic log of the main lithological and structural features in trench R2 (R2-a - NW wall and R2-b - SE wall). Thrust contact of Cretaceous and Permian-Carboniferous sediments is located at base-distance 3.5-3.7 m. Positions of dated sample USI-4B shown by black-and-white disc.

Úsilné R1-a

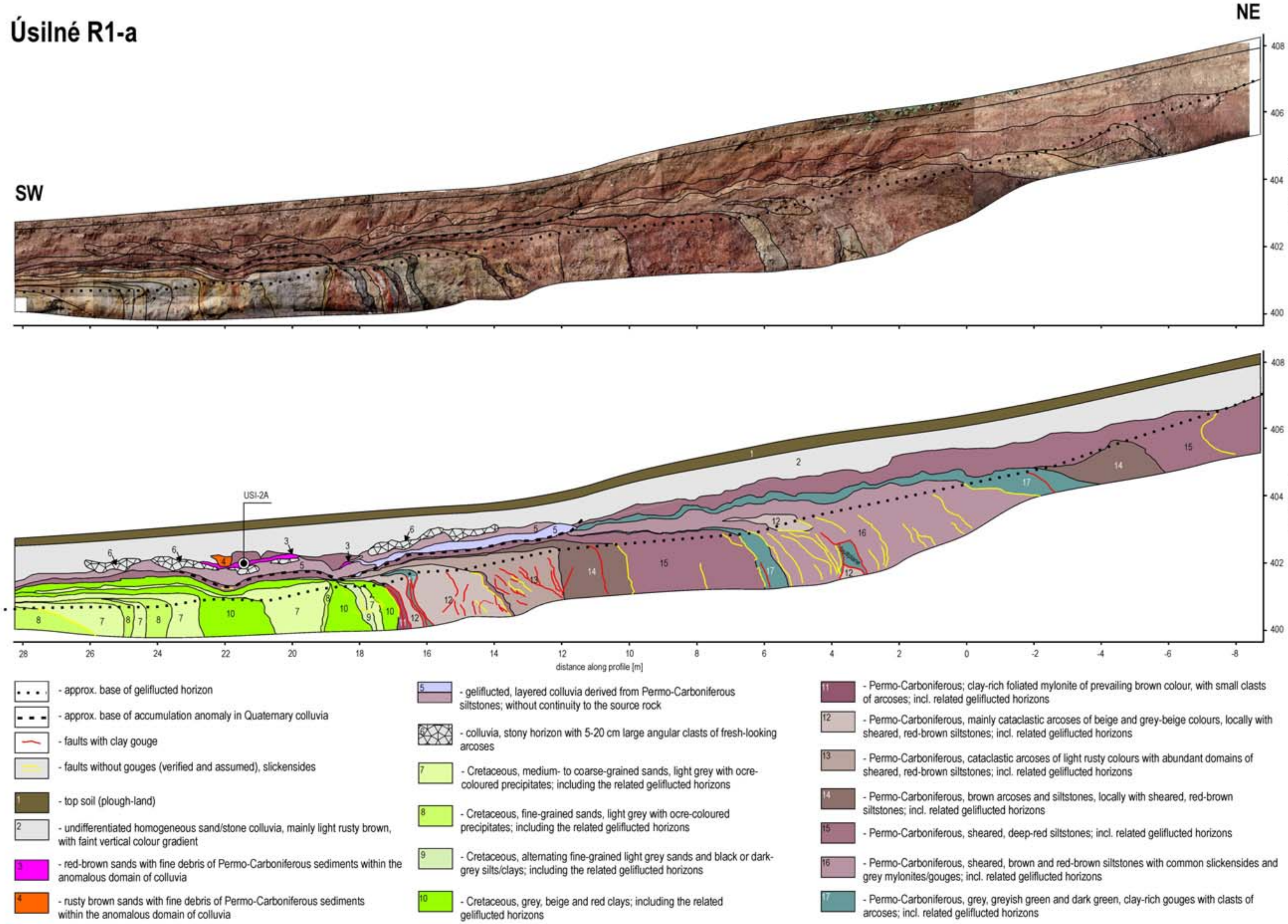
SW
NE
elevation [m a.s.l.]
408
406
404
402
400
USI-2A
distance along profile [m]
28
26
24
22
20
18
16
14
12
10
8
6
4
2
0
-2
-4
-6
-8
- approx. base of gelifluted horizon
- approx. base of accumulation anomaly in Quaternary colluvia
- faults with clay gouge
- faults without gouges (verified and assumed), slickensides
1 - top soil (plough-land)
2 - undifferentiated homogeneous sand/stone colluvia, mainly light rusty brown, with faint vertical colour gradient
3 - red-brown sands with fine debris of Permo-Carboniferous sediments within the anomalous domain of colluvia
4 - rusty brown sands with fine debris of Permo-Carboniferous sediments within the anomalous domain of colluvia
5 - gelifluted, layered colluvia derived from Permo-Carboniferous siltstones; without continuity to the source rock
- colluvia, stony horizon with 5-20 cm large angular clasts of fresh-looking arcoses
7 - Cretaceous, medium- to coarse-grained sands, light grey with ocre-coloured precipitates; including the related gelifluted horizons
8 - Cretaceous, fine-grained sands, light grey with ocre-coloured precipitates; including the related gelifluted horizons
9 - Cretaceous, alternating fine-grained light grey sands and black or dark-grey silts/clays; including the related gelifluted horizons
10 - Cretaceous, grey, beige and red clays; including the related gelifluted horizons
11 - Permo-Carboniferous; clay-rich foliated mylonite of prevailing brown colour, with small clasts of arcoses; incl. related gelifluted horizons
12 - Permo-Carboniferous, mainly cataclastic arcoses of beige and grey-beige colours, locally with sheared, red-brown siltstones; incl. related gelifluted horizons
13 - Permo-Carboniferous, cataclastic arcoses of light rusty colours with abundant domains of sheared, red-brown siltstones; incl. related gelifluted horizons
14 - Permo-Carboniferous, brown arcoses and siltstones, locally with sheared, red-brown siltstones; incl. related gelifluted horizons
15 - Permo-Carboniferous, sheared, deep-red siltstones; incl. related gelifluted horizons
16 - Permo-Carboniferous, sheared, brown and red-brown siltstones with common slickensides and grey mylonites/gouges; incl. related gelifluted horizons
17 - Permo-Carboniferous, grey, greyish green and dark green, clay-rich gouges with clasts of arcoses; incl. related gelifluted horizons

Úsilné R2-a

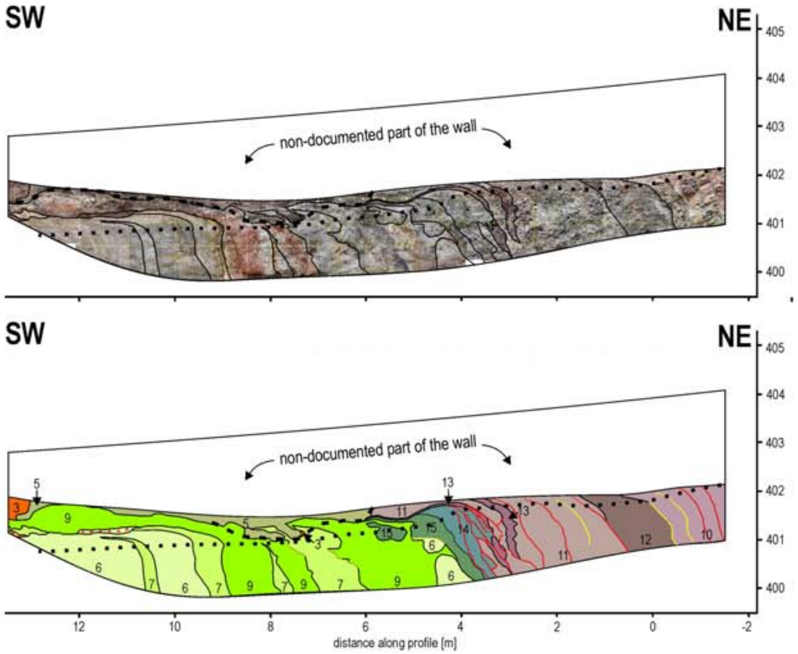

Úsilné R2-b

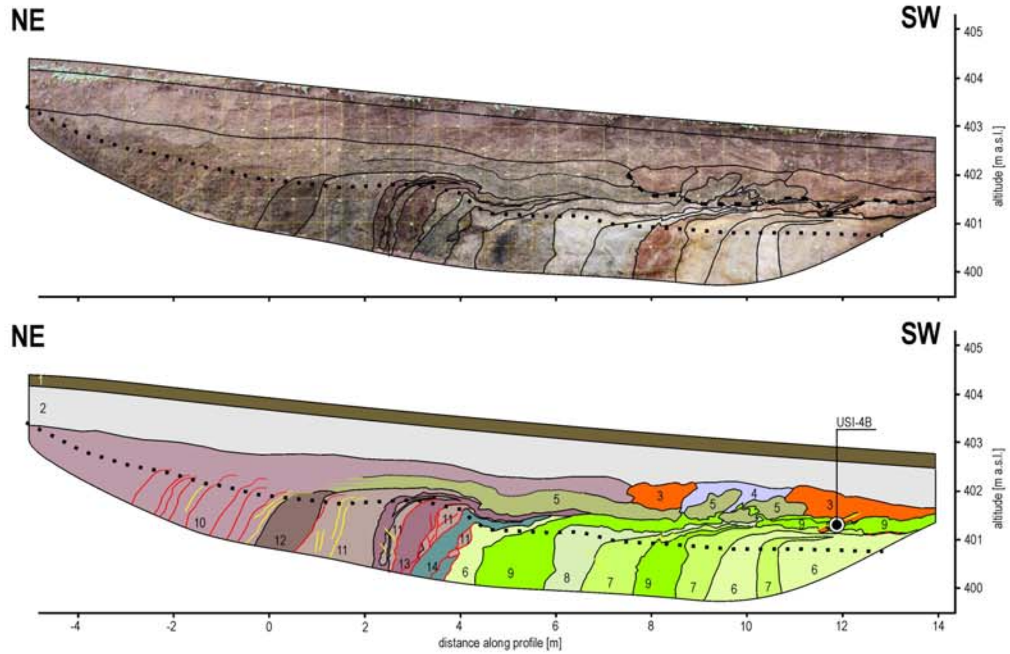

- approx. base of gelifluted horizon
- approx. base of accumulation anomaly in Quaternary colluvia
- faults with clay gouge
- faults without gouges (verified and assumed), slickensides
- top soil (plough-land)
- undifferentiated homogeneous sand/stone colluvia, mainly light rusty brown, with faint vertical colour gradient
- rusty brown sands with debris of Permo-Carboniferous sediments within the colluvia
- gelifluted, layered colluvia derived from Permo-Carboniferous sediments; without continuity to the source rock
- horizon of green-brown colluvia with unclear continuity to Permo-Carboniferous source-rock, and unclear upper margin in NE part
- deep rusty brown weathered horizons wiithin gelifluted Cretaceous sands
- Cretaceous, medium- to coarse-grained sands, light gre, locally with ocre-coloured precipitates; including the related gelifluted horizons
- Cretaceous, fine-grained sands, light grey with ocre-coloured precipitates; incl. related gelifluted horizons
- Cretaceous, medium-grained sands with intercalations of clays, both light grey, with ocre-coloured precipitates; incl. related gelifluted horizons
- Cretaceous, grey, beige and red clays/silts; including the related gelifluted horizons
- Permo-Carboniferous, alternating rusty brown arcoses (dm-size) and sheared, deep- red-brown siltstones (cm-size); incl. related gelifluted horizons
- Permo-Carboniferous, fractured and cataclased, rusty brown arcoses, locally with sheared siltstones; incl. related gelifluted horizons
- Permo-Carboniferous, dark brown cataclased arcoses; incl. related gelifluted horizons
- Permo-Carboniferous, deep red-brown fine-grained arcoses and siltstones; incl. related gelifluted horizons
- Permo-Carboniferous, grey, brownish or greenish clay gouge with clasts of arcoses; incl. related gelifluted horizons
- Melange of clay gouge with clasts of arcoses and Cretaceous clastic sediments; incl. related gelifluted horizons

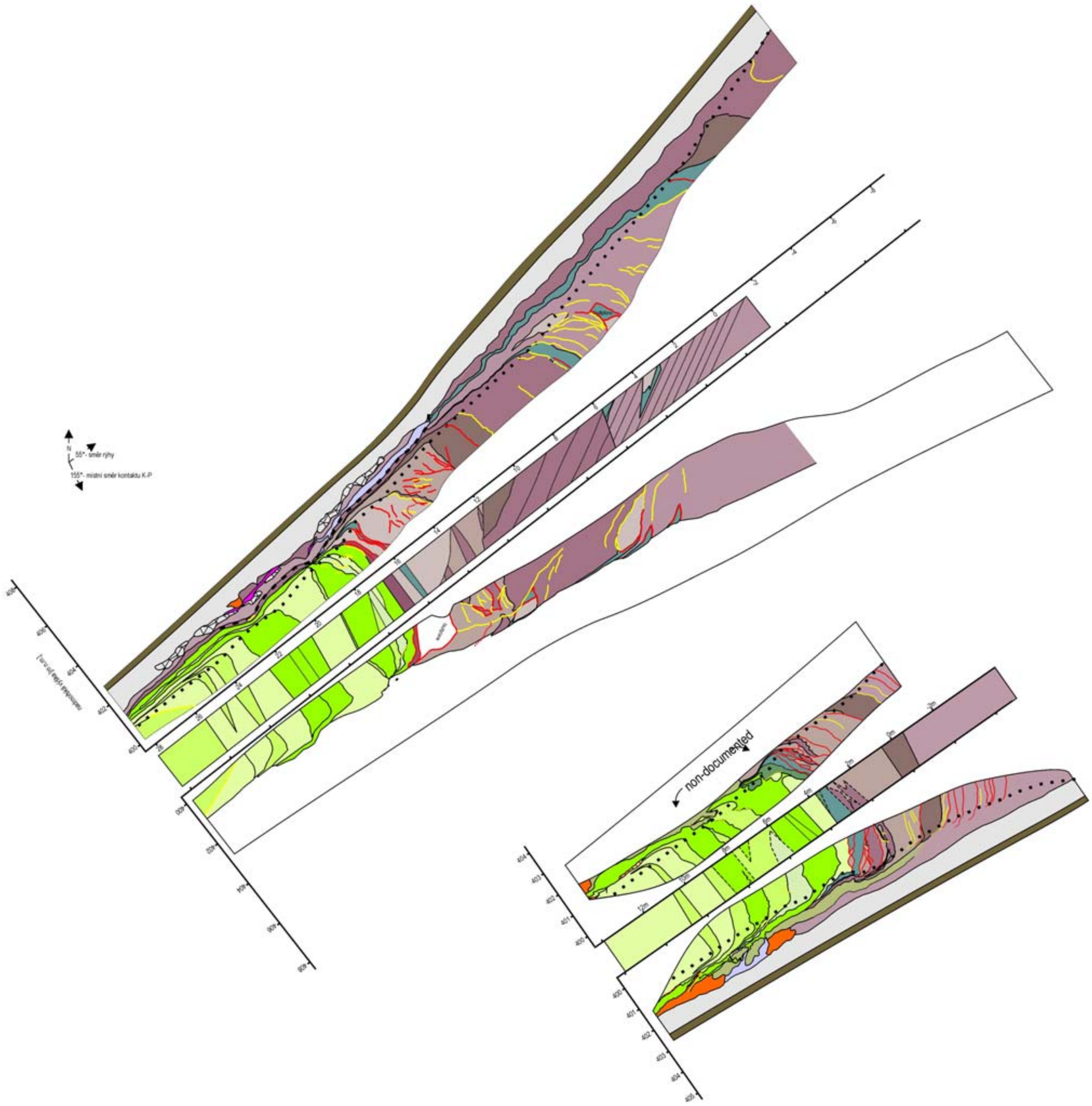

Fig. 4.7.2-11: Schematic plan- and side-view logs of the lithologies and structures exposed in trenches R1 and R2 shown in real geographical orientation. Plan views are approximative, partly derived from the observations in the walls. Legend as in Figs. 4.7.2-9 and 10.

4.7.2.4. Analysis of fault structures

In trench R1 two major fault systems with nearly perpendicular strikes were exposed: the Hluboká Fault system with mean NW-SE strike (fault planes with azimuth 140-150°) and a group of faults with NNE-SSW to NE-SW strikes (fault planes with azimuth 25-55°, Fig. 4.7.2-14). The average strike in the latter fault system is close to the azimuth of the elongation axis of the Permo-Carboniferous Blanice Graben and its local marginal faults (20-35°). In trench R2 the faults of this system were nearly absent.

As outlined above, the faults of the Hluboká Fault system have significant thrusting component - most of the lithological boundaries, slickensides and fault gauges display steep to moderate dips to the NE. In non-consolidated Cretaceous sediments the deformation is ductile or semiductile and this domain can be interpreted as an overturned limb of a large fold. Only locally, minor small-scale fault structures were observed in laminated clays (Fig. 4.7.2-12). In consolidated Permo-Carboniferous sediments the faults of this system are usually accompanied by strong mylonitization, clay gauges of variable character and chemical alterations probably connected to fluid activity (Fig. 4.7.2-13). Locally, these faults contain slickensides, but slickenlines are usually missing.

Fig. 4.7.2-12. Detailed view of conjugated system of small-scale faults in the laminated clays within the overturned limb of Cretaceous sequence, 2m from the contact with Permo-Carboniferous (R1-a, view from SE). Reference grid spacing is 50×50 cm.

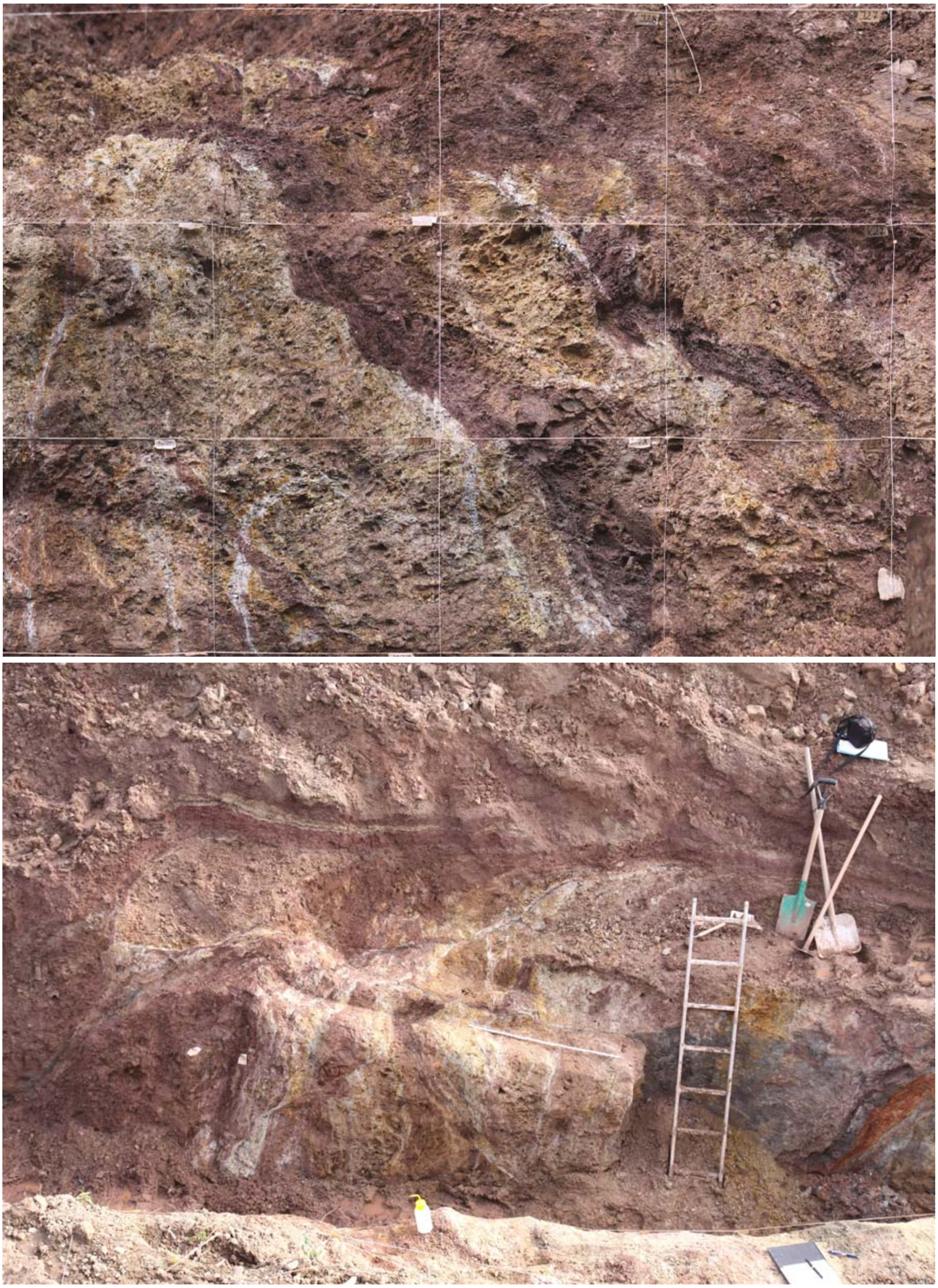

Fig. 4.7.2-12. Complicated thrusting in a zone of mixed cataclased arcoses, sheared siltstones and clay gouges developed within the Permo-Carboniferous sequence next to the contact with Cretaceous sediments. Top: R1-A, view from SE (50cm grid). Below: R1-b, view from NW (width of the area shown is 6.5 m). None of these structures continue to the gelifluted colluvia.

The second group of NNE-SSW to NE-SW strike contains faults which were activated in various times, as indicated by large scatter in orientations and mutual cross-cuttings of faults with contrasting gouges developed within the same lithologies. These faults are preferentially concentrated in a 6-7m wide shear zone in Permo-Carboniferous sequence in trench R1 with the system of nearly penetrative slickensides developed in its central part (mean dip direction/dip orientation 310/70). Away from the shear zone the faults of this orientation are less common and they were virtually not observed in trench R2. Slickenlines are usually well developed having mean orientation 203/45. In some cases two or more systems of slickenlines were observed on a single slickenside.

The determination of shear sense was problematic, since different kinematic indicators were often contradictory (assymetric steps, Riedel shears, S-C structures). In Cretaceous sands a cryptic, sub-horizontal cleavage was locally observed, manifested as the planes of preferred break-up on the cleaned walls. The intersection of this cleavage with steeper slickensides results in sub-horizontal striation on these planes, which, however, do not have any kinematic meaning.

To analyse the internal fabric of clay gouges and deformed clay-rich sediments we studied the anisotropy of magnetic susceptibility on 36 samples taken from both systems of faults. The mean susceptibility (30 to 100 × 10^{-6} SI) and its thermal dependence indicate that paramagnetic phyllosilicates are dominant magnetic carriers. In system of NNE-SSW striking faults most samples show magnetic fabric compatible with macroscopically observed slickenlines and some samples probably reflect kinematic interference with NW-SE faults. In Cretaceous clays and fault gouges associated with NW-SE faults the magnetic fabric is characterised by sub-horizontal to moderately dipping lineations scattered around mean NW-SE direction. In case of sedimentary clays this can be due to the partial reorientation of clay minerals from bedding planes into the micro-fault planes, which then could not be used as a kinematic indicator. However, since the magnetic fabric of the fault gouges is similar to the clay-rich sediments, it can rather indicate a significant strike-slip component of fault slip (by analogy to the NNE-SSW striking faults). Nevertheless, the interpretations must be made with caution, since the complex and often largely unknown long-term slip history of the faults studied can result in unexpected relations between the latest fault slip direction and the fabric of the fault gouge.

On following page:

Fig. 4.7.2-14. Compass structural measurements in trenches R1 and R2. Lower hemisphere, equal-area diagrams show the orientations of poles to re-oriented lithological boundaries, faults with gouges and slickensides (top right), the orientations of slickenlines (top left), principal directions of magnetic susceptibility tensors (AMS) in Cretaceous clay strata and fault gouges in Permo-Carboniferous with NW-SE orientation (bottom right) and with NNE-SSW orientation (bottom left). Schematic drawing in the middle is a plan-view map of R1 trench showing the spatial distribution of the two dominant types of planar features highlighted: Blue - the NW-SE planes with thrusting component; Red - NE-SW to NNE-SSW striking faults. Accordingly, these two systems are colour-coded in the top right diagram. Red dots in top left orientation diagram indicate slickenlines associated with the NNE-SSW striking faults. Note the concentration of the NNE-SSW striking faults in a several meters wide zone in Permian-Carboniferous domain.

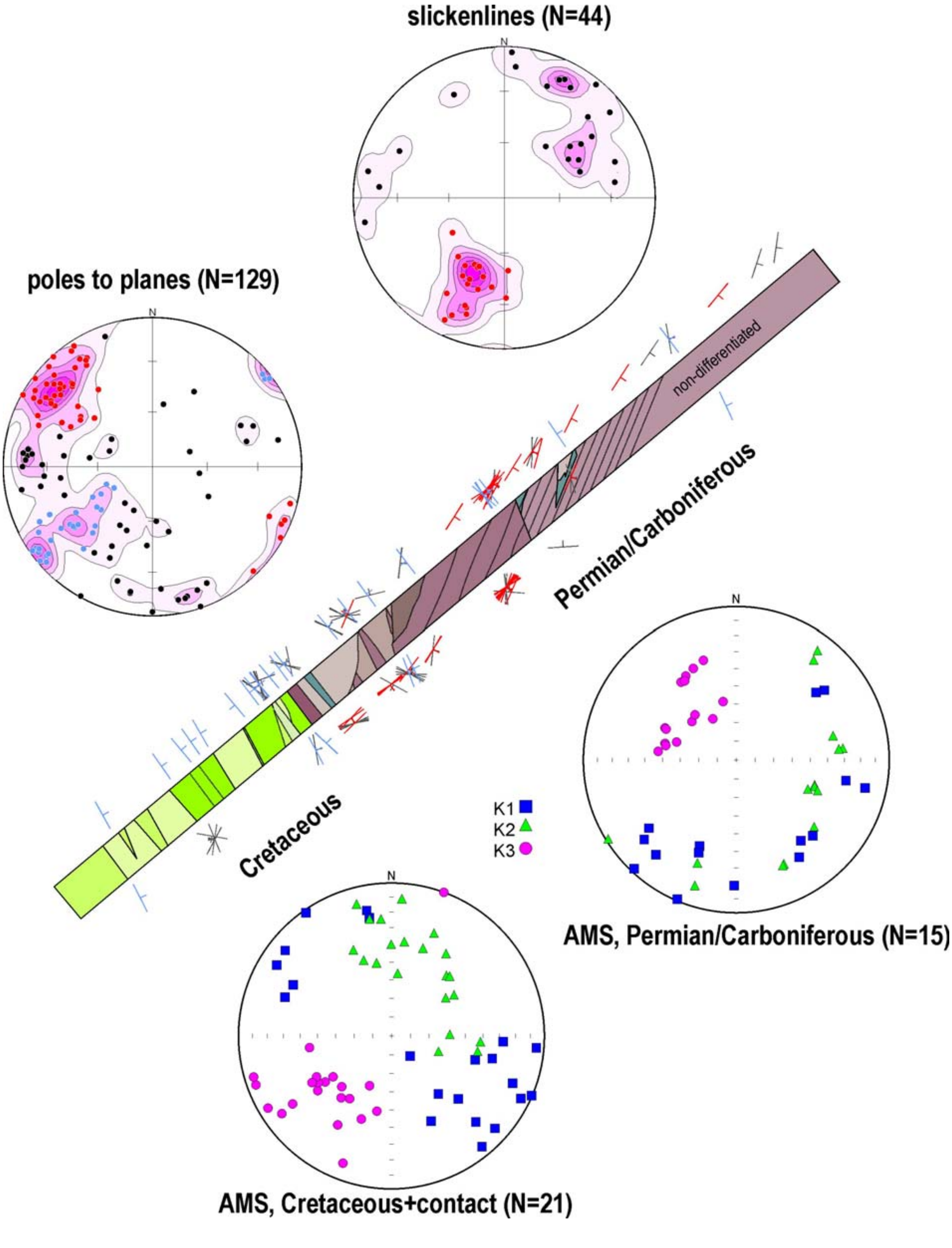
slickenlines (N=44)
N
poles to planes (N=129)
N
non-differentiated
Permian/Carboniferous
Cretaceous
N
K1
K2
K3
AMS, Permian/Carboniferous (N=15)
N
AMS, Cretaceous+contact (N=21)

The ambivalent cross-cutting relations between the two fault systems (NW-SE faults cross-cut by NNE-SSW faults and vice versa) indicate multiphase reactivation of at least one of the faults.

The presence of multiple slickenlines on single slickenside, the absence of striations on NW-SE faults as well as many other structural observations in the fault zone suggests that the reactivation history of both fault systems was rather complex. Furthermore, due to the lack of outcrops in Cretaceous and younger formations the observations in the trenches can not be complemented by other data (in older rocks of the area the deformation is too complex to be included in the analysis). In such setting the feasible estimation of paleostress can not be carried out. In spite of that, we analysed the dataset of compass measurements from the trenches using *MARK* program (Kernstocková 2005) to test the uniqueness and stability of the paleostress solutions. The program finds the best solutions, taking into account the similarity of shape parameters of reduced stress tensors calculated for all possible combinations of the input data. Manual separation of paleostress phases is avoided in the algorithm. The results show that the inversion problem is non-unique and that the individual solutions only partly satisfy the input data. Between the large number of solutions the one presented in Fig. 4.7.2-15 seems to be dominant: sub-horizontal, NNW-SSE maximum compressive stress (sigma1) and sub-horizontal, E-W to ENE-WSW striking least compressive stress (sigma3). This solution does not satisfy mainly the moderately dipping NW-SE thrusts observed in Permo-Carboniferous domain close to the contact with Cretaceous sequence in the trench R1. The structures fitting this solution could correspond to synchronous re-activation of the Hluboká and Drahotěšice Faults in several post-Cretaceous periods including Eocene, Oligocene and Miocene (see Chapter 2.4). Quaternary re-activation can not be ruled out since the paleostress solution is also close to the present-day stress in the Bohemian Massif.

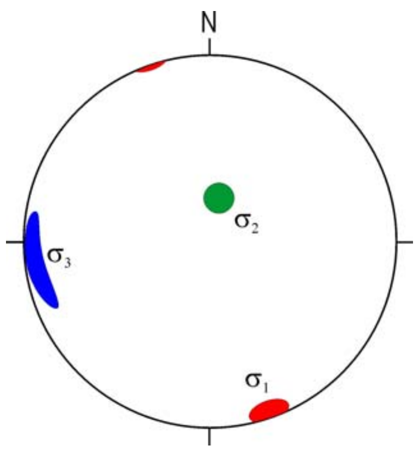

Fig. 4.7.2-15. Best solution of stress inversion of the compass measurements from the trenches R1 and R2 (re-oriented lithological boundaries, slickensides and slickenlines). Equal-area projection on lower hemisphere.

4.7.2.5. Brittle structures of non-tectonic origin

Locally, indistict sub-vertical gashes were observed in lower parts of the colluvia and the upper parts of the in-situ Cretaceous strata in trenches R1 and R2. These gashes cross-cut geliflucted horizons and evidently post-date the gelifluction, however, they are associated only with small (mm-scale) displacements as indicated by the absence of offsets at cross-cutting lithological boundaries, of gouges or slickensides. A fading-downward tendency was observed in most of these gashes. We interpret these structures as tension gashes formed by a non-tectonic deformation on gravitationally instable slope.

In trench R2 (R2b profile, base distances 8-9m and 12m) cm-dm-scale thrust or fold-and-thrust structures were observed within the geliflucted horizons of colluvia. In all cases these structures are local, clearly terminated both at the top and bottom which indicates that these structures are due to gravity-driven transport on the slope during gelifluction process.

On the base of the accumulation anomaly in trench R1 a small, sub-horizontal slickenside was observed, having clearly developed slickenlines parallel to the dip of the slope. This structure is intrepreted as a potential basal plane of a paleo-landslide.

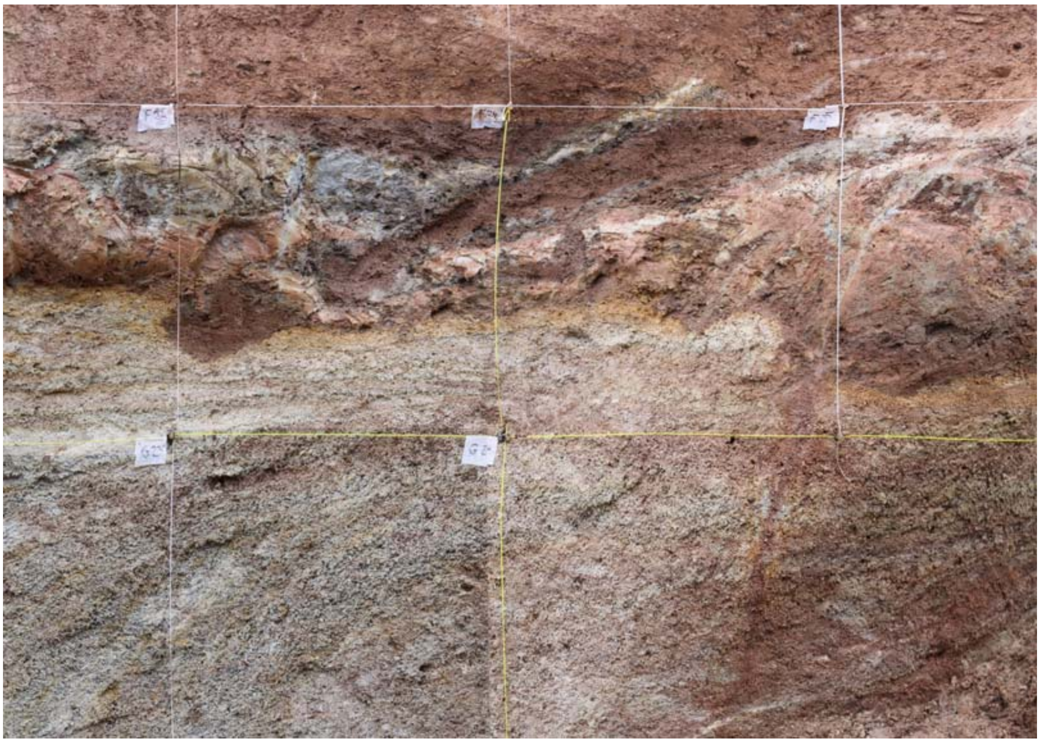

Fig. 4.7.2-16. Thrust plane developed within the geliflucted colluvia (top middle) near the contact of two lithological (rheological) domains and steeply dipping tension gash cutting through the colluvia and in-situ Cretaceous strata (right). Both structures are of non-tectonic origin, being associated with gravity-driven forces. Grid dimension 50cm.

4.7.3. TRENCH R3

4.7.3.1. Situation and geophysical indication

Trench R3 was excavated approx. 170 m to the NW from trench R1, in the area of expected trace of segment 3 of the Hluboká Fault (Fig. 4.7.3-1). As explained above, the existence of this fault segment is inferred as a necessary geometrical link between the distinct segments 2 and 4. However, the character of the gravity indication of the fault is diffuse, suggesting a complicated structure of the Hluboká Fault in this area most probably resulting from the interference with the NNE-SSW striking Drahotěšice Fault. Thick sequences of Cretaceous sediments are developed on both wings of the fault and the lack of geomorphological expression at the contact of easily eroded soft sediments makes the detailed location of the fault trace difficult. Two resistivity profiles (USI-4 and USI-5) in the eastern part of the segment indicate the existence of steep lithological boundaries parallel to the local fault strike close to the contact with segment 4 (Figs. 4.7.3-1 and 4.7.3-2). These boundaries were interpreted as a trace of a broader deformation zone developed in the faulted domain (see white lines in Fig. 4.7.3-1).

Trench R3 (azimuth 170°, length 40 m incl. ramps, typical depth 2.5 m, max. depth 3.5 m) was excavated with the intent to verify the local fault trace and to study the fault-related deformation of fluvial and colluvial sediments on top of it. The trench was located between the resisitivity profiles and its position and orientation was limited by the protection zones of gas- and water pipelines, the electric line, and the expected level of water table. The flat terrain with slope between 1 and 2° was suitable with respect to the need of the in-situ position of the fluvial sediments which are present in the area.

The western wall was cleaned and documented in detail in a way similar to the other two trenches (reference grid with step of 0.5×0.5-1 m); the eastern wall and the bottom were used for supplementary analyses of selected structures.

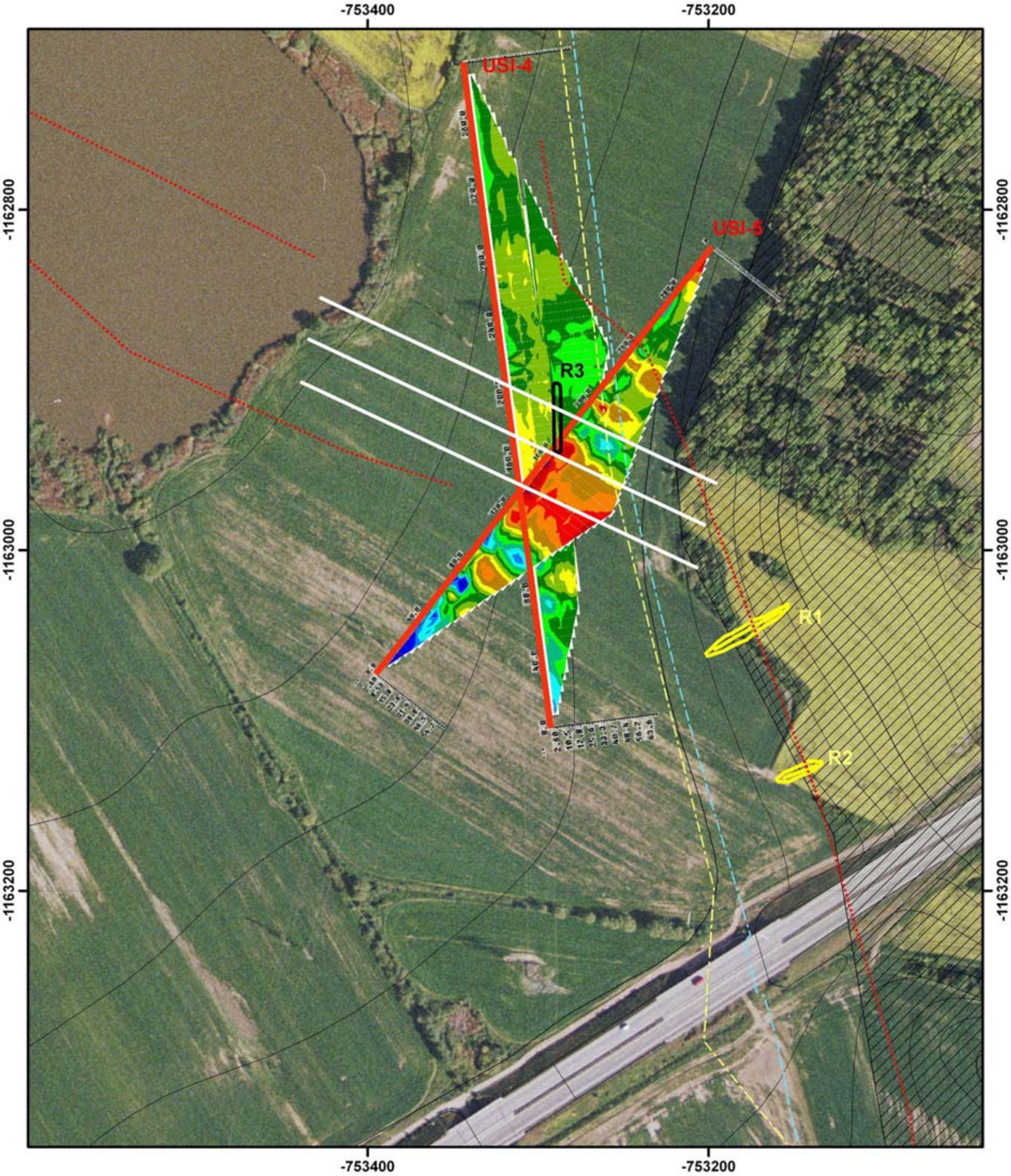

Fig. 4.7.3-1. Situation at the locality Úsilné showing the gravity indication (red dotted lines, manual redrawing of horizontal gravity gradient maxima), resistivity profiles USI-4 and USI-5 and the position of trenches (yellow and black line symbols). White lines show the expected minimum extent of the deformation zone related to segment 3 of the Hluboká Fault. Terrain contour lines with 2 m step. Dash-and-dot lines show the position of gas and water pipelines.

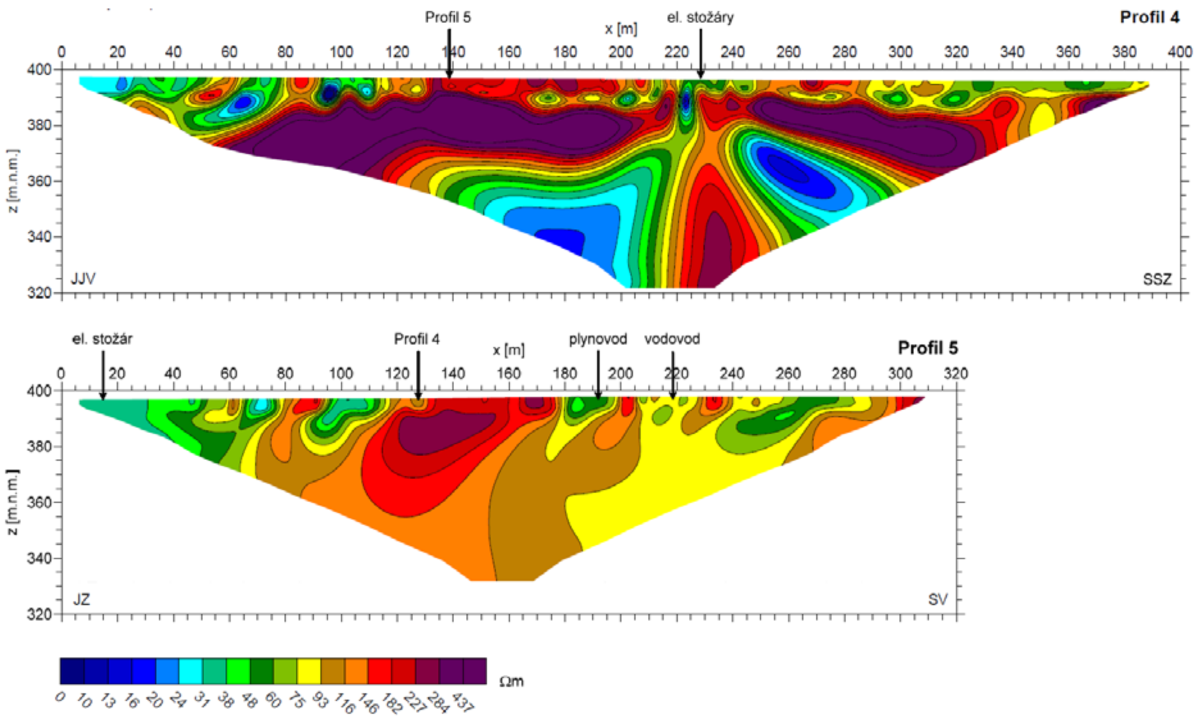

Fig. 4.7.3-2. Inverted resistivity profiles USI-4 and USI-5.

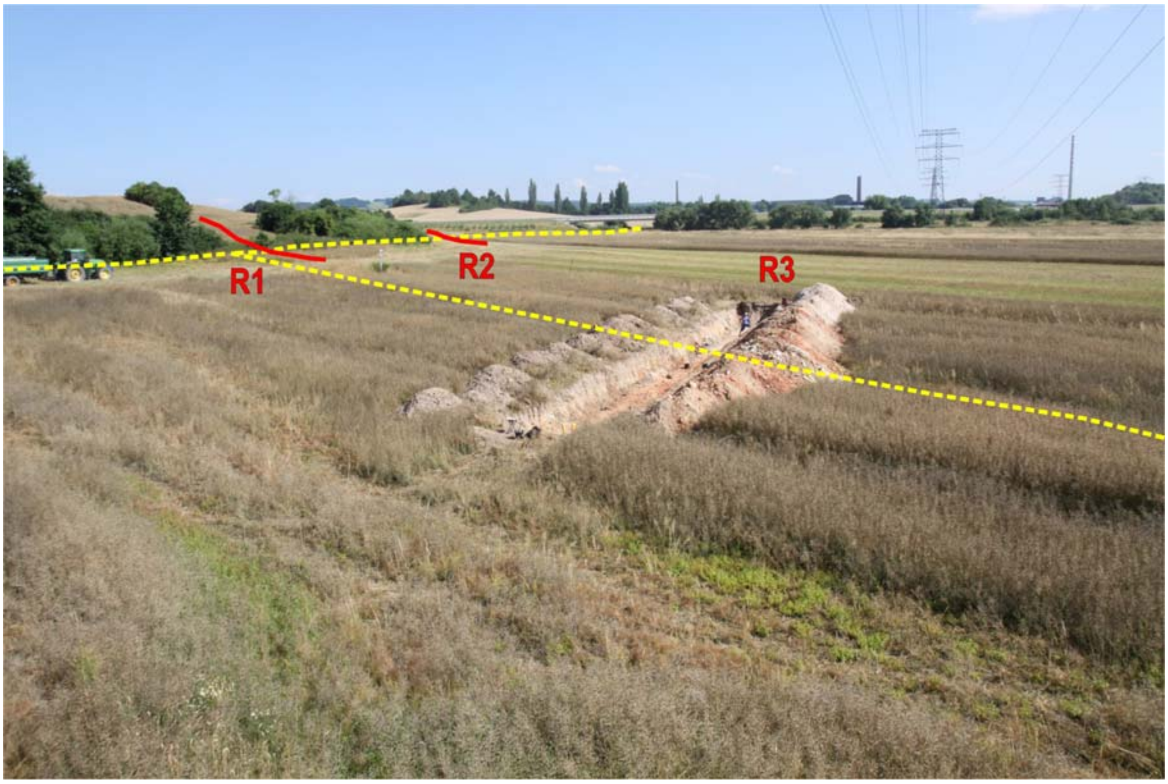

Fig. 4.7.3-3.: The overall situation at the locality Úsilné (Jul 2010) with R3 trench viewed from the NW. The positions of trenches R1 and R2 (landed up) shown by red lines. The traces of fault segments 3 and 4A shown by yellow dashed line.

4.7.3.2. Sub-surface structure of the deformation zone

Trench R3 exposed the near-surface parts of deformed Cretaceous clastics buried below Quaternary colluvia (Figs. 4.7.3-5 and 4.7.3-6). In the central part of the trench (15-23m) a zone of lithological change from sands (to the south) to clays (to the north) was observed, which corresponds well with the resistivity profiles measured. Steep lithological boundaries with strikes 100-120° and dips 70-85° to the SSW (Figs. 4.7.3-4) indicate large post-Santonian deformation of possibly similar character as observed in trenches R1 and R2.

No discrete deformation planes with slickensides or slickenlines were observed in Cretaceous sediments. Due to the poor consolidation of these clastics deformation was mainly ductile and it is very likely that the width of the deformation zone exceeds the extent of the trench.

Upper parts of the exposed profiles are represented by accumulations of Quaternary colluvia derived from the adjacent scarp. Cretaceous clays and sands largely prevail as a source material for these colluvia; these are of similar lithological character as the in-situ sediments below. The rare domains derived from Permo-Carboniferous sediments were found only as a fill of a narrow channel sub-parallel with the terrain dip (central part of the profile).

By analogy with the profiles in trenches R1 and R2 we suppose that at least a part of the colluvia were transported by solifluction *sensu lato*, but due the orientation of the trench relative to the transport direction (transport-perpendicular section in trench R3 vs. transport-parallel sections in trenches R1 and R2) direct comparison can not be made.

In spite of the mild dip of the terrain (below 2°), the thickness of the colluvia reaches approximately 2 m. Contrary to trenches R1 and R2 located directly on the scarp, in trench R3 located 70-80 m from the foot of the scarp such thick colluvia are probably due to the passive accumulation of the distal colluvia rather than an active in-situ gelifluction.

In central and northern parts of trench R3 three sand-rich domains were identified within the colluvial horizon. These lithologies have significant component of fine- to medium grained, partly sorted, quartz-rich sands with well-rounded grains mixed in variable ratios with sub-angular clasts of Permo-Carboniferous and Cretaceous sediments. Macroscopicaly, these sediments are similar to those found in colluvia exposed in trenches R1 and R2. The domains have dish-shaped bases and a width of 2-3 m in the top parts (Figs. 4.7.3-5 a 4.7.3-6). 3-D structural features indicate that these are the fills of narrow and long, slope-parallel channels partly filled by colluvia.

OSL dating of two samples taken from these sand-rich sediments (US3-1A, US3-3A, see Fig. 4.7.3-6) revealed their Holocene age, 8.22±0.44 and 8.38±0.46 ka, respectively (see Table 4.7.4-1).

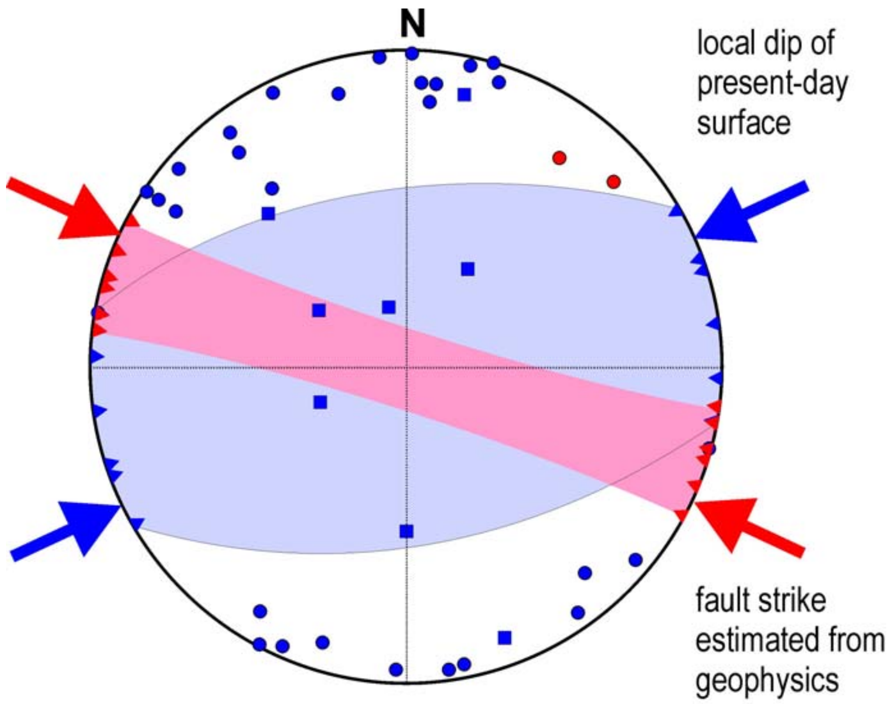

Fig. 4.7.3-4.: Synoptic diagram of structural features in trench R3. Red symbols show the structures of tectonic origin: large red arrow indicates the fault strike assumed on basis of geophysical data; red triangles and pink field show strikes of lithological boundaries measured in the trench base; red circles are poles to two boundaries between clay and sand measured in the lower part of the exposed wall. Blue symbols show the structures related to gravity-driven slope transport: large blue arrow indicates the local dip of the terrain slope; blue triangles and light blue field show the channel-axes and strikes of lithological boundaries in the colluvia (interpolated between the two trench walls); blue squares show the poles to lithological boundaries in colluvia measured directly in the wall; blue circles show the poles to major tension gashes.

On following pages:

Figs. 4.7.3-5 and 4.7.3-6.: Orthorectified photomosaic and schematic log of the main lithological and structural features in trench R3 (W wall). Positions of dated samples US3-1A and US3-3A shown by black-and-white discs.


Úsilné R3
SOUTH
NORTH
US3-1A
US3-2A
continued below
continued from above
distance along profile [m]
elevation [m a.s.l.]

Úsilné R3

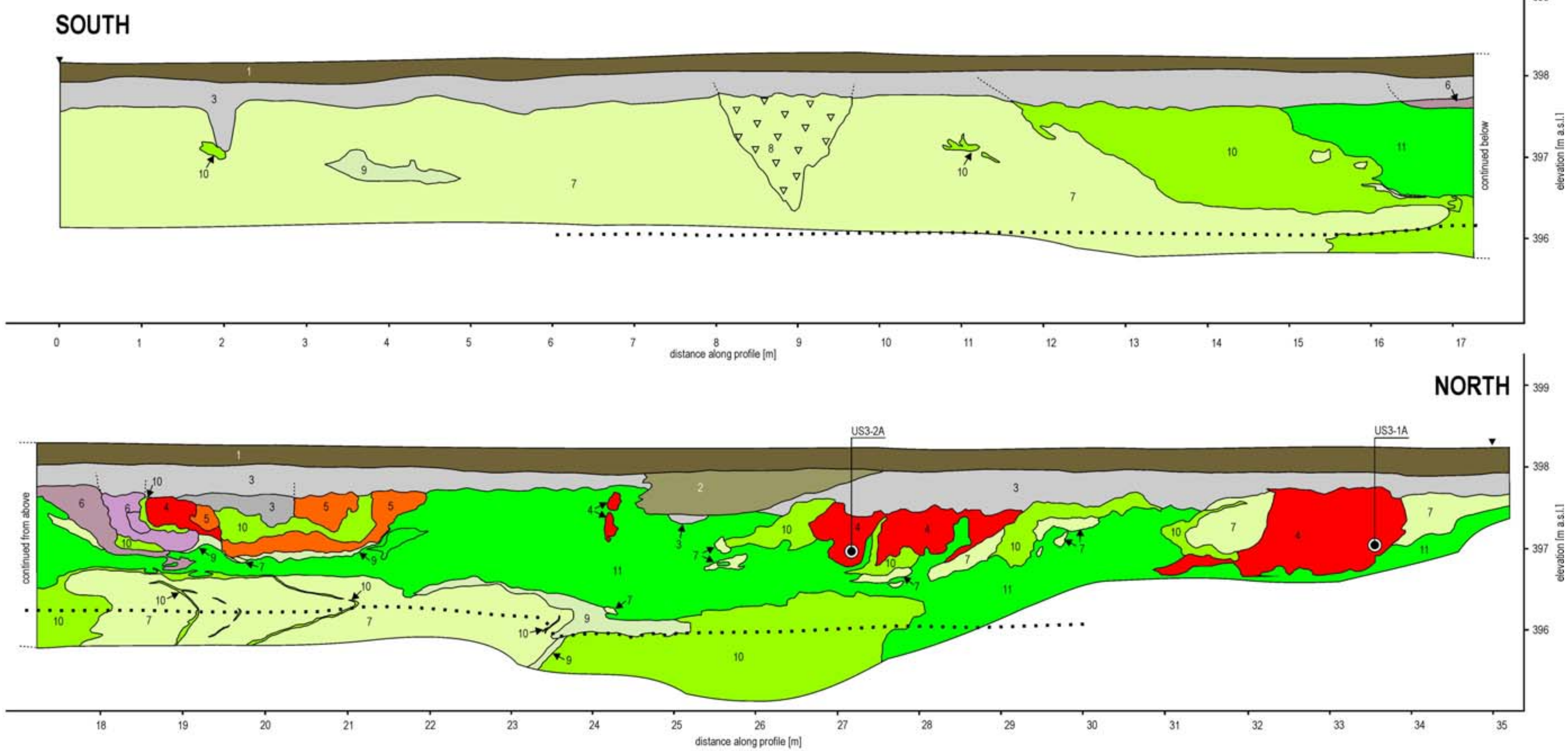

- approximate base of gelifluction
1 - top soil (plough-land)
2 - antrhropogenic fill of drainage trench
3 - undifferentiated sand-stone colluvia, largely homogenised by cryoturbation, with locally preserved sub-structures; light rusty brown colour
4 - rusty brown sands with subsidiary small debris derived from Permo-Carboniferous and Cretaceous sediments
5 - rusty brown sands with large amount of small sub-angular debris derived from Permo-Carboniferous and Cretaceous sediments
6 - gelifluctеd horizons derived from Permo-Carboniferous siltstones, mainly red-brown
7 - Cretaceous, medium- to fine-grained sands and gravels, light grey and cream-coloured, with ocre-coloured precipitates; including the related gelifluctеd horizons
8 - Cretaceous, dark grey to brown-grey, medium- to coarse-grained sands with debris of organic carbon
9 - Cretaceous, light grey, silty sands and sandy silts with ocre-coloured precipitates; including the related gelifluctеd horizons
10 - Cretaceous, light grey and yellow-red marbled clays; incl. the related gelifluctеd horizons
11 - Cretaceous, deep-red clays; incl. the related gelifluctеd horizons

4.7.3.3. Brittle structures of non-tectonic origin

In trench R3 a system of frequent, sub-vertical gashes, locally reaching depths of <2 m, is developed. Similarly as in trenches R1 and R3 these gashes cross-cut through the colluvia and are higjlighted by grey halo, likely resulting from reduction chemical reactions. Locally, they are filled with up to several mm thick clay of grey colour. In most cases fading-downward tendency was observed. These structures clearly post-date the accumulation of colluvia, but they display no shear displacement, since no offsets of lithological boundaries are associated with them. We explain these features as purely tensional gashes, likely developed as a result of gravitational instability of colluvia accumulated below the scarp. The gashes display preferred orientation with strikes sub-parallel to the terrain slope (Fig. 4.7.3-4). This can be explained for example as a result of lateral extension of local, anisometric, slope-parallel accumulations with positive elevation (channel-like structures filled by colluvia quickly slided from the scarp).

At the base of one of the sand-filled channels a thrust-like slab of clay was observed, with displacement >50 cm (Fig. 4.7.3-7). Similarly as in trench R2, this structure is interpreted as due to the gravity-driven flow-like transport of the sediments on the slope, with no relation to the tectonic forces (comp. with Fig. 4.7.2-16).

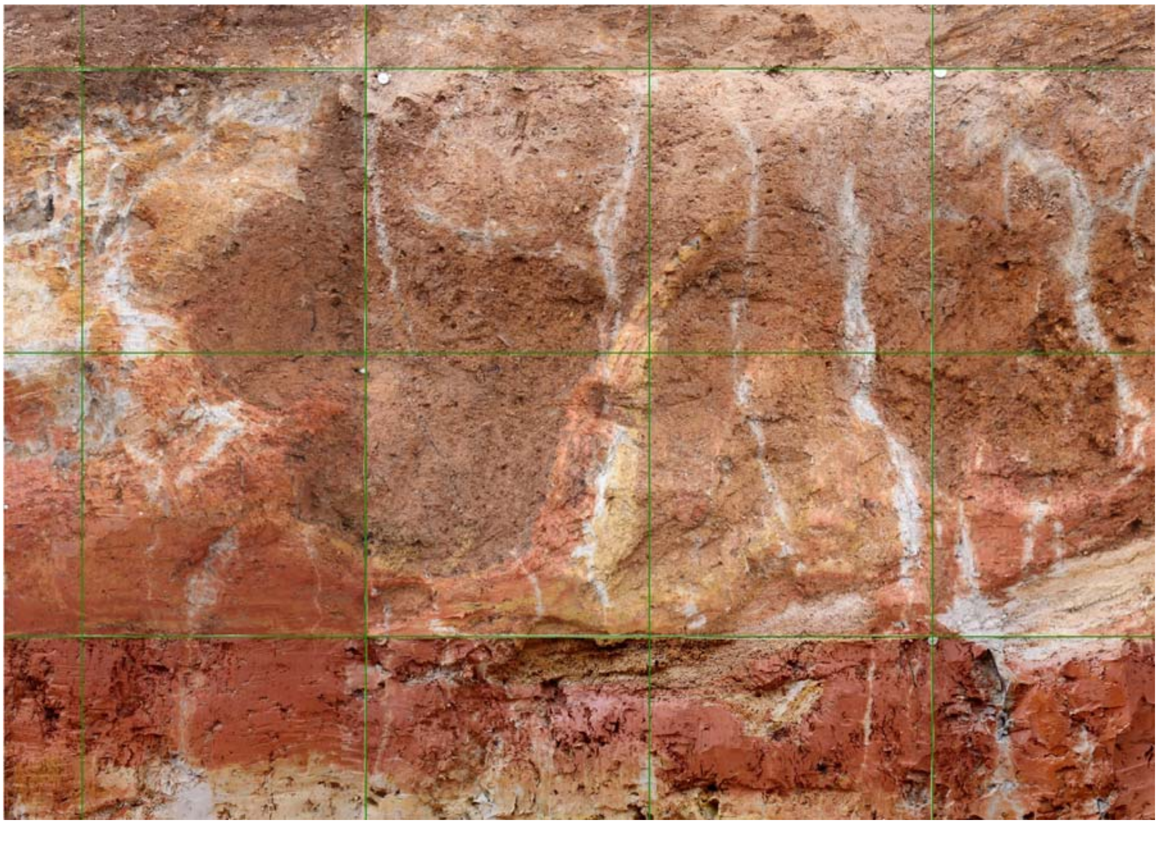

Fig. 4.7.3-7. Thrust-like structure and tension gashes in Quaternary colluvia. Both types of structure are due to the gravity-driven transport and they have no relation to the tectonic slip on the fault. Grid 50×50 cm.

4.7.4. LOCALITY ÚSILNÉ - THE AGE OF TECTONIC DEFORMATIONS AND POST-TECTONIC EVENTS

All deformation structures of tectonic origin observed in the three trenches are located in the lower parts of the exposed profiles, disturbing exclusively the sediments of Cretaceous and Permo-Carboniferous age. In the upper parts, the fault planes and steep lithological boundaries are uniformely bended as their host rocks are transported by gelifluction and other mechanisms (e.g. landslides) along the slope of the geomorphologically dominant scarp of fault segment 4A. In none of the three trenches we observed tectonic fault structures proceeding into colluvia continually and without change of orientation. The colluvia are only transected by tension gashes with small (sub-mm- or mm-scale) displacements which have not accomodated shear slip and which most likely relate to gravitational instability of the terrain slope.

The process of gelifluction, indicated by well developed uniform layering (locally lamination) with layers sub-parallel to the terrain surface, is therefore younger than tectonic slip on the fault and can serve as an indicator of its minimum age.

The precise dating of the formation of colluvial sediments is problematic, mainly in the lower parts, because they usually do not contain either organic matter suitable for radiocarbon dating, or fine-grained sediments which are expected to have been exposed to the sunlight during their transport (condition necessary for OSL dating). This problem, however, was solved by dating the anomalous domains of exotic, sand-rich material found locally within the colluvia in all three trenches. These sediments are composites of fine- to medium grained, partly sorted, quartz-rich sands with well-rounded grains mixed in variable ratios with sub-angular clasts of Permo-Carboniferous and Cretaceous sediments. In trench R1 these sediments were found within the domain interpreted as a part of a landslide (basal plane indicated by slickenslides with slickenlines). In trench R2 these sediments were found in two different structural positions: in the SE wall (R2-b, sample USI-4B) they form an integral component of the lower part of the colluvia, while in the NW wall (R2-a) they also seem to be affected by a landslide. In trench R3 these sand-rich sediments form several domains with dish-shaped bases representing the fills of narrow and long, slope-parallel channels partly filled by colluvia.

The results of the OSL dating of the four samples taken from these sediments are given in Table 4.7.4-1 together with the interpretation of the sedimentary environment and bleaching events.

Based on the observations in the three trenches, the OSL dating, and the situation of Quaternary sediments in the adjacent areas we suggest that in trenches R1 and R2 these mixtures of sands with fine-grained colluvia represent the alluvial facies deposited at the fault scarp synchronously with gelifluction of the colluvia which operated during Wurmian, i.e. MIS (Marine Isotope Stages) 2-3. It is not ruled out that some parts of colluvia containing these sands were affected by cryoturbation which possibly lead to bleaching. Farther from the fault scarp, in the area of trench R3 the age of the sands partly incorporated into the colluvia indicates the locally continuing channel transport of the scarp-derived sediments into the transitional alluvial/fluvial environment in Holocene.

The prevailing Wurmian age of the colluvia at the locality Úsilné is in agreement with the observations from other parts of the Bohemian Massif. In the Moravian loess successions containing the archeological artefacts and datable material the gelifluction was constrained to short interstaidals of the late MIS 3 (Škrdla et al., 2006, 2008). In the trenches across the fault scarps in southern Silesia (Rychlebské Mts.) the radiocarbon and OSL datings of coluvia indicate the age of gelifluction between 11 and 20 ka (Štěpančíková et al., 2010 and unpublished data). Together these data indicate that the latest climatic conditions optimal for the operation of gelifluction process were achieved in the end of Pleistocene when large temperature oscillations were associated with the transition from the last glacial period to the Holocene interglacial.

The age of the sediments and the indirect indications given above prove that the latest tectonic activity of segment 4A is pre-Holocene and probably older than 21 000 years. Most likely, this also applies to segment 3.

The maximum age of the observed fault structures ensues from the age of the deformed Cretaceous sediments, whose age has been constrained as Upper Coniacian to Santonian or Lower Campanian (80-85 milion years) based on paleontological data.

trench; sample	**lithology; position**	**age [ka ± 1 σ]**	**interpretation**
R1; USI-2A	mixed aluvial sands+colluvia; middle/lower parts of geliflucted colluvia	48.7 ± 2.6	older syn-gelifluction ?alluvial sediments emplaced into syn-gelifluction landslide; possible cryoturbation
R2; USI-4B	mixed aluvial sands+colluvia; middle/lower parts of geliflucted colluvia	21.8 ± 1.2	syn-gelifluction (re-)sedimentation in ?alluvial environment, possible cryoturbation
R3; US3-1A	mixed aluvial sands+colluvia; channel in upper/middle parts of colluvia	8.38 ± 0.46	post-gelifluction ?alluvial sedimentation, partial transport with colluvia in channels
R3; US3-2A	mixed aluvial sands+colluvia; channel in upper/middle parts of colluvia	8.22 ± 0.44	post-gelifluction ?alluvial sedimentation, partial transport with colluvia in channels

Table 4.7.4-1: Summary of lithologies, ages and interpretations of samples from locality Úsilné dated by OSL method.

4.8. SEGMENT 5 - LOCALITY ČERVENÝ VRCH

Approximately 500-1000 m SE of the locality Úsilné-1 a pronounced linear escarpment of NW-SE strike can be observed near the basin margin. Farther to the SE the slope and height of this escarpment are reduced. Near Červený vrch hill (height 429 m a.s.l.) a NW-SE elongated islet of crystalline rocks (amphibolite, aplite) crops out in Permian-Carboniferous sediments of the Lhotice basin, which is adjacent to the escarpment (Fig. 4.8-1). The rocks are partly exposed in a small, shallow, partly re-filled quarry on top of the hill.

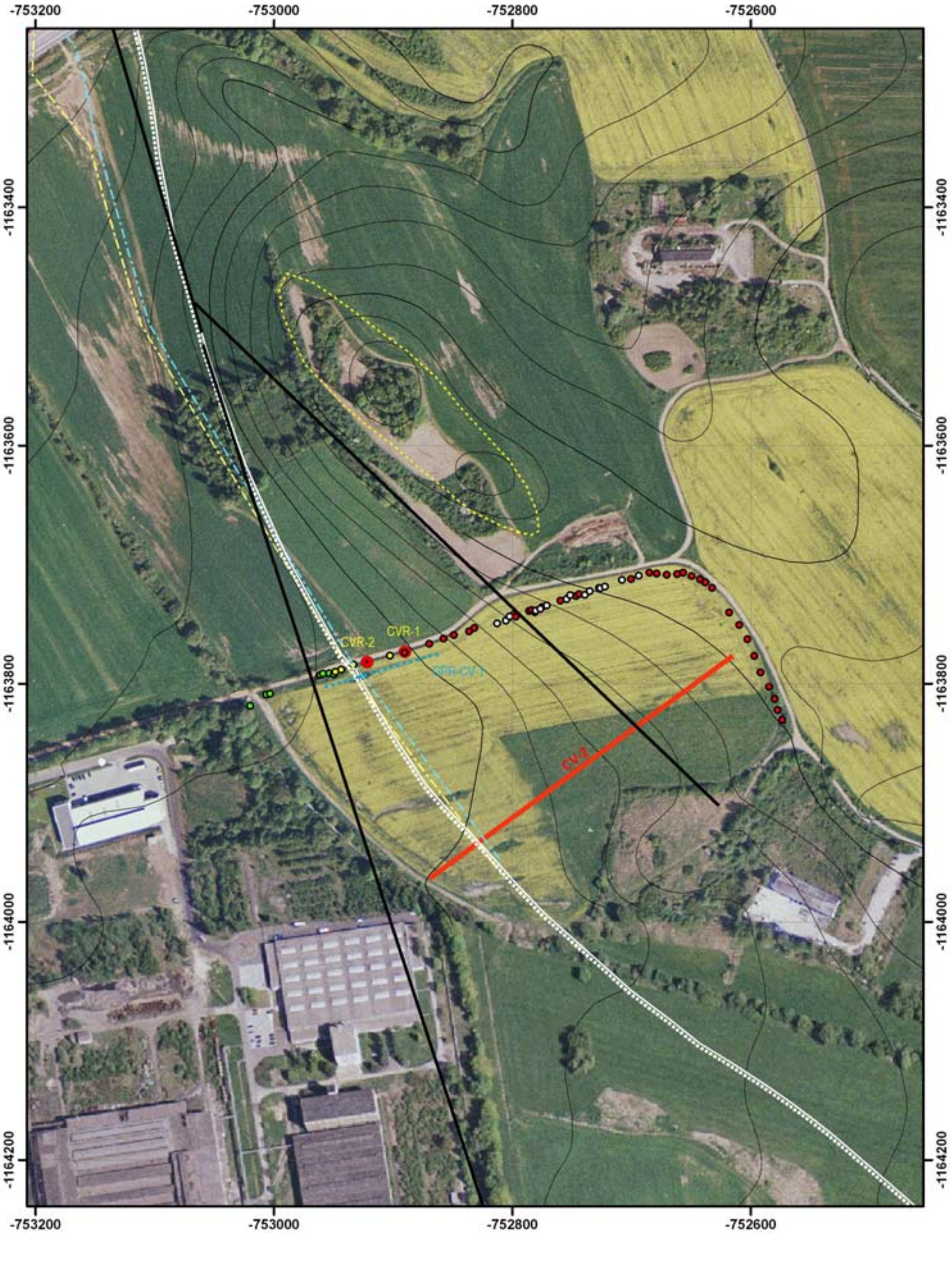

Fig. 4.8-1. Situation at the locality Červený vrch. Solid red and dotted blue lines: geophysical profiles CV-2 and GPR-CV1; small circles - documented points in shallow trench (red - Permo-Carboniferous, green - Cretaceous, yellow - Quaternary, grey - clay gouges); large circles - shallow boreholes. White line - approx. margin of Cretaceous basin. Black lines - approx. traces of main fault segments Dash-and-dot lines (yellow and blue) - gas and water mains. S-JTSK grid with 200 m step. Contour lines with 2 m step.

The shape and position of this exotic crystalline body within Permian-Carboniferous sediments clearly indicates that it is related to fault(s) with reverse slip component. In older mining reports from coal mines in Permian-Carboniferous sequence the faults of this strike are sometimes mentioned as reverse faults which locally lead to stratigraphical multiplications of coal seams (e.g. Kettner 1933). In geological maps of Czech Geol. Survey the fault is drawn on the SW margin of the crystalline body. This fault zone was described by Reininger (1909) for the first time, and it is sometimes called the „Reininger Fault“. Taking into account its strike and position near the basin margin this fault zone can be viewed as a part of the Hluboká Fault which can potentially provide important information on its late tectonic activity.

In March and April 2009 a long, 1 m deep trench for mains was excavated (Fig. 4.8-2) and exposed the shallow sub-surface levels of contact zone of crystalline and Cretaceous, including the above described fault zone. In spite of its shallow extent, the exposed alluvium and colluvium and locally the subcropping bedrock allowed to map the main lithological features of the contact zone as shown on a log in Fig. 4.8-3. The very contact of the Cretaceous and Permo-Carboniferous sediments, located >50 m to the west of the foot of the scarp is covered by a bed (probably thin) of Quaternary silts/clays rich in wood fragments. Using two shallow boreholes (CVR-1 and CVR-2, see Fig. 4.8-1) the contact was located at a close proximity to the gas and water mains, which makes a more detailed survey and trenching practically impossible.

Fig. 4.8-2. Shallow trench across the basin margin south of Červený vrch hill. View at the segment 5 fault scarp from the west. Dashed yellow line shows the approximate trace of the fault zone; dashed blue line corresponds to the lithological contact Cretaceous vs. Permian-Carboniferous. Tectonic clays and cataclasites were found in the area marked by red polygon.

In the alluvia and colluvia of Permian-Carboniferous sediments small domains of grey or locally black clays were observed in at least 100 m wide zone near the islet of crystalline rocks. In the NE part of this zone hard, dark grey, fine grained breccias approx 1-2 dm thick were found (Fig. 4.8-4). These clays and breccias are interpreted as likely tectonic gouges associated with the fault zone, probably corresponding to the terminating structure of the crystalline islet. The nature of the tectonic breccias (hard, compact rock, difficult to hammer) indicates their deep origin and hence the likely long-term activity of the fault zone probably going back to Variscan orogeny. Although some of the breccias have macroscopic appearance of cataclysed granitoids, they are probably derived from arcoses and the continuation of crystalline rocks to the trench was not confirmed. The contrasting lithologies of the fault-related rocks (clay gouges vs. hard breccias) likely corresponding to different burial depths suggest a long-term exhumation synchronous with the fault slip. Unfortunately, the shallow depth of the trench has not allowed a more detailed study of the indicated tectonic structures. By analogy with the locality Úsilné strong re-working of the colluvium with the observed lithologies by Late Pleistocene solifluction is expected.

Ground penerating radar profile GPR-CV-1 (200 MHz frequency), located across the contact of Cretaceous vs. Permian-Carboniferous and the lower part of the scarp, suggest only slight disturbance of the reflections near the foot of the scarp (Fig. 4.8-5). Although the structure is rather inconclusive, its association with the fault can not be excluded.

On following page:

Fig. 4.8-3: Schematic log of the profile across the basin margin and fault scarp exposed in the shallow trench near Červený vrch. Arrows with numbers show the documented points. The contact Permo-Carboniferous vs. Cretaceous is partly covered by Quaternary silts/clays with wood fragments. Boreholes CVR-1 and CVR-2 at the position 380-420 m has shown that the contact is located close to the mains (gas, water), which makes trenching practically impossible. Tectonic clay gouges occur at the position 190-320 m. Tectonic breccia was found at position 210 m. Profile GPR-CV-1 extends approximately at the position 49 to 59 m.

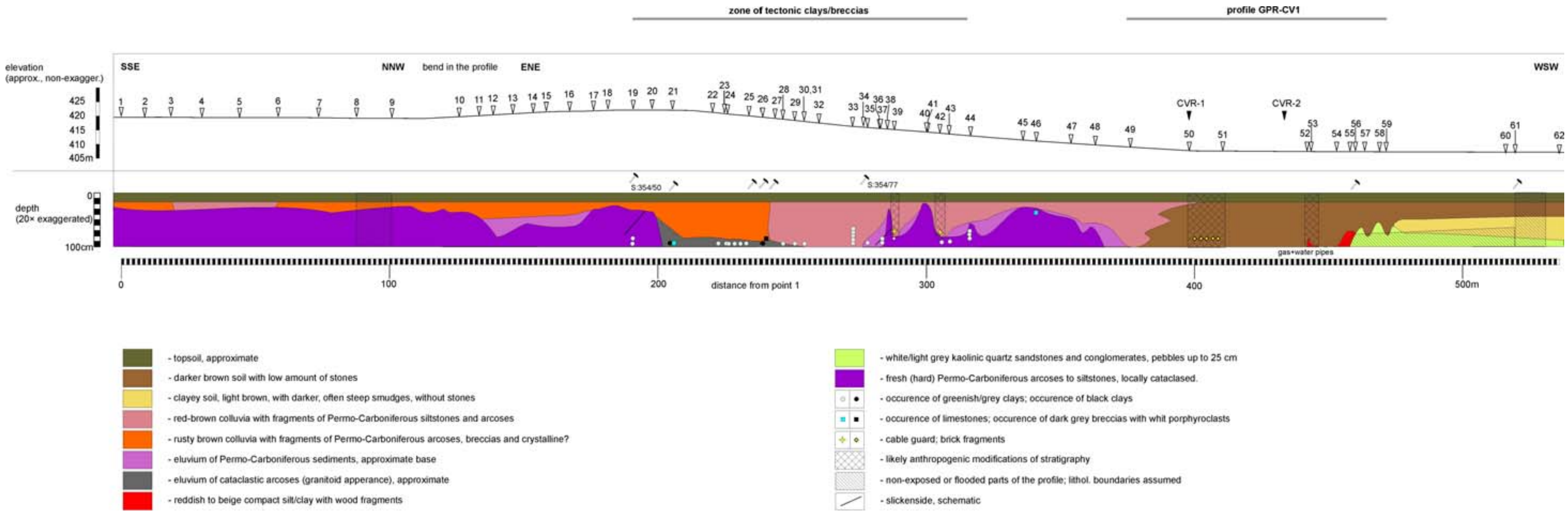
zone of tectonic clays/breccias
profile GPR-CV1
elevation (approx., non-exagger.)
425
420
415
410
405m
SSE
NNW
bend in the profile
ENE
WSW
CVR-1
CVR-2
S:354/50
S:354/77
depth (20× exaggerated)
0
100cm
gas+water pipes
0
100
200
300
400
500m
distance from point 1
- topsoil, approximate
- darker brown soil with low amount of stones
- clayey soil, light brown, with darker, often steep smudges, without stones
- red-brown colluvia with fragments of Permo-Carboniferous siltstones and arcoses
- rusty brown colluvia with fragments of Permo-Carboniferous arcoses, breccias and crystalline?
- eluvium of Permo-Carboniferous sediments, approximate base
- eluvium of cataclastic arcoses (granitoid apperance), approximate
- reddish to beige compact silt/clay with wood fragments
- white/light grey kaolinic quartz sandstones and conglomerates, pebbles up to 25 cm
- fresh (hard) Permo-Carboniferous arcoses to siltstones, locally cataclased.
- occurence of greenish/grey clays; occurence of black clays
- occurence of limestones; occurence of dark grey breccias with whit porphyroclasts
- cable guard; brick fragments
- likely anthropogenic modifications of stratigraphy
- non-exposed or flooded parts of the profile; lithol. boundaries assumed
- slickenside, schematic

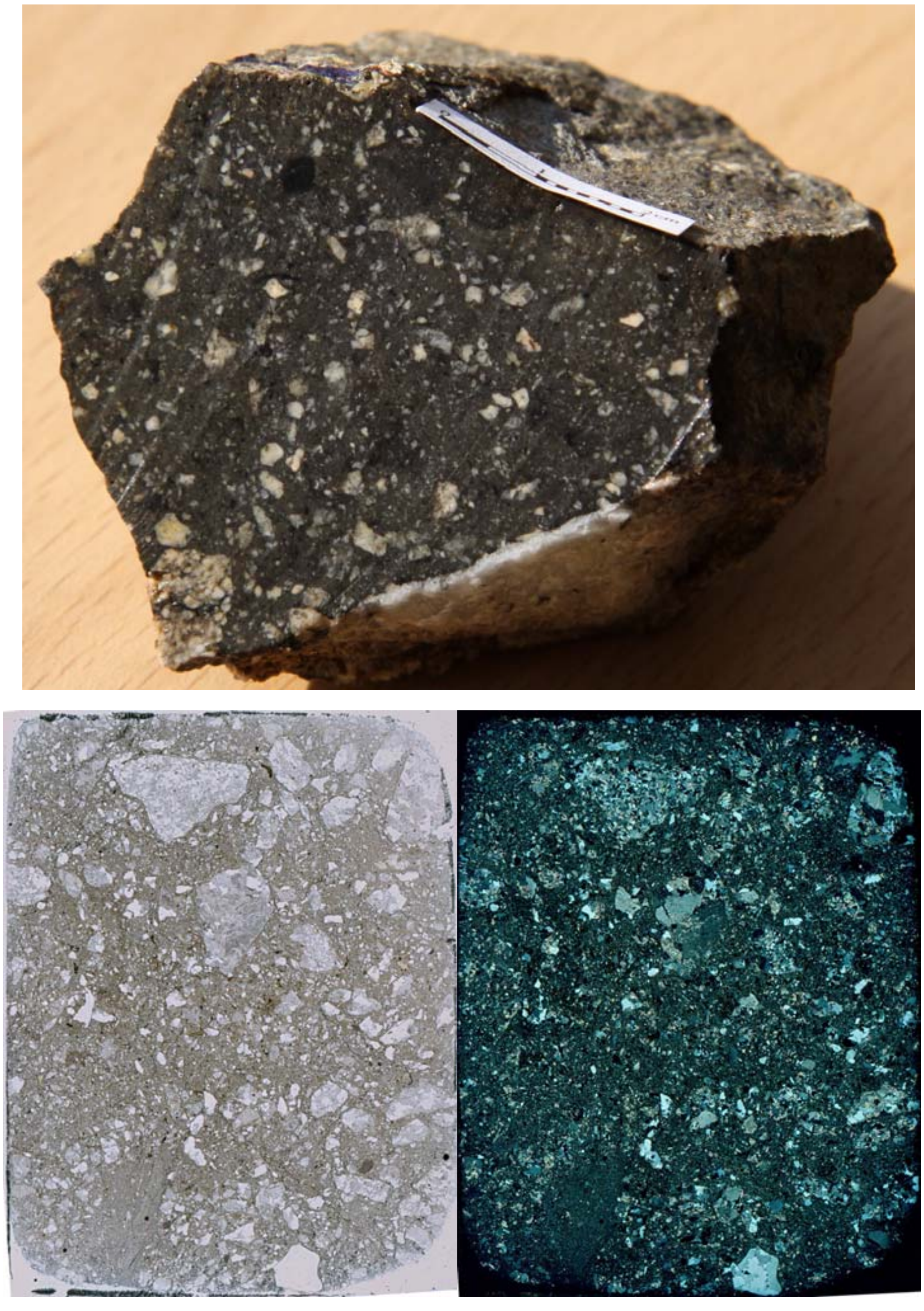

Fig. 4.8-4: Tectonic breccia derived from Permo-Carboniferous arcoses from the shallow trench near Červený vrch. Extremely fine-grained matrix indicates large strains accomodated. The compact nature of the rock indicates large depths of origin. Macrophotograph of the cut surface (top) and thin-section PPL and XPL photomicrographs (below, 2×3cm).

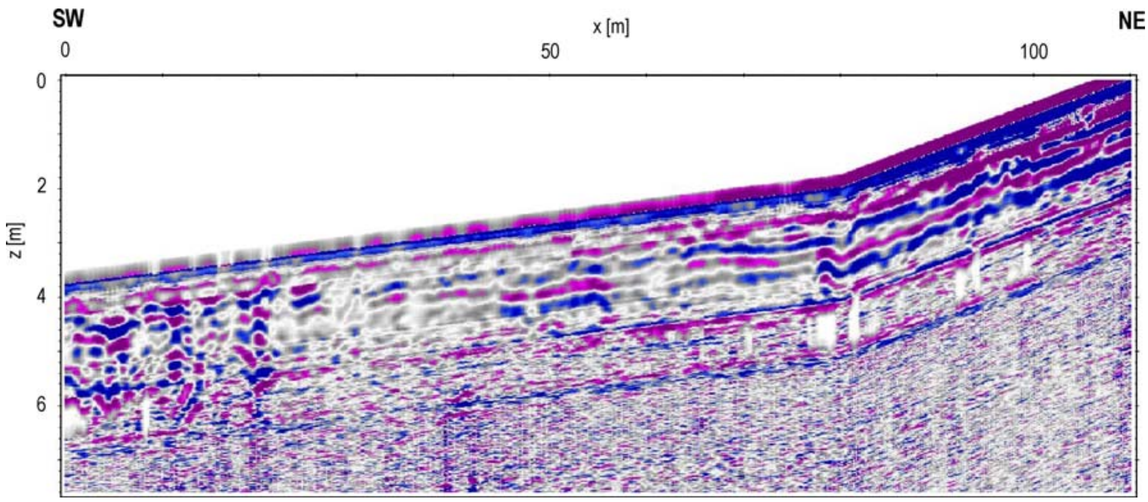

Fig. 4.8-5. Profile GPR-CV-1 (200 MHz). See Fig. 4.8-3 for lithological log across the profile. Author: F. Hubatka.

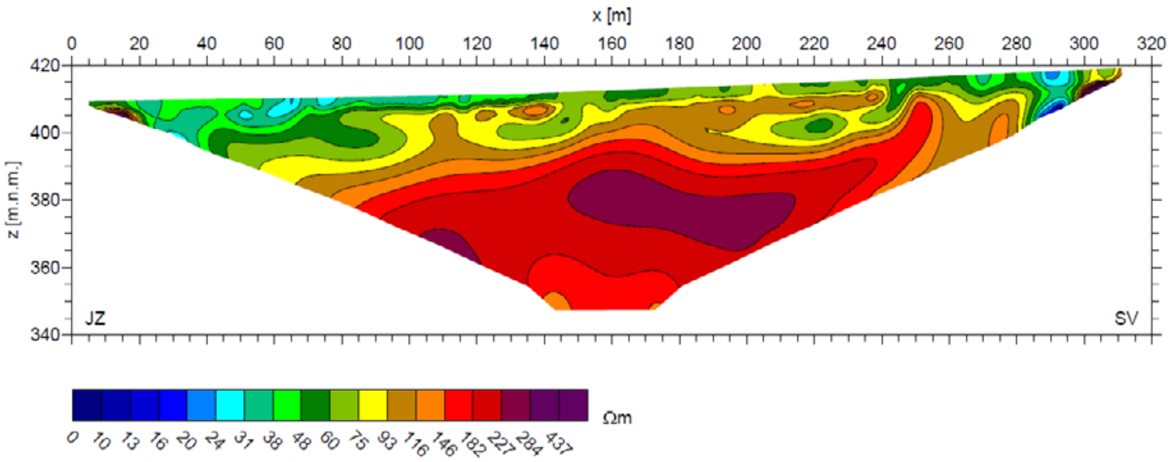

Fig. 4.8-6. Tomographic electrical resistivity section CV-2.

To constrain the fault trace farther to the SE we made electrical resistivity profile CV-2 (see Figs. 4.8-1 a 4.8-6) in the area of expected intersection of the fault zone with the locally thicker accumulation of colluvium, approx. 150 m to the SE of profile GPR-CV-1. The distribution of resistivity indicates relatively homogeneous lithology across the major part of the profile, including the position 150-250 m, where fault is expected to exist. Possibly, the features in the NE part indicate some steep lithological boundaries. The position of the fault thus remains unknown, although the trenching would be technically easy. Furthermore, strong gelifluction of the colluvia can be expected, similarly as at the locality Úsilné, and dating of the tectonic slip could be difficult to carry out. The continuation of the fault segment farther to the NE is completely unknown, because of the lack of geomorphological and geological indications (the contact Cretaceous vs. Permo-Carboniferous is clearly dissociated from the fault segment 5).

5

SUMMARY AND INTERPRETATION OF THE HLUBOKÁ FAULT SCARP

5. SUMMARY AND INTERPRETATION OF THE HLUBOKÁ FAULT SCARP

5.1 SUMMARY OF OBSERVATIONS

The primary intention of the project was to expose the shallow parts of the Hluboká Fault by trenches which would allow direct detailed study of the deformational structures, their dating and eventual paleoseismological analyses. However, for many reasons the trenching was not possible in large parts of the fault and it was limited to the external parts of the fault where only low scarps are developed and built-up area is not so extensive. In central parts of the fault we studied the continuity of the sediments covering the fault as an indirect alternative method of research, based on drilling and geophysical survey and dating of Quaternary terraces. However, In the whole region the possibility to date the tectonic activity was further limited by the Late Pleistocene periglacial mass wasting which affected both the colluvia and relics of higher fluvial terraces preserved at the slopes.
In some parts of the fault, a dissociation of the main marginal fault and the escarpment in terrain morphology was observed. In such cases we made effort to study both structures, taking into account the possibility of multiple faults in a broader fault zone.
In following paragraphs the main observations are briefly summarised for individual fault segments. However, since indirect indicators had to be used at many localities and because some results are not conclusive, the general assessment of the activity of the Hluboká Fault will have to be based on a combination of the results from all segments together.

Segment 1A

In this segment, between Munice and western margin of Hluboká nad Vltavou, the Hluboká Fault is buried beneath the Miocene sediments of the Mydlovary Fm. The mild escarpment at the basin margin is offset approx. 200 m to the NE from the surface trace of the fault. The reflection seismic profile performed by AIP team (Decker et al. 2010a) indicates that the sediments of the Mydlovary Fm. above the Hluboká Fault are not affected by faulting. Similarly, the borehole data do not indicate any significant change of thickness of the Mydlovary Fm. associated with the basin margin. It is suggested that the sedimentary fill of the „Northern River“ channel is more or less continuous along the whole profile Dobřejovice - Křesín - Hluboká-west - Hluboká-south. No indication of faulting was observed within sediments of Cretaceous and Miocene age exposed in two trenches which traversed both the surface trace of the fault and of the escarpment. The electrical resistivity profile across the escarpment suggests a mildly dipping, transgressive base of Miocene sediments below its foot.
In summary, the continuous stratigraphy of the Mydlovary Fm. suggests the long-term absence of significant fault slip at this segment since Middle to Late Miocene. The similar elevation of the base of relics of the Zliv. Fm. in the area also indicate the absence of vertical slip.

Segments 1C and 2A + hypothetical segment H

To the SE of Hluboká nad Vltavou the main marginal fault is covered by Quaternary fluvial sediments of the Vltava river and to the SE of Opatovice also by colluvio-alluvial fans. Number of boreholes and the gravity indication prove that the marginal fault (Hluboká Fault *sensu stricto*) is offset from the terrain escarpment up to 300m to the SW. This step-like geometry of the basin margin with sub-Quaternary crystalline ledge can be a result of (1) subsidence of the small-scale crystalline block with Cretaceous cover between multiple faults, (2) formation of erosional pediment within the crystalline at the foot of the single fault scarp or (3) combination of both scenarios. We defined an additional hypothetical segment H as a structure whose surface trace corresponds with the foot of the main terrain scarp, since the escarpment has conspicious morphology and its strike (140-145°) is close to that of segment 2. Since trenching was not possible in this area, our main aim was to test the continuity of terrace sediments across the whole fault zone to learn about the possible slip with vertical component in Quaternary. We focused on the lower terrace in this phase of research, since the sampling of the relict higher terraces turned out to be problematic.
The more or less constant thickness of the lower terrace across the basin margin (typically 5-8 m in the deepest parts) indicate the absence of vertical slip on the Hluboká Fault zone since the time of its deposition. To the south of segment H the OSL dating indicates concordant elevation/age relations across the basin margin in the timespan approximately 0-53 ka BP (boreholes HL-4, HL-5, HL-6, HL-8, HL-12, HL-14 and OP-1, (see Fig. 5.1). This is in agreement with the absence of morphological expression of the fault in colluvio-alluvial fan covering segment 2A.

To the NE of segment H, dating of the lower terrace was restricted to borehole HL-11 which was situated very close to the present-day river channel, in the place with moderate thickness of Quaternary. The OSL dating revealed the Holocene age of sands and gravels, which suggests that the older (Late Pleistocene, Würm) terraces were locally destroyed by continuing erosion in the river channel and are not preserved in the narrow neck of the valley in Hluboká-Zámostí. The lowest parts of the terrace remain undated and should be subject to continuing research in future. We assume, however, that Würmian sediments are represented in the lower parts of the terrace downstream, which are well below the present-day bottom of the river channel.

Dating of higher terraces turned out to be difficult since only spatially limited relics of sediments are easily accessible. Several relics sampled and dated within both CIP and AIP projects give strikingly young ages which could be interpreted as due to their apparent differential tectonic transport on the fault zone. However, such model would be in contradiction to other significant observations. Furthermore, these sedimentary relics do not display typical morphologies and lithologies which could be regarded as characteristic for the in-situ fluvial sediments and we suggest that their ages reflect times of re-deposition during Late Pleistocene. This is further discussed in following chapter.

Segment 2B

In this segment the Hluboká Fault is not associated with terrain scarp which is explained as due to the combined effect of tectonic quiescence and the absence of lithological contrast which would promote the differential erosion. Locally, 3-6 m thick sequence of Quaternary fluvial sediments cover the fault, whose position is confined by boreholes (large difference in thickness of Klikov Fm.), gravity indication and electrical resistivity profile. The smooth shape of base of Quaternary sediments observed in GPR and electrical resistivity profiles suggests the absence of vertical slip since the time of the their deposition. The dating of three samples indicates mostly Holocene and Late Würmian age of sedimentary sequence, with the age of basal parts around 40 ka.

Segment 3

In this short segment the gravity indication of the fault is rather diffuse and the geomorphological expression is missing. It is assumed that the geometry of this fault segment is complicated due to the interaction with the NNE-SSW striking Drahotěšice Fault. Trench Úsilné-R3 exposed the upper part of ductile deformation zone and overlying colluvia in place where steeply dipping lithological contacts were indicated by electrical resistivity profiles. The continuity of colluvia dated at 8.2-8.4 ka suggests the absence of slip in Holocene. However, this conclusion is only relevant for the exposed part of the zone, which is probably much broader than the part exposed by the trench.

Segment 4A

This fault segment coincides with the contact of Cretaceous sediments of the Budějovice Basin and Permian-Carboniferous sediments. Its position is well confined by gravity indication and shallow geophysical survey, as well as by mild terrain scarp. Two parallel trenches (Úsilné-R1 and Úsilné-R2) exposed the fault and the associated zone of deformation which was of ductile or semi-ductile character in non-consolidated Cretaceous sediments and largely brittle in consolidated Permian-Carboniferous sediments. The observed deformational structures are probably associated with both Hluboká and Drahotěšice Faults. The colluvium covering the fault is strongly geliflucted, continuous and all fault structures are uniformly bended into slope-parallel orientation at its base. Dating of mixtures of sand-rich domains in colluvia interptreted as alluvial facies deposited at the fault scarp synchronously with gelifluction, gives the ages 21.8 ka and 48.7 ka. It is inferred from the structural position of these sediments that the fault did not slip in the period 0-21 ka BP.

In segments 4B, 5, 6 and 7 the Quaternary activity of the fault has not been assessed, mainly because of its problematic location and the lack of Quaternary sediments deposited on top of the fault.

5.2 QUATERNARY SEDIMENT ARCHITECTURE IN CENTRAL PART OF THE FAULT: PRELIMINARY MODEL

As summarised above, the more or less constant thickness of the lower Vltava terrace across the basin margin suggests the absence of vertical slip on the Hluboká Fault zone since the time of its deposition, because the relative uplift of the NW block would lead to reduction of thickness of the lower terrace. Direct dating of lower terrace sediments, however, was possible only in the area to the to the south of the escarpment where OSL dating indicates concordant elevation/age relations across the Hluboká Fault sensu stricto in the timespan approximately 0-53 ka BP. To the north of the escarpment the sampling of lower terrace was not complete and the age is only assumed based on analogy with the area to the south.

To assess the vertical slip at the Hluboká Fault zone in the pre-Würmian period, it was desirable to compare the relative elevations and ages of Vltava terraces at higher levels above the present-day floodplain. However, the sampling of such sediments turned out to be problematic due to their complicated accessibility. To the north of the Hluboká Fault escarpment the higher terraces are preserved at larger area only in densely built-up areas of Hluboká-Zámostí, where sampling was not possible. To the south of the escarpment the higher terraces are covered by thick deposits of colluvio-alluvial fan between Opatovice and Hrdějovice and were also not sampled in this project for technical reasons. In this project we studied sediments in smaller and easily accessible relics where potentially fluvial origin was assumed. The OSL dating was performed both by AIP team (samples HR-1, DH5-1, HLR-1, DH-7, HL-16) and CIP team (samples OP-7, NO-1).

The well-sorted sands sampled in a shallow probe HLR-1 in the elevation 5.8 m above the reconstructed Vltava surface-level, reveals the Late Pleistocene age (23.33±2.29 ka, Decker et al. 2010b). Similar age (23.42±2.54 ka) has been determined for clay-laminated sands (sample DH5-1) studied by AIP team in an artificial outcrop in the slope of the left part of the valley, 6.5 m above the reconstructed Vltava surface-level. In case of these localities, however, the sampled sediments do not form characteristic terrace morphology. Loamy sands were also observed in borehole HR-1 at the elevation 13.4 m above the Vltava level for which OSL dating gives the age 53.6 ka. The lithology of these samples suggests that they may represent sediments of alluvial fans rather than relics of in-situ fluvial terraces. Similar loamy sands were observed in boreholes in the alluvio-colluvial fan west of Hrdějovice (H-1, H-2 and H-3). These are also exposed in a steep creek valley at the NW edge of the colluvio-alluvial fan, close to the foot of the fault escarpment near Skelná Huť (sample NO-1, >10m above the reconstructed Vltava surface-level, dated at 16.3 ka).

The sandy gravels taken from the basal parts of Quaternary fill of the narrow plateau in the main escarpment (sample OP-7, 7.75 m above the reconstructed Vltava surface-level) give the age 42.4 ka. These sediments seem to contain significant amount of fluvial component, however, the relatively large content of poorly rounded grains is not characteristic for purely fluvial sediments of the lower Vltava terraces, and mixing with colluvia is likely. Similarly, the sample HL-16 taken from a <50 cm thick bed of sandy gravels hosted within the relic of Quaternary sediments in a landslide cut-off approx. 13 m above the reconstructed Vltava surface-level, gives the Late Pleistocene, early Würmian age (approx. 80 ka, D. Homolová, pers. comm.). Although the gravel component is probably fluvial in origin, its re-deposition in the environment of alluvial fans (proluvium) can not be ruled out. Furthermore, strong re-working by cryoturbation is indicated for the whole sequence.

The sample DH-007 was taken from a relic of old terrace with small, but well developed morphological plateau on top of the rocky slopes in the left part of the river valley, north of Zámostí, approx. 18 m above the reconstructed Vltava surface-level. Although in this case the in-situ position of sub-horizontally bedded sandy gravels is likely, the age is beyond the range of OSL dating, > 140 ka (Decker et al. 2010b).

As given above, most of these samples give systematically younger ages than expected, taking into account their higher elevation and the similar range as the ages of sediments in the lower terrace (see Chapters 4.4 to 4.6, Figs. 4.4.3-3 and 5.1). On the other hand, as described in previous chapter, the similar thickness of Quaternary sediments of the lower Vltava terrace to the NE and SW of the escarpment suggests that no substantial vertical offset took place on the Hluboká Fault zone after the deposition of the lower terrace. The ages of the sediments at higher elevations are in contradiction to this significant observation and we suggest that these sediments do not represent the in situ terraces deposited by Vltava river. Most of these samples were taken in small relics without clear morphological signature and in such setting it is not possible to unequivocally assess its sedimentary environment or prove the in-situ position. In our preliminary model, the fine grained, often loamy sands (samples DH5-1, HLR-1, HR-1, NO-1) are interpreted as relics of alluvial fans. In case of sandy gravels (samples HL-16 and OP-7) we suggest that the ages of these sediments reflect the bleaching of their fine-grained component during re-deposition at the slopes and/or during cryoturbation. Furthermore, the ages and relative elevations of the sediments from higher levels are not perfectly concordant with each other and to explain this, a relatively complex tectonic model with several active faults would be required, for which the independent indications are missing. Nevertheless, the apparently systematic nature of the observed misfits is striking and data available do not allow to rule out the slip at the central fault segment in Quaternary. Therefore we strongly suggest that our present results should be complemented by further research in future.

The preliminary model of Quaternary sediment architecture at the basin margin compiled based on the observations and assumptions given above is presented in Fig. 5.1.

The three profiles in this figure represent three different morphostructural types of the basin margin at three different segments:

1) between Hrdějovice and Úsilné where the fault scarp is not developed and the Vltava river is relatively far from the Hluboká Fault, 2) between Hrdějovice and Opatovice where colluvio-alluvial fan covers the higher terraces and narrow pediment in crystalline is developed, and 3) near Hluboká where Vltava (and its floodplain) approaches the fault scarp, leaves the basin and enters the adjacent hilly land, crossing a broad pediment in crystalline.

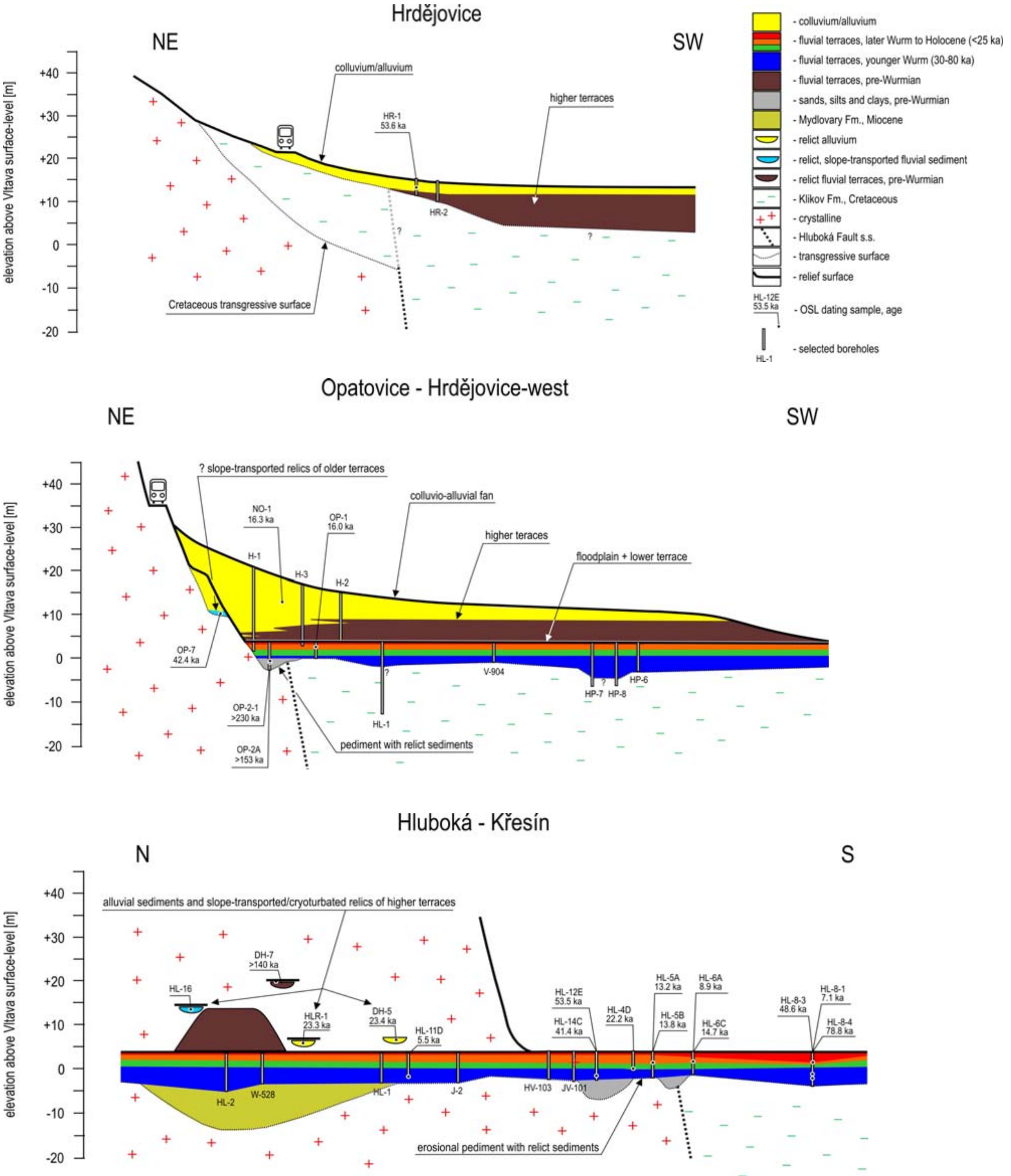

Fig. 5.1.: Schematic composite profiles showing the interpreted extent of Quaternary and Tertiary sediments at the basin margin east of Hluboká nad Vltavou. The three profiles represent three different morphostructural types of the basin margin at three different segments: 1) without fault scarp, distant from Vltava river floodplain (Hrdějovice), 2) at the border area of floodplain and colluvio-alluvial fan, with higher terraces partly preserved and narrow pediment in crystalline (segment Opatovice-Hrdějovice-west), 3) with fault scarp adjacent to Vltava river, without colluvio-alluvial fan and with broad pediment in crystalline (segment Hluboká - Křesín). Note that the lower profile is parallel to the Vltava river while the other two are near-perpendicular. Selected boreholes and OSL ages of the dated sediments are also shown.

5.3 THE HLUBOKÁ FAULT SCARP

The escarpment developed at the NE margin of the Budějovice Basin can be explained as a result of (1) long-term slip on a fault with significant vertical component during late Cenozoic, (2) differential erosion of basin-fill sediments on an inactive marginal fault, or (3) a combination of both processes.

In the latest geomorphological studies (summarised by Balatka and Přibyl, 1995) basin margin is described as „fault scarp strongly affected by exogenic processes“. These authors assume that the scarp was formed in Miocene and Pliocene, as a reaction to the regional uplift of the Bohemian Massif, which promoted the denudation of loose sediments of the Budějovice basin. The whole pronounced morphological depression associated with the basin was then explained as a result of the late Cenozoic differential erosion.

Differential erosion in the Budějovice Basin

Indeed, the morphology of the whole basin, of the relics of consolidated lithologies inside the basin and of the NE margin of the basin indicate that that differential erosion must have played major role in formation of the Hluboká Fault scarp. Three independent observations supporting this assumption are given below, as an example:

1) The absence of marginal lacustrine facies of the Mydlovary Fm. in the central part of the basin.

In the lower unit of the Mydlovary Fm. characteristic sedimentary sequence with lignite seams associated with diatomites is developed. These sediments were deposited in the marginal lacustrine environment (Slánská 1963, Řeháková 1963) in the swamp and peat bog facies, and the geological situation of the lignite seams near or beyond the present-day margins of the Budějovice Basin indicates that this sequence must have continued towards the central parts of the basin with flat paleorelief. As shown in Fig. 5.2, several relics of these sediments are located just beyond the marginal faults of the basin, which probably offset some of these relics (Olšovice – Vlhavy Fault, Kamenný Újezd – Dubné Fault) and their original continuation into the basin is very likely. In spite of that, these sediments were never found in the numerous boreholes in the central parts of the basin. It seems likely that this younger unit of the Mydlovary Fm. once covered large parts of the basin and was largely destroyed by denudation in later periods. The denudation began already during Miocene, when the upper units of the Mydlovary Fm. were deposited, and it was probably the largest in Pliocene and Quaternary, when Vltava river terraces were formed.

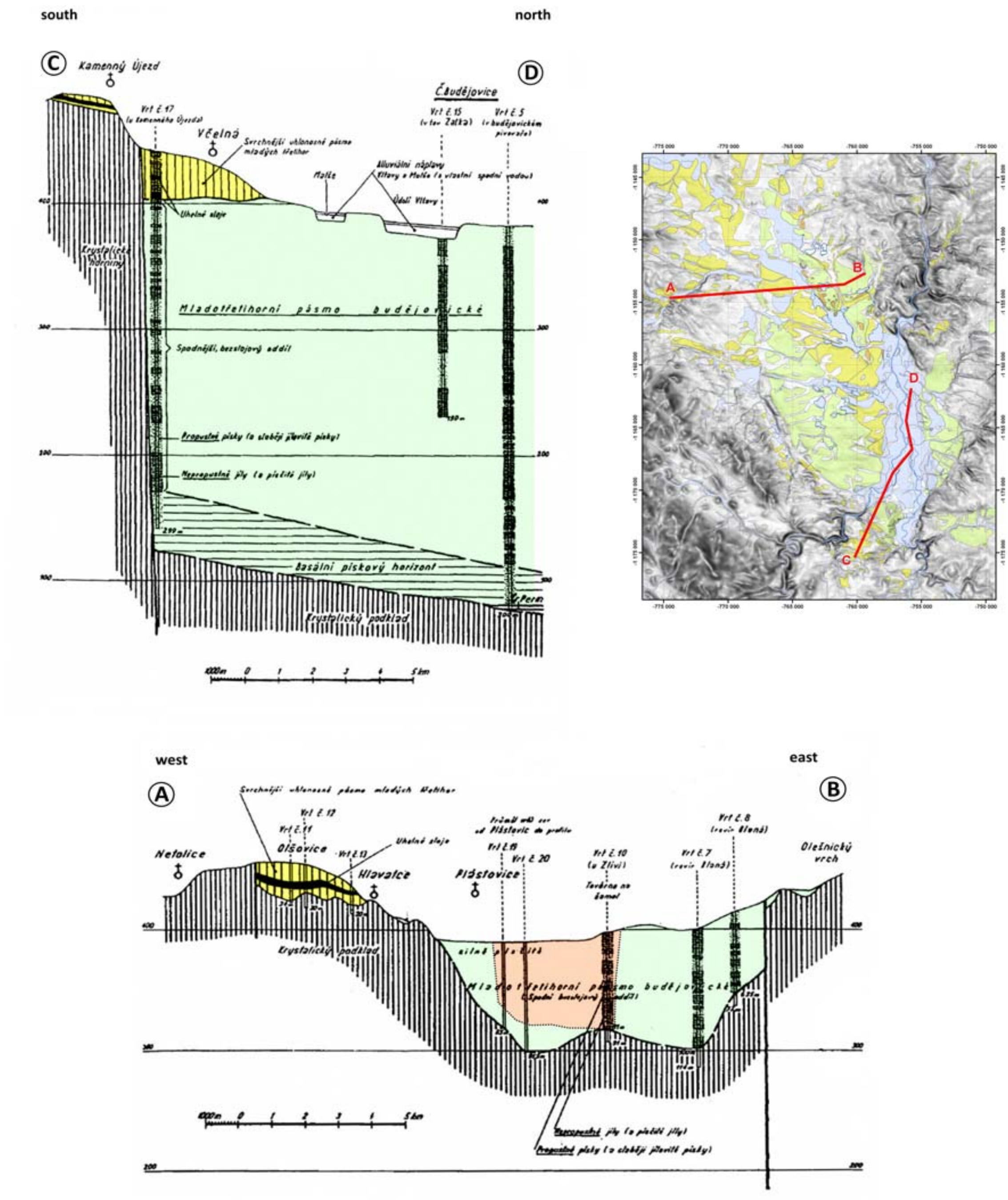

Fig. 5.2. Two structural profiles across the Budějovice Basin after Hynie (1949), modified. The situation of profiles is shown in a map (top right). Green - Klikov Fm., yellow - lower unit of Mydlovary Fm.; purple orange - upper unit of Mydlovary Fm., approximate extent.

2) The positive relief of the Zliv Fm.

In the area between Zliv and Munice the important role of differential erosion in the formation of the basin morphology is well demonstrated by the relief of the relics of Zliv Fm.

The sandstones/conglomerates of the Zliv Fm. represent the most consolidated sediments of the basin fill, which resist the erosional forces. In this area these relics are systematically associated with pronounced elevations 15-30 m above the flat relief developed on the sediments of Klikov Fm. (Fig. 5.3).

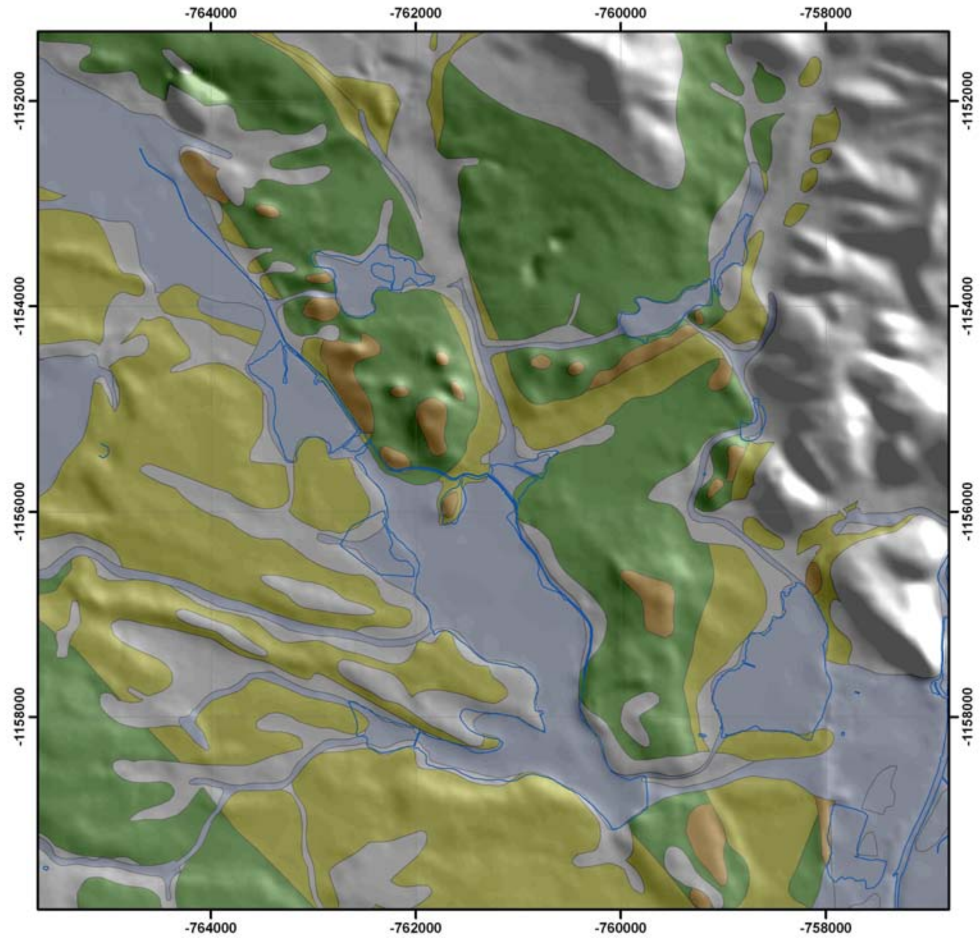

Fig. 5.3. Relief (shaded gradient map, illumination from NE) and surface geology of the area between Mydlovary and Hluboká nad Vltavou. Green - Klikov Fm., orange - Zliv Fm., yellow - Mydlovary Fm. Note the correlation of the positive elevations in the flat basin relief with occurences of Zliv Fm. relics.

3) The absence of the Hluboká Fault scarp in the areas of sediment promontories

Another clear indication of large differential erosion can be found just on the trace of the Hluboká Fault (Fig. 5.4). The escarpment of the NW-SE direction is first seen to the E and SE of Munice, where erosion-resistant crystalline rocks (paragneisses) emerge from the loose sediments of the Mydlovary Fm. (the elevated relief to the NW of Munice is possibly controlled by the relic of Zliv Fm., see above). Farther to the SE, at the western outskirts of Hluboká nad Vltavou, the escarpment is interrupted by the Tertiary „Northern River“ channel filed with sediments of the Mydlovary Fm. The local water divide is located close to the basin margin and no active fluvial system is present in this valley in Late Quaternary. Between Hluboká and Hrdějovice the scarp developed in the crystalline rocks is <50 m high with slope 15-35° and it is interrupted only by the Vltava river valley. In the area Hrdějovice-Borek-Úsilné (fault segments 2B and 3) where sediments of the Klikov Fm. exceed the fault trace in a local promontory, the scarp is missing again and mildly dipping slope is developed (<2° above the fault). South of Úsilné the scarp is developed at the contact of basin sediments with Permo-Carboniferous, having height of approx. 10 m and slope of 5-8°.

This systematic spatial coincidence of the fault scarp with surface contacts of lithologically contrasting rocks and its absence in areas where such contrasts are not present, clearly proves that the present-day morphology of the basin margin in this area is mainly a result of deep differential erosion.

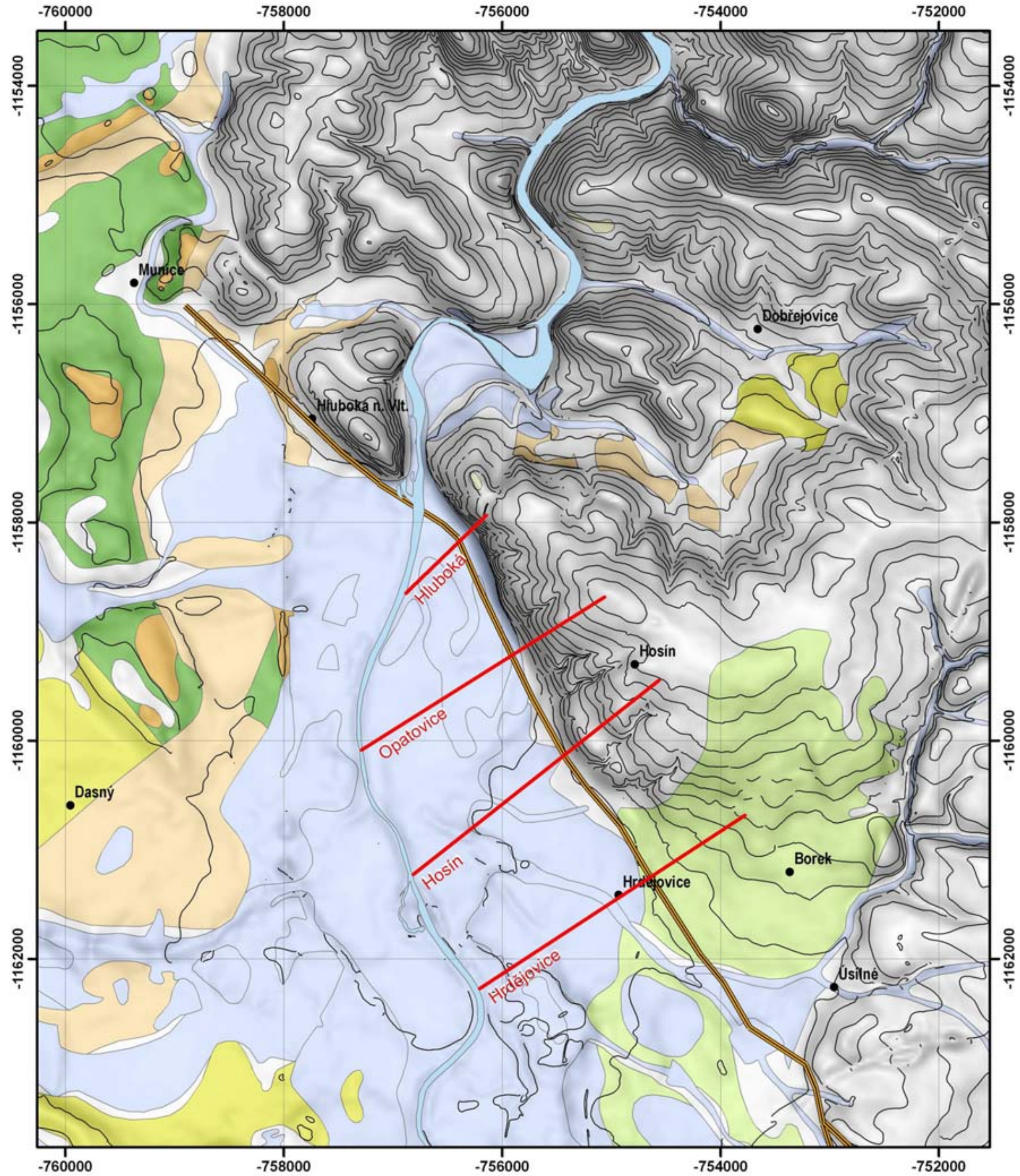

Fig. 5.4.: Composite map of the NE margin of the Budějovice Basin to demonstrate the lithological control of the Hluboká Fault scarp. Coloured areas show the extent of the sedimentary fill of the basin (green - Klikov Fm., yellow, purple and ocre - Mydlovary and Zliv Fm., blue - Quaternary fluvial sediments). Grey shaded areas represent the solid rocks of Proterozoic and Paleozoic age and their colluvia. Hluboká Fault is shown by bold brown line. Red lines indicate the positions of profiles shown in Fig. 5.5.

Fault scarp morphology and its evolution

In the geomorphological maps of Balatka and Přibyl (1994) and Demek (1994) only the lower part of the escarpment developed between Munice and Vráto is assigned as the „exogenically re-modelled fault scarp“. In the central segment this level of the escarpment has the elevation range approx. 375 – 440 m a.s.l., the typical slope is >20° and the height of the scarp locally exceeds 60 m. The upper part of the escarpment, on the other hand, has a milder slope <15° and was explained as denudation slope by Balatka and Přibyl (1994). The combined effect of these two levels with different slopes is the general convex shape of the whole scarp, a feature which is often explained as due to the long-term active slip on the fault (with vertical slip component) where the degradation of the older upper part of the scarp is more advanced than in the lower part where continuing active slip on the fault plane keeps the scarp steep.

This morphology is also reflected in lateral and longitudinal profiles of short (0.4-2 km) creek valleys incised into the scarp between Hluboká and Hrdějovice. In the upper, denudated part of the scarp, broader hanging valleys with milder slope are developed while below the inflexion points the creeks form narrow steeper valleys. The longitudinal (thalweg) profiles, though strongly affected by the railway corridor and possibly by other artificial modifications (relics of small dams were identified on some creeks) are generally convex, in several cases even in the lower parts of the scarp. They can reflect fast relative lowering of erosional base. This feature, similarly as the morphology of the scarp itself, is characteristic for scarps of active faults in which lithological pre-disposition does not exist.

The morphology of the Hluboká scarp, however, is laterally strongly variable and complex, as shown by four elevation profiles in Fig. 5.5 which are characteristic for the segment Hluboká – Hrdějovice. Several plateaus (ledges) with limited lateral extent are developed in the scarp at various elevations; e.g. the most pronounced plateau on the Hosín profile, approx. 430 m a.s.l. (Fig. 5.5) or the narrrow plateau with Quaternary sediments north of Opatovice around 390 m a.s.l. (base of the sediments at approx. 380 m a.s.l., see Chapter 4.5 and Fig. 5.1).

Amongst other features, it is notable that the steepest scarp is developed in the area adjacent to the Vltava river, where floodplain approaches the foot of the scarp and colluvium is narrow. It is straightforward to explain this by the locally increased lateral erosion of Vltava river in Late Pleistocene, which led both to destruction of higher terraces and colluvia and steepening of the scarp.

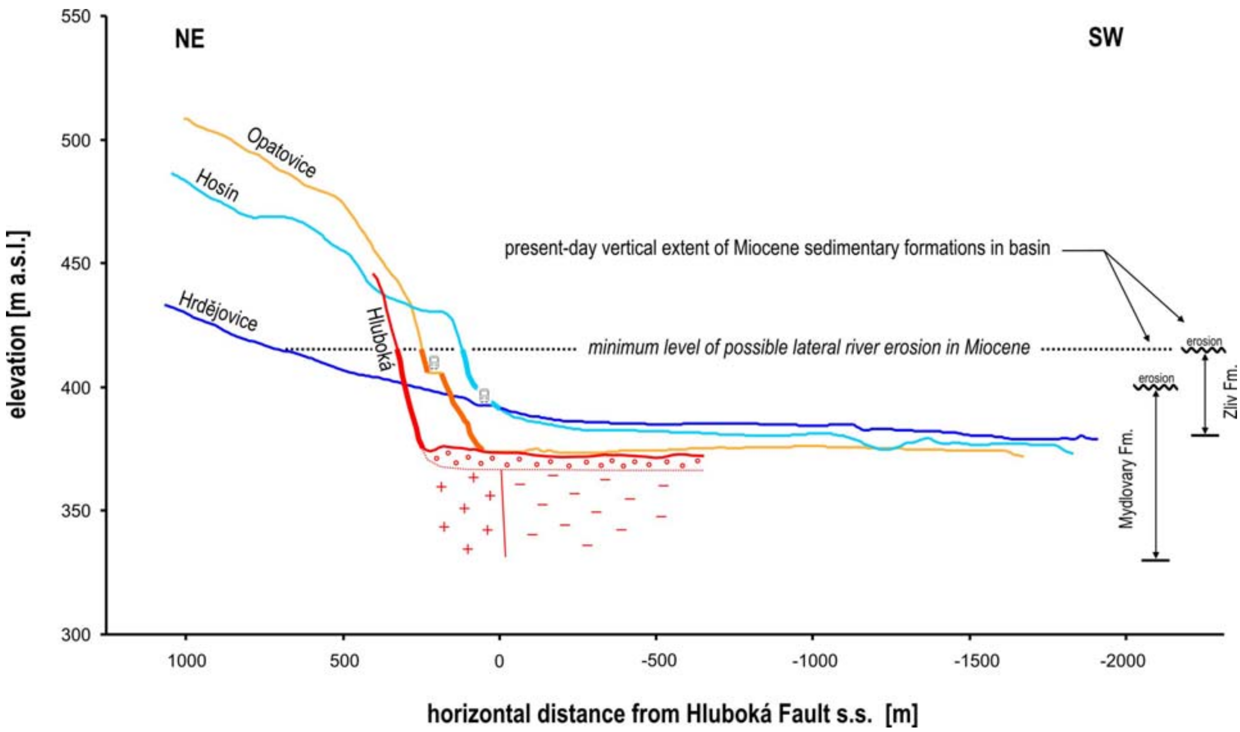

Fig. 5.5: Four representative elevation profiles across the basin margin between Hluboká and Hrdějovice. See Fig. 5.4 for location. The subsurface geology is schematically shown for profile Hluboká (red). Also shown is the present-day vertical extent of the relics of Mydlovary Fm. and Zliv Fm. in the adjacent areas within the basin which indicate the minimum level of possible degradation of the exposed fault scarp by lateral river erosion in Miocene (those parts of the scarp which are below this level are highlighted in bold). Note the absence of fault scarp at the Hrdějovice profile where unconsolidated sediments of Klikov Fm. are developed at both wings of the fault. Also note the broad pediment in crystalline at Hluboká profile with the steepest scarp.

It is also notable that to the east of Hluboká the ledge in the crystalline buried beneath floodplain is much broader (up to 300 m) than indicated beneath the higher terraces and the colluvio-alluvial fan farther to the SE, between Opatovice and Hrdějovice (comp. Figs. 5.1, 5.4 and 5.5). This ledge is interpreted as an erosional pediment with locally preserved relics of sands, silts and clays (observed in boreholes OP-2, HL-12, HL-13 and HL-14). The age of these sediments is unknown, but its lithological features and OSL dating (sample OP-2) suggest that they are post-Santonian and pre-Würmian. This indicates that the formation of the pediment must have occured earlier than in Late Pleistocene. In accordance with Balatka and Přibyl (1995), we suggest that this most probably occured in Neogene. The present day vertical extent of sediments of the Mydlovary Fm. and Zliv Fm. in the areas of the basin which are close to the scarp is approx. 330-400 m and 385-420 m a.s.l., respectively. This means that in Miocene, the regional erosional base was at the elevation range which overlaps with the elevations of the pediment, as well as at least some of the plateaus higher in the scarp. Thus, all these morphological features could represent the stepwise, long-term process of scarp degradation (possibly by lateral river erosion) which operated at least in Miocene and continued again in Pliocene and Quaternary when the erosional base was returning to the level of the present-day river-system.

Regarding this fact and all the observations from the area given above, we conclude that the escarpment developed at the NE margin of the Budějovice Basin between Munice and Hrdějovice represents an exhumed and degraded part of the Hluboká Fault sensu stricto. The well pronounced morphology in its central part is due to the extreme erosion of the basin sediments by Vltava river in Pleistocene. The generally linear character of the escarpment is inherited from the Hluboká Fault *sensu stricto*, and can also partly reflect the existence of fault-parallel planar fabric (possibly including other fault planes) developed in its deformation zone. As discussed above, we suggest that no differential movement at the hypothetical fault associated with the scarp occured in Late Pleistocene, but this statement should be supported by more data during further research.

6

CONCLUSIONS AND SUGGESTIONS FOR CONTINUING RESEARCH

6. CONCLUSIONS AND SUGGESTIONS FOR CONTINUING RESEARCH

• We performed a detailed mapping of the Hluboká Fault sensu stricto between the villages Munice and Vráto, where it has distinct geological, geophysical and geomorphological expression, representing the main marginal fault of the Budějovice basin. The fault is bounded by other fault systems of N-S and NNE-SSE strike and its continuation farther to the NW and SE is not supported by observations. Although it is composed of several segments with strike differences of up to 30°, in terms of reactivation potential it can be regarded as a single structure with the length of 13 km.

• In spite of the first order coincidence of the fault with distinct morphological escarpment, the detailed survey confirmed that the surface trace of the main lithological boundary between Cretaceous sediments and crystalline rocks and the foot of escarpment are locally separated by a distance of up to 200-300 m. This raised the hypothesis of a zone with multiple fault structures developed along the main lithological boundary which has been further critically tested.

• Extensive amount of data relevant for the assessment of Quaternary slip in the fault zone was gathered at several localities on individual segments, using observations on surface, in trenches, geophysical sections and boreholes, and dating of sediments overlying the fault zone:

1) Observations which contraindicate the Late Quaternary activity of the fault:

In segment 1A the continuous stratigraphy of the Mydlovary Fm. suggests the long-term absence of (vertical) fault slip since Middle to Late Miocene. This is also suported by similar elevation of relics of the Zliv Fm. on both wings of the fault.

In segments 1C and 2A the continuity of Holocene and Late Würmian (0-45 ka) fluvial sediments indicates the absence of vertical slip on the Hluboká fault in this period. The similar thickness of Quaternary sediments of the lower Vltava terrace to the NE and SW of the escarpment suggests that this applies to the whole fault zone, including the hypothetical segment H.

In segments 2B and 3 the absence of vertical slip in Holocene, and probably in Late Würm, is indicated by continuity of fluvial sediments.

In segment 4A we proved the absence of slip at the marginal fault at least for a period 0-22 ka based on direct observations in trenches.

2/ Observations indicating possible ongoing slip in the fault zone:

Morphological features of the escarpment associated with the fault zone between Hluboká and Hrdějovice, which displays complicated profile of generally concave-up geometry.

Elevations of relict Quaternary sediments sampled at higher levels above the Vltava floodplain near Hluboká, which are larger to the NE of the fault escarpment than expected based on the elevations of sediments of similar age observed in the SW.

The arguments for tectonic quiescence at the Hluboká Fault zone prevail and we suggest that the apparent indications of Quaternary slip can be explained atectonically:
The present-day morphology of the escarpment is explained mainly as due to the differential erosion of unconsolidated sediments of the basin fill and long-term, probably multiphase, degradation of the fault scarp since Tertiary. The crystalline ledge developed below the foot of the scarp and buried beneath Quaternary terraces, is interpreted as pediment.
The observed vertical separation of the sediments of similar age can be explained as due to the bleaching of their fine-grained component during re-deposition at the slopes (alluvial and colluvial environments) and/or cryoturbation. All the apparently younger sediments were sampled in small relics without clear morphological signature. In such position it is not possible to unequivocally assess its sedimentary environment and in-situ position. The observed constant thickness of the lower terrace is contraindicative to the vertical slip on the fault. Nevertheless, the apparently systematic nature of the observed misfits is striking and data available do not allow to rule out the slip at the central fault segment in Quaternary. Therefore we strongly suggest to continue the research in this area to resolve the conflicting dates.

• No indications of paleoseismic events were found in geological record during the current research. However, it must be kept in mind that other fault structures which do not necessarily have pronounced surface manifestation, can theoretically produce stronger earthquake. It is therefore essential to continue the monitoring of microseismicity in the region using local seismic network. In case that an increased seismic activity appears to be spatially associated with any fault structures mapped on the surface, it is suggested to carry out a detailed paleoseismological research of such structures.

• Newly revised catalogues of historical and instrumentally observed seismicity in the area within 70 km from Temelín NPP indicate only very weak activity with magnitudes not exceeding $M_{I(1km)}$ = 3.2 in period 1591-1991 and M_L=2.6 in period 1991-2009. In broader area of the Hluboká Fault only two questionable historical events with the intensity 4-5° MSK are located.

• Current research has not revealed any new facts which would require the revision of seismic hazard assessment in the area of the NPP Temelín. Nevertheless, to solve some enigmatic observations which can possibly be indicative of vertical slip on the Hluboká Fault in Quaternary we suggest to carry out a complementary study, with the main points outlined below:

1. Complementary datings of the lower Vltava terrace and of the relics of higher terraces. Dating of sediments sampled by several boreholes at the elevations 363-390 m a.s.l. near Hluboká-Zámostí and Opatovice/Skelná Huť will allow to assess the vertical slip at segment H during the last 100-150 ka.

2. Detailed geophysical and borehole survey of the Northern River channel near Hluboká. The refined profile of the base of this Tertiary paleovalley will allow to assess the slip on fault segment 1A back to 15 Ma and to locate or rule out eventual latent faults of the Hluboká Fault zone.

3. Trenching in segment 2B. Current research suggests that north of Nemanice the Hluboká Fault should be accessible in shallow depths beneath datable Quaternary sediments.

4. Trenching in segment 5. Although the faults in this segment are not well constrained in places with datable Quaternary sediments, it is likely that these can be reached in trenches and their activity assessed at least for Holocene period.

REFERENCES

Ambrož V. (1935): Studie o krystaliniku mezi Hlubokou a Týnem nad Vltavou. - MS PřF UK Praha.

Balatka B. (1993): Geomorfologická analýza oblasti jaderné elektrárny Temelín z hlediska morfostrukturní stability. Výzkumná zpráva o řešení úkolu HS 248/93 na území zákl. mapy 1:25 000 list 22-441 Březí u Týna nad Vltavou, 27s + 6 příl., geomorfol. mapa. - MS Kat. FGG PřF UK v Praze.

Balatka B., Přibyl V. (1994): Geomorfologická analýza území České Budějovice-Lišov z hlediska morfostrukturní stability. Výzkumná zpráva o řešení úkolu HS 404, 23s. + 4 příl. geomorfol. mapa 1:25 000. - MS Kat. FGG PřF UK v Praze.

Balatka B., Přibyl V. (1995): Syntéza geomorfologického vývoje zájmového území JE Temelín v mladším kenozoiku. Souhrnná výzkumná zpráva. 15s. + 1 příl. - MS Kat. FGG PřF UK v Praze.

Balatka B., Přibyl V. (1997): Geomorfologické poměry západní části Lišovského prahu přilehlé části Blatské pánve. - Acta Universitatis Carolinae, Geographica, No. 2, 15-30.

Bárta V. and Benda V. (1966): Geophysical survey in the South Bohemian basins using the VES method. - MS Geofond Praha.

Bouška et al. (1993): Vysvětlivky ke geologické mapě 1:50 000 list 22-44 Hluboká nad Vltavou. - ČGÚ, Praha, 46s.

Březinová D., Cimbálníková A., Kužvart M., Pacltová B., Špinar Z. (1965): Ložisko jílu u Jehněda. - Čas. Mineral. Geol., roč. 10, č. 3, s. 301-311. Praha.

Čech V. et al. (1962): Vysvětlivky k přehledné geologické mapě ČSSR, 1:200 000, M-33-XVII (České Budějovice) a M-33-XXXIII (Vyšší Brod). - ÚÚG Praha, 196 str.

Cepák L. (1967): Zhodnocení hydrogeologických vrtů státní pozorovací sítě HMÚ pro první horizont podzemních vod v povodí IV. - horní Vltava a VII. - střední Vltava. - MS Vodní zdroje, Praha GF P020833

Čepek L. (1929): Poznámka k lignitové sloji u Mydlovar. - Věst. Stát. Geol. Úst., V, č. 2-3, 177-181. Praha.

Čepek L. (1935): O vzniku jihočeského antracitu. - Věst. Stát. geol. Úst., roč. IX, č. 1-2, s. 1-8. Praha.

Chábera S. (1982): Geologické zajímavosti jižních Čech. - Jihočes. Muz. České Budějovice.

Chocholáč M. (1985): Stavebně-geologický průzkum pro výstavbu přípojky plynu do Šamotových závodů Zliv. - MS, Keramoprojekt, Brno. GF P046834

Čtyroký P. and Fejfar O. (1962): Ein Fund von Süßwassergastropoden und Säugetieren in der Mydlovary-Schichtenfolge in Südböhmen. - N. Jb. Geol. Paläont., Mh. 3. Stuttgart.

Daněk A. (2001): Zpráva o hydrogeologickém průzkumu Borek - sportovní areál, zdroj podzemní vody. - MS, Hydroprůzkum České Budějovice, s.r.o., České Budějovice, GF P100985

DECKER K, HNTERSBERGER E., HOMOLOVÁ D. (2010a): Paleoseismology of Temelin's near-regional faults. Interim report 2. - MS Department of Geodynamics and Sedimentology, University of Vienna.

DECKER K., HINTERSBERGER E., HOMOLOVA D. (2010b): Paleoseismology of Temelin's Near-Regional Faults - Interim Report 3. - MS Department of Geodynamics and Sedimentology, University of Vienna.

DEMEK J. (1994): Geomorfologická mapová studie listu základní mapy 1: 25 000 Zliv (Hluboká nad Vltavou) 22-443. Výzk. zpráva o řešení úkolu HČ 5/220/93-3, 14s. + 4 příl., geomorfol. mapa. - MS PřF UP, Olomouc.

DEMEK J., MACKOVČIN P. (ED.) A KOL. (2006): Hory a nížiny. - In: Zeměpisný lexikon ČR. AOPK ČR, Brno, 582 s.

DÈZES P., SCHMID S.M., ZIEGLER P.A. (2004): Evolution of the European Cenozoic Rift System: interaction of the Alpine and Pyrenean orogens with their foreland. – Tectonophysics, 389, 1-33.

DOMÁCÍ L. (1979): Některé aspekty sedimentace klikovského souvrství. - Acta Univ. Carol., Geol., No. 3-4, 149-166.

DORNIČ J., GABRIELOVÁ N., KNOBLOCH E., MALECHA A., ŘEHÁKOVÁ Z., ŘEZÁČ B., SLÁNSKÁ J., VOJTĚCH S. (1966): Vysvětlivky k základní geologické mapě 1:50000 list M-33-101-D (Hluboká n.Vltavou). - Ústřední ústav geologický, Praha. GF P018881, GF V056099, GF V056100, GF V056101

FENCL J., HROMADA K. (1956): Zpráva o pedogeologickém mapování blat Cepského, Kočičího a části Žofinky v jižních Čechách. - Zprávy o geol. výzkumech v roce 1955, str. 36-38.

GABRIELOVÁ N., MALECHA A., ŘEHÁKOVÁ Z. AND SLÁNSKÁ J. (1964): Další doklady o geologické pozici a stáří zlivského souvrství jihočeských pánví. - Věstník ÚÚG, 34, 243-249. Praha.

HAGEDOORN J.G. (1959): The plus-minus method of interpreting seismic refraction sections. - Geophysical Prospecting, 7, 158–182.

HANŽLOVÁ R., HUDOVÁ Z., MÁLEK J., NOVOTNÝ O., PAZDÍRKOVÁ J., ZEDNÍK J. (2007b): Recent Earthquakes in the Orlík Reservoir Region. - Transactions of the VŠB – Technical University of Ostrava, Civil Engineering Series, No. 2, Vol. VII, pp. 189 – 195, Ostrava.

HANŽLOVÁ R., MATTUŠOVÁ I., PAZDÍRKOVÁ J., VLACH R., OTRUBA J., KRATOCHVÍL T., VYSLOUŽIL P. (2010): Detailní seismické rajonování; Seismologické monitorování okolí JE Temelín: Zpráva č. 66 za rok 2009. MS ÚFZ Brno.

HANŽLOVÁ R., NEHYBKA V., OTRUBA J., ŠVANCARA J., VLACH R. (2007a): Nová seismologická síť monitorující JE Temelín. - Bezpečnost jaderné energie, č. 7/8. Praha.

HOLUB V., KALIBOVÁ-KAISEROVÁ M. (1965): K otázce nejjižnějších výskytů permokarbonu blanické brázdy. - Sb. Jihočes. Muz. v Čes. Budějovicích, přír. Vědy, V, s. 73-77. České Budějovice.

HOMOLKA M. (2003): Č. Budějovice - Budvar - HV-2A. - MS, Hydroprůzkum České Budějovice, s.r.o., České Budějovice, GF P106580

HOMOLKA M. (2004): České Budějovice - náhradní a doplňkové zdroje pitné vody - severní část pánve, průzkumný vrt BP-4. Zpráva o hydrolgeologickém průzkumu. - MS, Hydroprůzkum Č. Budějovice - GF P110137

Hynie O. (1949): Vodárensky využitelné vydatné nádrže podzemních vod v Čechách. - Geotechnika, Sv. 8, Stát. Geol. Úst., Praha

Kadlec E., Odstrčil J., Bartoš V. (1975): Detailní gravimetrické mapování v oblasti jihočeských pánví a moldanubika vodňanského. MS – Geofyzika n.p. Brno, Geofond Praha.

Karlín P. (1987): Podrobný inženýrsko-geologický průzkum pro výstavbu prodejny zeleniny v Hluboké nad Vltavou, okres České Budějovice. - MS, Stavební geologie Praha, závod České Budějovice. GF P056399

Karlín P. (2007): Zpráva o výsledcích podrobného geotechnického průzkumu pro řízený podvrt pod řekou Vltavou v Hluboké nad Vltavou. - MS, Stavební geologie Praha. GF P117413

Kárník V., Michal E., Molnár A. (1957): Erdbebenkatalog der Tschechoslowakei bis zum Jahre 1956. - Travaux. Inst. Geophys. Tchecosl. Acad. Sci., 69, NČSAV Praha.

Kárník V., Procházková D., Brouček I. (1981): Catalogue of Earthquakes for the Territory of Czechoslovakia for the Period 1957 - 1980. - Geofyzikální sborník No 555, Geofyzikální ústav ČSAV, Praha.

Kettner R. (1933): Geologický posudek o permské budějovické pánvi se zvláštním zřetelem k výskytu antracitové sloje u Lhotic. - Geofond P488, 45 stran. Praha.

Klečka M. et al. (1988): Tektonika střední části Českého moldanubika v širším okolí JE Temelín. - MS Ústav geologie a geotechniky ČSAV Praha, 72 str.

Koláček F. (1921): Seznam otřesů pozorovaných na půdě Republiky Československé. - Spisy Přírodověd. fakulty Masarykovy univ., č. 7, Brno 1921.

Kodym O., Fusán O., Matějka A. (1967): Geologická mapa ČSSR, měřítko 1:500 000. – ÚÚG. Praha.

Koroš I. (2001): Úsilné US-2A. - MS Geofond Praha, P101250.

Kroupa J. (1991): České Budějovice - Budvar, hydrogeologický průzkum. - MS, Stavební geologie Praha, závod České Budějovice. GF P074222

Kůst J. (1947): Vrt na vodu v Hrdějovicích.- MS, ARTESIA, Praha, GF V021011

Lána V. (1973): Zhodnocení průzkumného hydrogeologického vrtu 45-1. - MS, Vodní zdroje, Praha, GF V070452

Lehmann B. (2007): Seismic traveltime tomography for engineering and exploration applications. - EAGE Publications BV, Houten, Nizozemí.

Lenhardt, W.A., Hammerl, Ch. (2010): Seismologische Analyse historischer Erdbebeninformation aus Niederösterreich seit 1000 n.Chr., Erfassung von lokalen Erdbebenauswirkungen und Interpretation im Vergleich mit der rezenten Erdbebentätigkeit zur Schaffung einer Grundlage für Fragestellungen der Bauwerkssicherheit, Raumordnung, des Zivil- und Katastrophenschutzes. Projekt der Niederösterreichischen Landesregierung, Baudirektion, Abt. Allgemeiner Baudienst, Geologischer Dienst, Projektbericht NC 65-2006, BD1-G-5101/001-2006

Linsser H. (1967): Investigation of tectonics by gravity detailing. -Geophysical Prospecting 15, No.3, p. 480-515.

Loke M.H. & Barker R.D. (1996): Rapid least-squares inversion of apparent resistivity pseudosections using a quasi-Newton method. - Geophysical Prospecting, 44, 131–152.

Loke M.H. & Dahlin T. (2002): A comparison of the Gauss-Newton and quasi-Newton methods in resistivity imaging inversion. - Journal of Applied Geophysics, 49, 149–162.

Malecha A. (1966): Geologické výsledky strukturních vrtů v severovýchodní části budějovické pánve. - Zprávy o geol. výzk. v roce 1964, 327-329, ÚÚG Praha.

Malecha A. (1994): Geologická a tektonická stavba jihovýchodní části budějovické pánve a její vývoj. - MS, Dolní Bukovsko, 18 str.

Malecha A. et al. (1966): Vysvětlivky k základní geologické mapě 1:50 000, list M-33-101-d, Hluboká n./Vlt. - MS Archiv ÚÚG Praha. (GF Praha, P 18881).

Malecha A. and Mrázek Z. (1960): Geologická generální mapa 1:200 000 list České Budějovice, část - jihočeské pánve. MS GF V046625

Malecha A., Pícha F. (1963): Geologický vývoj jihozápadní části třeboňské pánve. - Věst. ÚÚG, XXXVIII, s. 297-310. Praha.

Malecha A., Suk M., Zikmund J. (1964): Stavba a podloží jihočeských pánví. - Sbor. geol. Věd, Ř. G, sv. 4, s. 97-120. Praha.

Malkovský M. (1987): The Mesozoic and Tertiary basins of the Bohemian Massif and their evolution. – Tectonophysics 137, 31-42.

Matznerová L. (1969): Hluboká - hotel, závěrečná zpráva. - Stavební geologie, Praha. GF V061169

Michal E. (1928): Seznam zemětřesení v Českém masivu do r. 1896. - Bulletin Sismique, Année II, No 1, Inst. Géophys. Nat. Tchéchosl., Praha 1928.

Mísař Z., Dudek A., Havlena V., Weiss J. (1983): Geologie ČSSR I. Český masív. – SPN, 336 stran.

Mrázek A. (1960): Svrchní křída a terciér jihočeských pánví. - MS, Ústřední ústav geologický, Praha, GF P012010

Nehybka V., Hanžlová R., Otruba J., Švancara J., Vlach R. (2006): New Local Seismological Network in Southern Bohemia. - Acta Geodynamica et Geomaterialia, Vol. 3, No. 4, pp. 87-101, Praha.

Pacltová B. (1961): Některé rostlinnémikrofosilie ze sladkovodních uloženin svrchní křídy (senon) v jihočeských pánvích. - Sbor. ÚÚG, 26, odd. paleont., 47-102. Praha.

Pazderník O. (1984): Předběžný inženýrsko-geologický průzkum v trase projektovaného vodovodního řadu Hluboká nad Vltavou – Zliv, okres České Budějovice. - MS, Stavební geologie, Praha. GF P047243

Petr J. (1977): Budějovická pánev - roční zpráva. MS, Vodní zdroje, Praha. GF P025997

Plachký F. (1989): Hluboká nad Vltavou - Kulturní dům – Doplňující vrty na staveništi, inženýrsko-geologický průzkum. - MS, Stavoprojekt, České Budějovice. GF P073792

Plachký F. (1989): Kulturní dům Hluboká nad Vltavou, inženýrsko-geologický průzkum základových poměrů. - MS, Stavoprojekt, České Budějovice. GF P073775

Plachký F. (1996): Zpráva o inženýrsko-geologickém průzkumu na staveništi plaveckého areálu - plavecký bazén v Hluboké nad Vltavou. - MS, ATELIERY A1, s.r.o., České Budějovice. GF P085791

Plachký F. (1999): Zpráva o průzkumu základových poměrů na staveništi zimního stadionu v Hluboké nad Vltavou. - MS, PRŮZKUMNÉ PRÁCE s.r.o., České Budějovice. GF P095549

PLACHKÝ F. (2004): Zpráva o inženýrsko-geologickém průzkumu staveniště Prodejny potravin Plus Hluboká nad Vltavou. - MS, PRŮZKUMNÉ PRÁCE s.r.o., České Budějovice. GF P109457

PLACHKÝ F. (2005): Zpráva o doplňujícím inženýrsko-geologickém průzkumu pro přístavbu a modernizaci Parkhotelu, Hluboká nad Vltavou. - MS, PRŮZKUMNÉ PRÁCE s.r.o., České Budějovice. GF P113401

POPP F. (1990): Hluboká nad Vltavou – kotelna. Průzkum základových poměrů. - MS, Stavoprojekt, České Budějovice. GF P073835

PŘIBYL V. (1993): Geomorfologická analýza území listu 22-423 Týn nad Vltavou zákl.mapy 1:25000 z hlediska morfostrukturní stability. Výzkumná zpráva o řešení úkolu HS 248/93, 24s + 6 příl., geomorfol. mapa. - MS, Kat. FGG PřF UK v Praze.

PUPÍK V. (2007): Hluboká nad Vltavou - mosty 146-001 a 146-002, podrobný geotechnický průzkum. - Stavební geologie-Geotechnika, a.s., Praha, GF P116281

REININGER H. (1909): Das Tertiarbecken von Budweis. - Jb. geol. Reichsanst. (1908), 58/3, 469-526. Wien.

ROUT J. (2008): Závěrečná zpráva inženýrsko-geologického průzkumu na stavby: Plavební komora Hluboká nad Vltavou a Zajištění plavebních hloubek ve zdrži VD Hněvkovice. - MS, Stavební geologie-Geotechnika, a.s., Praha, GF P120279

RŮŽIČKA M. (1973): Fluviální sedimenty řeky Moravy v okolí Olomouce. – Sborník Geologických Věd, řada Antropozoikum, 9, 7-38.

ŘEHÁKOVÁ Z. (1963): Jihočeské pánevní sedimenty ve světle diatomových analýz. - Věst. ÚÚG, XXXVIII, s. 311-323. Praha.

SEDLÁK J., GNOJEK I., ZABADAL S. (2009): Detailed Gravity Survey of the Hluboká Fault Zone. - MS, Miligal, s.r.o., Brno.

SLÁNSKÁ J. (1961): Zpráva o petrografickém výzkumu strukturních vrtů GB-3 až GB-13 v jihočeských pánvích. - MS, Archiv Geofondu Praha.

SLÁNSKÁ J. (1963): Výsledky petrografického výzkumu klikovského a mydlovarského souvrství. - Věst. ÚÚG, XXXVIII, s. 367-385. Praha.

SLÁNSKÁ J. (1967): Sedimentologie jihočeských pánví. MS, Nepublikovaná kandidátská disertační práce, UK a ČSAV. Praha.

SLÁNSKÁ J. (1974): Continental Cretaceous and Tertiary sedimentation in the South Bohemian basins, Czechoslovakia. - N. Jb. Geol. Palaeont. Abh. 146, 3, 385-406.

ŠEFARA J. (1973): Interpretation of vertical density boundaries using a map of gravity anomalies by means of digital computers. - J. Geol. Sci., Applied Geophysics, vol. 21, 19-30.

ŠETINA L. (1981): Zpráva o výsledcích inženýrsko-geologického průzkumu pro přeložky a objekty v Hluboké nad Vltavou, V. dílčí část. - MS, Stavební geologie Praha. GF P034617

ŠETINA L. (1972): Závěrečná zpráva inženýrsko-geologického průzkumu pro čerpací stanici pohonných hmot v Hluboké n. Vltavou. - MS, Stavební geologie, Praha. GF V068630

ŠIMEK J. (1966): Zpráva o základových poměrech na staveništi 45 bytových jednotek v Hluboké nad Vltavou. - MS, Stavoprojekt, České Budějovice. GF V054304

ŠIMEK J. (1990): Hluboká nad Vltavou – 72 bytových jednotek, průzkum základových poměrů. - MS, Stavoprojekt, České Budějovice. GF P073862

Šimek J. (2001): Čerpací stanice odpadních vod Hluboká nad Vltavou, inženýrsko-geologický průzkum. - MS, PRŮZKUMNÉ PRÁCE s.r.o., České Budějovice. GF P101580

Šimek J. (2002): Přeložka vodovodu - protlak, Hluboká nad Vltavou, inženýrsko-geologický průzkum. - MS, František Plachký - IG průzkum, České Budějovice, GF P101572

Šimůnek P. (2005): Hluboká nad Vltavou, relaxační a rekondiční centrum, vyhodnocení vrtu HRC-1. - MS, Energoprůzkum Praha, spol. s r.o. GF P114996

Šimůnek P., Prachař I., Barták V., Buben J., Domácí L., Piskač J. (1994): Lokalita výstavby JE Temelín. Doplňující geologické a seismologické průzkumy. Část A – Tektonika. - MS, Energoprůzkum Praha,83 p.

Šimůnek P., Prachař I., Barták V., Domácí L., Piskač J. (1995): NPP Temelín Construction Site. Supplementary geological and seismological surveys. Part A: Tectonics. Part B: Seismic Risk. - MS, Energoprůzkum Praha.

Škoda S. (1988): Zpráva o geologickém průzkumu půdních poměrů v trase STL plynovodu Hluboká n. Vlt. – Zámostí. - MS, Stavoprojekt, České Budějovice . GF P063034

Štěpančíková P., Hók J., Nývlt D., Dohnal J., Sýkorová I., Stemberk J. (2010): Active tectonics research using trenching technique on the south-eastern section of the Sudetic Marginal Fault (NE Bohemian Massif, central Europe). – Tectonophysics 485, 269-282.

Švancara J., Hanžlová R., Havíř J., Špaček P. (2010): Detailní seismické rajonování: Komplexní vyhodnocení seismotektonických, gravimetrických a geologických dat. Zpráva č. 9 za roky 2007, 2008 a 2009. MS, ÚFZ Brno.

Švancara J., Špaček P. (2007): Detailní seismické rajonování: Komplexní vyhodnocení seismotektonických, gravimetrických a geologických dat. Zpráva č. 8 za roky 2004, 2005 a 2006. MS, ÚFZ Brno.

Švancara J. (2004): Tíhová mapa České republiky. - Československý časopis pro fyziku, vol. 54, no. 4, s. 217-220.

Švára O. (1960): Zpráva o průzkumu základové půdy na staveništi hotelu v Hluboké nad Vltavou. - Státní projektový ústav pro výstavbu měst a vesnic Č. Budějovice. GF V045752

Švára O. (1984): 68 bytových jednotek. Hluboká nad Vltavou. Průzkum staveniště. - MS, Stavoprojekt, České Budějovice. GF P045946

Švára O. (1986): Zpráva o průzkumu základových poměrů na staveništi obytného trojdomu se 48 byt. jednotkami v Hluboké nad Vltavou. - MS, Stavoprojekt, České Budějovice. GF P060991

Tomek Č. (1974): Řešení obrácené gravimetrické úlohy a její aplikace na morfologii středočeského plutonu. - Conference „Plutonity, jejich geneze a postmagmatické přeměny". - Čas. Min. Geol., 19, 217, Praha.

Uličný D., Laurin J., Čech S. (2008): Controls on clastic sequence geometries in a shallow-marine, transtensional basin: the Bohemian Cretaceous Basin, Czech Republic. - Sedimentology, doi: 10.1111/j.1365-3091.2008.01021.x

Vašta V. (1968): Vyhodnocení prvé etapy hydrogeologického průzkumu pro pivovar Budvar v Českých Budějovicích. - MS, IGHP, závod Praha, GF V057399

Vašta V. (1969): České Budějovice - pivovar. Závěrečná zpráva. - MS, Stavební geologie Praha, závod České Budějovice, GF V062599.

Vavřínová M. (1946): Geologie jihozápadního podhůří Orlických hor v okolí Kynšperka a jeho saxonská tektonika. – Sbor. Stát. geol. Úst., Odd. geol., 13, 343-373.

Volšan V. (1961): Českobudějovicko. Surovina: štěrkopísky. - MS, Geoindustria Praha, GF P012368

Woldřich J.N. (1893): Příspěvek k seznání budějovické pánve permské a třetihorní. - Věst. Čes. spol. nauk, 4, 11s. Praha.

Zedník J., Pazdírková J. (2009): Seismic activity in the Czech Republic in 2007. Studia geophysica et geodaetica 53, 2, 269-274.

Zeman A., Havlíček P., Minaříková D., Růžička M., Fejfar O. (1980): Kvartérní sedimenty střední Moravy. – Sborník Geologických Věd, řada Antropozoikum, 13, 37-91.

Ziegler P.A., Dèzes P. and Verniers J. (2006): Crustal evolution of Western and Central Europe. – In: Gee D., Stephenson R.A. (eds.): European Lithosphere Dynamics, Geological Society of London, Memoirs, 32, 43-56.

LIST OF APPENDICES